International Journal of Polymer Science

Polymeric Biomaterials for Tissue Engineering Applications 2011

Guest Editors: Shanfeng Wang, Lichun Lu, Chun Wang, Changyou Gao, and Xiaosong Wang

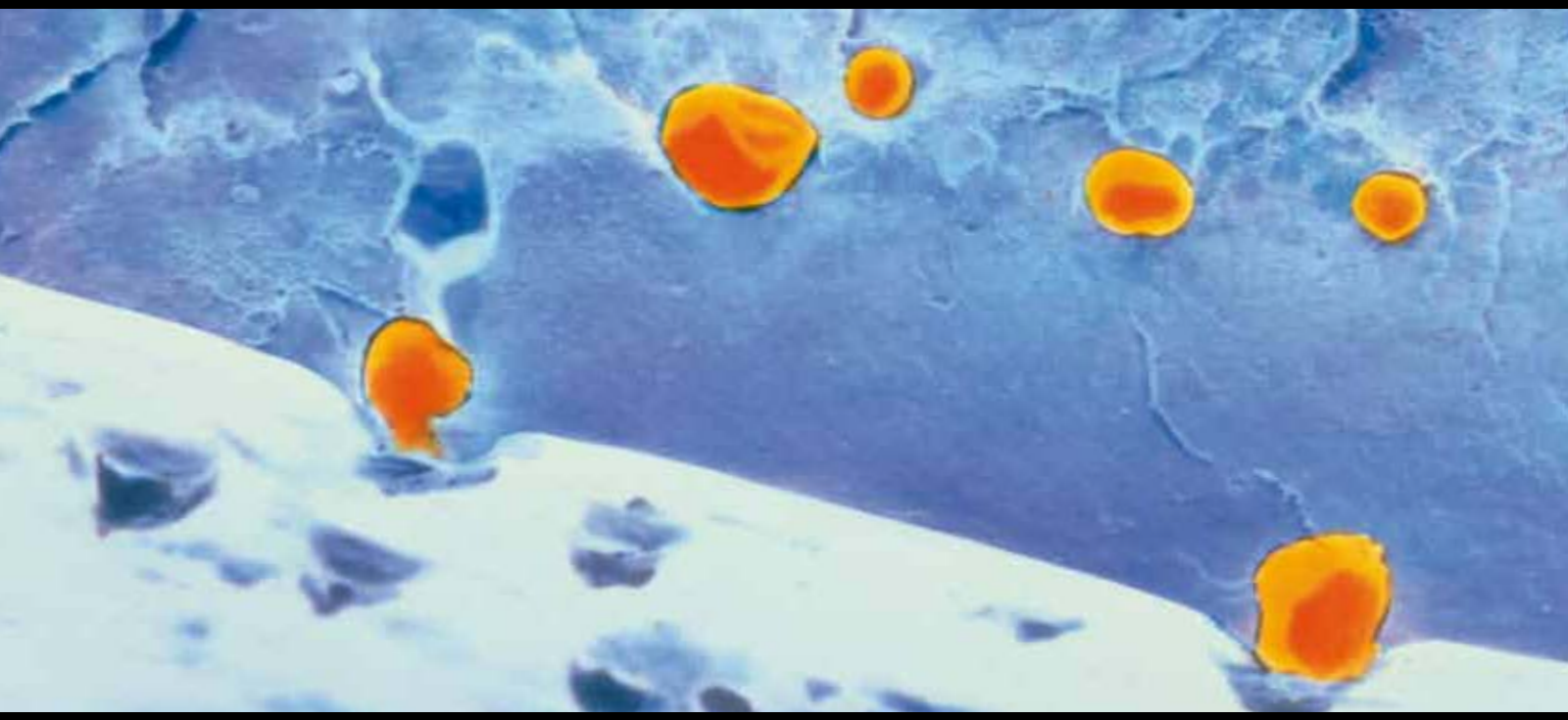

Polymeric Biomaterials for Tissue Engineering Applications 2011

International Journal of Polymer Science

Polymeric Biomaterials for Tissue Engineering Applications 2011

Guest Editors: Shanfeng Wang, Lichun Lu, Chun Wang, Changyou Gao, and Xiaosong Wang

Editorial Board

Contents

Hindawi Publishing Corporation
International Journal of Polymer Science
Volume 2011, Article ID 184623, 2 pages
doi:10.1155/2011/184623

Editorial

Polymeric Biomaterials for Tissue Engineering Applications, 2011

Shanfeng Wang,[1,2] Lichun Lu,[3] Chun Wang,[4] Changyou Gao,[5] and Xiaosong Wang[6]

[1] *Department of Materials Science & Engineering, The University of Tennessee, Knoxville, TN 37996, USA*
[2] *Biosciences Division, Oak Ridge National Laboratory, Oak Ridge, TN 37831, USA*
[3] *Departments of Biomedical Engineering and Orthopedic Surgery, Mayo Clinic College of Medicine, Rochester, MN 55905, USA*
[4] *Department of Biomedical Engineering, University of Minnesota, MN 55455, USA*
[5] *Department of Polymer Science and Engineering, Zhejiang University, Hangzhou 310027, China*
[6] *Department of Chemistry, Waterloo Institute of Nanotechnology, University of Waterloo, Waterloo, ON, Canada N2L 3G1*

Correspondence should be addressed to Shanfeng Wang, swang16@utk.edu

Received 14 November 2011; Accepted 14 November 2011

The interdisciplinary field of biomaterials and tissue engineering has been one of the most dynamic and rapidly expanding disciplines in the past two decades. Polymers are very attractive and useful in this area because of their tailorable chemical structures and physical properties. Many noncytotoxic and biodegradable polymers have been fabricated into medical devices for diverse applications, including tissue repair, drug delivery, cancer therapy, and nonviral gene therapy. Novel synthetic, supramolecular, and biomimetic strategies have been developed for advancing exploration of polymeric biomaterials. By tuning polymer structural parameters and morphologies at different length scales, controllable physical properties can be achieved for satisfying diverse clinical needs and regulating cell behavior. Polymeric biomaterials can also be incorporated with natural materials and inorganic nanoparticles to obtain novel, unique, and synergetic properties for better performance.

The aim of this annual special issue is to highlight recent significant developments in the synergy between material design strategies and biological evaluations through contributions from active researchers in the field. The first special issue was launched in 2010, and it proved to be very successful. The nine papers in that issue have garnered ten citations in one year according to Web of Science. This special issue has thus become an annual special issue to be published each year. Such a series can have a long-term impact and in time gather a community around it. The 2011 issue here covers various topics related to polymeric biomaterials for tissue engineering applications. Five original research articles and four reviews are included to stimulate the continuing efforts in developing novel polymeric systems, which is crucial to improve our fundamental understanding of cell/tissue-material interactions and tissue repair and regeneration. The editors of this annual special issue make every effort to ensure rapid and high-quality review process. The elapsed time for each accepted paper in this issue ranged from 24 to 54 days with an average value of 44.4 days.

Aliphatic polymer esters such as poly(L-lactide) (PLLA), polyglycolide (PGA), and their copolymers are widely used in tissue engineering applications. In the first paper "*Fast and convenient synthesis of amine-terminated polylactide as a macroinitiator for ω-benzyloxycarbonyl-* L*-lysine-N-carboxyanhydrides*" M. Ju et al. report synthesis of amine-terminated PLLA (NH_2-PLLA) with different molecular weights and then polymerization of ω-benzyloxycarbonyl-L-lysine-*N*-carboxyanhydrides using NH_2-PLLA as a macroinitiator. *In vivo* biocompatibility was also evaluated by implantation of the block copolymer and NH_2-PLLA in nude rats.

Polyhydroxybutyrate (PHB) is a semicrystalline degradable biomaterial produced by microorganisms. Its brittle nature and high crystallinity limit its potential tissue engineering applications. In the second and third papers "*Application of polyethylene glycol to promote cellular biocompatibility of polyhydroxybutyrate films*" and "*Manipulation of*

polyhydroxybutyrate properties through blending with ethyl-cellulose for a composite biomaterial" R. T. H. Chan et al. report modification of PHB by blending with poly(ethylene glycol) (PEG) and ethyl-cellulose (EtC), respectively. Both PEG and EtC can decrease PHB crystallinity. Neural-associated olfactory ensheathing cells were found to attach and proliferate better on PEG-modified PHB films while did not change on EtC-modified ones.

Fiber-reinforced polymer composites can be engineered for specific tissue performance, in particular, bone repair. On a per-weight basis, their mechanical properties can be many times greater than structural aluminum, titanium, or steel. In the fourth paper "*Bisphenyl-polymer/carbon-fiber-reinforced composite compared to titanium alloy bone implant*" R. C. Peterson reports aerospace/aeronautical thermoset bis-phenyl-polymer/carbon-fiber-reinforced composites, aiming to replace metal bone implants. They also performed *in vivo* bonemarrow tests with Sprague-Dawley rats and examined osteoconductivity of the polymer composites compared to titanium alloy controls.

Chitosan, a copolymer of D-glucosamine and *N*-acetyl-D-glucosamine, is a biodegradable polysaccharide obtained from *N*-deacetylation of chitin, which can be extracted from the shells of crabs and shrimps. Chitosan has been used as biocompatible wound dressings and also has intrinsic would-healing abilities. In the fifth paper "*In Vitro evaluation of a biomedical-grade bilayer chitosan Porous Skin regenerating template as a potential dermal scaffold in skin tissue engineering*" C. K. Lim et al. report a method to prepare a biomedical-grade bilayer chitosan porous skin regenerating template as a potential dermal scaffold. Cultured primary human dermal fibroblasts were able to penetrate the scaffold, and pore sizes between 50 and 150 μm were found to be cytocompatible, as indicated by no additional production of interleukin-8 (IL-8) and tumor necrosis factor-α (TNF-α).

Review articles in this issue cover different aspects in scaffolds and hydrogels for tissue engineering applications. In the sixth paper "*Polymeric scaffolds in tissue engineering application: a review*" B. Dhandayuthapani et al. give an overview of different types of scaffolds, materials properties, and fabrication techniques. The seventh paper "*Hydrogel contact lens for extended delivery of ophthalmic drugs*" contributed by X. Hu et al. summarizes hydrogel contact lenses for extended delivery of ophthalmic drugs. Strategies to modify the conventional contact lenses as well as novel contact lenses are discussed. In the eighth paper "*Poly(amidoamine) hydrogels as scaffolds for cell culturing and conduits for peripheral nerve regeneration*" F. Fenili et al. review biodegradable poly(amidoamine) hydrogels as scaffolds for cell culturing and conduits for peripheral nerve regeneration. The last paper of this issue "*Hydrogel synthesis directed toward tissue engineering: impact of reaction condition on structural parameters and macroscopic properties of xerogels*" contributed by B. Adnadjević and J. Jovanović discusses xerogel preparation and impact of reaction condition on structural parameters and macroscopic properties after a brief review of applications of hydrogels in tissue engineering.

Acknowledgment

We thank all the contributing authors and reviewers for their efforts in putting together this special issue.

Shanfeng Wang
Lichun Lu
Chun Wang
Changyou Gao
Xiaosong Wang

Hindawi Publishing Corporation
International Journal of Polymer Science
Volume 2011, Article ID 381076, 7 pages
doi:10.1155/2011/381076

Research Article

Fast and Convenient Synthesis of Amine-Terminated Polylactide as a Macroinitiator for *ω*-Benzyloxycarbonyl-L-Lysine-*N*-Carboxyanhydrides

Mingjie Ju, Feirong Gong, Shujun Cheng, and Yun Gao

Key Laboratory for Ultrafine Materials of Ministry of Education, School of Materials Science and Engineering, East China University of Science and Technology, Shanghai 200237, China

Correspondence should be addressed to Feirong Gong, gongfeirong@yahoo.com.cn

Received 26 May 2011; Accepted 29 June 2011

Academic Editor: Shanfeng Wang

Amine-terminated poly (L-lactide) (NH_2-PLLA) with various chain lengths were successfully synthesized by sequential tert-butyl-*N*-(3-hydroxypropyl) carbamate initiated bulk ring-opening polymerization (ROP) of L-lactide (L-LA) in the presence of Stannous(II) 2-ethylhexanoate ($Sn(Oct)_2$) and deprotection of the *N-tert*-butoxycarbonyl (Boc) group at the end of the polymer chain. The polymers obtained were characterized by FT-IR, ^{1}H NMR, and GPC method. NH_2-PLLA thus prepared was used to initiate the polymerization of *ω*-benzyloxycarbonyl-L-lysine-*N*-carboxyanhydride (Lys (Z)-NCA), and the result confirmed the high nucleophilicity of the terminal amine group. This method was not only suitable for the preparation of low molecular weight NH_2-PLLA, but also quite efficient in the synthesis of high molecular weight samples.

1. Introduction

During the last few years, aliphatic polyesters based on hydroxyalkanoic acid, such as polylactides (PLLA), polyglycolide (PGA), poly (caprolactone) (PCL), and their copolymers have become the most important biopolymers because of their biodegradability and good biocompatibility for pharmaceutical and biomedical applications. However, the scope of further application of PLLA is limited for the lacking of highly reactive groups as triggers of chemical reaction, and the surface of PLLA is very hydrophobic [1]. Chemical modification, especially end functionalization, is an important method to expand the applications area of these polymers [2]. The end-functionalized polymers are also important intermediates which can react at the end of the chain with other molecules containing reactive groups such as acid chlorides, sulfonyl chlorides, acid anhydrides, and activated esters for the synthesis of novel polymeric materials [3, 4]. NH_2-PLLA can be used to conjugate with lactose to form a new bioabsorbable material which shows high biodegradability and gives a microphase separation structure [1]. Especially, they were investigated as a macroinitiator for the ring-opening polymerization (ROP) of amino acid N-carboxyanhydrides (NCAs) to prepare a block copolymer containing polypeptide segments which showed quite different properties from other polymers [5–14].

The synthesis of NH_2-PLLA was based on a method first reported by Gotsche et al. in 1995 [5]. The main idea of his point was capping the hydroxyl end group of PLLA with BOC-L-Phe which containing a protective amino group using N,N′-dicyclohexylcarbodiimide (DCC) as the condensing agent. However, conversion of the hydroxyl group into an N-protected amino acid ester with the acylation of DCC is always not sufficient, possibly because of the low reactivity of the terminal hydroxyl group and the steric hindrance of the huge polymer chain [7]. Fan et al. [8] synthesized a mixed acid anhydride of BOC-L-Phe and trimethylacetyl chloride (TMAC) to improve the reactivity of the coupling agent. The complete end capping of the end hydroxyl group of PLLA was achieved by reacting with the mixed acid anhydride under the existence of 4-(1-pyrrolidinyl) pyridine. Finally, the protective group was removed to form the free amino group at the chain end of PLLA. Caillol et al. [6] synthesized amino-functionalized PLLA through

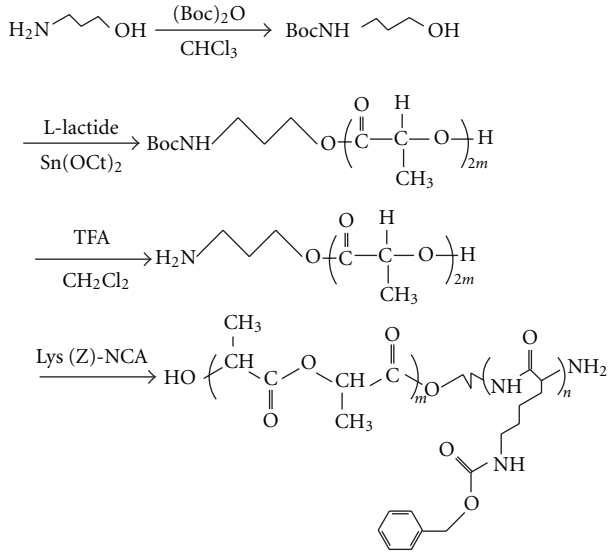

Figure 1: Synthesis of NH_2-PLLA and PLLA-*b*-PZLys block copolymer.

ring-opening polymerization of L-LA initiated by zinc alkoxide that was obtained from the reaction between diethylzinc and tert-butyl-*N*-(3-hydroxypropyl) carbamate. Lately, Ouchi et al. [1] synthesized NH_2-PLLA through anionic ROP of L-LA in dry tetrahydrofuran using Boc-amino-OK as an initiator. But in our opinion, the initiators mentioned above were so sensitive to environmental factors such as humidity and oxygen that they were so difficult to handle and store.

Stannous(II) 2-ethylhexanoate ($Sn(Oct)_2$) is one of the most widely used compounds for catalyzing the ROP of various lactones and lactides [15–18]. Despite the fact that the mechanism and the initiating complex remain unclear, both mechanisms are thought to be alcohol initiated [19–23], since the degree of polymerization is clearly dependent on the monomer-to-alcohol ratio [24], and the end groups of the polymers have hydroxyl functionalities. In the present research, we proposed a novel three-step method to achieve the complete end capping of PLLA with amine group by tert-butyl-*N*-(3-hydroxypropyl) carbamate initiated bulk ring-opening polymerization of L-LA catalyzed by $Sn(Oct)_2$. In order to control the molecular weight, alcohols have been widely used to initiate the bulk ring-opening polymerization of L-LA, but to our knowledge, the synthetic method of NH_2-PLLA initiated by tert-butyl-*N*-(3-hydroxypropyl) carbamate under the catalyzing of $Sn(Oct)_2$ has not been published. The outline of the synthetic route is illustrated in Figure 1. At first, the amine group of 3-amino-1-propanol was protected by reaction with di-tert-butyl dicarbonate under the existence of triethylamine. Then, tert-butyl-*N*-(3-hydroxypropyl) carbamate synthesized above was used to initiate the polymerization of L-LA to prepared Boc-amino terminated PLLA (BocNH-PLLA). Finally, the Boc group at the chain end was removed by the treatment of trifluoroacetic acid. The synthesized NH_2-PLLA (NH_2-PLLA) was used as a macroinitiator for the ROP of Lys (Z)-NCA to prepare the block copolymer of L-lactide and *ω*-benzyloxycarbonyl-L-lysine (PLLA-*b*-PZLys).

2. Experimental

2.1. Materials. L-LA was purchased from PURAC and recrystallized twice from anhydrous ethyl acetate. Anhydrous trifluoroacetic acid (TFA), $Sn(Oct)_2$ were from Sigma and distilled twice before use. Di-tert-butyldicarbonate, triphosgene, and *ω*-benzyloxycarbonyl-L-lysine were purchased from GL biochemical of Shanghai and used as received. Lys (Z)-NCA was prepared according to the previously method [25]. The purity of the obtained NCA was checked by DSC analysis from the position and the shape of the melting process. The melting endotherm of Lys (Z)-NCA was about 100°C-101°C with a highly asymmetric peak, showing the absence of residual chloride. Other reagents were commercially available and used as received. All solvents were thoroughly dried and distilled before use.

2.2. Synthesis

2.2.1. Synthesis of Tert-Butyl-N-(3-Hydroxypropyl) Carbamate. 3-amino-1-propanol (1.52 g, 20 mmol) and triethyamine (2.22 g, 22 mmol) were dissolved in chloroform (50 mL) in a flask equipped with a magnetic stirrer, and di-tert-butyldicarbonate (4.8 g, 22 mmol) in chloroform (20 mL) was added dropwise to the solution in 1 h with continuous stirring. After reaction for another 1 h, the concentrated solution was diluted with 5% potassium hydrogen sulfate aq. Soln. and extracted with ethyl acetate and dried over $MgSO_4$. After filtration and evaporation of the solvent, purification of the compound was carried out by column chromatography on silica gel using ethyl acetate and hexane as eluent. The purity of tert-butyl-*N*-(3-hydroxypropyl) carbamate obtained as colorless viscous oil was found to be over 98.7% by HPLC analysis. Yield: 86.2%.

2.2.2. Preparation of BocNH-PLLA, $PLLA_{25}$. PLLA was synthesized by ROP of L-LA initiated by tert-butyl-*N*-(3-hydroxypropyl) carbamate and catalyzed by $Sn(Oct)_2$. L-LA (14.4 g, 100 mmol) and tert-butyl-*N*-(3-hydroxypropyl) carbamate (700 mg, 4 mmol) were weighted in a glove box and introduced in an oven-dried schlenk bottle, and 72 mg of $Sn(Oct)_2$ (0.5 of L-LA) was added as a 0.02 g/mL solution in dry dichloromethane. After vacuumized and purged with Ar three times, the bottle was degassed under a high vacuum for 2 h to remove the residue dichloromethane. The bottle was then flame-sealed and immersed in a 130°C oil bath for 6 h. The obtained white solid was dissolved in dichloromethane, and the catalyst $Sn(Oct)_2$ was removed by precipitating the polymer solution in a large amount of chilled methanol, filtered and dried in vacuum at room temperature. The polymer was recovered over 85% yield with a stannous content less than 20 ppm.

2.2.3. Synthesis of Amine-Terminated PLLA. 1 g of PLLA was introduced in a flask which has been dried, purged with Ar

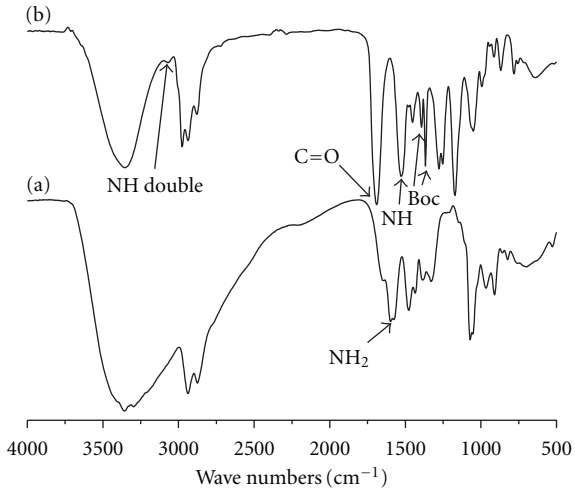

Figure 2: FT-IR spectra of 3-amino-1-propanol (a) and tert-butyl-*N*-(3-hydroxypropyl) carbamate (b).

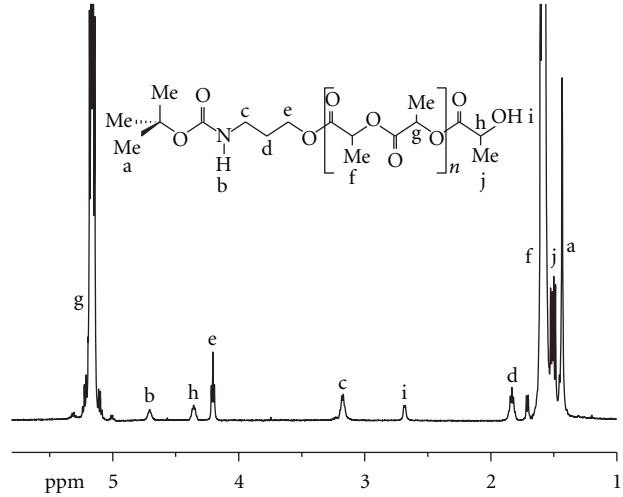

Figure 3: ^{1}NMR spectra of BocNH-PLLA in $CDCl_3$.

and vacuumized several times. Freshly distilled methylene chloride (12 mL) was added, followed by a large excess of anhydrous trifluoroacetic acid (6 mL). The solution was stirred at room temperature for 1 h, after which time all solvents were evaporated, the polymer was redissolved in dichloromethane and washed with aqueous $NaHCO_3$ (5%) and water and finally dried over $MgSO_4$. After filtration, the solution was precipitated in chilled methanol and dried in a vacuum at room temperature. The polymer was recovered over 80% yield.

2.2.4. Synthesis of PLLA-b-PZLys Block Copolymer. 2 g (6.5 mmol) or 5 g (16.3 mmol) of Lys (Z)-NCA was dissolved in 50 mL of CH_2Cl_2. The resultant solution was added to a solution of NH_2-$PLLA_{25}$ (1 g, 0.27 mmol) in 15 mL CH_2Cl_2. The reaction mixture was stirred under an inert atmosphere for 24 h at room temperature. The viscous solution obtained was poured into a large quantity of chilled diethyl ether, followed by filtration and drying under reduced pressure to give a white powder over 90% yield.

2.2.5. In Vivo Tissue Responses. Boc-PLLA (DP_{LA} = 100), NH_2-PLLA (DP_{LA} = 100), and PLLA-*b*-PZLys (DP_{LA} = 25, DP_{ZLys} = 24) were dissolved in CH_2Cl_2 at a concentration of 10% (w/v) in the watch glass. Polymer films were obtained by evaporating the solution under room temperature and dried in vacuum for 3 days. Nude rats weighing 200–250 g were implanted with the polymer films (n = 4 for each polymer) in legs. Animals with polymer films were allowed to survive 28 days after implantation and then terminated. The surgical wounds were reopened, and the leg musculature was removed with the polymer remnant and fixed in 10% formalin for histological analysis. Specimens were prepared for H-E staining analysis.

2.3. Measurements. ^{1}H-NMR spectra were recorded at room temperature on a Bruker DRX-500 using $CDCl_3$ as the solvent. Gel permeation chromatography (GPC) was carried out on a Waters HPLC system equipped with a Model 2690D separation module, a Model 2410 refractive index detector, and Shodex columns (K802.5, K803, and 805). Chloroform was used as eluent at the flow rate of 1.0 mL/min. Calibration was fulfilled with narrow-molar-mass distributed polystyrene standards. The infrared spectral analysis of the samples was performed on a FT-IR spectrophotometer (Nicolet Magna-IR550).

3. Result and Discussion

The general synthetic routes for the preparation of tert-butyl-*N*-(3-hydroxypropyl) carbamate, BocNH-PLLA, NH_2-PLLA, and PLLA-*b*-PZLys were shown in Figure 1.

3.1. Synthesis of Tert-Butyl-N-(3-Hydroxypropyl) Carbamate. Boc was chosen as the protective group for amine group of 3-amino-1-propanol because of its stability under the designed temperature of polymerization of L-LA and it can be easily removed under mild conditions. Tert-butyl-*N*-(3-hydroxypropyl) carbamate was obtained from the reaction of 3-amino-1-propanol and di-tert-butyldicarbonate at room temperature under the existence of triethylamine. The complete protection of the amine group was confirmed by IR spectra (Figure 2). The absorption peak at 1649.0 cm^{-1} assigned to primary amine was completely disappeared in tert-butyl-*N*-(3-hydroxypropyl) carbamate, and the peaks at 1527.0 cm^{-1} ($\nu_{CO\text{-}NH}$) and 1689.6 cm^{-1} (ν_{CO}) were attributed to second amide, indicating the successive protection of amine group by *t*-butoxycarbonyl. The peaks at 1366.7 cm^{-1} and 1392.8 cm^{-1} belonged to the Boc group were also characteristic of the formation of tert-butyl-*N*-(3-hydroxypropyl) carbamate.

3.2. Synthesis of NH_2-PLLA. Amino-functionalized PLLA was synthesized through ROP of L-LA with tert-butyl-*N*-(3-hydroxypropyl) carbamate. The bulk polymerization can be easily carried out at 130°C because of the stabilization of

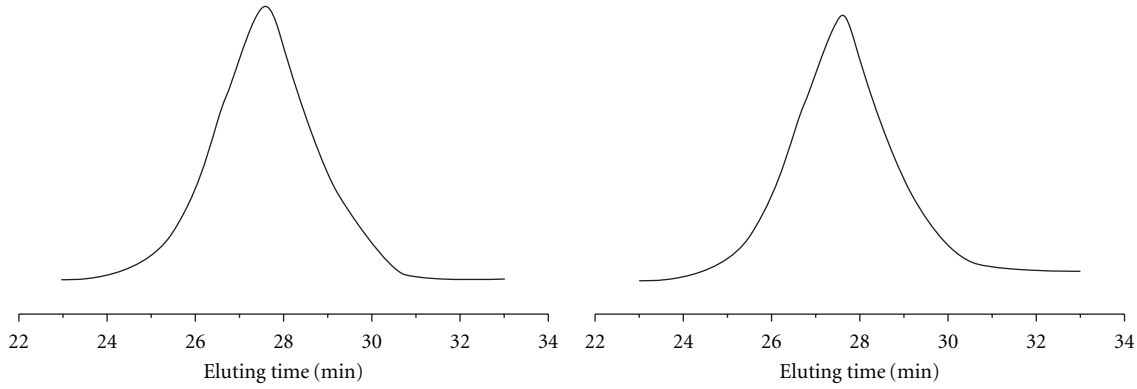

Figure 4: GPC curves of BocNH-PLLA (a) and NH_2-PLLA (b).

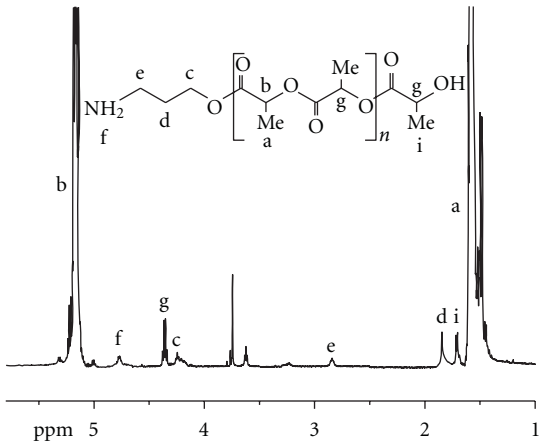

Figure 5: ^{1}H NMR spectra of NH_2-PLLA in $CDCl_3$.

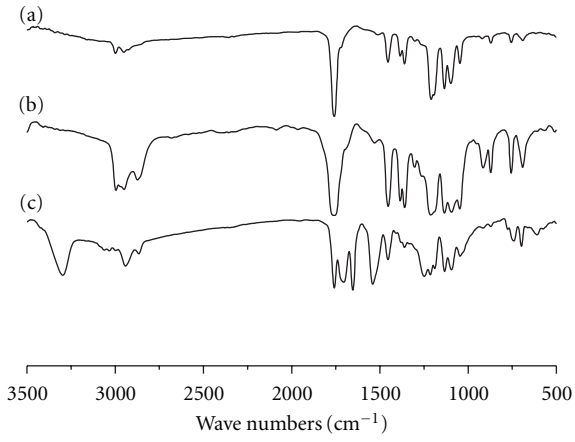

Figure 6: FT-IR spectra of BocNH-PLLA (a), NH_2-PLLA (b), and PLLA-*b*-PZLys (c).

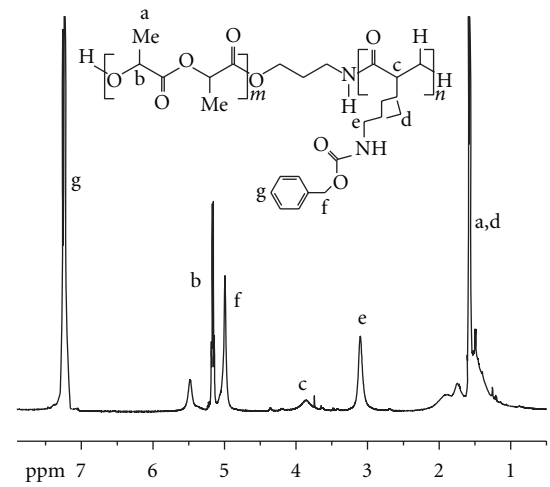

Figure 7: ^{1}H NMR spectra of the block copolymer of PLLA-*b*-PZLys.

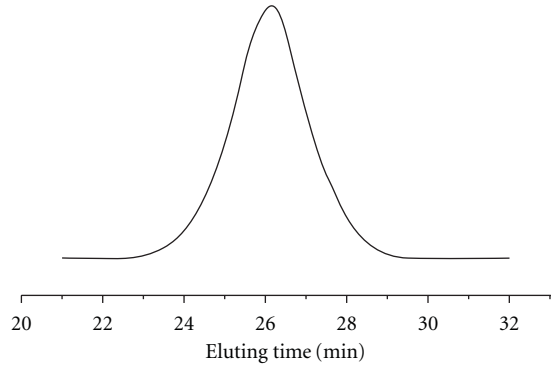

Figure 8: GPC trace of the block copolymer of PLLA-*b*-PZLys.

Boc group under this temperature in 12 h with high yields in recovered polymer between 85% and 98%. In this study, the polymerization of L-LA was carried out under rigorously anhydrous conditions to avoid any initiation of water, which will lead to a mixture of carboxyl acid terminated PLLA and BocNH-PLLA. The degree of polymerization of BocNH-PLLA was found to be easily controlled by changing the feed molar ratio of L-LA to tert-butyl-*N*-(3-hydroxypropyl) carbamate. The characteristics of the synthesized polymers are reported in Table 1.

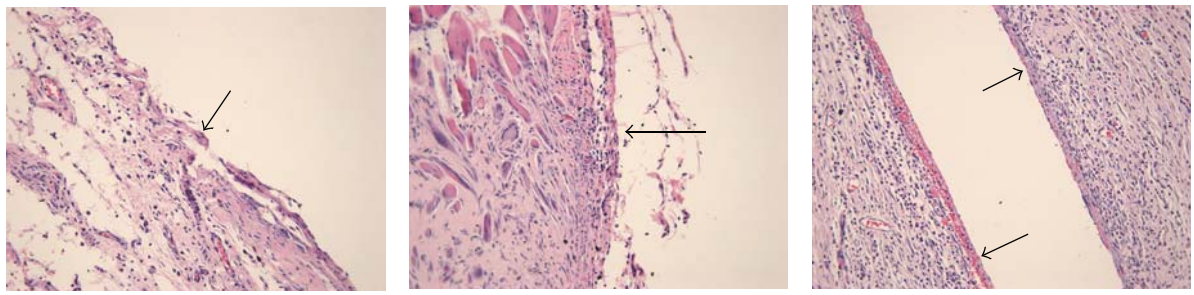

Figure 9: *In vivo* biocompatibility of the polymer films (interface surfaces are denoted by arrows).

Table 1: Molecular weight characterization of BocNH-PLLA homopolymers.

Sample	M_0/I_0 (mol)	Mn[a]	Mn[b]	Mn[c]	PDI	Mn[d]	Mn[b]/Mn[d]
$PLLA_{10}$	10	1440	1544	2680	1.21	1527	1.01
$PLLA_{25}$	25	3600	3487	6423	1.24	3661	0.95
$PLLA_{50}$	50	7200	7663	13848	1.52	7893	0.97
$PLLA_{100}$	100	14400	15295	28657	1.48	16334	0.94
$PLLA_{150}$	150	21600	22927	39569	1.46	22554	1.02
$PLLA_{200}$	200	28000	33295	55436	1.61	31599	1.05

[a]Calculated from the free ratio. [b]Calculated from the ^{1}H NMR (see Figure 2). [c]Obtained from GPC based on the PS calibration. [d]Corrected GPC result, $Mn^c \times 0.57$.

The functionality of the end group of the polymer was determined by comparing the molecular weight obtained from GPC and that determined by ^{1}H NMR [6] using the signals of a, c, or e attributed to the end group and that of lactide units g or f (Figure 3). In all cases, the functionality was found close to 1, which means that all polymer chains were capped with BocNH groups. The GPC trace of the resulted polymer (Figure 4(a)) is a single peak, and the molecular weight distribution of the product is narrow, showing that only one type of polymer corresponding to the expecting end group.

The next step removal of the Boc group of the terminal residue from the obtained polymer was realized by treatment in the mixed solvent of TFA and CH_2Cl_2 at room temperature for 1 hour. This reaction deprotected all primary amine functions at the end of the polymer, without lowering the molecular weight, as shown by the GPC trace (Figure 4(b)). This was also confirmed by ^{1}H NMR (Figure 5) with the complete disappearance of methyl peak at 1.43 ppm corresponding to the terminal Boc group. The signal of $–CH_2–N$ shifted from 3.16 to 2.75 ppm. The ratio between this peak and that of lactide units (a and b) remained also constant after the deprotection, showing the degree of polymerization not changed.

3.3. Block Copolymerization. It is well known that primary amines, being more nucleophilic than basic, can be used to initiate the ROP of NCAs to prepare polypeptide containing block copolymers. Among all polypeptides, poly (L-lysine) (PLL) is unique due to its hydrophilicity and functional side NH_2 groups which can help to improve the affinity to proteins and cells, or to ionically combine with drugs, antibodies or DNAs, and thus may lead to breakthrough in fields of targeting drug delivery and gene delivery [26, 27]. Therefore, in order to test the reactivity of the amine-terminated polymer prepared above, NH_2-PLLA was used as a macroinitiator for the ROP of lys (Z)-NCA. FT-IR spectra of BocNH-PLLA, NH_2-PLLA, and PLLA-*b*-PZLys were illustrated in Figure 6. The absorption at 1758 cm^{-1} belong to the carbonyl group, 1951 cm^{-1} to methyl, and 1046 and 1098 cm^{-1} to C–O–C bond. In the spectrum of the block copolymer, two amide I bands at 1653 cm^{-1} and 1704 cm^{-1} were observed, most likely for the main chain amide linkage and the side amide group, respectively. The amide II band was also observed at 1540 cm^{-1}.

Figure 7 illustrates the ^{1}H NMR spectra of the block copolymer. Besides the signals of PLLA, new peaks at about 7.23, 4.96, 3.85, and 3.03 ppm corresponding to the lysine residue appeared. From the integral ratio of lactide unit to lysine unit, the average degree of polymerization (DP) of the polypeptide block can be easily calculated to be 21 and 53, which is very close to the feed molar ratio of NCA monomer to the macroinitiator, confirming the high initiation reactivity of NH_2-PLLA. The GPC trace of the resulting copolymer (Figure 8) showed a unimodal shape. This further indicated complete amine-end-capping of PLLA, and the copolymerization was completed successfully, and there was no homopolymer in the copolymer.

3.4. In Vivo Tissue Responses. The *in vivo* biocompatibility of Boc-PLLA, NH_2-PLLA, and PLLA-*b*-PZLys was evaluated via implantation of the polymer films in rats (Figure 9).

The polymeric implants and surrounding tissues were collected at day 28. Despite the difference in molecular weight and structures, there was no significant difference in inflammatory reactions between the polymers as assessed by fibrotic band thickness and lymphocytes infiltration, as shown in Figure 9. The three polymer films caused same fibrotic band thickness and the surrounding tissues showed an abundant perivascular infiltration of lymphocytes, which was most probably caused by the degradation of the polymer films.

4. Conclusion

Compared to the methods that have been published, a novel, very simple, and highly efficient approach for the synthesis of amine-terminated polylactide (may also be used for other kinds of polylactones and polylactides) with various chain lengths based on tert-butyl-*N*-(3-hydroxypropyl) carbamate initiated bulk ring-opening polymerization has been developed and shown to be successful. The deprotection of the Boc group can be easily carried out under mild condition without breaking up of the polymer chain. This method was confirmed not only suitable for the preparation of low molecular weight NH_2-PLLA, but also quite efficient in the synthesis of high molecular weight samples.

Acknowledgment

The authors would like to thank the National Basic Research Program of China (no. 81000105) for the financial support to this work.

References

[1] T. Ouchi, T. Uchida, H. Arimura, and Y. Ohya, "Synthesis of poly(L-lactide) end-capped with lactose residue," *Biomacromolecules*, vol. 4, no. 3, pp. 477–480, 2003.

[2] F.-Z. Lu, X.-Y. Xiong, Z.-C. Li, F.-S. Du, B.-Y. Zhang, and F.-M. Li, "A convenient method for the synthesis of amine-terminated poly(ethylene oxide) and poly(ε-caprolactone)," *Bioconjugate Chemistry*, vol. 13, no. 5, pp. 1159–1162, 2002.

[3] P.-R. Ashton, S.-E. Boyd, C.-L. Brown et al., "Synthesis of glycodendrimers by modification of poly(propylene imine) dendrimers," *Chemistry*, vol. 3, no. 6, pp. 974–984, 1997.

[4] P. Degee, P. Dubois, R. Jerome, and P. Teyssie, "Macromolecular engineering of polylactones and polylactides. 9. Synthesis, characterization, and application of ω-primary amine poly (ε-caprolactone)," *Macromolecules*, vol. 25, no. 17, pp. 4242–4248, 1992.

[5] M. Gotsche, H. Keul, and H. Höcke, "Amino-termined poly (L-lactide)s as initiators for the polymerization of N-carboxyanhydrides: synthesis of poly(L-lactide)-block-poly(α-amino acid)s," *Macromolecular Chemistry and Physics*, vol. 196, no. 12, pp. 3891–3903, 1995.

[6] S. Caillol, S. Lecommandoux, A.-F. Mingotaud et al., "Synthesis and self-assembly properties of peptide-polylactide block copolymers," *Macromolecules*, vol. 36, no. 4, pp. 1118–1124, 2003.

[7] N. Kang and J.-C. Leroux, "Triblock and star-block copolymers of *N*-(2-hydroxypropyl)methacrylamide or *N*-vinyl-2-pyrrolidone and d,l-lactide: synthesis and self-assembling properties in water," *Polymer*, vol. 45, no. 26, pp. 8967–8980, 2004.

[8] Y. F. Fan, G. Chen, J. Tanaka, and T. Tateishi, "L-Phe end-capped poly(L-lactide) as macroinitiator for the synthesis of poly(L-lactide)-b-poly(L-lysine) block copolymer," *Biomacromolecules*, vol. 6, no. 6, pp. 3051–3056, 2005.

[9] M.-L Yuan and X.-M Deng, "Synthesis and characterization of poly(ethylene glycol)-block-poly(amino acid) copolymer," *European Polymer Journal*, vol. 37, no. 9, pp. 1907–1912, 2001.

[10] Z.-G Yang, J. Yuan, and S.-Y Cheng, "Self-assembling of biocompatible BAB amphiphilic triblock copolymers PLL(Z)-PEG-PLL(Z) in aqueous medium," *European Polymer Journal*, vol. 41, no. 2, pp. 267–274, 2005.

[11] H.-Y. Tian, C. Deng, H. Lin et al., "Biodegradable cationic PEG-PEI-PBLG hyperbranched block copolymer: synthesis and micelle characterization," *Biomaterials*, vol. 26, no. 20, pp. 4209–4217, 2005.

[12] C. Deng, H. Tian, P. Zhang, J. Sun, X.-S. Chen, and X.-B. Jing, "Synthesis and characterization of RGD peptide grafted poly(ethylene glycol)-*b*-poly(L-lactide)-*b*-poly(L-glutamic acid) triblock copolymer," *Biomacromolecules*, vol. 7, no. 2, pp. 590–596, 2006.

[13] C. Deng, X. Chen, H. Yu, J. Sun, T. Lu, and X. Jing, "A biodegradable triblock copolymer poly(ethylene glycol)-*b*-poly(l-lactide)-*b*-poly(l-lysine): synthesis, self-assembly, and RGD peptide modification," *Polymer*, vol. 48, no. 1, pp. 139–149, 2007.

[14] J. Rao, Z. Luo, Z. Ge, H. Liu, and S. Liu, "'Schizophrenic' micellization associated with coil-to-helix transitions based on polypeptide hybrid double hydrophilic rod-coil diblock copolymer," *Biomacromolecules*, vol. 8, no. 12, pp. 3871–3878, 2007.

[15] D.-K. Gilding and A. M. Reed, "Biodegradable polymers for use in surgery-poly(ethylene oxide) poly(ethylene terephthalate) (PEO/PET) copolymers: 1," *Polymer*, vol. 20, no. 12, pp. 1454–1458, 1979.

[16] D.-W. Grijpma, G.-J. Zondervan, and A.-J. Pennings, "High molecular weight copolymers of L-lactide and ε-caprolactone as biodegradable elastomeric implant materials," *Polymer Bulletin*, vol. 25, no. 3, pp. 327–333, 1991.

[17] H.-R. Kricheldorf and J. Meier-Haack, "Polylactones, 22 ABA triblock copolymers of L-lactide and poly (ethylene glycol)," *Macromolecular Chemistry and Physics*, vol. 194, no. 2, pp. 715–725, 1993.

[18] A.-C. Albertsson and M. Gruvegård, "Degradable high-molecular-weight random copolymers, based on ε-caprolactone and 1,5-dioxepan-2-one, with non-crystallizable units inserted in the crystalline structure," *Polymer*, vol. 36, no. 5, pp. 1009–1016, 1995.

[19] Y.-J. Du, P.-J. Lemstra, A.-J. Nijenhuis, A.-M. Van Aert, and C. Bastiaansen, "ABA type copolymers of lactide with poly(ethylene glycol). Kinetic, mechanistic, and model studies," *Macromolecules*, vol. 28, no. 7, pp. 2124–2132, 1995.

[20] A. Schindler, Y.-M. Hibionada, and C.-G. Pitt, "Aliphatic polyesters. III. Molecular weight and molecular weight distribution in alcohol-initiated polymerizations of ε-caprolactone," *Journal of polymer science: Part A*, vol. 20, no. 2, pp. 319–326, 1982.

[21] X.-C. Zhang, D.-A. Macdonald, M.-F.-A. Goosen, and K.-B. Mcauley, "Mechanism of lactide polymerization in the presence of stannous octoate: the effect of hydroxy and carboxylic acid substances," *Journal of Polymer Science: Part A*, vol. 32, no. 15, pp. 2965–2970, 1994.

[22] A.-J. Nijenhuis, D.-W. Grijpma, and A.-J. Pennings, "Lewis acid catalyzed polymerization of L-lactide. Kinetics and mechanism of the bulk polymerization," *Macromolecules*, vol. 25, no. 24, pp. 6419–6424, 1992.

[23] M. Ryner, K. Stridsberg, A.-C. Albertsson, H. Von Schenck, and M. Svensson, "Mechanism of ring-opening polymerization of 1,5-dioxepan-2-one and L-lactide with stannous 2-ethylhexanoate. A theoretical study," *Macromolecules*, vol. 34, no. 12, pp. 3877–3881, 2001.

[24] A. Kowalski, A. Duda, and S. Penczek, "Mechanism of cyclic ester polymerization initiated with tin(II) octoate. 2. 1 macromolecules fitted with tin(II) alkoxide species observed directly in MALDI-TOF spectra," *Macromolecules*, vol. 33, no. 3, pp. 689–695, 2000.

[25] D. S. Porche, M. Moore, and J. L. Bowles, "An unconventional method for the prepration of NCAs," *Synthetic Communications*, vol. 29, pp. 843–852, 1999.

[26] Y. Kakizawa, A. Harada, and K. Kataoka, "Glutathione-sensitive stabilization of block copolymer micelles composed of antisense DNA and thiolated poly(ethylene glycol)-block-poly(L-lysine): a potential carrier for systemic delivery of antisense DNA," *Biomacromolecules*, vol. 2, no. 2, pp. 491–497, 2001.

[27] S. Park and K. E. Healy, "Nanoparticulate DNA packaging using terpolymers of poly (lysine-g-(lactide-*b*-ethylene glycol))," *Bioconjugate Chemistry*, vol. 14, no. 2, pp. 311–319, 2003.

Hindawi Publishing Corporation
International Journal of Polymer Science
Volume 2011, Article ID 473045, 9 pages
doi:10.1155/2011/473045

Research Article

Application of Polyethylene Glycol to Promote Cellular Biocompatibility of Polyhydroxybutyrate Films

Rodman T. H. Chan,[1] Helder Marçal,[1] Robert A. Russell,[1,2] Peter J. Holden,[2] and L. John R. Foster[1]

[1] *Bio/Polymer Research Group, Centre for Advanced Macromolecular Design, School of Biotechnology and Biomolecular Science, University of New South Wales, Sydney, NSW 2052, Australia*
[2] *Australian Nuclear Science & Technology Organisation, Lucas Heights, Sydney, NSW 2234, Australia*

Correspondence should be addressed to L. John R. Foster, j.foster@unsw.edu.au

Received 1 July 2011; Accepted 22 August 2011

Academic Editor: Shanfeng Wang

Polyhydroxybutyrate (PHB) is a biomaterial with potential for applications in biomedical and tissue engineering; however, its brittle nature and high crystallinity limit its potential. Blending PHB with a variety of PEGs produced natural-synthetic composite films composed of FDA-approved polymers with significant reductions in crystallinity, from 70.1% for PHB films to 41.5% for its composite with a 30% (w/w) loading of PEG2000. Blending also enabled manipulation of the material properties, increasing film flexibility with an extension to break of 2.49 ± 1.01% for PHB films and 8.32 ± 1.06% for films containing 30% (w/w) PEG106. Significant changes in the film surface properties, as measured by porosity, contact angles, and water uptake, were also determined as a consequence of the blending process, and these supported greater adhesion and proliferation of neural-associated olfactory ensheathing cells (OECs). A growth rate of 7.2×10^5 cells per day for PHB films with 30% (w/w) PEG2000 loading compared to 2.5×10^5 for PHB films was observed. Furthermore, while cytotoxicity of the films as measured by lactate dehydrogenase release was unaffected, biocompatibility, as measured by mitochondrial activity, was found to increase. It is anticipated that fine control of PEG composition in PHB-based composite biomaterials can be utilised to support their applications in medicinal and tissue engineering applications.

1. Introduction

Polyhydroxybutyrate (PHB, Figure 1(a)) is a semicrystalline biopolymer produced by a wide variety of bacteria when subjected to conditions of essential nutrient limitation with excess carbon [1, 2]. The monomer component of microbial PHB, 3-hydroxybutyric acid (HBA), is recognised by mammalian enzymes; mammalian HBA is one of three ketone bodies and an essential source of mobile carbon for sufferers of starvation and diabetes mellitus [3]. Furthermore, the use of microbial HBA in mammals does not trigger any cytotoxic response [4]. First commercialised by W. R. Grace and Co. in the early 1950s, microbially produced PHB is an FDA- (Food and Drug Administration, USA) approved biomaterial investigated for application in a variety of medical devices [5, 6]. For example, microbial PHB has been used as a nerve conduit to fill a 10 mm gap in injured sciatic nerve of Spague-Dawley rats and did not trigger any immune and inflammatory responses or cause anastomotic failures [7].

While PHB has a thermoplastic capability and a tensile strength comparable to polypropylene, its comparatively high crystallinity results in a brittle nature and relatively long degradation time under physiological conditions [7, 8]. However, blending PHB with various additives provides a relatively simple and cost-effective opportunity to manipulate properties of PHB-based biomaterials [9].

PEG (Figure 1(b)) is an ideal candidate for blending with PHB, a flexible polymer with good solubility in both water and organic solvents; it is used in protein purification processes, as well as a drug carrier and various other pharmaceutical applications [10, 11]. A range of PEGs can be synthesised with average molecular weights (Mn) from 106

(diethylene glycol, DEG) to 20,000. Also FDA-approved PEG is biocompatible with both blood and tissue, nontoxic to cellular system, nonimmunogenic, and an excellent conjugate for polymer graft materials [12, 13].

Blending PHB with polyethylene glycol (PEG) reduces crystallinity and other physiochemical properties of the composite biomaterial [11, 14]. Tan et al. reported that PEG polymer chains remained mobile when PHB underwent crystallisation and moved to intra- and interspherulitic regions [15]. Thus, the presence of PEG in blends reduced the PHB crystallisation rate which promoted the formation of smaller spherulites and hindered nucleation; as a result, the PHB/PEG films became more flexible in comparison with their PHB counterparts. Zhang et al. reported that the crystallinity of PHB-based films decreased while their toughness was improved as the loading of PEG-20,000 increased from 10 to 20% (w/w) [16]. Similarly, Rodrigues et al. demonstrated that PHB is completely miscible with PEG-300 and the crystallinity was decreased as the PEG content increased in blends [17].

While there are a number of studies reporting blends of PHB with various PEGs, their focus has been on changes in crystallisation behaviour and subsequent physiochemical and material properties. In addition to blending, chemical grafting of PEG (PEGylation) to PHB and other members of the polyhydroxyalkanoate (PHA) family has also been investigated [18, 19]. However, PEGylation reduces the molecular mass of the biopolymer to an extent where solubilisation may readily occur. More recently Foster and coworkers have shown that PEG-modulated biological synthesis of PHAs results in "endcapping" of the hydrophobic PHA chains with hydrophilic PEG molecules (bioPEGylation) [20]. While physiochemical and material changes due to bioPEGylation are comparatively minor, the presence of the covalently bound PEG groups promoted cell cycle progression in satellite stem cells [21]. In contrast to bioPEGylation, blending is a more simple process and provides greater flexibility in the loading and type of PEG that can be added. In the study here, we report on the influence of PEG loading and molecular mass on the physiochemical and material properties of PHB/PEG composite biomaterials. Furthermore, we report, for the first time, the influence that different PEG molecular weights and loadings has on cell adhesion and proliferation to PHB/PEG biomaterial films.

2. Experimental

2.1. Reagents. Polyhydroxybutyrate (PHB) of natural origin, polyethylene glycol (PEG) (molecular weights of 106, diethylene glycol (DEG) and 2000), and trypsin were purchased from Sigma Aldrich (Sydney, Australia). Analytical grade chloroform and dimethyl sulfoxide (DMSO) were purchased from Univar (Seven Hills, Australia). Mammalian cell growth medium, fetal bovine serum (FBS), and penicillin/streptococcus antibiotic were obtained from Gibco-Invitrogen (Sydney, Australia). OECs were routinely cultured in Dulbecco's Modified Eagle's Medium (DMEM/F12) supplemented with 10% FBS purchased from Lonza

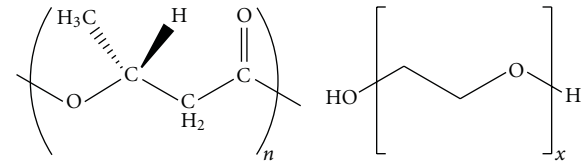

(a) (b)

Figure 1: Chemical formulae for biomacromolecules (a) poly(3-hydroxybutyrate): (PHB) and (b) poly(ethylene glycol): (PEG).

Table 1: Nomenclature of biomaterial films prepared in this study.

Sample	Loading (% w/w)		
	PHB	PEG106	PEG2000
PHB	100	0	0
PHB/PEG106-10	90	10	0
PHB/PEG106-20	80	20	0
PHB/PEG106-30	70	30	0
PHB/PEG2000-10	90	0	10
PHB/PEG2000-20	80	0	20
PHB/PEG2000-30	70	0	30

(Portsmouth, NH, USA). CellTiter 96 aqueous one solution cell proliferation assay and in vitro lactic dehydrogenase-based toxicology kit were purchased from Promega (Madison, WI, USA) and Sigma Aldrich, respectively.

2.2. Film Fabrication. Biopolymer films were produced by solvent casting technique as described in the study by Rodrigues et al. [17]. Powdered PHB and PEG samples with respective weight ratios of 100 : 0, 90 : 10, 80 : 20, and 70 : 30 (w/w) were dissolved in heated chloroform in a sterile sealed vessel (2% w/v, 160 rpm, 50°C). The solution was allowed to cool (22°C, 160 rpm, 15 mins) before pouring into sterile, glass Petri dishes, and the solvent evaporated by standing (12 hours, 22°C). The resulting films, labelled as per Table 1, were subsequently maintained at 40°C under vacuum for 48 hours to remove any solvent residues.

2.3. Material Characterisation. Material properties of biopolymer films were analysed using a tensile testing instrument (Instron-5543, Norwood, MA, USA) at 22°C with 30% relative humidity. Films samples (30 × 15 mm) were fixed using pneumatic grips of a calibrated tensile testing instrument and slowly moved apart (20 mm min^{-1}). The maximum load, tensile strength, and extension at break were calculated using Bluehill computer software (Norwood, MA, USA). Means from at least ten samples were determined ($n = 10$).

The porosity of the biopolymer films were measured by ethanol displacement method [22]. The samples were cut into 50 × 10 mm sizes and immersed in a measuring cylinder with a known volume of ethanol (V_1). The total volume of ethanol and the films (V_2) was recorded after 5 mins of immersion. The ethanol-impregnated film was removed, and the remaining ethanol volume was recorded (V_3). Means of

five samples were determined ($n = 5$). The porosity of the film was calculated by following formula:

$$\text{Porosity } (\%) = \frac{(V_1 - V_3)}{V_2 - V_3} \times 100\%. \quad (1)$$

X-ray diffraction patterns of the biopolymer films were acquired using a Philips X'pert Material Research Diffraction (MRD) System (Eindhoven, Netherlands). Film samples (20 × 20 mm) were secured on glass slides and aligned with 2θ, z-axis, and omega scans (scattering angle range of $2\theta = 10-30^\circ$ and scan step size of 0.02° continuous scan type). A radiation wavelength of 1.5406 Å (Cu K-Alpha) was used to generate a power of 45 kV and tube current of 40 mA. The crystallinity (Xc) was calculated with the following equation and carried out using X'pert Highplus software and Excel software:

$$\text{Crystallinity } (\%) = \left[\frac{Fc}{Fc + Fa}\right] \times 100\%, \quad (2)$$

where Fc and Fa are the areas of crystal (peak) and non-crystal regions (under the curve), respectively.

Water uptake (WU) by the films was measured using gravimetry before and after water immersion [23]. The biopolymer films were cut into 40 × 10 mm sizes and 20 μm thickness, weighed, and immersed into RO water at 37°C for 50 mins (W_1). The hydrated film was removed and weighed after drying the surface water with Kimwipes (Ringwood, Australia) (W_2). The water uptake was calculated by the following formula:

$$\text{WU } (\%) = \frac{(W_2 - W_1)}{W_1} \times 100\%, \quad (3)$$

where WU is the percentage of water uptake, W_1 and W_2 were the weight of sample film before and after immersion. Means of five samples were determined ($n = 5$).

The contact angle was measured by sessile drop method using contact angle meter at room temperature (22°C, rH 30%) to examine the hydrophilicity of polymer surface (KSV Cam 200, Espoo, Finland) [24]. Biopolymer films were cut into 40 × 30 mm and microsyringed water droplets slowly allowed to fall onto their surfaces. Contact angles between the water droplet and the biopolymer films were recorded using KSV instrument software. Means of ten readings were calculated for each sample ($n = 10$).

2.4. Degradation Studies. Preweighed samples of biopolymer films (30 × 15 mm) samples were sterilised through gamma-irradiation and placed into Eppendorf tubes (2 mL). Samples were incubated (37°C, 150 rpm) following the addition of 2 mL phosphate-buffered saline (0.1 M, pH 7.4) with penicillin (100 units mL^{-1}), streptomycin (100 μg mL^{-1}), and fungizone-amphotericin B (2.5 μg mL^{-1}). At periodic intervals over an 84-day timescale, samples were removed, filtered, and dried in a dessicator (40°C, 24 h) before allowing to acclimatise at 22°C (atmospherically equilibrated weight). The weight loss of the films was calculated with weight loss (%), defined by (3):

$$W\ (\%) = \frac{W_t}{W_0} \times 100\%, \quad (4)$$

where W is the percentage weight loss, W_0 and W_t were the initial weight and weight after incubation. Means of four samples per time point, per sample were determined ($n = 4$) [25].

2.5. Cell Studies. Murine olfactory ensheathing cells (OECs) were cultivated in medium consisting of DMEM, 10% FBS, 250 unit penicillin, 250 μg mL^{-1} streptomycin, and 1 μg mL^{-1} and fungizone-amphotericin B in T-75 tissue culture flasks incubated at 37°C with 5% CO_2 [26]. OECs were removed from the flask using trypsin (2.5%) at 70% confluence. A cell population of approximately 4×10^4 cells mL^{-1} was used to inoculate films samples (13 × 13 mm). At periodic intervals over a 10-day timescale, samples were sacrificed and the films were twice rinsed with 10 mL of PBS; 2 mL of trypsin (2.5%) was subsequently added before incubation (37°C, 2 mins). Cell viability was then calculated using a haemocytometer and the trypan blue exclusion technique. Samples were conducted in triplicate ($n = 3$). Cell proliferation was also observed under a light microscope (Leica DFC 280, London, UK).

2.6. Microscopy. Film samples that had been cultivated with OECs were rinsed twice with 1% phosphate buffer saline (PBS) and fixed for four hours at 22°C in 2.5% glutaraldehyde in 0.1 M PBS buffer (pH 7.2). Subsequently, films were washed with PBS buffer three times for 5-minute duration. After another buffer wash, samples were dehydrated for 10 minutes in a series of ethanol washes (30, 50, 70, 80, 90, 95, and 100%) and critical point dried using liquid carbon dioxide. All specimens were mounted on aluminium stubs and surface coated with a layer of gold particles using a sputter coater (Emitech K550x, Ashford, England). Samples were subsequently examined using scanning electron microscopy (Hitachi S3400-I, Tokyo, Japan) at 15 kV and 750 mA, a procedure adapted from Chung et al. [27].

2.7. MTS Assay. Mitochondrial function in the OEC populations were assessed using a CellTiter 96 aqueous one solution cell proliferation assay [28]. OECs were cultured in DMEM with 10% FBS, harvested by trypsinisation, counted, and plated into 96-well plates with films of PHB, PHB/PEG106-20, PHB/PEG106-30, PHB/PEG2000-20, and PHB/PEG2000-30 (w/w). Cells cultivated in the absence of the biomaterials were used as control. 3000 cells were cultivated in each well and incubated for 48 hours (37°C with 5% CO_2); 30 μL of MTS (3-(4,5-dimethylthiazol-2-yl)-2,5-diphenyltetrazolium bromide) solution was then added to each well, and the plate incubated for a further 4 hours. MTS concentrations were determined at an absorbance of 490/690 nm using a microtitre plate spectrophotometer. A mean of 5 samples was determined ($n = 5$).

2.8. Lactate Dehydrogenase (LDH) Assay. LDH assays were used to detect cytotoxicity in the OECs population as a consequence of their incubation with PHB and PHB/PEG films [29]. Cells were cultured in DMEM with 10% FBS, harvested by trypsinisation, counted, and plated into 96-well

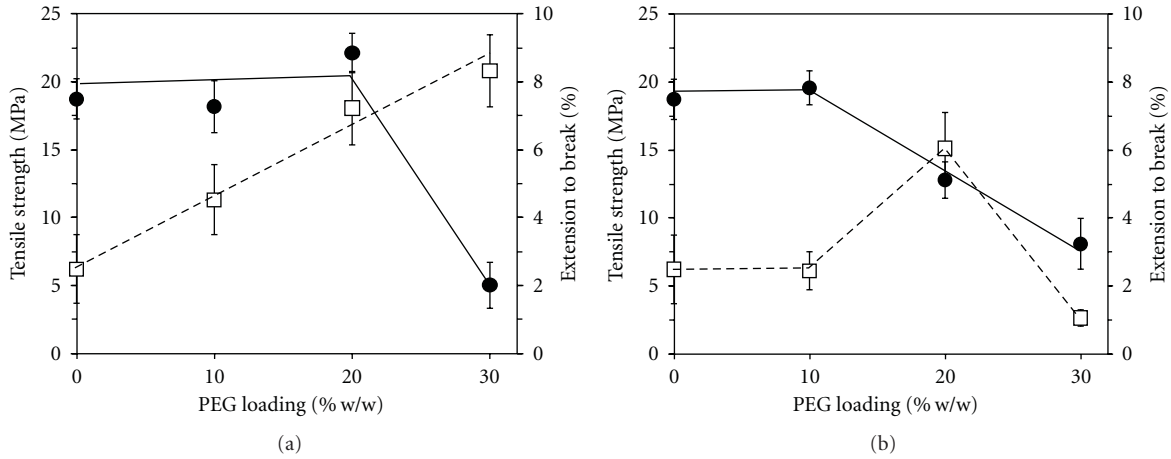

Figure 2: Change in material properties for PHB/PEG composite films with variations in PEG loading (% w/w), (a) PEG106 and (b) PEG2000; (•) tensile strength (MPa) and (□) extension to break (%).

plates with films of PHB, PHB/PEG106-20, PHB/PEG106-30, PHB/PEG2000-20, and PHB/PEG2000-30. Cells cultivated in the absence of the biomaterials were used as healthy controls. 3,000 cells were cultivated in each well and incubated for 48 hours (37°C, 5% CO_2). At 45 minutes prior to the endpoint, 10 μL samples of lysis solution were added to 5 of the wells and these served as positive controls. The plate was centrifuged for 5 minutes at 250 g at room temperature (22°C, rH 30%). 50 μL samples of the supernatants were then transferred to a sterile 96-well plate and 100 μL of LDH mixture added to each well before incubating in the dark for 30 minutes (37°C, 5% CO_2). LDH analysis was performed at absorbances of 490 and 650 nm using microtitre plate spectrophotometer. Means of 5 samples were determined ($n = 5$).

2.9. Statistical Analysis. Mean values for data were calculated with standard deviation of each group. A Student's t-test was performed for significance with 95% confidence.

3. Result and Discussion

3.1. PHB/PEG Film Characterisation. Blending is recognised as a cost-effective technique for the manipulation of material and physiochemical properties of polymeric biomaterials. In the study here, the material properties of the solvent cast PHB films were similar to previous reports, with a tensile strength of 19 ± 1.7 MPa and extension to break of 2.5 ± 1.8% [26]. While blending with up to 20% (w/w) PEG106 had no significant effect on the tensile strength of the PHB/PEG composite films, a loading of 30% (w/w) (PHB/PEG106-30) significantly reduced the strength to 5.2 ± 1.9 MPa (Figure 2(a), $P > 0.005$). In contrast, the extension to break of the PHB/PEG106 films increased linearly to 8.3 ± 1.1% with a 30% (w/w) loading. As the molecular mass of the PEG was increased, the reduction in tensile strength PHB was observed after 10% (w/w) PEG loading with a linear loss to 8.2 ± 2.1 MPa for PHB/PEG2000-30 films (Figure 2(b)). In

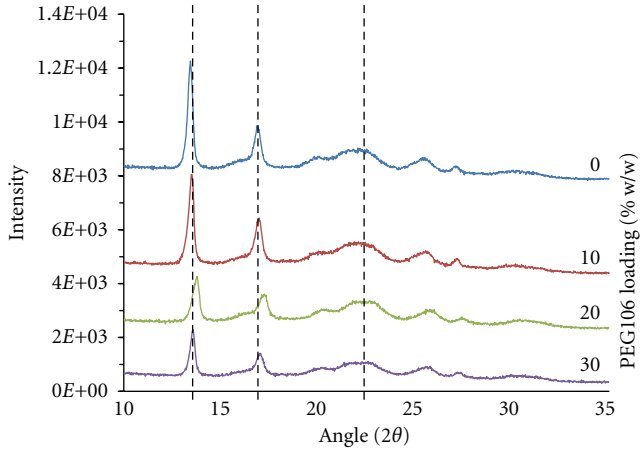

Figure 3: X-ray diffractograms of PHB/PEG composite films with variations in PEG106 loading (% w/w).

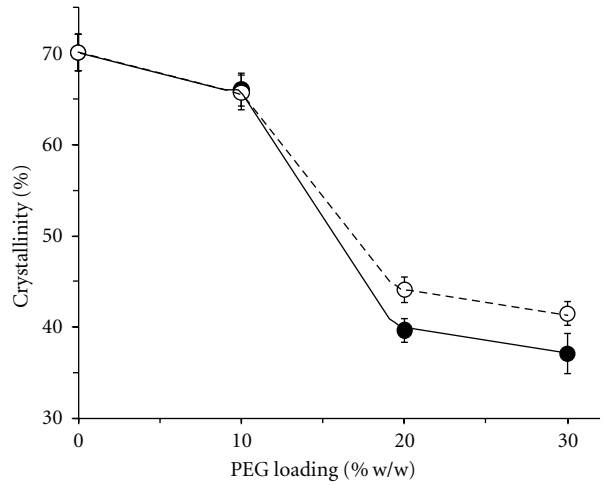

Figure 4: Change in crystallinity of PHB/PEG composite films with variations in PEG loading (% w/w); (•) PEG106 and (◦) PEG2000.

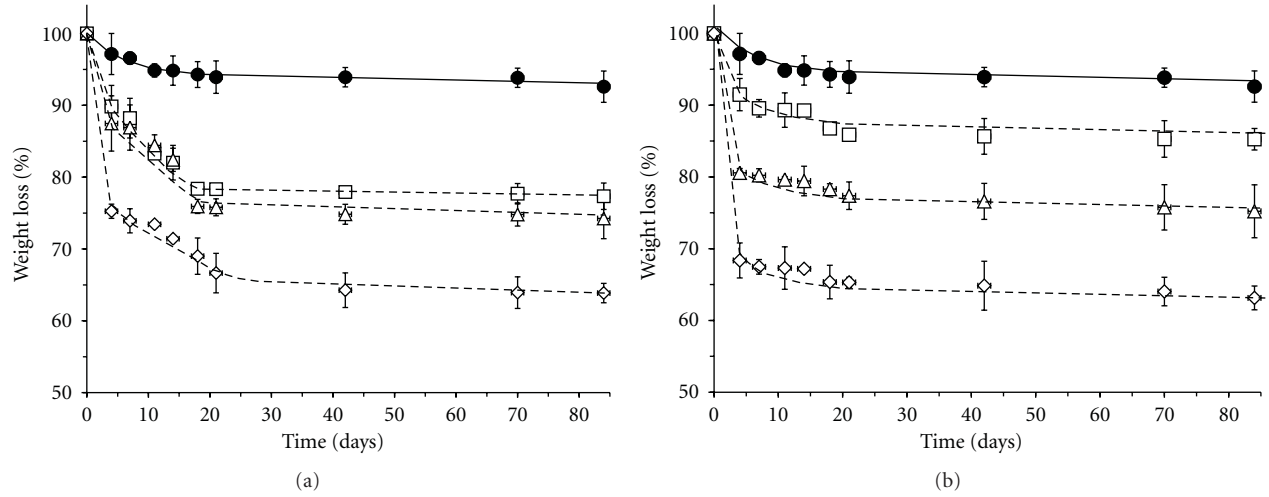

Figure 5: Change in weight loss profiles for PHB/PEG composite films with different PEG loadings (% w/w) when incubated under physiological conditions (37°C, pH 7.4, 120 rpm), (a) PEG106 and (b) PEG2000; (•) 0%—PHB, (□) 10%, (Δ) 20%, and (◇) 30%.

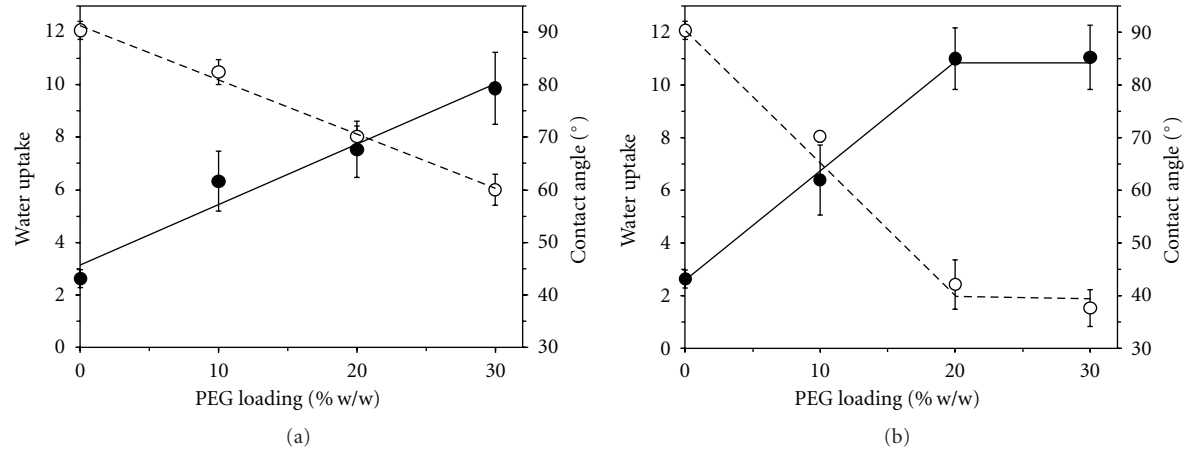

Figure 6: Change in water contact angles (•) and water uptakes (◦) for PHB/PEG composite films with different PEG loadings (% w/w), (a) PEG106 and (b) PEG2000.

contrast to the blends with PEG106, PHB/PEG2000-20 films showed an increase in flexibility but decreased again as the PEG loading increased to 30% (w/w). Thus, blending PHB with PEG generally increased the flexibility of the composite films when compared to the comparatively brittle PHB, with the changes being concentration dependent. The extension to break of both the PHB/PEG106-20 and PHB/PEG2000-20 films exhibited similar flexibilities to sutures fabricated from poly(tetrafluoroethylene) (PTFE), but was less flexible when compared to nylon and silk [30].

PHB is a semicrystalline biopolymer; the increases in extension to break of its composites with PEG suggest a change in crystallinity. X-ray diffraction patterns and maxima, observed at 14°, 17°, and 22° for PHB and PHB/PEG106 composite films, were found to be consistent with previous studies (Figure 3) [31]. As the PEG106 loading in the films increased, the intensity of the diffraction peaks was reduced (Figure 3). Similar X-ray diffraction patterns were also observed with the PHB/PEG2000 blends (data not shown). Consequently the crystallinity of the PHB/PEG films was observed to decrease from 70% for PHB films to approximately 45% for films blended with 30% (w/w) PEG106 and PEG2000, PHB/PEG106-30 and PHBPEG2000-30, respectively (Figure 4). The results suggest that the PHB crystal structure remained intact with separation of the crystalline PHB from amorphous PHB and DEG regions into semicrystalline matrices. Similar changes in PHB blends with cellulose acetate butyrate (CAB) are reported by Wang et al. [32].

It is known that PHB has a relatively slow degradation rate under physiological conditions and blending has been used to manipulate its degradation behaviour [33]. In the study here, PHB films showed little weight loss after 84 days of incubation under the physiological conditions (Figure 5). In contrast, films with ascending PEG loadings exhibited significant weight losses only after 10 days (Figure 5). However, Figure 5 clearly shows that the initial weight loss approximated the initial PEG loadings; these losses occurred within 20 days of incubation for PHB/PEG106 films and 10 days for

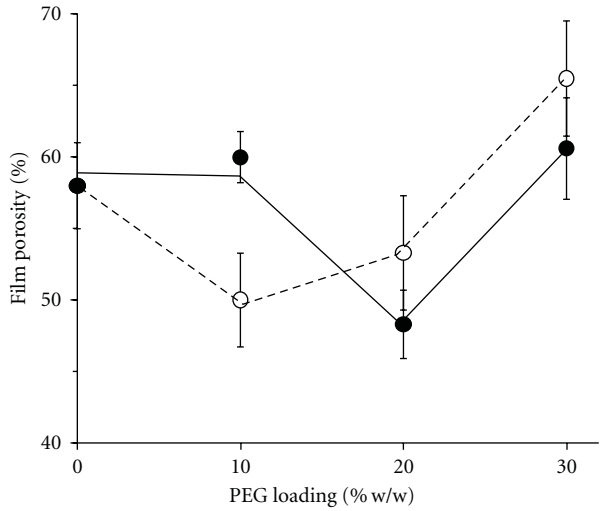

Figure 7: Change in porosity of PHB/PEG composite films with increasing PEG loading (% w/w), (∘) PEG106 and (•) PEG2000.

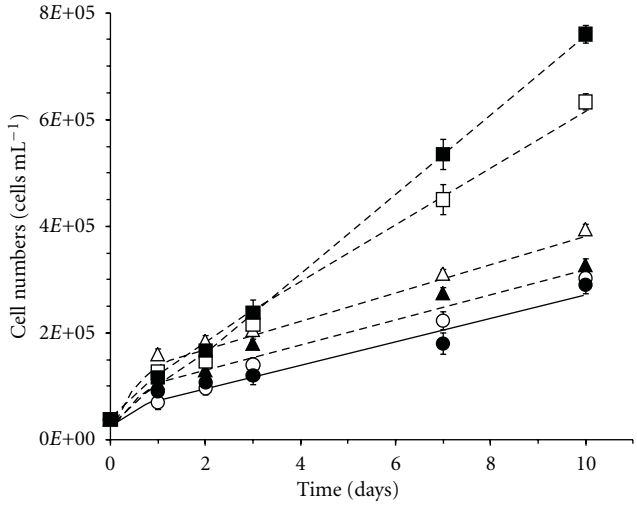

Figure 8: Change in growth of olfactory ensheathing cells (no. mL^{-1}) when cultivated on PHB/PEG composite films with different PEG loadings (% w/w); (∘) cell culture dish, (•) PHB film, PHB/PEG106 films with 20 (Δ) and 30 (▲) % w/w loadings, PHB/PEG2000 films with 20 (□) and 30 (■) % w/w loadings.

the PHB/PEG2000 films. Degradation of the residual films was negligible over the remaining duration of the study, consistent with the behaviour of PHB films (Figure 5) [34]. This initial dissolution of the relatively small, hydrophilic PEG groups from the hydrophobic PHB matrix is consistent with previous studies of PHB-pectin composites, where the relatively smaller pectin was solubilised and released from within PHB films [35]. Initial dissolution of the pectin was shown to subsequently promote weight loss of the remaining PHB film after a plateau period of apparent stability.

PHB is a hydrophobic biopolymer with films here exhibiting a water contact angle of 90.3 ± 1.7°; blending with PEG106 reduced the contact angles of the composites films in a linear fashion, with PHB/PEG106-30 possessing an angle of 60.0 ± 3.0° (Figure 6) [24]. Thus, blending PEG with PHB can improve the hydrophilicity of the films, and this was evident with an increase in water uptake, from 2.62 ± 0.34% for PHB to 9.86 ± 1.37% for PHB/PEG106-30 (Figure 6(a)). PEG of a higher molecular weight had a proportional greater influence on the hydrophilicity of the composite films, a linear decrease in water contact angle with increasing PEG2000 loading occurred to 20% loading before stabilising at approximately 39° (Figure 6(b)). Similarly, the water uptake increased to a maximum of 11.04 ± 1.22% for PHB/PEG2000-30. A number of studies have suggested that the hydrophilic-hydrophobic relationship on biomaterial surfaces to influence cellular adhesion and proliferation [36].

Consistent with previous reports, PHB films in this study had a porosity of 58 ± 3.0% [33]. Blending the PHB with PEG resulted in slight but significant changes to the porosity of the films, ranging from 48.3 ± 4.0% for PHB/PEG106-20 films to 65.5 ± 3.6% for PHB/PEG2000-30 films as illustrated in Figure 7. Saad et al. have shown that osteoblasts tend to attach and grow into the pores and grooves of a highly porous scaffold, suggesting that surface porosity had an important role in cell attachment [37]. Increases in porosity of the PHB-based biomaterials have also been shown to accelerate its physiological degradation rate [38]. Thus, surface properties reported to influence cell attachment could be adjusted in PHB films by blending with PEGs of different molecular weights and loadings.

3.2. Cellular Responses to the PHB/PEG Films. Consistent with changes to the composite surface properties, adult olfactory ensheathing cells (OECs) cultivated on the films showed significant changes in attachment and proliferation (Figure 8). The growth patterns of OECs on the polystyrene tissue culture plate (control) were similar to those of the PHB films with steady increases over a ten-day incubation period. Blending with PEG106 increased the initial cell attachment although their subsequent growth rates were similar to those cultivated on PHB. In contrast, blending with PEG2000 had a much greater influence, with PHB/PEG2000-30 exhibiting a growth rate of 7.2×10^5 cells mL^{-1} per day compared to 2.7×10^5 cells mL^{-1} dy^{-1} for PHB/PEG106-30 and 2.5×10^5 cells mL^{-1} dy^{-1} for PHB films (Figure 8). Thus, blending with PEG promoted the growth of OECs on the PHB-based composite films.

PEG, or its high molecular weight equivalent, polyethylene oxide (PEO), can be used to develop protein-repelling surfaces. Consequently, PEG has been incorporated onto biomaterial surfaces through grafting [39], adsorption surface treatments [40], and through bulk incorporation via crosslinking [41] or block copolymerization [42]. The design of most PEG-derivatized surfaces has sought to eliminate cell and protein adhesion using high PEG surface concentrations. However, Tziampazis et al. have suggested that the conformation of the adhered proteins can also play a crucial role in determining cell adhesion and proliferation and have used small surface concentrations of PEG to regulate cell adhesion and differentiation [42]. Furthermore, Zhang et al. have clearly shown that blending with PEG effectively improved

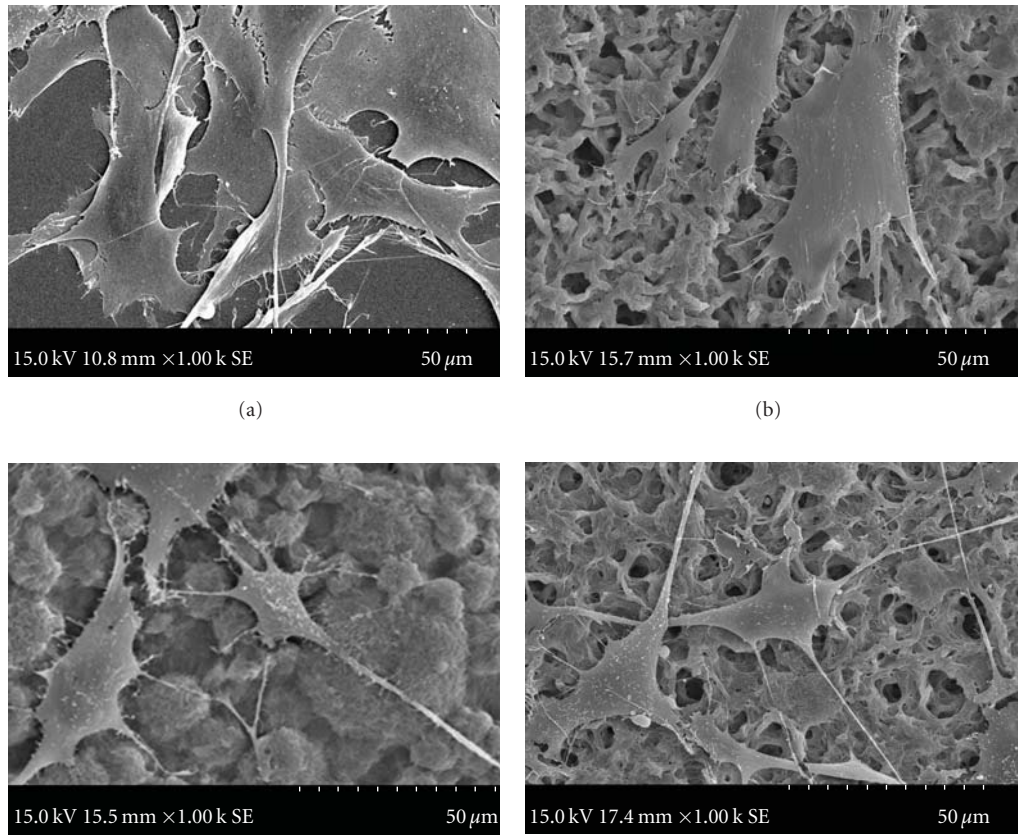

Figure 9: Scanning electron micrographs illustrating morphology of olfactory ensheathing cells attached to various surfaces after 24 hours of cultivation: (a) Polystyrene slide, (b) PHB film, (c) PHB/PEG106 with 20% w/w loading, and (d) PHB/PEG2000 with 20% w/w loading.

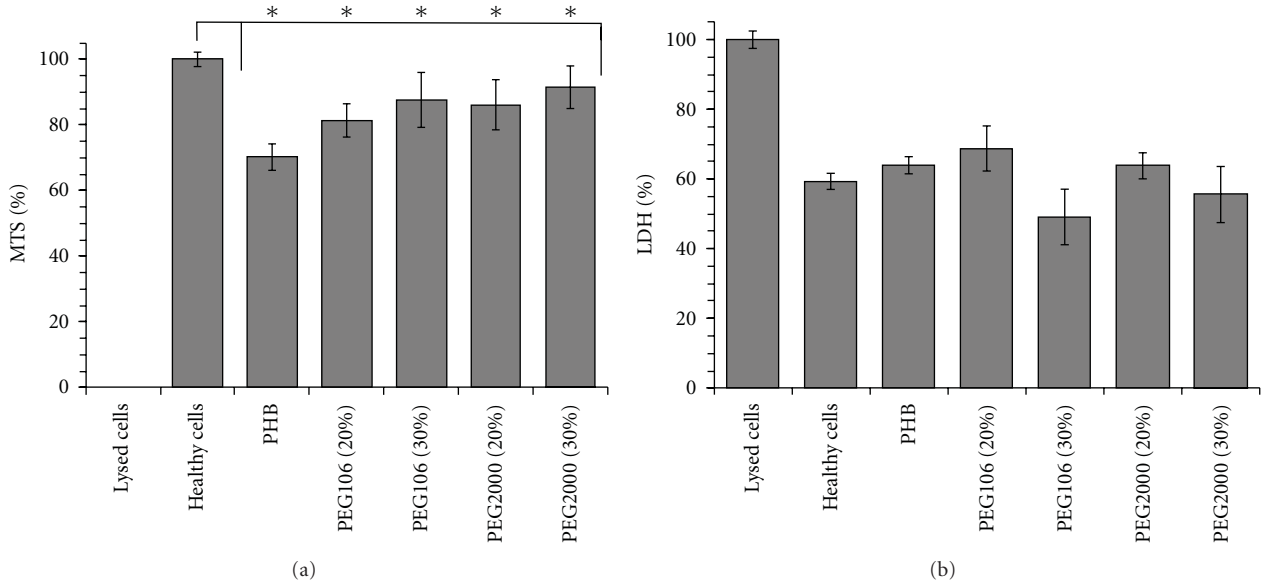

Figure 10: Changes in cellular activity relative to healthy cells, for olfactory ensheathing cells cultivated on PHB and PHB/PEG composite films: (a) MTS concentrations and (b) LDH release ($^*P > 0.005$ significance, $n = 10$).

the biocompatibility of chitosan films [43]. Thus, in the solvent evaporated PHB/PEG blends reported here, one can speculate that the bulk of the PEG was used to modify the material properties while small surface concentrations enhanced cell adhesion and proliferation.

Qualitative examination of OECs attached to the films showed revealed no abnormal cell morphology. The healthy cells appeared flat with many filopodial extensions (Figure 9). These filopodia play an important role in neuron regeneration, which is the first step in growth cone formation [44]. Ahmed et al. have also reported that the actin-containing filopodial extensions in OECs cultivated on PHB films provided cell mobility and greater cell-cell communication [45]. Over three days of incubation, OECs proliferated profusely consistent with the control (Figure 9).

The MTS assay measures the mitochondrial activity of the cells by reducing the substrate, yellow MTS tetrazolium salt into purple formazan compound and can be used as an indicator of cell viability [45]. In the study here, the percentages of MTS for cells cultivated on the PHB and PHB/PEG composite films were significantly different when compared to a control of healthy cells. Furthermore, OECs grown on the PHB/PEG composite films exhibited MTS levels closer to that exhibited by the control of healthy cells than the cells grown on PHB films ($P > 0.005$, Figure 10(a)). When under stress cell membranes exhibit increased permeability and a subsequent release of lactate dehydrogenase (LDH). LDH in the cultivation medium provides an indication of cellular cytotoxicity [28]. In the study here, the concentration of LDH released from cells cultivated on the PHB and PHB/PEG composite films was statistically similar to healthy cells ($P > 0.005$, Figure 10). The results suggest that none of the films investigated were cytotoxic; however, blending with PEG enhanced cell viability. Thus, the presence of PEG in the PHB films supported initial attachment of OECs and their subsequent proliferation despite the PEGs being released from the biopolymer matrices within the first 5 days of incubation.

4. Conclusions

The biopolymer PHB is an FDA-approved biomaterial; however, its relatively high crystallinity and brittle nature greatly reduce its potential for application in biomedical devices. Blending is a cost-effective and comparatively simple technique to modify the final properties of PHB-based composites. Blending PHB with a variety of PEGs produced natural-synthetic composite films composed of FDA-approved polymers with significant reductions in crystallinity and enabled manipulation of the material properties and degradation potential of the composites. Flexibility of the PHB/PEG composite films was improved compared to PHB, as was the hydrophilicity. Changes to surface morphology and hydrophilicity were found to increase the attachment and proliferation of OECs promoting the biocompatibility of the composite biomaterials compared to PHB. It is anticipated that fine control of PEG composition in PHB-based composite biomaterials can be utilised to support their applications in medicinal and tissue engineering applications.

References

[1] F. M. Kapritchkoff, A. P. Viotti, R. C. P. Alli et al., "Enzymatic recovery and purification of polyhydroxybutyrate produced by *Ralstonia eutropha*," *Journal of Biotechnology*, vol. 122, no. 4, pp. 453–462, 2006.

[2] H. Mitomo, W. -C. Hsieh, K. Nishiwaki, K. Kasuya, and Y. Doi, "Poly(3-hydroxybutyrate-co-4-hydroxybutyrate) produced by *Comamonas acidovorans*," *Polymer*, vol. 42, no. 8, pp. 3455–3461, 2001.

[3] X. Hang, Z. Lin, J. Chen, G. Wang, K. Hong, and G. -Q. Chen, "Polyhydroxyalkanoate biosynthesis in *Pseudomonas pseudoalcaligenes* YS1," *FEMS Microbiology Letters*, vol. 212, no. 1, pp. 71–75, 2002.

[4] L. J. R. Foster and B. J. Tighe, "Enzymatic assay of hydroxybutyric acid monomer formation in poly(β-hydroxybutyrate) degradation studies," *Biomaterials*, vol. 16, no. 4, pp. 341–343, 1995.

[5] M. Zinn, B. Witholt, and T. Egli, "Occurrence, synthesis and medical application of bacterial polyhydroxyalkanoate," *Advanced Drug Delivery Reviews*, vol. 53, no. 1, pp. 5–21, 2001.

[6] P. Vandamme and T. Coenye, "Taxonomy of the genus Cupriavidus: a tale of lost and found," *International Journal of Systematic and Evolutionary Microbiology*, vol. 54, no. 6, pp. 2285–2289, 2004.

[7] S. Philip, T. Keshavarz, and I. Roy, "Polyhydroxyalkanoates: biodegradable polymers with a range of applications," *Journal of Chemical Technology and Biotechnology*, vol. 82, no. 3, pp. 233–247, 2007.

[8] I. M. Arcana, A. Sulaeman, K. D. Pandiangan, A. Handoko, and M. Ledyastuti, "Synthesis of polyblends from polypropylene and poly(R,S)-β-hydroxybutyrate, and their characterization," *Polymer International*, vol. 55, no. 4, pp. 435–440, 2006.

[9] C. Chen, X. Zhou, Y. Zhuang, and L. Dong, "Thermal behavior and intermolecular interactions in blends of poly(3-hydroxybutyrate) and maleated poly(3-hydroxybutyrate) with chitosan," *Journal of Polymer Science Part B: Polymer Physics*, vol. 43, no. 1, pp. 35–47, 2005.

[10] J. M. Harris, *Poly(Ethylene Glycol) Chemistry: Biotechnical and Biomedical Applications*, Plenum Press, New York, NY, USA, 1992.

[11] G. X. Cheng, T. Z. Wang, Q. Zhao, X. L. Ma, and L. G. Zhang, "Preparation of cellulose acetate butyrate and poly(ethylene glycol) copolymers to blend with poly(3-hydroxybutyrate)," *Journal of Applied Polymer Science*, vol. 100, pp. 1471–1478, 2006.

[12] X. Li, K. L. Liu, J. Li et al., "Synthesis, characterization, and morphology studies of biodegradable amphiphilic poly[(R)-3-hydroxybutyrate]-alt-poly(ethylene glycol) multiblock copolymers," *Biomacromolecules*, vol. 7, no. 11, pp. 3112–3119, 2006.

[13] S. Zalipsky, "Synthesis of an end-group functionalized polyethylene glycol-lipid conjugate for preparation of polymer-grafted liposomes," *Bioconjugate Chemistry*, vol. 4, no. 4, pp. 296–299, 1993.

[14] R. D. Ashby, F. Shi, and R. A. Gross, "Use of poly(ethylene glycol) to control the end group structure and molecular weight of poly(3-hydroxybutyrate) formed by *Alcaligenes latus* DSM 1122," *Tetrahedron*, vol. 53, no. 45, pp. 15209–15223, 1997.

[15] S. M. Tan, J. Ismail, C. Kummerlöwe, and H. W. Kammer, "Crystallization and melting behavior of blends comprising poly(3-hydroxy butyrate-co-3-hydroxy valerate) and poly(ethylene oxide)," *Journal of Applied Polymer Science*, vol. 101, no. 5, pp. 2776–2783, 2006.

[16] Q. Zhang, Y. Zhang, F. Wang, L. Liu, and C. Wang, "Thermal properties of PHB/PEG blends," *Journal of Materials Science and Technology*, vol. 14, no. 1, pp. 95–96, 1998.

[17] J. A.F.R. Rodrigues, D. F. Parra, and A. B. Lugão, "Crystallization on films of PHB/PEG blends evaluation by DSC," *Journal of Thermal Analysis and Calorimetry*, vol. 79, no. 2, pp. 379–381, 2005.

[18] L. J. R. Foster, "Biosynthesis, properties and potential of natural-synthetic hybrids of polyhydroxyalkanoates and polyethylene glycols," *Applied Microbiology and Biotechnology*, vol. 75, no. 6, pp. 1241–1247, 2007.

[19] B. Hazer and A. Steinbüchel, "Increased diversification of polyhydroxyalkanoates by modification reactions for industrial and medical applications," *Applied Microbiology and Biotechnology*, vol. 74, no. 1, pp. 1–12, 2007.

[20] V. Sanguanchaipaiwong, C. L. Gabelish, J. Hook, C. Scholz, and L. J. R. Foster, "Biosynthesis of natural-synthetic hybrid copolymers: polyhydroxyoctanoate-diethylene glycol," *Biomacromolecules*, vol. 5, no. 2, pp. 643–649, 2004.

[21] H. Marçal, N. S. Wanandy, V. Sanguanchaipaiwong et al., "BioPEGylation of polyhydroxyalkanoates: influence on properties and satellite-stem cell cycle," *Biomacromolecules*, vol. 9, no. 10, pp. 2719–2726, 2008.

[22] R. Zhang and P. X. Ma, "Poly(α-hydroxyl acids)/hydroxyapatite porous composites for bone- tissue engineering. I. Preparation and morphology," *Journal of Biomedical Materials Research*, vol. 44, no. 4, pp. 446–455, 1999.

[23] X. Li, K. L. Liu, M. Wang et al., "Improving hydrophilicity, mechanical properties and biocompatibility of poly[(R)-3-hydroxybutyrate-co-(R)-3-hydroxyvalerate] through blending with poly[(R)-3-hydroxybutyrate]-alt-poly(ethylene oxide)," *Acta Biomaterialia*, vol. 5, no. 6, pp. 2002–2012, 2009.

[24] K. J. Townsend, K. Busse, J. Kressler, and C. Scholz, "Contact angle, WAXS, and SAXS analysis of poly(β-hydroxybutyrate) and poly(ethylene glycol) block copolymers obtained via Azotobacter vinelandii UWD," *Biotechnology Progress*, vol. 21, no. 3, pp. 959–964, 2005.

[25] T. Freier, C. Kunze, C. Nischan et al., "In vitro and in vivo degradation studies for development of a biodegradable patch based on poly(3-hydroxybutyrate)," *Biomaterials*, vol. 23, no. 13, pp. 2649–2657, 2002.

[26] T. Ahmed, H. Marçal, M. Lawless, N. S. Wanandy, A. Chiu, and L. J. R. Foster, "Polyhydroxybutyrate and its copolymer with polyhydroxyvalerate as biomaterials: influence on progression of stem cell cycle," *Biomacromolecules*, vol. 11, no. 10, pp. 2707–2715, 2010.

[27] R. S. Chung, A. Woodhouse, S. Fung et al., "Olfactory ensheathing cells promote neurite sprouting of injured axons in vitro by direct cellular contact and secretion of soluble factors," *Cellular and Molecular Life Sciences*, vol. 61, no. 10, pp. 1238–1245, 2004.

[28] L. Braydich-Stolle, S. Hussain, J. J. Schlager, and M. C. Hofmann, "In vitro cytotoxicity of nanoparticles in mammalian germline stem cells," *Toxicological Sciences*, vol. 88, no. 2, pp. 412–419, 2005.

[29] C. Y. Xia, C. X. Yuan, and C. G. Yuan, "Galanin inhibits the proliferation of glial olfactory ensheathing cells," *Neuropeptides*, vol. 39, no. 5, pp. 453–459, 2005.

[30] J. M. Garcia Paez, A. Carrera San Martin, J. V. Garcia Sestafe et al., "Resistance and elasticity of the suture threads employed in cardiac bioprostheses," *Biomaterials*, vol. 15, no. 12, pp. 981–984, 1994.

[31] B. L. Hurrell and R. E. Cameron, "A wide-angle X-ray scattering study of the ageing of poly(hydroxybutyrate)," *Journal of Materials Science*, vol. 33, no. 7, pp. 1709–1713, 1998.

[32] T. Wang, G. Cheng, S. Ma, Z. Cai, and L. Zhang, "Crystallization behavior, mechanical properties, and environmental biodegradability of poly(β-hydroxybutyrate)/cellulose acetate butyrate blends," *Journal of Applied Polymer Science*, vol. 89, no. 8, pp. 2116–2122, 2003.

[33] C. W. Pouton and S. Akhtar, "Biosynthetic polyhydroxyalkanoates and their potential in drug delivery," *Advanced Drug Delivery Reviews*, vol. 18, no. 2, pp. 133–162, 1996.

[34] L. J. R. Foster and B. J. Tighe, "Centrifugally spun polyhydroxybutyrate fibres: accelerated hydrolytic degradation studies," *Polymer Degradation and Stability*, vol. 87, no. 1, pp. 1–10, 2005.

[35] L. J. R. Foster and B. J. Tighe, "In vitro hydrolytic degradation of centrifugally spun polyhydroxybutyrate-pectin composite fibres," *Polymer International*, vol. 58, no. 12, pp. 1442–1451, 2009.

[36] Z. Kai, D. Ying, and C. Guo-Qiang, "Effects of surface morphology on the biocompatibility of polyhydroxyalkanoates," *Biochemical Engineering Journal*, vol. 16, no. 2, pp. 115–123, 2003.

[37] B. Saad, P. Neuenschwander, G. K. Uhlschmid, and U. W. Suter, "New versatile, elastomeric, degradable polymeric materials for medicine," *International Journal of Biological Macromolecules*, vol. 25, no. 1–3, pp. 293–301, 1999.

[38] G. Q. Chen and Q. Wu, "The application of polyhydroxyalkanoates as tissue engineering materials," *Biomaterials*, vol. 26, no. 33, pp. 6565–6578, 2005.

[39] B. Wesslen, M. Kober, C. Freij-Larsson, A. Ljungh, and M. Paulsson, "Protein adsorption of poly(ether urethane) surfaces modified by amphiphilic and hydrophilic polymers," *Biomaterials*, vol. 15, no. 4, pp. 278–284, 1994.

[40] K. Bergstrom, K. Holmberg, A. Safranj et al., "Reduction of fibrinogen adsorption on PEG-coated polystyrene surfaces," *Journal of Biomedical Materials Research*, vol. 26, no. 6, pp. 779–790, 1992.

[41] P. D. Drumheller and J. A. Hubbell, "Densely crosslinked polymer networks of poly(ethylene glycol) in trimethylolpropane triacrylate for cell-adhesion-resistant surfaces," *Journal of Biomedical Materials Research*, vol. 29, no. 2, pp. 207–215, 1995.

[42] E. Tziampazis, J. Kohn, and P. V. Moghe, "PEG-variant biomaterials as selectively adhesive protein templates: model surfaces for controlled cell adhesion and migration," *Biomaterials*, vol. 21, no. 5, pp. 511–520, 2000.

[43] M. Zhang, X. H. Li, Y. D. Gong, N. M. Zhao, and X. F. Zhang, "Properties and biocompatibility of chitosan films modified by blending with PEG," *Biomaterials*, vol. 23, no. 13, pp. 2641–2648, 2002.

[44] M. Hammarlund, P. Nix, L. Hauth, E. M. Jorgensen, and M. Bastiani, "Axon regeneration requires a conserved MAP kinase pathway," *Science*, vol. 323, no. 5915, pp. 802–806, 2009.

[45] T. Ahmed, H. Marçal, M. Lawless, N. S. Wanandy, A. Chiu, and L. J. R. Foster, "Polyhydroxybutyrate and its copolymer with polyhydroxyvalerate as biomaterials: influence on progression of stem cell cycle," *Biomacromolecules*, vol. 11, no. 10, pp. 2707–2715, 2010.

Hindawi Publishing Corporation
International Journal of Polymer Science
Volume 2011, Article ID 651549, 8 pages
doi:10.1155/2011/651549

Research Article

Manipulation of Polyhydroxybutyrate Properties through Blending with Ethyl-Cellulose for a Composite Biomaterial

Rodman T. H. Chan,[1] Christopher J. Garvey,[2] Helder Marçal,[1] Robert A. Russell,[1,2] Peter J. Holden,[2] and L. John R. Foster[1]

[1] *Bio/Polymer Research Group, Centre for Advanced Macromolecular Design, School of Biotechnology and Biomolecular Science, University of New South Wales, Sydney, NSW 2052, Australia*
[2] *Australian Nuclear Science and Technology Organisation, Lucas Heights, NSW 2234, Australia*

Correspondence should be addressed to L. John R. Foster, j.foster@unsw.edu.au

Received 6 May 2011; Accepted 30 May 2011

Academic Editor: Shanfeng Wang

Polyhydroxybutyrate (PHB) is widely used as a biomaterial in medical and tissue-engineering applications, a relatively high crystallinity limits its application. Blending PHB with ethyl-cellulose (EtC) was readily achieved to reduce PHB crystallinity and promote its degradation under physiological conditions without undue influence on biocompatibility. Material strength of composite films remained unchanged at 6.5 ± 0.6 MPa with 40% (w/w) EtC loadings. Phase separation between the two biopolymers was determined with PHB crystallinity decreasing from 63% to 47% for films with the same loading. This reduction in crystallinity supported an increase in the degradation rates of composite films from 0.39 to 0.81% wk^{-1} for PHB and its composite, respectively. No significant change in morphology and proliferation of olfactory ensheathing cells were observed with the composites despite significant increases in average surface roughness (R_a) of the films from 2.90 to 3.65 μm for PHB and blends with 80% (w/w) EtC, respectively.

1. Introduction

Polyhydroxyalkanoates (PHAs) are a family of biopolyesters synthesised by a range of microbial species under conditions of environmental stress with excess of carbon [1]. Currently, PHAs consisting of one or more of over 150 different monomer unit have been identified and include the commercially produced polyhydroxybutyrate (PHB) [2, 3]. PHB is the most commonly studied member of the PHA family is biodegradable and biocompatible and used as both a bioplastic and biomaterial for medical devices (Figure 1) [4].

Microbial PHB is comprised of β-hydroxybutyric acid (HBA) monomer units, which is also one of the ketone bodies produced by mammalian cells under conditions of starvation and diabetes and is thought to facilitate biocompatibility in its microbial counterpart which, in the absence of endotoxins, does not trigger any cytotoxic response in mammals [5]. Foster and Tighe have shown that microbial HBA is chemically identical to the mammalian HBA and is recognised by mammalian enzymes [5, 6]. Microbially produced PHB does not trigger an immune and inflammatory response or cause anastomotic failures [7]. As a biomaterial, PHB has been used for various biomedical devices such as sutures, prosthetic devices, and drug delivery systems and for surgical applications [8]. However, the crystalline nature of PHB, its brittleness and low flexibility, long degradation rate under physiological conditions, and poor processability limit its potential for tissue engineering [9]. Modification of PHB physiochemical and material properties through copolymerising and blending have demonstrated successful manipulation of these properties particularly as a bioplastic for environmental applications but with limited success in biomedical scenarios [10, 11].

Similar to PHB, ethyl-cellulose (EtC) is also an FDA-(Food and Drug Administration, USA) approved biomaterial and is widely used as a blood coagulant, coatings for pharmaceutical tablets, and matrices for poorly soluble drugs

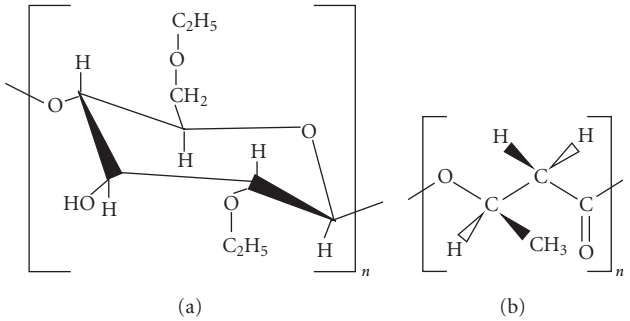

Figure 1: Chemical formulae for biomacromolecules (a) EthylCellulose (EtC) and (b) Poly(3-hydroxybutyrate), (PHB).

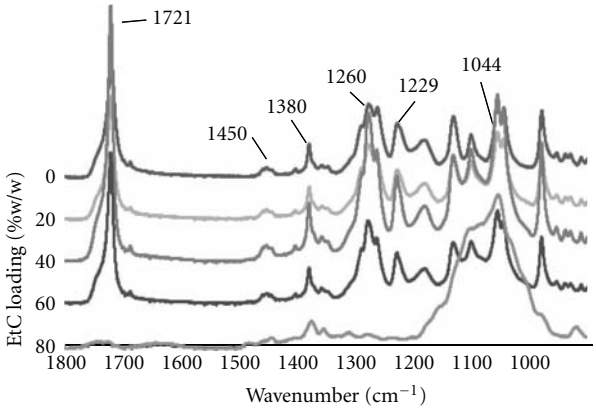

Figure 2: FTIR spectra for PHB-EtC composite films with varying loads of EtC (%w/w).

[12]. Ethyl-cellulose has also been used as a framework in drug-delivery systems for stabilising drug release through the cellulose hydrophilic surface interface [13]. Furthermore, studies have shown that EtC is susceptible to enzyme digestion in human body [14]. In contrast, degradation of PHB proceeds through abiotic hydrolysis and under physiological conditions is a slow process taking years to completely degrade [15]. The rate of PHB degradation has been enhanced by blending PHB with other polymers such as cellulose triacetate (CTAc) and PEG [16, 17].

While there are a variety of reports on PHB-based blends, studies using cellulose derivatives are limited. In the study here, we report on the manipulation of PHB physiochemical and material properties through the addition of ethyl-cellulose as a blending agent with the production of composite PHB-Etc biomaterial films (Figure 1).

2. Experimental

2.1. Reagents. Polyhydroxybutyrate (PHB) of natural origin, ethyl cellulose (48% ethoxyl) and Trypsin were purchased from Sigma Aldrich (Sydney, Australia; Figure 1). Analytical grade chloroform and dimethyl sulfoxide (DMSO) were purchased from Univar, (Seven Hills, Australia). Mammalian cell growth medium, fetal bovine serum (FBS) and Penicillin/Streptococcus antibiotic were obtained from Gibco-Invitrogen (Sydney, Australia). OECs were routinely cultured

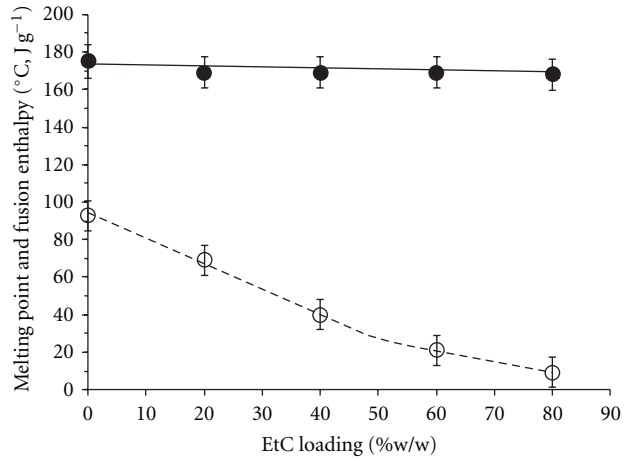

Figure 3: Change in thermal properties for PHB-EtC composite films with variations in EtC loading (%w/w); (●) melting point (°C) and (○) fusion enthalpy (J g^{-1}).

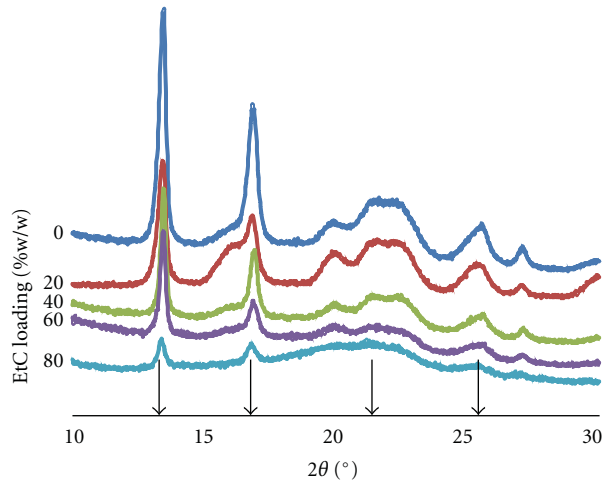

Figure 4: X-ray diffractograms of PHB-EtC composite films with variations in EtC loading (%w/w).

in Dulbecco's Modified Eagle's Medium (DMEM/F12) supplemented with 10% FBS purchased from Lonza (USA).

2.2. Film Fabrication. Biopolymer films were produced by solvent casting as per Zhang et al. [18]. PHB and EtC samples with weight ratios of 100 : 0, 80 : 20, 60 : 40, 40 : 60, and 20 : 80 (w/w) were dissolved in heated chloroform in a sterile sealed vessel (5% w/v, 160 rpm, 50°C). The solution was allowed to cool (22°C, 160 rpm, 15 mins) before pouring into sterile, glass Petri dishes and the solvent evaporated by standing (12 hours, 22°C). The resulting films were subsequently maintained at 40°C under vacuum for 48 hours to remove any solvent residues before annealing at 70°C for 10 days.

2.3. Material characterisation. Material properties of PHB and PHB-EtC films were analysed using a tensile testing instrument (Instron-5543, USA) at 22°C with 30% relative humidity. Films samples (30 mm × 15 mm) were clamped

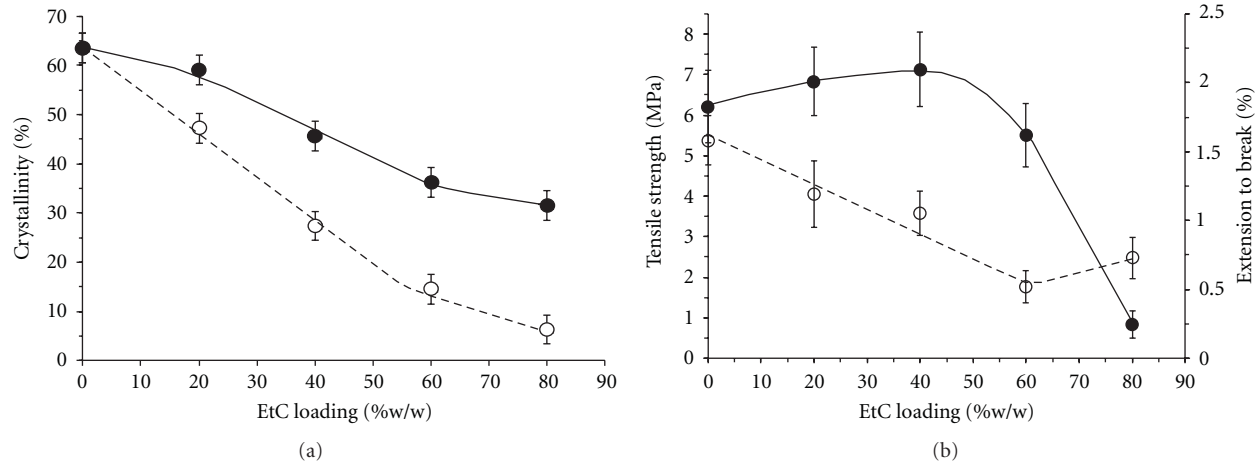

Figure 5: Change in (a) crystallinity: (●) PHB crystallinity, (○) bulk crystallinity (%) and (b) tensile strength (●, MPa) and extension to break (○, %) for PHB-EtC composite films with variation in EtC loading (%, w/w).

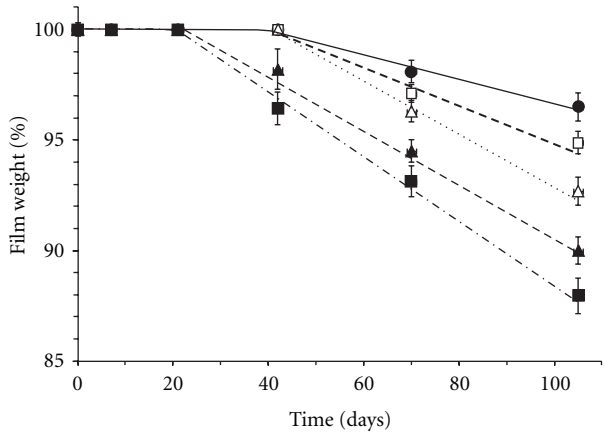

Figure 6: Change in degradation of PHB-EtC composite films with variations in EtC loading (● 0; □ 20; Δ 40; ▲ 60, ■ 80%, w/w) under physiological conditions (37°C, pH 7.4, 140 rpm).

to the calibrated tensiometer using pneumatic grips which slowly moved apart (20 mm min^{-1}). The maximum load, tensile strength and extension at break were calculated using Bluehill computer software (USA). Means from at least 10 samples were determined ($n = 10$).

Thermal properties of the PHB-EtC films were examined using a DSC-1 Star^e system (Mettler Toledo, USA). Samples (5 mg) were sealed in pans and heated at 10°C min^{-1} from 25°C to 200°C to obtain the melting temperature (T_m) and enthalpy of fusion (ΔH_f). Samples were then cooled at the same rate from 200°C to −50°C and reheated from −50°C to 25°C to obtain glass transition temperatures (T_g). The blend (Blend-X_c) and PHB (PHB-X_c) phase crystallinity were calculated using (1), respectively [19]

$$\text{Blend-}X_c = \frac{\Delta Hf}{\Delta H_f^\circ} \times 100,$$
$$\text{PHB-}X_c = X_c \frac{\text{blend}}{W_{\text{PHB}}} \times 100\%, \quad (1)$$

where ΔH_f° is the enthalpy of fusion for PHB (146 Jg^{-1}) [19] and W_{PHB} is the percentage of PHB in the blended film. Means of at least 15 samples were determined ($n = 15$).

X-ray diffraction patterns of the PHB-EtC composites were acquired using a Philips X'pert Material Research Diffraction (MRD) System (Holland). Film samples (20 × 20 mm) were secured on glass slides and aligned with 2θ, z-axis and omega scans (scattering angle range of 2θ = 10–30° and scan step size of 0.02° continuous). Radiation of wavelength 1.5406 Å (Cu K-Alpha) were generated using a power of 45 kV and tube current of 40 mA.

Fourier transform infra-red (FTIR) were made on the PHB-EtC films using a Nicolet iS10 FTIR spectrometer (Thermo scientific, USA). FTIR spectra were acquired between 900 and 1800 cm^{-1} wave numbers by accumulating 64 scans at a resolution of 0.5 cm^{-1}. Optics were purged with nitrogen to suppress signals from carbon dioxide and water vapour.

2.4. Degradation Studies. Preweighed samples of PHB-EtC films (25 × 10 mm) were sterilised through gamma-irradiation and placed into 2 ml Eppendorf tubes. Samples were incubated (37°C, 150 rpm) following the addition of phosphate buffered saline (0.1 M, pH 7.4) with penicillin (100 units mL^{-1}), streptomycin (100 μg mL^{-1}) and fungizone-amphotericin B (2.5 μg mL^{-1}). At periodic intervals samples were removed, filtered, and dried in a dessicator (40°C, 24 h) before allowing to acclimatise at 22°C (atmospherically equilibrated weight). Means of four samples per time point, per sample, were determined. The degradation experiment, modified from Foster et al., was carried out over 105 days [6]. Weight loss (%) was calculated as:

$$W\ (\%) = \frac{W_t}{W_0} \times 100\%, \quad (2)$$

where W is the percentage weight loss and W_0 and W_t are the initial weight and weight after incubation, respectively; means of 5 samples were determined ($n = 5$).

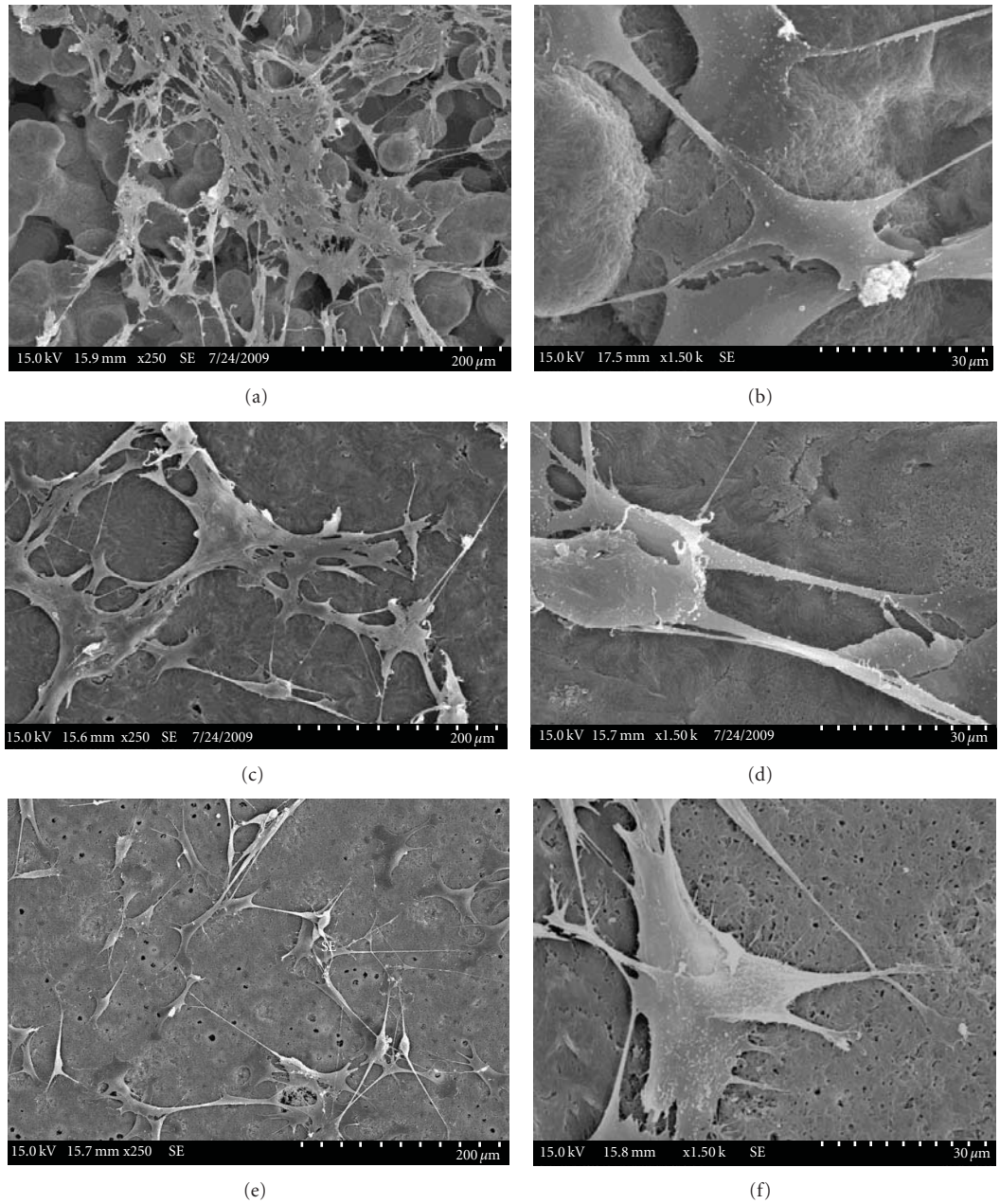

Figure 7: SEMs illustrating attachment of olfactory ensheathing cells (OECs) on PHB-EtC composite films with variations in EtC loadings after 24 hours cultivation (a, d) PHB films with 0% (b, e) 20% and (c, f) 40% (w/w) ETC loadings; (a–c) ×250 magn, bar = 200 μm, (d–f) ×1500 magn, bar = 30 μm.

2.5. Cell Studies. Murine olfactory ensheathing cells (OECs) were cultivated in medium containing (DMEM, 10% FBS, 250 unit penicillin, 250 μg mL^{-1} streptomycin and 1 μg mL^{-1} fungizone-amphotericin B) in T-75 tissue culture flasks incubated at 37°C with 5% CO_2 [20] . OECs were removed from the flask using trypsin (2.5%) at 70% confluence and cell populations of approximately 2×10^5 cells mL^{-1} used to inoculate films samples (13 × 13 mm). At periodic intervals, samples were sacrificed, and the films were rinsed twice with 10 mL of PBS, 2 mL of trypsin (2.5%) was subsequently added before incubation (37°C, 2 mins). Cell proliferation was observed over 3 days and cell viability was calculated using a haemocytometer and the trypan blue exclusion technique [20]. Samples were conducted in triplicate ($n = 3$).

2.6. Microscopy. Cell attachment to PHB-based films were visualised using microscopy. Films were rinsed twice with phosphate buffer saline (PBS, 1%) and fixed in 2.5% glutaraldehyde in 0.1 M PBS buffer (pH 7.2, 4°C, 12 hours). Films were then washed with PBS buffer three times for 5 minutes duration and postfixed in 1% osmium tetroxides (OsO_4, 1 hour). After a buffer wash, samples were sequentially dehydrated in ethanol (30%, 50%, 70%, 80%, 90%, 95%, and 100%, 10 minutes each) and critical point

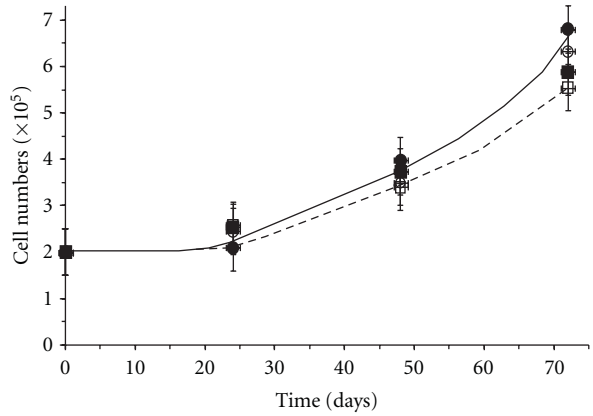

Figure 8: Change in proliferation of OECs as number of cells attached to PHB-EtC films with time for variations in EtC loadings (%, w/w); (●) 0, (○) 20, (■) 40, (□) 60, (▲) 80% (w/w).

dried, adapted from Chung et al. [21]. Specimens were mounted on aluminium stubs and surfaces were coated with a layer of gold particles using a sputter coater (Emitech K550x, England). Samples were subsequently examined using scanning electron microscopy (Hitachi S3400-I, Japan) at 15 kV and 750 mA.

The microtopographies of the PHB-EtC films were mapped using the reflection mode of a confocal scanning laser microscope (CSLM, Leica model TCS-SP, Germany) at excitation and emission wavelengths of 458 and 440–470 nm, respectively. Multiple images through the z-plane were recorded (step size = 2.5 μm). A total of 30 images were used to generate a 3D depth map and calculate average surface roughness values (R_a) according to ISO 4298 (2000) using ImageJ software (National Institute of Health, USA):

$$R_a = \frac{1}{L}\int_0^L |z|dx, \tag{3}$$

where the average surface roughness (R_a) was calculated from the sampling length (L), the plane (z) and the variations of irregularities (dx) from the mean line [3].

2.7. Statistical Analysis. The data are displayed as a mean value with standard deviation of each group. A Student's t-test was performed to test significance with 95% confidence.

3. Results and Discussion

3.1. PHB-Etc Film Characterisation. FTIR is sensitive to local molecular environments and as a consequence has been widely applied to investigate interactions between macromolecules during crystallisation [22]. In the study here, FTIR measurements on the solvent cast PHB films showed a characteristic spectrum with peaks at 1721 and 1229 cm^{-1} assigned to stretching of the C=O groups and C-O-C bonds, respectively, in the crystalline matrix. While peaks at 1450 and 1380 cm^{-1} were characteristic of asymmetric and symmetric methyl group deformation, those at 1260, 1229 and 1044 cm^{-1} were assigned to C-O-C stretching with C-H deformation, C-O-C stretching in the amorphous regions and C-CH_3 stretching [23, 24]. Blending PHB with increasing loads of EtC gradually reduced the peak intensities in the spectra belonging to crystalline PHB as the amorphous content of the composites increased. Contrary to Kumagai et al. who reported blends of PHB with cellulose triacetate [16], we did not resolve spectral shifts in peaks suggesting no specific interactions between the two biopolymer components (i.e., hydrogen bonding). The spectra appeared to be simple linear combinations of semicrystalline PHB and EtC (Figure 2).

Differential scanning calorimetry (DSC) showed no significant change in the melting point (mp, 175 ± 4°C) and glass transition temperature (Tg, 1 ± 1°C) of PHB in the composite (Figure 3). However, PHB fusion enthalpies (ΔH_f) decreased from 92 to 10 $J\,g^{-1}$ in films with 80% (w/w) EtC loading. X-ray diffraction patterns and maxima, observed at 14, 17, 22 and 26°, of the PHB-Etc composites were consistent with previous studies (Figure 4) [25]. As the EtC loading increased the relative peak intensities were reduced, such that the composite with 80% (w/w) EtC loading showed a much broader spectrum with the peaks at 14 and 17° only just noticeable. No disruption of the PHB crystal structure was observed, further supporting FTIR data suggesting the apparent separation of crystalline PHB from amorphous PHB and EtC regions into semicrystalline matrices with EtC chains trapped in the PHB lamellae [26, 27]. The results reported here are consistent with that of Scandola who investigated phase behaviour in PHB and Etc blends and the influence this blending had on environmental degradation of these composites [27].

Differentiation between the crystalline and amorphous regions revealed that as the EtC content in the blend increased, the percentage crystallinity of the films decreased from 63.5 ± 3.3% [19] in PHB films to 9.2 ± 1.5% when the films possessed only 20% (w/w) PHB. (Figure 5(a)). Similarly, the increasing load of EtC disrupted the crystalline process for the PHB which decreased by approximately 32% to 31.5 ± 4.2% with 80% (w/w) EtC loading consistent with the work of Zhang et al. who reported blends of PHB with starch acetate (Figure 5(a)) [18].

Changes in film crystallinity as a consequence of blending with EtC, anticipates an influence on the material properties of the PHB-EtC composite films. However, Figure 5(b) shows no significant change in tensile strength as the EtC loading increased to 40% (w/w) before a dramatic decrease from approximately 6.83 ± 1.05 to 0.84 ± 0.33 MPa (Figure 5(b)). In contrast, extension to break of the films showed an apparently linear decrease from 1.58 + 0.38% for PHB to 0.52 + 0.12% for composites containing 60% (w/w) EtC ($P < 0.05$). Garvey et al. have shown that crystallisation increases in annealed PHB-EtC films when compared to similarly annealed PHB films [28]. Furthermore, The use of relatively high temperatures during film fabrication has been shown to support nucleation and spherulite formation in PHB films while reducing the distance between the PHB granules in the matrix [9]. In the study here, PHB-EtC composites with 20% (w/w) EtC loadings annealed at 25°C exhibited optimal mechanical properties, since tensile

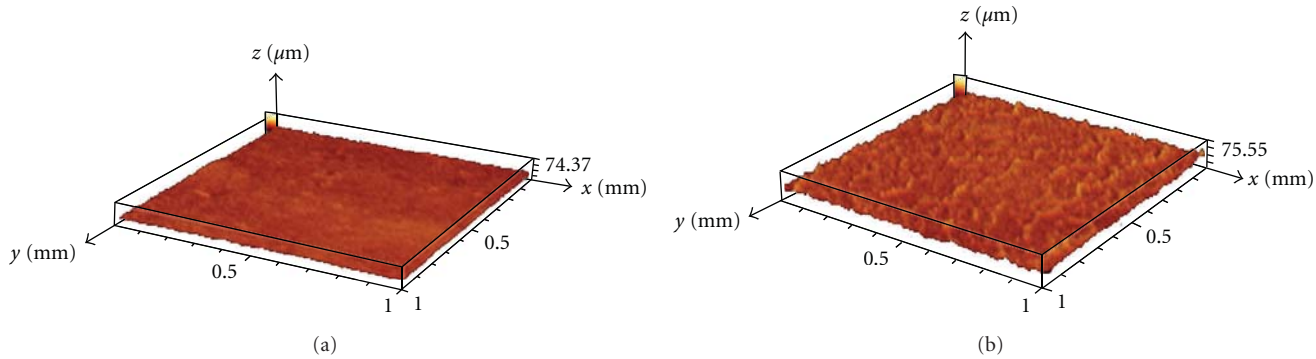

Figure 9: Surface microtopographies of (a) PHB and (b) PHB-EtC composite with 80% EtC (w/w) films.

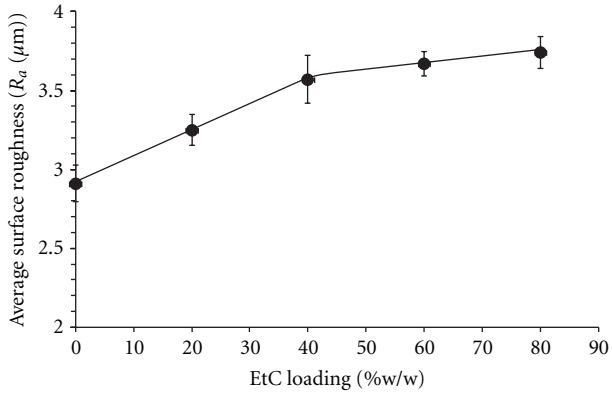

Figure 10: Change in average surface roughness (R_a, μm) of PHB-EtC composite films with variations in EtC loading (%, w/w).

strength and extension at break point were maintained (Figure 5(b)).

3.2. Film Degradation. In addition to influencing material properties, crystallinity can also dictate abiotic degradation behaviour. Reduction of PHB fractional crystallinity makes films more permeable to water molecules and consequently increase hydrolysis of the ester bonds [29]. When incubated under physiological conditions (pH 7.4, 37°C, 160 rpm) PHB and composites films with loadings up to 40% (w/w) EtC no significant weight loss for the first 40 days, while films with higher EtC loadings exhibited weight loss earlier after only 20 days (Figure 6). Figure 6 clearly shows that increasing the EtC loading in the PHB-EtC films increased their degradation, such that PHB films had lost approximately 3.5% of their initial weight after 105 days incubation while composites with 20% (w/w) PHB lost about 12% of their initial weight. Furthermore, weight loss rates were linear and increased significantly ($P > 0.005$) from 0.39% wk^{-1} for PHB films to 0.81 and 1.34% wk^{-1} for PHB blended with 40 and 80% (w/w) EtC, respectively.

3.3. Cellular Responses to PHB-Etc Films. Blends of PHB with EtC are commercially attractive as both biopolymers are FDA approved and have demonstrated success as biomedical devices. Blending with EtC reduces the PHB crystallinity and permits manipulation of film material properties and more favourable degradation under physiological conditions. In the study here, the influence of EtC on biocompatibility on the PHB films was compared using adult olfactory ensheathing cells (OECs). Figure 7 shows that OECs readily attached to PHB and its composite with 20% (w/w) EtC and exhibited healthy morphology with many filament extensions comparable to cells in an asynchronous control with the absence of biomaterials. Furthermore, while cell proliferations appeared to be slightly greater for the PHB homopolymer, these were not significant in the course of this study (Figure 8). In all cases, OEC viability was maintained over 95% for each of the films during duration of the study.

Irregular porous surfaces of PHB-based films have been shown to influence cell adhesion and growth [29]. Microtopographies of the films clearly show changes in surface structures as a consequence of EtC blending (Figure 9). Depth maps derived from these images were used to determine the average surface roughness's (R_a) as per ISO 4298 (Figure 10). PHB films exhibited a R_a 2.91 ± 0.12 μm, as the EtC content increased the R_a also increased. Composite films with 80% (w/w) EtC loadings had the most irregular surface with a significantly greater R_a value of 3.74 ± 0.10 μm (Figure 10, $P > 0.001$). In comparison to the study here, Zhao et al. have reported that increasing surface roughness in PHA films reduced murine fibroblast attachment, with cells apparently preferring a smoother surface [30].

4. Conclusions

The highly crystalline nature of PHB limits its applications as a biomaterial for medical devices. Manipulation of composition and processing are used to promote more favourable properties in PHB-based devices [31, 32]. In the research reported here, we have combined PHB with another FDA-approved biomaterial, ethyl cellulose. Blending of these two components produced composite films with significant reductions in crystallinity which promoted their degradation under physiological conditions but did not significantly compromise their material properties or biocompatibility. It is anticipated that with the added control of annealing we can effectively "tailor" PHB-based biomaterials through

blending to support biomedical device fabrication such as nerve conduits for neuronal regeneration as well as the development of tissue engineering matrices.

References

[1] F. M. Kapritchkoff, A. P. Viotti, R. C. P. Alli et al., "Enzymatic recovery and purification of polyhydroxybutyrate produced by Ralstonia eutropha," *Journal of Biotechnology*, vol. 122, no. 4, pp. 453–462, 2006.

[2] T. Freier, "Biopolyesters in tissue engineering applications," *Advances in Polymer Science*, vol. 203, no. 1, pp. 1–61, 2006.

[3] C. A. Woolnough, T. Charlton, L. H. Yee, M. Sarris, and L. J. R. Foster, "Surface changes in polyhydroxyalkanoate films during biodegradation and biofouling," *Polymer International*, vol. 57, no. 9, pp. 1042–1051, 2008.

[4] L. J. Chen and M. Wang, "Production and evaluation of biodegradable composites based on PHB-PHV copolymer," *Biomaterials*, vol. 23, no. 13, pp. 2631–2639, 2002.

[5] L. J. R. Foster and B. J. Tighe, "Enzymatic assay of hydroxybutyric acid monomer formation in poly(β-hydroxybutyrate) degradation studies," *Biomaterials*, vol. 16, no. 4, pp. 341–343, 1995.

[6] L. J. R. Foster and B. J. Tighe, "In vitro hydrolytic degradation of centrifugally spun polyhydroxybutyrate-pectin composite fibres," *Polymer International*, vol. 58, no. 12, pp. 1442–1451, 2009.

[7] S. Philip, T. Keshavarz, and I. Roy, "Polyhydroxyalkanoates: biodegradable polymers with a range of applications," *Journal of Chemical Technology and Biotechnology*, vol. 82, no. 3, pp. 233–247, 2007.

[8] Z. W. Dai, X. H. Zou, and G. Q. Chen, "Poly(3-hydroxybutyrate-co-3-hydroxyhexanoate) as an injectable implant system for prevention of post-surgical tissue adhesion," *Biomaterials*, vol. 30, no. 17, pp. 3075–3083, 2009.

[9] J. W. You, H. J. Chiu, and T. M. Don, "Spherulitic morphology and crystallization kinetics of melt-miscible blends of poly(3-hydroxybutyrate) with low molecular weight poly(ethylene oxide)," *Polymer*, vol. 44, no. 15, pp. 4355–4362, 2003.

[10] K. Zhao, Y. Deng, J. C. Chen, and G. Q. Chen, "Polyhydroxyalkanoate (PHA) scaffolds with good mechanical properties and biocompatibility," *Biomaterials*, vol. 24, no. 6, pp. 1041–1045, 2003.

[11] C. Chen, C. H. Yu, Y. C. Cheng, P. H. F. Yu, and M. K. Cheung, "Biodegradable nanoparticles of amphiphilic triblock copolymers based on poly(3-hydroxybutyrate) and poly(ethylene glycol) as drug carriers," *Biomaterials*, vol. 27, no. 27, pp. 4804–4814, 2006.

[12] M. M. Crowley, B. Schroeder, A. Fredersdorf et al., "Physicochemical properties and mechanism of drug release from ethyl cellulose matrix tablets prepared by direct compression and hot-melt extrusion," *International Journal of Pharmaceutics*, vol. 269, no. 2, pp. 509–522, 2004.

[13] H. Dong, Q. Xu, Y. Li, S. Mo, S. Cai, and L. Liu, "The synthesis of biodegradable graft copolymer cellulose-graft-poly(l-lactide) and the study of its controlled drug release," *Colloids and Surfaces B: Biointerfaces*, vol. 66, no. 1, pp. 26–33, 2008.

[14] J. Chen, S. Jo, and K. Park, "Polysaccharide hydrogels for protein drug delivery," *Carbohydrate Polymers*, vol. 28, no. 1, pp. 69–76, 1995.

[15] D. S. Rosa, N. T. Lotto, D. R. Lopes, and C. G. F. Guedes, "The use of roughness for evaluating the biodegradation of poly-β-(hydroxybutyrate) and poly-β-(hydroxybutyrate-co-β-valerate)," *Polymer Testing*, vol. 23, no. 1, pp. 3–8, 2004.

[16] Y. Kumagai, Y. Kanesawa, and Y. Doi, "Enzymatic degradation of microbial poly(3-hydroxybutyrate) films," *Makromolekular Chemie*, vol. 193, no. 1, pp. 53–57, 1992.

[17] X. J. Loh, K. K. Tan, X. Li, and J. Li, "The in vitro hydrolysis of poly(ester urethane)s consisting of poly[(R)-3-hydroxybutyrate] and poly(ethylene glycol)," *Biomaterials*, vol. 27, no. 9, pp. 1841–1850, 2006.

[18] L. Zhang, X. Deng, and Z. Huang, "Miscibility, thermal behaviour and morphological structure of poly(3-hydroxybutyrate) and ethyl cellulose binary blends," *Polymer*, vol. 38, no. 21, pp. 5379–5387, 1997.

[19] P. J. Barham, A. Keller, E. L. Otun, and P. A. Holmes, "Crystallization and morphology of a bacterial thermoplastic: poly-3-hydroxybutyrate," *Journal of Materials Science*, vol. 19, no. 9, pp. 2781–2794, 1984.

[20] H. Marçal, N. S. Wanandy, V. Sanguanchaipaiwong et al., "BioPEGylation of polyhydroxyalkanoates: influence on properties and satellite-stem cell cycle," *Biomacromolecules*, vol. 9, no. 10, pp. 2719–2726, 2008.

[21] R. S. Chung, A. Woodhouse, S. Fung et al., "Olfactory ensheathing cells promote neurite sprouting of injured axons in vitro by direct cellular contact and secretion of soluble factors," *Cellular and Molecular Life Sciences*, vol. 61, no. 10, pp. 1238–1245, 2004.

[22] C. Vogel, E. Wessel, and H. W. Siesler, "FT-IR imaging spectroscopy of phase separation in blends of poly(3-hydroxybutyrate) with poly(L-lactic acid) and poly(ε-caprolactone)," *Biomacromolecules*, vol. 9, no. 2, pp. 523–527, 2008.

[23] T. Furukawa, H. Sato, R. Murakami et al., "Structure, dispersibility, and crystallinity of poly(hydroxybutyrate)/ poly(L-lactic acid) blends studied by FT-IR microspectroscopy and differential scanning calorimetry," *Macromolecules*, vol. 38, no. 15, pp. 6445–6454, 2005.

[24] L. J. R. Foster, V. Sanguanchaipaiwong, C. L. Gabelish, J. Hook, and M. Stenzel, "A natural-synthetic hybrid copolymer of polyhydroxyoctanoate-diethylene glycol: biosynthesis and properties," *Polymer*, vol. 46, no. 17, pp. 6587–6594, 2005.

[25] B. L. Hurrell and R. E. Cameron, "A wide-angle X-ray scattering study of the ageing of poly(hydroxybutyrate)," *Journal of Materials Science*, vol. 33, no. 7, pp. 1709–1713, 1998.

[26] T. Wang, G. Cheng, S. Ma, Z. Cai, and L. Zhang, "Crystallization behavior, mechanical properties, and environmental biodegradability of poly(β-hydroxybutyrate)/cellulose acetate butyrate blends," *Journal of Applied Polymer Science*, vol. 89, no. 8, pp. 2116–2122, 2003.

[27] M. Scandola, "Polymer blends based on bacterial poly(3-hydroxybutyrate)," *Canadian Journal of Microbiology*, vol. 41, supplement 1, pp. 310–315, 1995.

[28] C. J. Garvey, R. A. Russell, V. M. Garamus, F. Boue, L. J. R. Foster, and P. J. Holden, *Small Angle Neutron Scattering Study of the Interface between Ethylcellulose and Polyhydroxyalkanoate Blends during Annealing*, Abstract, SAS2009, ANSTO, Oxford, UK, 2009.

[29] I. I. Muhamad, L. K. Joon, and M. Noor, "Comparing the degradation of poly-β-(hydroxybutyrate), 39-46 poly-β-(hydroxybutyrate-co-β-valerate)(PHBV) and PHBV/cellulose triacetate blend," *Malaysian Polymer Journal*, vol. 1, no. 1, pp. 39–46, 2006.

[30] Z. Kai, D. Ying, and C. Guo-Qiang, "Effects of surface morphology on the biocompatibility of polyhydroxyalkanoates," *Biochemical Engineering Journal*, vol. 16, no. 2, pp. 115–123, 2003.

[31] L. J. R. Foster, "Biosynthesis, properties and potential of natural-synthetic hybrids of polyhydroxyalkanoates and polyethylene glycols," *Applied Microbiology and Biotechnology*, vol. 75, no. 6, pp. 1241–1247, 2007.

[32] B. Hazer, "Amphiphilic poly(3-hydroxyalkanoate)s: potential candidates for medical applications," *Energy and Power Engineering*, vol. 2, no. 1, pp. 31–38, 2010.

Hindawi Publishing Corporation
International Journal of Polymer Science
Volume 2011, Article ID 168924, 11 pages
doi:10.1155/2011/168924

Research Article

Bisphenyl-Polymer/Carbon-Fiber-Reinforced Composite Compared to Titanium Alloy Bone Implant

Richard C. Petersen

Department of Biomaterials, University of Alabama at Birmingham, Birmingham, AL 35294-0007, USA

Correspondence should be addressed to Richard C. Petersen, richbme@uab.edu

Received 21 March 2011; Revised 22 April 2011; Accepted 3 May 2011

Academic Editor: Shanfeng Wang

Aerospace/aeronautical thermoset bisphenyl-polymer/carbon-fiber-reinforced composites are considered as new advanced materials to replace metal bone implants. In addition to well-recognized nonpolar chemistry with related bisphenol-polymer estrogenic factors, carbon-fiber-reinforced composites can offer densities and electrical conductivity/resistivity properties close to bone with strengths much higher than metals on a per-weight basis. *In vivo* bone-marrow tests with Sprague-Dawley rats revealed far-reaching significant osseoconductivity increases from bisphenyl-polymer/carbon-fiber composites when compared to state-of-the-art titanium-6-4 alloy controls. Midtibial percent bone area measured from the implant surface increased when comparing the titanium alloy to the polymer composite from 10.5% to 41.6% at 0.8 mm, $P < 10^{-4}$, and 19.3% to 77.7% at 0.1 mm, $P < 10^{-8}$. Carbon-fiber fragments planned to occur in the test designs, instead of producing an inflammation, stimulated bone formation and increased bone integration to the implant. In addition, low-thermal polymer processing allows incorporation of minerals and pharmaceuticals for future major tissue-engineering potential.

1. Introduction

Foremost advancements are expected in stem-cell/osteoprogenitor/osteoblast tissue-engineering for the next generation of bone implants as a result of new materials available from the stealth-electronic technology aeronautical/aerospace era. Through a better understanding of the microstructure and electron-transfer properties for matter, polymer-based fiber-reinforced materials can be bioengineered to provide important new materials for broad significant bone implant applications. In the world of materials, fibers are the strongest and possibly stiffest known forms of a substance matter [1]. When combined into an appropriate matrix like a polymer, much of the fiber mechanical-strength properties can be transferred through the bulk material [1, 2]. Such multiconstituent materials, referred to as composites, have led the way in the aeronautical/aerospace age, primarily as a means to provide stronger lighter structural parts. The basic polymer used for advanced design capability has been a class of thermosetting organic resins that cure by electron free-radical crosslinking [1, 2]. The thermoset resins generally contain similar interconnecting bisphenyl double-aromatic ring molecules that can be reinforced by chemical coupling with fibers for highly developed mechanical properties [1, 2]. The bisphenol-derived polymer function was further identified in 1936 through a pharmaceutical study as one of the first synthetic estrogens [3]. Estrogen in turn has a stimulating anabolic effect on bone formation and differentiation of osteoblasts [4–7].

In terms of material biocompatibility, polymers have extensively long hydrocarbon backbone chains and are more similar to carbon-based tissue cells than metals or ceramics. Chemical similarity between neutrally active nonpolar polymer materials and lipid hydrocarbon cellular membrane interfaces are then expected to improve biocompatibility for many new important biomedical applications. Various assorted polymers are currently already used for the transition artificial heart organ, vascular grafts, tendon/ligament repair, guided tissue regeneration, articular joint components, orthopedic medical cements, resorbable scaffolds for tissue growth and resorbable sutures [8, 9]. In fact, polymer materials are well-known primordial biologic-derived hydrocarbons that were geologically degraded and then recovered by the petroleum industry and separated as pure monomeric

Table 1: Biomaterial properties.

Material	Density (g/cm^3)	Resistivity[a] (Ωm)	Tensile strength (MPa)	Yield strength (MPa)	Modulus (GPa)
Bone longitudinal-radial hydrated [8, 9]	1.8–2.1	46–150	70–150	30–70	15–30
Titanium grades 1–4 [9, 18]	4.5–4.51	10^{-7}	240–550	170–485	104–110
Titanium-6-4aluminum vanadium alloy [8, 9, 18]	4.4–5.0	10^{-8}	860–1103	795–1034	116–120
Bisphenyl Unidirectional CF[b] [1, 2, 18, 19]	1.6	5	780–1850		145–325
Bisphenyl Unidirectional CF[b] 4-pt. bend [1, 2, 19]	1.6	5	790–1800		120–255
Bisphenyl/QF[b] Exp.Uni-woven laminate 4-pt. bend [17, 19]	1.49 (.01)[c]	5	963 (240)[c]	774 (176)[c]	64 (14.4)[c]
Bisphenyl 3-D Woven E-Glass 3-pt. Bend X-Y planes [17]			576 (129)[c]	441 (75)[c]	26 (18)[c]

[a]Resistivity = 1/conductivity.
[b]CF: carbon fiber; QF: quartz fiber.
[c]Experimental standard deviations in parentheses.

units. Highly advanced biologically derived structural composites developed for military aircraft and aerospace structures are thus now ready for biomedical application.

Free-radical cure thermoset bisphenyl resins are processed at relatively low temperatures, between room temperature and below 200°C to produce the hardened cured polymer [2]. So, other organic compounds can be added into the resin before curing and safely processed. Similarities in nonpolar chemical relationships between thermoset resins and many organic therapeutics consequently appear to be a major opportunity toward establishing biocompatible cell/tissue interfaces with implants. For example, due to molecular parallel chemistry interactions nonpolar pharmaceuticals can be blended into resins and cured into a polymer implant interface [10, 11] for long-term release and interfacial interactions with adjacent cells and tissue. Nonpolar hydrocarbon additives have subsequently shown the ability to entangle with the main polymer backbone chain to improve matrix toughness properties [11]. A tougher, less brittle composite then aids in making thinner parts [12] which becomes more important for small biomedical devices. In addition, polarized inorganic fillers similar to bone mineral are commonly included in thermoset free-radical cure bisphenyl polymers to improve mechanical/physical properties and control manufacturing process consolidation [2, 13, 14]. Eukaryote mammalian cells then extensively require inorganic calcium and phosphates derived from a large bone source to insulate and seal lipid membrane compartments and establish voltage potentials [15–17]. With a negative membrane potential, cells then have the ability to do work and develop [15–17].

Polymer-matrix fiber-reinforced composites can therefore be engineered for specific tissue performance with potential mechanical properties many times greater than structural aluminum, titanium, or steel on a per-weight basis [2, 18] (Table 1 on density, mechanical and electrical conduction properties). Bisphenyl-polymer/carbon-fiber composite electrical-conduction/resistivity properties [9, 17–19] are similar to bone [9, 17] with design capability to better simulate conditions favorable to the approximate −70 mV plasma cell membrane resting potential [16, 17] and complex electron-transfer reactions that form the fundamental units for the varied multitude of biologic processes [15–17]. In addition, when compared to metals or ceramics, the modulus or stiffness of polymer composites (Table 1) can be engineered to accommodate stress-transfer conditions with surrounding bone tissue and associated living cells [17]. Modulus mismatch between bone and metals consequently has been a problem with current implant loosening related to stress transfer between the bone and implant [20]. Density in turn is related to modulus through force-interatomic-distance equilibriums [18].

In order to test the hypothesis that bisphenyl-polymer/carbon-fiber composite was more biocompatible than titanium-6aluminum-4vanadium alloy implant material for mesenchymal stem-cell recruitment with osteoprogenitor/osteoblast proliferation/differentiation, an *in vivo* rat tibia model [21] was used to measure bone growth by histomorphometry. Statistics were calculated using Microsoft Excel for a t test of unequal variances to compare differences between groups. The marginal level of uncertainty was set at $\alpha = 0.05$.

2. Materials and Methods

2.1. Materials and In Vivo Animal Test Model. Unidirectional bisphenyl-polymer/carbon-fiber rods 1.5 mm in diameter were placed for two weeks *in vivo* using an engineered Sprague-Dawley rat tibia model that has been previously described elsewhere by McCracken and Lemons et al. [21]. As a result, previous tissue slides for 1.5 mm diameter titanium-6-4 alloy (90% titanium; 6% aluminum; 4% vanadium) material controls were consequently available for comparison [21] to measure percent bone area (PBA) at a specified tibia intramedullary distance from the implant using Bioquant software (Nashville, TN). The titanium alloy screws measured 1.5 mm diameter × 8 mm length (Walter Lorenz Surgical Inc. Jacksonville, FL). The bisphenyl-epoxy-polymer/carbon-fiber composite was composed of 60 volume percent unidirectional carbon fibers with 40 volume percent polymer processed into 1.5 mm diameter rods using a bisphenol-derived epoxy thermoset resin (Aerospace Composite Products, Livermore, CA). The bisphenyl polymers originate from two interconnecting aromatic rings as

a bisphenol [2] that has been compared pharmaceutically to the molecular structure estrogen [3].

2.2. Animal Preparation. Animals were maintained according to standards set by the American Association for Accreditation of Laboratory Animal Care following the Guide for Care and Use of Laboratory Animals proposed through the National Research Council (1996). Ten male Sprague-Dawley rats weighing 350 to 375 g (4 months old) were obtained for each of the two groups separately comparing PBA surrounding implants for the titanium alloy historical controls and new bisphenyl-polymer/carbon-fiber composite. Two additional rats were also included for an alternate histology imaging characterization for the bisphenyl-polymer/carbon-fiber composite. All rats were weighed to the nearest gram. Animals were provided food and water during the experimental procedure *ad libitum*. The room was maintained at 23°C, with 12-hour light-dark cycles.

The animals were anesthetized using Isofluorane from a precision vaporizer inducing at 4-5% and maintaining at 1-2%. Rats were also administered intraperitoneal anesthetics with ketamine at 10 mg per 100 g and xylazine at 1 mg per 100 g. Rats were shaved, scrubbed, and draped to provide a surgical field. A 1.5-cm incision was made on the medial-proximal surface of the tibia above the tibial protuberance. Tissue was reflected to expose the flat portion of the tibia below the joint.

Using a slow-speed surgical handpiece with a no. 4 round bur and copious warm saline irrigation, a pilot hole was drilled in the tibia 8 mm proximal to the tibial cortical bone protuberance. A 1.3 mm diameter surgical implant twist drill bit was used to create an oblique-transverse osteotomy, traveling through the medullary canal and the opposite cortical shaft. Rather than drilling perpendicular to the bone, an oblique path of implant placement was used to optimize the implant surface area in the canal for each specimen. A no. 6 round bur was used to increase the size of the hole in the medial aspect of the tibia. The osteotomy was irrigated with 20 mL of warm saline. The titanium-6Al-4V allow screws were placed by hand to engage the opposite cortical shaft but did not engage the medial cortical bone shaft, which had been enlarged with the no. 6 round bur. The bisphenyl-epoxy-polymer/carbon-fiber composite rods were cut to 5.0 mm lengths, washed, cleaned by ultrasonic vibration and sterilized by autoclave. Autoclave sterilization without ultrasonic cleaning was not used for two alternate composite rat tibia tests which were later sectioned horizontally through the implant at right angles to all other samples for slide analysis. A 1.5 mm surgical implant twist drill bit was used to create an oblique-transverse osteotomy, traveling through the medullary canal and the opposite cortical shaft as before. The bisphenyl polymer/carbon fiber composite rods were inserted with some pressure and lightly tapped into place. Primary closure was achieved for each animal by approximating the muscle layers with resorbable sutures and closing the skin with surgical staples.

2.3. Histomorphic Analysis. After healing for 14 days, the rats were euthanized with carbon dioxide inhalation and exsanguinated by cardiac incision with sharp scissors. Tibiae were removed, cleaned of soft tissue, and immediately imaged by X-rays and photographs for later characterization and comparison with the histology. Tibial specimens were then fixed in phosphate-buffered paraformaldehyde for a minimum of 12 hours. Subsequent specimens were dehydrated with progressive alcohols under vacuum, cleared with xylene, infiltrated and embedded with methylmethacrylate and polymerized by ultraviolet light. Samples were prepared for light microscopy by cutting and grinding techniques that provided a lateral section of the implant. The final sample thickness was less than 60 um with specimens mounted on clear plastic slides. Slides for the 20-rat group statistical analysis were stained with toluidine blue to identify live bone. One sample from the original polymer composite statistical analysis group was stained with a modified H&E medium after partially exposing the upper cortical plate to examine the bone inside the tibia canal before solvent dehydration. Sanderson's stain was further used for two additional rat tibia slides not included in the statistical analysis which were prepared with cuts horizontal at right angles through the composite implants.

Percent Bone Area (PBA) was defined as the area occupied by bone within 0.8 mm and 0.1 mm of the implant inside the bone-marrow space of the tibia between the cortical bone plates. Previous PBA measurements had been determined with the titanium alloy at 1.5 mm [21]. A distance of 0.8 mm was now used as this measure was considered a rough approximation of the physiologic cortical-plate thickness for the Sprague-Dawley rats under study. A distance of 0.1 mm was also considered as a physiologic estimate for initial osseointegration with basic oxygen diffusion limits. Data was analyzed using BioQuant Software (Nashville, TN). Measurements for the PBA statistical analysis were all completed at 2x magnification with an Olympus microscope on a 19-inch-by-19-inch monitor and were reconfirmed when necessary at 4x or 10x visually for accuracy. All stained areas were measured as live bone. Comparisons of different measurements between groups were analyzed using a t-test with unequal variances. Results were considered significant at alpha = 0.05. Imaging was further completed at 20x and 40x for more in-depth evaluations.

3. Results

3.1. PBA Statistics. After two weeks, major breakthrough significant statistical differences were found when comparing histological tibia intramedullary PBA results for bisphenyl-polymer/carbon-fiber composites to titianium-6-4 metallurgy (Figures 1(a) and 1(b)). At a tibia-marrow/implant distance of 0.8 mm, PBA increased from 10.5 ± 5.3 to 41.6 ± 13.9 when comparing the titanium alloy to the polymer composite, respectively, $P < 10^{-4}$. At a tibia-marrow/implant distance of 0.1 mm, PBA increased from 19.3 ± 12.3 to 77.7 ± 7.0 when comparing titanium alloy to the polymer composite, respectively, $P < 10^{-8}$. The bisphenyl-polymer/carbon-fiber composite and titianium-6-4 alloy both increased PBA approximately almost double from 41.6 to 77.7 and 10.5 to 19.5 correspondingly when

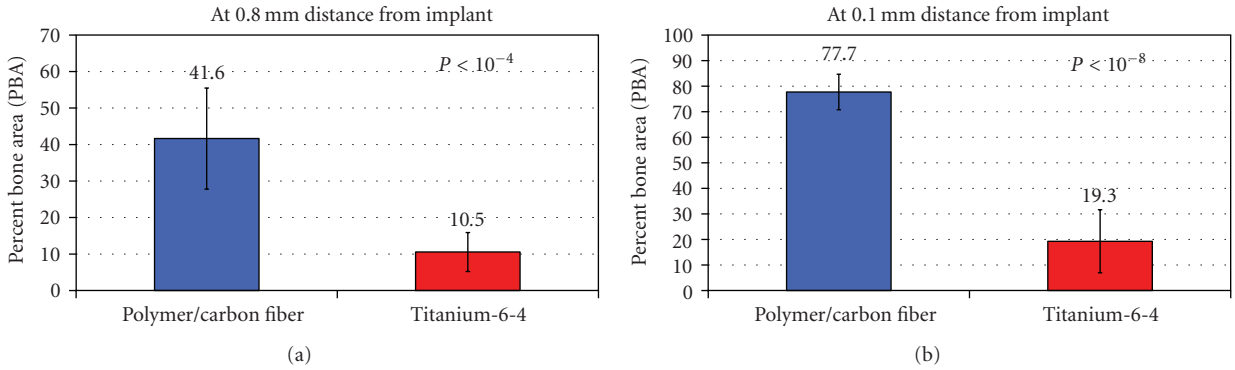

Figure 1: *In vivo* implant rat tibia PBA cross-sectional results at 0.8 mm and 0.1 mm from the implant surface at midcanal showing highly significant increases for the bisphenyl-polymer/carbon-fiber composite compared to titanium-6-4 alloy. (a) Comparisons for cross-sectional Group Mean PBA out to 0.8 mm from the implant, $P < 10^{-4}$. (b) Comparisons for cross-sectional Group Mean PBA out to 0.1 mm from the implant, $P < 10^{-8}$. The PBA was averaged from both distal and mesial implant surfaces separately at both 0.8 mm and 0.1 mm. All data presented as the set average ± one standard deviation error bars. The sample size was 10 for all groups.

comparing results at an implant distance of 0.8 mm to the much closer distance of 0.1 mm.

3.2. Imaging. As part of the investigation, imaging characterization was completed by gross photography observation in Figures 2(a)–2(f), with X-rays in Figures 3(a) and 3(b), and from histological slides at magnifications ranging from 1.25x to 40x in Figures 4(a)–4(d) and 5(a)–5(f). The three imaging techniques revealed important biocompatibility potential with significant osseoconductive responses for the bisphenyl-polymer/carbon-fiber implants that greatly exceeded the titanium-6-4 alloy standard bone implant screws. Bone growth was stimulated along the entire surface of the bisphenyl-polymer/carbon-fiber implants through the tibia canal bone-marrow space, filled in surgical space between the implant and cortical bone, grew above the normal cortical bone surface levels along the implant and even partially over the end of many exposed composite rods.

Photograph imaging (Figures 2(a)–2(f)) of the 1.5 mm diameter bisphenyl-polymer/carbon-fiber implants and tissue shows tough collagenous calcifying osteoid in Figures 2(a) and 2(b) that would follow the implant surface above the upper cortical bone plate approximately 1.0 mm and sometimes also start to grow over the implant end. Fracture of the bone after fixation in Figure 2(c) and before solvent dehydration with embedding for histological section in Figure 4(c) shows that the newly formed intramedullary tibial bone appears somewhat dense and more similar to cortical bone (arrow) rather than trabeculated bone. Separate tests not included in the statistical analysis incorporated minor insignificant bisphenyl-polymer/carbon-fiber fragments as particulate cuttings retained along the implant before surgery which resulted in an overly exuberant collagenous osteoid response extruded on the lower cortical plate over the implant end in Figure 2(d). Dissection of the soft tissue away from the upper cortical plate always became more difficult at the bisphenyl-polymer/carbon-fiber implant interface where soft tissue is shown lifted up from the cortical bone and an extremely tough fibrous cuff surrounds the entire implant circumference in Figure 2(e). An easy dissection around the entire band of tough fibrous cuff tissue that surrounded a bisphenyl-polymer/carbon-fiber implant which protruded only minimally above the cortical bone indicates that soft tissue integration is associated with carbon-fiber fragments of fine particulate in Figure 2(f).

X-ray imaging in Figure 3 of the 2-week rat tibial 1.5 mm diameter unidirectional bisphenyl-polymer/carbon-fiber implant shows an X-ray frontal view in Figure 3(a) with enhanced cortical-like bone growing around the implant. The vertical X-ray bone density of the tibia around the implant could generally approximate and often greatly even surpass the highest levels for cortical edge density. The increased X-ray bone density is particularly apparent from the top as bone grew both through the intramedullary canal and also up the implant outer surface. A typical X-ray lateral view in Figure 2(b) shows cortical-like bone growing along the implant through the tibial canal where bone is not normally physiologically found.

As a comparison reference for low magnification imaging at the 0.8 mm distance from the implant (Figures 4(a) and 4(b)) average mesial and distal PBAs for both the titanium alloy (11.2 mesial and 9.9 distal) and bisphenyl-polymer/carbon fiber composite (38.8 mesial and 44.4 distal) were very similar and no significant statistical differences were apparent. The titanium alloy (Figure 4(a)) shows pieces of bone integrating along the implant surface whereas the bisphenyl-polymer/carbon-fiber (Figure 4(b)) shows more extensive coordinated bone formation along the implant surface. High power magnifications from Figure 5 detected some minor fiber fracture and fiber fragments. However, all carbon-fiber exposure to the biologic environment stimulated bone growth immediately at the fiber surface. Some broken fibers were even incorporated directly into the growing bone cell unit. Intense osseoconductivity was accentuated most at surface implant defects for the bisphenyl-polymer/carbon-fiber composites (Figure 5(e)). Some light staining measured directly from the slides as bone on a 19-inch-by-19-inch monitor screen that could include higher

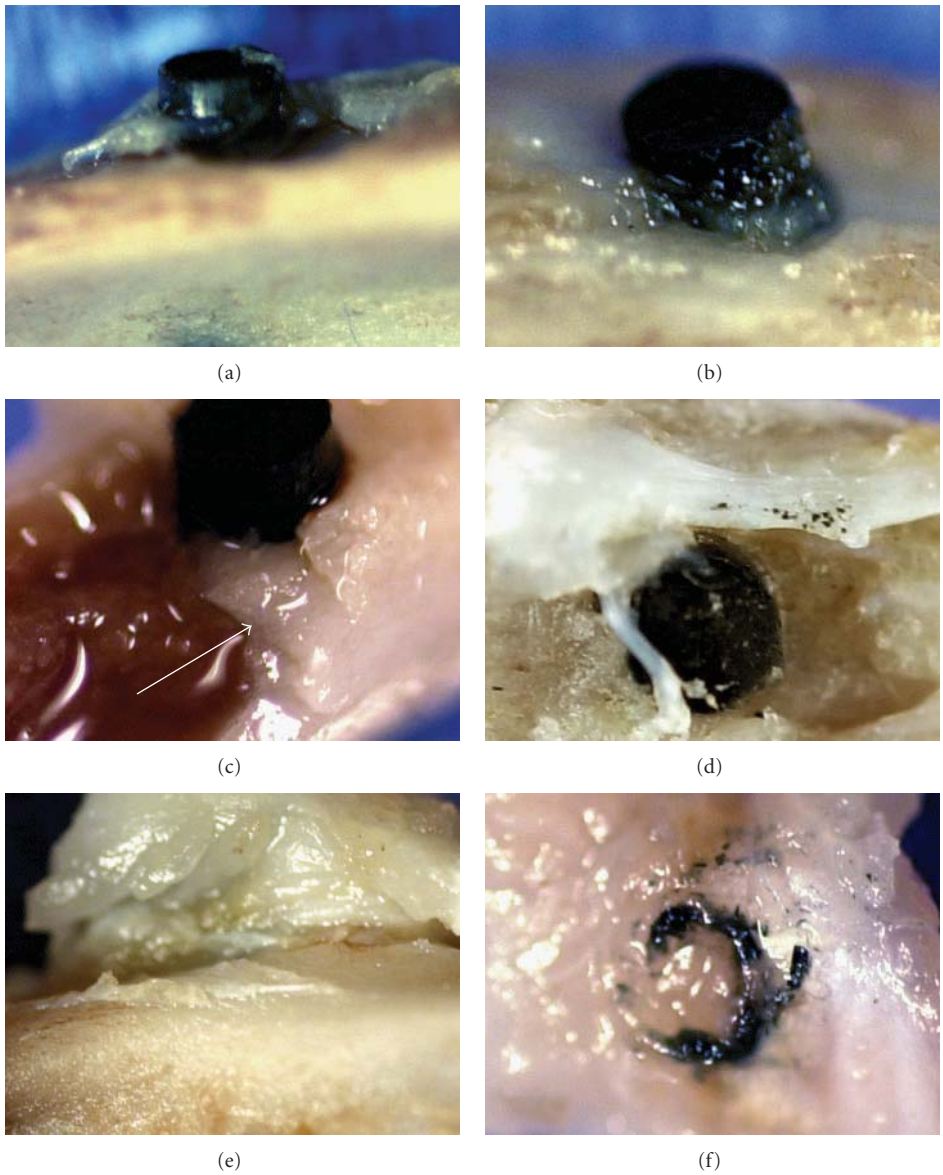

Figure 2: Photograph imaging of 1.5 mm diameter bisphenyl-polymer/carbon-fiber implants and tissue: (a, b) upper cortical bone plate with osteoid growing up the composite implant surface. (c) Fracture of the bone after fixation. (d) Separate tests not included in the statistical analysis incorporated minor insignificant bisphenyl-polymer/carbon-fiber fragments as particulate cuttings retained along the implant before surgery which resulted in an overly exuberant collagenous osteoid response extruded on the lower cortical plate over the implant end. (e) Dissection exposes an extremely tough fibrous cuff surrounding the entire implant circumference. (f) Tissue dissection of the fibrous cuff provides evidence of carbon fine particulate and fiber fragments.

power confirmation may not be entirely apparent in the reproduced images at lower magnification.

4. Discussion

4.1. Material Analysis Accentuated Biocomplex Comparisons. From the rat tibia *in vivo* intramedullary bone-marrow study comparing titanium alloy to bisphenyl-polymer/carbon-fiber composite, material differences were accentuated during extreme osseous formation in the exceedingly low *P*-value PBA study. Osteoblasts/osteocytes are the parenchyma tissue cells involved in the highly biocomplex synthesis and deposition of bone extracellular matrix for ossification that can arise from bone-marrow mesenchymal stem-cell progenitors [22, 23]. Therefore, possible complex chemistry and biological electron-transfer relationships could be more easily considered with two extreme differences in materials and biological tissue reactions. Through such new emphasized material comparisons, bone appears to be stimulated by bone cell recruitment, proliferation and differentiation from a bisphenyl-polymer/carbon-fiber composite with many potential advantages when compared with the metal

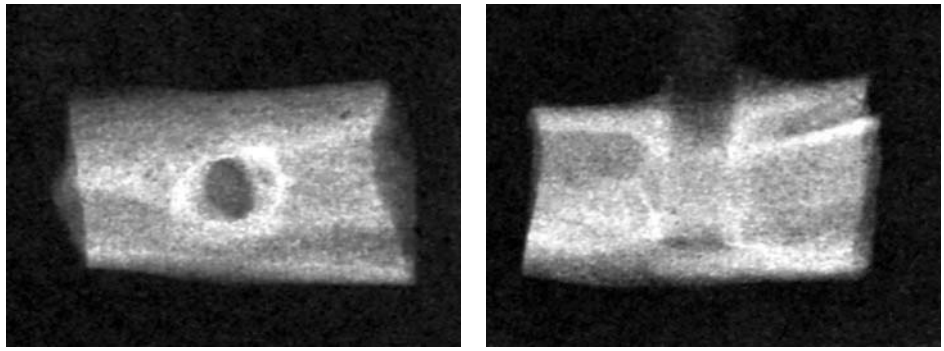

(a) (b)

Figure 3: X-ray Imaging: (a) Frontal view. (b) Lateral view.

Table 2: Resistivity[a] of different engineering and biological materials (Ωm).

Material	Type	Resistivity
Titanium pure	Conductor	$4.2–5.2 \times 10^{-7}$ [18]
Titanium-6Al-4V alloy	Conductor	1.7×10^{-8} [18]
Bisphenol-polymer/carbon Fiber Composite	Semiconductor	5 [19]
Bone longitudinal	Semiconductor	46 [9]
Bone radial	Semiconductor	150 [9]
Physiologic saline	Semiconductor	0.72 [9]
Silicon pure	Semiconductor	3000 [26]
Silicon phosphorous Doped	Semiconductor	20–80 [27]
Lipid phosphate headgroup/water interface	Semiconductor	100 [28]
Carbon fibers	Conductor	$0.95–1.8 \times 10^{-5}$ [18]
Thermoset bisphenyl polymer	Insulator	10^{10}–10^{13} [18]
General metals	Conductors	$\sim 10^{-6}$–10^{-9} [18]
Pure quartz fiber	Insulator	10^{20} [29]

[a] Resistivity = 1/conductivity.

titanium alloy. To elucidate on such new important composite material properties, nonpolar and steroid-like polymer factors with possible carbon-fiber biocircuit antioxidant-type electron-withdrawing effects that might occur can be described in further detail.

4.2. Polymer Nonpolar and Estrogen Factors. Nonpolar or hydrophobic polymer surfaces have previously demonstrated superior cell growth and adhesion over more polar or hydrophilic calcium phosphate hydroxyapatite *in vitro* [24, 25]. Therefore, another possible biocompatible influence may include nonpolar-nonpolar chemical similarities between the bisphenyl polymer and the bone-marrow bilipid-cell membranes that may promote attractive nonbonded Lennard-Jones parameters and London-type instantaneous-induced-dipole van der Waals dispersion forces. The bisphenyl-polymer backbone will stimulate estrogen steroid-like hormone factors, known to enhance stem-cell differentiation with bone formation [3–7]. Bone-marrow stem-cell proliferation further appears possibly linked to the nonpolar aromatic molecules that indirectly produce differentiation effects based on increased cell division, cell packing, and density for more uniform stress transfer as mineralizing cells assume closer relationships to the parenchyma tissue or bisphenol-polymer/carbon-fiber implant. Bisphenyl-polymer nonpolar hydrophobicity for water repulsion may even help favorable biological reactions to proceed at the implant interface by minimizing degrading effects from biological fluids locally. In addition, polymers do not release more polar metallic Lewis acids into biologic fluids for a stable neutral pH interface.

4.3. Electrical Conductivity/Resistivity for Semiconducting Potential. A bisphenyl-polymer/carbon-fiber implant interface with an overall resistivity of 5 Ωm [19] (Table 2) is about within an order of magnitude for bone mineral longitudinal and radial resistivity of approximately 46 Ωm and 150 Ωm, respectively [9]. Conversely, titanium alloy resistivity is vastly lower than bone by extensive orders of magnitude at about 10^{-8} Ωm [18]. Physiologic saline represents another biological comparison to composite resistivity at 0.72 Ωm [9]. Pure silicon semiconductor has a resistivity that is 3000 Ωm [26] and phosphorous-doped silicon used in high-energy physics has a resistivity of 20–80 Ωm [27]. As another comparison for plasma cell membrane electric biocompatibility performance, *in vitro* phosphate-head lipid resistivity at the interface between the phosphate head groups and water has been measured at approximately 100 Ωm [28]. The bisphenyl-polymer/carbon-fiber implant resistivity can further be increased by replacing carbon fibers, $0.95–1.8 \times 10^{-5}$ Ωm [18], with pure quartz fibers having a resistivity of 10^{20} Ωm [29]. Conversely, composite implant resistivity can be lowered by adding conducting metallic particulate with resistivities of about 10^{-6}–10^{-9} Ωm [18] into the thermoset bisphenyl polymer, 10^{10}–10^{13} Ωm [18]. Instead of a metal short circuit or polymer/ceramic insulation, the new fiber-reinforced composite has semiconducting potential. Related to safe efficient electron-transfer speeds, bone actually is

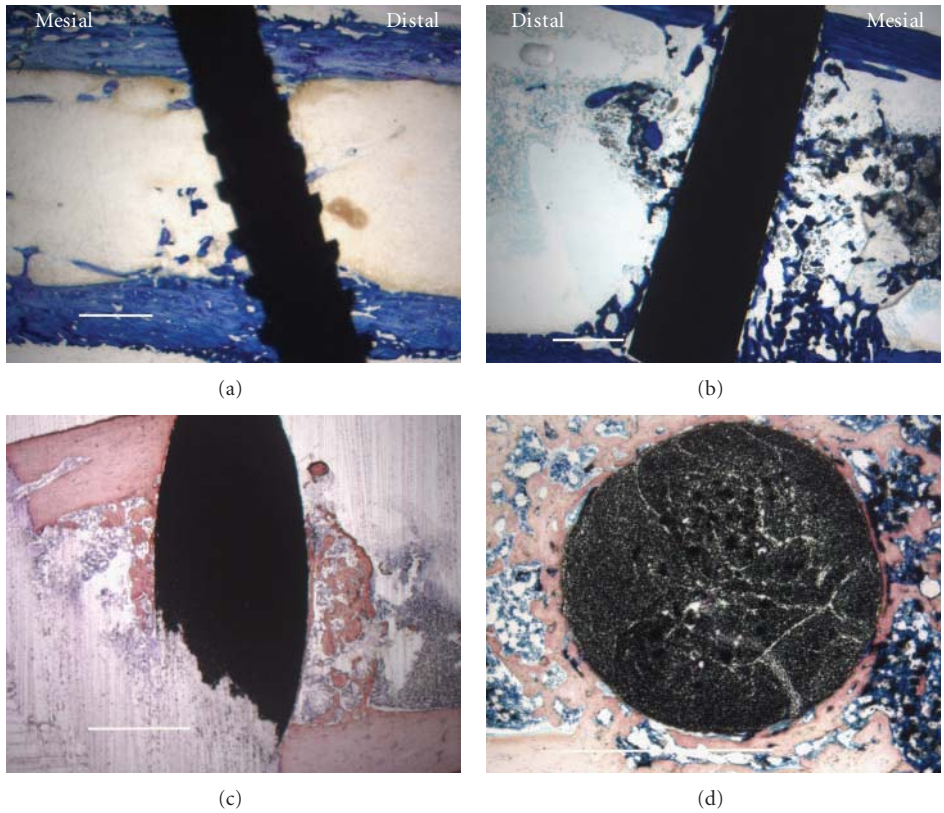

Figure 4: Histological low-magnification imaging with all scale bars approximately 1.0 mm. (a) Lateral section of titanium-6-4 alloy implant as a representative image at the 0.8 mm implant distance (7.1 PBA from 10.5 PBA average) with toluidine blue stain. (b) Lateral section of bisphenyl-polymer/carbon-fiber composite implant was chosen as a representative image at the 0.8 mm implant distance (42.3 PBA from 41.6 PBA average) with toluidine blue stain. (c) Lateral intramedullary section of a bisphenyl-polymer/carbon-fiber composite implant from the fractured sample in Figure 2(c) that appears as dense cortical bone before alcohol and xylene solvent dehydration and clearing, respectively, instead provides contrast with a more trabeculated appearance after some osteoid removal using a modified H&E stain. So, additional osteoid not seen by histology is a probable *in vivo* structure at some level associated with the bisphenyl-polymer/carbon fiber implants. (d) Horizontal section of a bisphenyl-polymer/carbon-fiber implant from an extra tibial study not included in the statistical analysis provides an alternate view of the cut fiber ends to better appreciate the unidirectional composite with a Sanderson's stain. The original implant diameters in all cases were approximately 1.5 mm.

a well-established piezoelectric tissue that polarizes during bending with a negative electron-transfer potential forming in compression where the healing callus forms *in vivo* [30], so that a reduced medical fracture is donating electrons and bonds are formed by electron pairing.

4.4. Carbon-Fiber Conducting Biocircuit and Antioxidant Effect. Carbon-fiber resistivity at about $10^{-5}\,\Omega$m is electrically conducting that compares at a level similar to metals such as cobalt-base Haynes superalloy [18]. Therefore, when carbon fibers are exposed, electron transfer is achievable at the biologic interface into a relative "sea of electrons" where the polymer insulation creates a micro-biocircuit that may prevent redeposition of potentially damaging free radicals locally back into the original surgical inflammatory zones. Direct carbon-fiber exposure to the bioenvironmental surroundings then might efficiently remove damaging electron energy by a simple electrochemical concentration gradient effect to a more positively charged low electron-level tissue. Alternatively, by the same electrochemical concentration gradient effect electrons could be effectively donated to reduce fracture or grow tissue such as the fiber cuff stimulated by fiber fragments in Figures 2(e) and 2(f). In addition to surgically induced inflammation from tissue-cell damage, during cellular energy synthesis excess free radicals subsequently further occur during hypoxic metabolic respiration when oxygen is absent [15–17] which is the common state at the implant interface. Without the final oxygen electron acceptor, metabolic acid cannot combine to form the normal physiologic waste product as water [15–17].

4.5. Carbon-Fiber Oxidation for Covalent Bonds. In addition to hydrophobic or nonpolar bisphenyl-polymer cellular biocompatibility, carbon fibers might be highly compatible with bioorganic carbon-based structures. Although bisphenyl-polymer/carbon-fiber composites are considered nonpolar materials, carbon-fiber outer surfaces are polarized by approximately 20% through oxidation as received thus

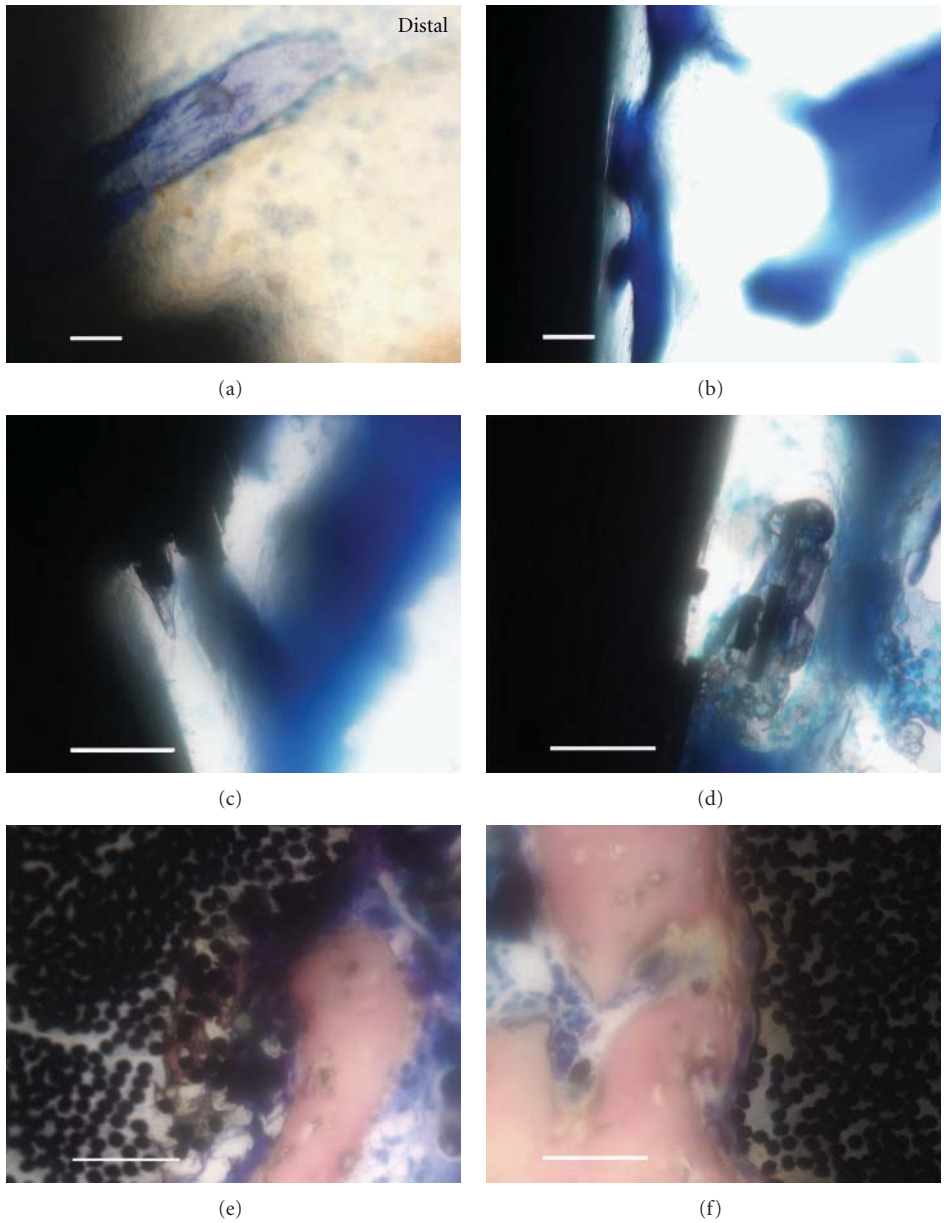

Figure 5: Histological high-magnification imaging with all scale bars approximately 50 μm. (a) Lateral section of the titanium-6-4 alloy image from Figure 4(a) on distal reveals some implant/bone particle integration using toluidine blue stain. (b) Lateral section of a bisphenyl-polymer/carbon-fiber implant exhibits a typical osseointegrated interface with a sophisticated pore-architecture remodeling that may have contained more *in vivo* osteoid using toluidine blue. (c) Lateral section of a bisphenyl-polymer/carbon-fiber implant presents a fractured composite surface that appears to stimulate bone directly onto an area that represents 2 multiple fiber-fracture ends with toluidine blue. (d) Lateral section of a bisphenyl-polymer/carbon-fiber implant shows an osseointegrating interface with multiple fractured fiber-fragment pieces debonded from the composite and encased in bone with toluidine blue. (e) Horizontal section of a bisphenyl-polymer/carbon-fiber composite implant not included in the statistical analysis expresses calcifications as intense bone integration into the implant surrounding individual carbon fibers of approximate 7 μm diameter after removing portions of the polymer matrix utilizing Sanderson's stain. The surface defect is approximately 200 μm deeply. (f) Horizontal section of a bisphenyl-polymer/carbon-fiber composite implant also not included in the statistical analysis shows fibers being pulled away from the implant at the bone interface that would necessarily entail polymer degradation or softening, using Sanderson's stain.

forming R-COOH or R-COH monolayers [31] to provide the possibility of biologically safe more hydrophilic condensation reactions with living cell membranes through peptide amino acids or lipid fatty acids and sugar or glycerol molecules. Cells may then possibly covalently bond directly to the carbon fibers by either the lipid membrane or glycolipids and glycoprotein linkages with only water as a byproduct. As examples, carbon fibers with polymer that acted as substrates for bone formation at the implant interface (Figure 5(b)) were further incorporated directly

into the growing bone (Figures 5(c) and 5(d)) anchored new bone around individual fibers (Figure 5(e)) and were even pulled outward away from the polymer at the implant (Figure 5(f)).

4.6. Bone and Material Stress Transfer. Stress-transfer "shielding" related to differences in modulus between the cortical bone (15–30 GPa) and other materials [20] did not apparently play a role in the polymer/carbon-fiber success (145–325 GPa) compared to titanium-6-4 alloy (116–120 GPa) (Table 1). With both the fiber-reinforced composite and titanium alloy materials displaying moduli of comparative magnitude, stress transfer with bone should be moderately similar. Nonetheless, *in vivo* static forces were basically in play for the intramedullary bone-marrow implants placed. While not another apparent factor in the present low-stress-transfer study, the density mass/volume relationship (g/cm^3) for the bisphenyl-polymer/carbon-fiber composite (1.49–1.6 g/cm^3) is still more similar to cortical bone (1.8–2.1 g/cm^3) than titanium alloy (4.4–5.0 g/cm^3) (Table 1). A lower density material may then improve subsequent biomaterial performance in movement for large implants and proprioception responsive interplay for smaller implants. Also, equivalent density is a probable factor with modulus for uniform stress transfer at the tissue/biomaterial interface, particularly with osseointegration. Further, polymer softening involved in degradation of the composite surface at the bone-tissue interface (Figures 5(c)–5(f)) could improve stress transfer at the molecular and cell levels. Subsequent stress transfer distributed overall more evenly over a greater area through similar modulus/density properties would result in less harmful forces as energy is better dispersed and adsorbed to reduce damage at the molecular and cell levels. Stress transfer then appears to play a possible role in cell differentiation during cell packing at optimum tissue density levels similar to surrounding parenchyma tissue to best reduce molecular damage by equalizing energy adsorption most effectively over a larger volume. Soft polymer/stiff fiber viscoelastic energy damping by the composite [1, 9] could subsequently be another factor in idealized stress transfer between the implant and adjacent mineralizing new bone.

4.7. Nitric Acids and Polymer Degradation. Of all acids (97% sulfuric, 37% hydrochloric, 97% phosphoric, and 70% nitric), nitric acid is the only acid that appreciably reacts with the composite thermoset free-radical cure bisphenyl polymer [17]. In fact, nitric acid reacts many times faster and aggressively with the cured thermoset bisphenyl polymer than the other acids, degrading the polymer entirely into solution while generating an intense green decomposition seen experimentally in our laboratory [17] (Figure 6). Nitric-acid polymer greenish decomposition has also been previously described for epoxy aromatic rings produced from bisphenol [32].

By similar nitric-acid chemical interactions with the bisphenyl polymer, acid concentrating enzymes may provide a nitric-acid type of osseointegrating biopathway [17]. Proteins are the most plentiful physiologic buffering systems for acid [15, 16] that might subsequently produce safe enzymatic polymer degradation. Moreover along with nitric acid, other strong acids similar to the ones mentioned previously or a weak nitrous acid may further be involved in softening the highly structural crosslinked aerospace thermoset bisphenyl polymer at the surface interface. Related nitric-acid ester precursors have already been described biologically as a process that produces a tolerance to nitric oxide and cardiovascular vasodilation [33]. From basic chemistry nitric oxide is unstable with an odd number of electrons [34] and will add to oxygen to form nitrogen dioxide even at room temperature with a decreasing rate with acid by simply dissolving in water [34]. As a consequence, wherever nitric oxide gas forms to reverse the side effects of hypoxic cell mitochondrial free radicals [15–17], nitric acid can ultimately develop [34] whereby negatively charged globular proteins that can further possibly act as enzymes would then be needed for buffering to control pH [15–17]. Nitric acid chemistry with other acids thus appears as a major biochemical need for enzymes that must dissolve difficult biological substrates with aromatic rings. Delocalized free radicals in the protein enzymes should further contribute potential energy with basic components to complement acid degradation. Although toxic breakdown byproducts were considered primarily with the acids and free radicals, the overall abundant bone growth response associated with osseointegration around the carbon fibers suggests that bisphenyl-like molecular structures were further formed as another dominate influence.

4.8. Potential Pharmaceutical and Bone Mineral Polymer Additives. With regard to polymer degradation during periods of oxygen stress at the implant interface, organic therapeutic drugs or inorganic fillers can be designed for incorporation into and release from thermoset polymer-based implants due to low-temperature cures ranging from room temperature to less than 200°C [1, 2]. On the other hand, most metals or ceramics are processed at melting temperatures that can range from approximately 1000 to 3000°C [18] so that pharmaceutical or bone mineral incorporation is impossible. Conversely, by low-thermal process, polymer matrix implants can be designed with therapeutic pharmaceuticals to help recruit, proliferate and differentiate bone-marrow mesenchymal stem cells/osteoprogenitors/osteoblasts for optimum successful results. For instance, Triclosan, a broad-spectrum aromatic molecular antimicrobial diphenyl ether with multiple Food and Drug Administration approvals for medical devices, compatibilizes with similar bisphenyl resins to strengthen and toughen the cured polymer while also reducing resin viscosity to improve resin wetting during fiber impregnation [10, 17]. Related compatible phenyl-aromatic or ring-structured or other organic-type pharmaceuticals may provide numerous biocompatibility avenues for thermoset polymer implant device stem-cell tissue engineering. In fact, aromatic structures compare on a level with amines as a basis for pharmacological therapeutics [35]. Further, ring-structured aromatic molecules are well-known conjugates for estrogens [36] and have been used in the design of

(a) (b)

Figure 6: (a) Typical composite bar exposed to sulfuric acid, hydrochloric acid, or phosphoric acid. (b) Composite bar exposed to nitric acid over a similar time period then washed and dried.

synthetic estrogen-stimulating proteins [37]. Prime examples for thermoset free-radical cure bisphenyl-polymer additive incorporation might include the ring-structured cholesterol derivatives that include vitamin D, anti-inflammatory corticosteroids or steroid tissue-forming androgens and estrogens [15–17]. Further, inorganic bone mineral substitutes can also be cured into the surface ideally engineered for crystallinity or amorphous solubility for long-term or quick release, respectively, for improved osseointegration with respect to continuing stability or immediate bone ingrowth correspondingly.

5. Conclusions

In order to prevent fiber loss in reinforced polymer-based composites planned for future use in medical/dental bone-implant devices, fundamental safety factors can now be included during the design with a proper knowledge of material composite micromechanics and macromechanics. Bisphenyl-polymer/carbon-fiber implants provide performance with mechanical properties comparable to current pure titanium grade metals at lower density with one third of the weight. In addition, the bisphenyl-polymer matrix composite further offered a synthetic estrogen nonpolar osseoconductive bone response that provides polymer-type insights into cellular membrane physiology for strong mesenchymal-stem/osteoprogenitor/osteoblast bone-marrow cell recruitment, proliferation and differentiation. Initial concerns for carbon-fiber fragments appear unwarranted now, as all imaging clearly shows increased bone formation associated with loose fibers. Polymeric-insulated carbon fibers appear to stimulate bone through a possible efficient biocircuit electron-transfer antioxidant effect in addition to direct bone integration by possible condensation with biologic molecules. Implant defects, where hypoxic oxygen concentrations would be expected to be low and saturating tissue with mitochondrial free radicals or acids, were associated with deeper implant osseointegration as polymer was even removed and bone surrounded individual electrical conductive carbon fibers. With the ability to specifically engineer polymer-based high-strength carbon-fiber-reinforced composites that minimally expose fragments and mimic body tissues, future bone implants should be expected to provide longer patient service with improved lightweight performance.

Acknowledgments

This paper is funded through the National Institutes of Health Grant no. T32DE14300. Thanks are due to Jack E. Lemons, M.D., Ph.D., Experimental Procedure, Director Laboratory Surgical Implant Research and Implant Retrieval Analysis Center Department of Surgery, School of Medicine and Department of Biomedical Engineering, School of Engineering, University of Alabama at Birmingham; Michael S. Reddy, DMD, DMS, Biological Technical Advice, Chair Department of Periodontology, University of Alabama at Birmingham; Michael S. McCracken, DDS, PhD, Surgery and Surgical Procedure, Associate Dean School of Dentistry and Department of Biomedical Engineering, University of Alabama at Birmingham; Director Patricia F. Lott, Center for Metabolic Bone Disease-Histomorphometry and Molecular Analysis Core Laboratory, University of Alabama at Birmingham, National Institutes of Health Grant no. P30-AR46031. Preston R. Beck, epoxy/carbon-fiber composite acid testing, Department of Biomaterials, University of Alabama at Birmingham.

References

[1] K. K. Chawla, *Composite Materials*, Springer, New York, NY, USA, 2nd edition, 1998.

[2] S. T. Peters, *Handbook of Composites*, Chapman and Hall, New York, NY, USA, 2nd edition, 1998.

[3] E. C. Dodds and W. Lawson, "Synthetic estrogenic agents without the phenanthrene nucleus [10]," *Nature*, vol. 137, no. 3476, p. 996, 1936.

[4] J. B. Lewis, F. A. Rueggeberg, C. A. Lapp, J. W. Ergle, and G. S. Schuster, "Identification and characterization of estrogen-like components in commercial resin-based dental restorative materials," *Clinical Oral Investigations*, vol. 3, no. 3, pp. 107–113, 1999.

[5] L. Gennari, R. Nuti, and J. P. Bilezikian, "Aromatase activity and bone homeostasis in men," *Journal of Clinical Endocrinology and Metabolism*, vol. 89, no. 12, pp. 5898–5907, 2004.

[6] R. Okazaki, D. Inoue, M. Shibata et al., "Estrogen promotes early osteoblast differentiation and inhibits adipocyte differentiation in mouse bone marrow stromal cell lines that express estrogen receptor (ER) α or β," *Endocrinology*, vol. 143, no. 6, pp. 2349–2356, 2002.

[7] M. N. Weitzmann and R. Pacifici, "Estrogen deficiency and bone loss: an inflammatory tale," *Journal of Clinical Investigation*, vol. 116, no. 5, pp. 1186–1194, 2006.

[8] B. D. Ratner, A. S. Hoffman, F. J. Schoen, and J. E. Lemons, *Biomaterials Science*, Elsevier, San Diego, Calif, USA, 2nd edition, 2004.

[9] B. J. Park and R. S. Lakes, *Biomaterials*, Plenum Press, New York, NY, USA, 2nd edition, 1992.

[10] R. C. Petersen, J. E. Lemons, and M. S. Reddy, "Triclosan antimicrobial for medical/dental devices," in *Proceedings of the 2nd Annual South East Tissue Engineering and Biomaterials Workshop*, p. 52, Birmingham, Ala, USA, February 2005.

[11] D. Sudhin and D. J. Lobse, *Polymeric Compatibilizers*, Hanser, New York, NY, USA, 1996.

[12] A. S. Brown, "Revolution in thermoset composites," *Aerospace America*, vol. 27, no. 7, pp. 18–23, 1989.

[13] R. C. Petersen, J. E. Lemons, and M. S. McCracken, "Micromechanics for fiber volume percent with a photocure vinyl ester composite," *Polymer Composites*, vol. 28, no. 3, pp. 294–310, 2007.

[14] J. V. Milewski, "A study of the packing of milled fibreglass and glass beads," *Composites*, vol. 4, no. 6, pp. 258–265, 1973.

[15] L. Sherwood, *Human Physiology*, Thompson, Belmont, Calif, USA, 5th edition, 2004.

[16] B. Alberts, D. Bray, J. Lewis, M. Raff, K. Roberts, and J. D. Watson, *Molecular Biology of the Cell*, Garland Publishing, New York, NY, USA, 3rd edition, 1994.

[17] R. Petersen, *Micromechanics & Fiber-Reinforced Composites in Biomedical Research*, VDH, Saarbrücken, Germany, 2008.

[18] W. D. Callister, *Materials Science and Engineering*, John Wiley & Sons, New York, NY, USA, 1997.

[19] Y. Ramadin, S. A. Jawad, S. M. Musameh et al., "Electrical and electromagnetic shielding behavior of laminated epoxy-carbon fiber composite," *Polymer International*, vol. 34, no. 2, pp. 145–150, 1994.

[20] G. Ryan, A. Pandit, and D. P. Apatsidis, "Fabrication methods of porous metals for use in orthopaedic applications," *Biomaterials*, vol. 27, no. 13, pp. 2651–2670, 2006.

[21] M. McCracken, J. E. Lemons, F. Rahemtulla, C. W. Prince, and D. Feldman, "Bone response to titanium alloy implants placed in diabetic rats," *International Journal of Oral and Maxillofacial Implants*, vol. 15, no. 3, pp. 345–354, 2000.

[22] A. J. Friedenstein, R. K. Chailakhyan, and U. V. Gerasimov, "Bone marrow osteogenic stem cells: in vitro cultivation and transplantation in diffusion chambers," *Cell and Tissue Kinetics*, vol. 20, no. 3, pp. 263–272, 1987.

[23] J. J. Minguell, A. Erices, and P. Conget, "Mesenchymal stem cells," *Experimental Biology and Medicine*, vol. 226, no. 6, pp. 507–520, 2001.

[24] S. A. Redey, M. Nardin, D. Bernache-Assolant et al., "Behavior of human osteoblastic cells on stoichiometric hydroxyapatite and type A carbonate apatite: role of surface energy," *Journal of Biomedical Materials Research*, vol. 50, no. 3, pp. 353–364, 2000.

[25] P. Zanchetta and J. Guezennec, "Surface thermodynamics of osteoblasts: relation between hydrophobicity and bone active biomaterials," *Colloids and Surfaces B*, vol. 22, no. 4, pp. 301–307, 2001.

[26] D. Halliday, R. Resnick, and J. Walker, *Fundamentals of Physics*, John Wiley & Sons, New York, NY, USA, 4th edition, 1993.

[27] B. S. Avset, "Evaluation of silicon diodes made on a variety of high-resistivity phosphorus-doped substrates," *Nuclear Instruments and Methods in Physics Research A*, vol. 385, no. 1, pp. 137–144, 1997.

[28] G. L. Jendrasiak and R. L. Smith, "The interaction of water with the phospholipid head group and its relationship to the lipid electrical conductivity," *Chemistry and Physics of Lipids*, vol. 131, no. 2, pp. 183–195, 2004.

[29] 29. Kossuth, Quartzel Fused Quartz Textiles, Saint Gobain, Advanced Ceramic Division, Quartz Technology Department, 77793 Nemours Cedex, France. Paris, April 2/1/002E, 1998.

[30] E. Fukada, "History and recent progress in piezoelectric polymers," *IEEE Transactions on Ultrasonics, Ferroelectrics, and Frequency Control*, vol. 47, no. 6, pp. 1277–1290, 2000.

[31] D. Youxian, W. Dianxun, and S. Mujin, "A study of the surface of carbon fiber by means of X-ray photoelectron spectroscopy-III," *Composites Science and Technology*, vol. 30, no. 2, pp. 119–126, 1987.

[32] J. A. Bornmann and C. J. Wolf, "Reaction of nitric acid with a solid epoxy resin," *Journal of Polymer Science*, vol. 22, no. 3, pp. 851–856, 1984.

[33] H. Burkhard and H. Schroder, "Nitrate tolerance is specific for nitric acid esters and its recovery requires an intact protein synthesis," *Biochemical and Biophysical Research Communications*, vol. 1998, no. 1, pp. 232–235, 1998.

[34] S. S. Zumdahl, *Chemistry*, D. C. Heath and Company, Lexington, Mass, USA, 1993.

[35] A. G. Gilman, L. S. Goodman, T. W. Rall, and F. Murad, *The Pharmacological Basis of Therapeutics*, Macmillan Publishing Company, New York, NY, USA, 7th edition, 1985.

[36] S. Christoph and F.-J. Meyer-Almes, "Novel fluorescence based receptor binding assay method for receptors lacking ligand conjugates with preserved affinity: study on estrogen receptor α," *Biopolymers*, vol. 72, no. 4, pp. 256–263, 2003.

[37] R. Kasher, B. Gayer, T. Kulik et al., "Design, synthesis, and evaluation of peptides with estrogen-like activity," *Biopolymers*, vol. 76, no. 5, pp. 404–420, 2004.

Hindawi Publishing Corporation
International Journal of Polymer Science
Volume 2011, Article ID 645820, 7 pages
doi:10.1155/2011/645820

Research Article

In Vitro Evaluation of a Biomedical-Grade Bilayer Chitosan Porous Skin Regenerating Template as a Potential Dermal Scaffold in Skin Tissue Engineering

Chin Keong Lim,[1] Ahmad Sukari Halim,[1] Ismail Zainol,[2] and Kartini Noorsal[3]

[1] *Reconstructive Sciences Unit, School of Medical Sciences, Universiti Sains Malaysia, Kelantan, 16150 Kubang Kerian, Malaysia*
[2] *Department of Chemistry, Faculty of Science and Mathematics, Universiti Pendidikan Sultan Idris, 35900 Tanjung Malim, Perak, Malaysia*
[3] *Advanced Materials Research Centre (AMREC) SIRIM Berhad, Lot 34, Jalan Hi-Tech 2/3, Kulim Hi-Tech Park, Kedah, 09000 Kulim, Malaysia*

Correspondence should be addressed to Ahmad Sukari Halim, ashalim@kb.usm.my

Received 18 May 2011; Revised 10 July 2011; Accepted 10 July 2011

Academic Editor: Shanfeng Wang

Chitosan is a copolymer of *N*-acetylglucosamine and glucosamine. A bilayer chitosan porous skin regenerating template (CPSRT) has been developed for skin tissue engineering. The pore size of the CPSRT was assessed using a scanning electron microscopy (SEM). The *in vitro* cytocompatibility of the CPSRT was tested on primary human epidermal keratinocyte (pHEK) cultures by measuring lactate dehydrogenase (LDH) levels and skin irritation by western blot analysis of the interleukin-8 (IL-8) and tumor necrosis factor-α (TNF-α) secretions. The ability of the CPSRT to support cell ingrowth was evaluated by seeding primary human dermal fibroblasts (pHDFs) on the scaffold, staining the cells with live/dead stain, and imaging the construct by confocal microscopy (CLSM). The CPSRT with pore sizes ranging from 50 to 150 μm was cytocompatible because it did not provoke the additional production of IL-8 and TNF-α by pHEK cultures. Cultured pHDFs were able to penetrate the CPSRT and had increased in number on day 14. In conclusion, the CPSRT serves as an ideal template for skin tissue engineering.

1. Introduction

Biopolymers are naturally synthesized compounds that are produced by living organisms. These materials participate in the natural biological cycle and are eventually degraded and reabsorbed by their environment. Chitin, a biopolymer, can be obtained at relatively low cost from the shells of shellfish (mainly crabs, shrimps, and lobsters), which are a waste product of the seafood processing industry [1]. Chitin and derivatives such as chitosan have a natural basicity that provides properties such as biocompatibility, biodegradability, antibacterial activity, heavy metal ion chelation ability, gel-forming properties, hydrophilicity, and remarkable protein affinity [2].

Chitosan is the primary biopolymer derivative of *N*-deacetylated chitin and consists of *N*-acetylglucosamine and glucosamine. Chitosan possesses an abundance of amino and hydroxyl groups that allow it to be chemically modified by processes such as acylation, *N*-phthaloylation, alkylation, Schiff base formation, reductive alkylation, tosylation, *O*-carboxymethylation, *N*-carboxyalkylation, and graft copolymerization [3, 4]. These modifications allow chitosan's properties to be tailored to a specific application.

Tissue regeneration is a complex biological process that involves inward migration and proliferation of cells into a defect area or scaffold, as well as the secretion of an extracellular matrix to support new tissue formation. Biocompatible tissue engineering constructs can provide cues for cell migration and differentiation to promote wound-healing, tissue formation, and vascular network regrowth. Tissue engineering uses polymer scaffolds to promote cell adhesion, proliferation, and differentiation *in vitro*. Although chitosan has been used in various types of biocompatible wound dressings, such as films, pastes, sheets, and porous templates

[5–8], it also has intrinsic wound-healing abilities [9]. A novel biomedical-grade bilayer chitosan porous skin regenerating template (CPSRT) was developed for use as a dermal scaffold for skin tissue engineering to take advantage of these wound-healing abilities as well as the biocompatible nature of chitosan. The pore size of the CPSRT was assessed using SEM analysis. However, the cytocompatibility and skin irritation of the CPSRT were tested *in vitro* using pHEK cultures. The *in vitro* cellular ingrowth into the CPSRT scaffold was evaluated using pHDF and was observed by CLSM.

2. Materials and Methods

2.1. Preparation and Microstructure Examination of CPSRT. CPSRT was developed at the Advanced Materials Research Centre (AMREC-SIRIM), Malaysia and in accordance with the methods described by Zainol et al. [10]. Pharmaceutical-grade chitosan powder with molecular weight at 634 kDa and deacetylation degree (DD) at 89% was purchased from Hunza Nutriceuticals Sdn Bhd, Perak, Malaysia. Chitosan was dissolved in 1% (v/v) acetic acid to prepare a 2% (w/v) chitosan solution. About 20% (w/w) glycerol were added as a plasticizer, followed by neutralization with sodium bicarbonate to achieve a pH of 6.2. The chitosan solution was then poured into a polytetrafluoroethylene (PTFE) mold and was casted and left dry at room temperature for the preparation of chitosan film. To create the porous structure of the CPSRT, the chitosan solution was frozen at −20°C and lyophilized for 24 hours. The chitosan bilayer CPSRT was fabricated through the attachment of both chitosan film and chitosan sponge using chitosan solution as the glue. The CPSRT was sterilized using ethylene oxide (EO) according to the International Standards Organization (ISO) guidelines (Part 10993–7:1995: Ethylene Oxide Sterilization Residuals).

The microstructure of the CPSRT was then observed *via* an SEM system. Briefly, the CPSRT was fixed in 2.5% glutaraldehyde for 1 hour followed by fixation in 2% Osmiumtetroxid for 30 minutes at room temperature. The CPSRT was then washed two times in distilled water, and the dehydration was performed using a graded series of ethanol (25%, 50%, 75%, and 100% ethanol for 5 minutes each).

2.2. pHEK and pHDF Cultures. Skin samples were obtained from consenting patients who had undergone elective surgery at Hospital Universiti Sains Malaysia, Kubang Kerian, Kelantan, after being approved by the Human Ethic Committee of Universiti Sains Malaysia.

The epidermal layer was lifted from the dermal layer after incubation in a dispase solution (2.4 units/mL). Keratinocytes were released from the epidermal layer using 0.25% trypsin-EDTA for 15 minutes at 37°C. The trypsin was deactivated by adding Dulbecco's minimal Eagle's medium (DMEM) supplemented with 10% fetal bovine serum (FBS). The pHEKs were centrifuged for 7 minutes at 200 ×*g* and were resuspended in CnT-07 (CELLnTEC Advanced cell system) growth medium. pHEK cells were seeded at a density of 2×10^5 viable cells/mL in culture flasks and were incubated at 37°C with 5% CO_2.

The remaining dermal layer was minced into smaller pieces and digested using collagenase type-I (200 cu/mL of DMEM) for 12 hours at 37°C to extract the pHDFs. The dissociated fibroblasts were washed with DPBS, and the cell pellets were sieved through a 70 μm strainer before being centrifuged at 200 ×*g* for 10 minutes. The pHDFs were seeded at 2×10^5 viable cells/mL in DMEM supplemented with 10% FBS and 1% penicillin-streptomycin.

2.3. Cytotoxicity of CPSRT by LDH Assay. The pHEK cultures at passage 3 were seeded at a density of 5×10^4 cells/mL in 24-well plate. CPSRT was sized into 5×5 mm^2 and was washed twice in the CnT-07 medium. The CPSRTs were then placed on 70% confluent cultures of pHEK in the same manner as a direct-contact test. The experiment was performed for 72 hours on 5 skin samples.

At each time point, 100 μL of supernatant was removed and added to an optically clear 96-well flat bottom microplate. This was mixed with 100 μL of LDH reaction mixtures (diaphorase/NAD^+ + iodotetrazolium chloride and sodium lactate) and incubated for 30 minutes at room temperature, as described in the instruction manual of the LDH Cytotoxicity Detection kit (Roche). The optical density (OD) of the test samples and the controls was measured at 490 nm using an enzyme-linked immunosorbent assay (ELISA) plate reader. The reference wavelength was set to 620 nm. pHEK cultures treated with 1% triton-X solution served as the positive control, whereas pHEKs with only growth medium served as the negative control. Background absorbance was measured using growth medium alone. The cytotoxicity was expressed as a percentage of the positive control, as shown in the following equation:

$$\text{Cytotoxicity (\%)} = \frac{(\text{Experimental OD} - \text{Negative control})}{(\text{Positive control} - \text{Negative control})} \times 100\%. \quad (1)$$

2.4. Western Blot Analysis of IL-8 and TNF-α Skin Proinflammatory Cytokines. This experiment was performed according to the western blotting protocols described by Millipore and Coufal et al. [11] with minor modifications. Cultured pHEKs in direct contact with CPSRTs were removed from the 6-well plates at 24 and 72 hours using Accutase.

Protein was extracted from 5×10^6 pelleted cells ($n = 3$) in 1 mL of RIPA buffer with salt (0.4 M sodium chloride, 50 mM Tris-HCl at pH 7.4, 1% NP-40, 0.1% sodium dodecyl sulphate (SDS), 1% Na-deoxycholate, 1 mM EDTA and 1 mM phenylmethanesulphonyl fluoride) at 4°C on a shaker for 5 hours. The lysed cells were then centrifuged at 15,700 ×*g* for 20 minutes at 4°C.

A 10% resolving gel (monomer solution acrylamide, 4X running gel buffer pH 8.8, 10% ammonium persulphate (APS), 10% SDS, TEMED and ddH_2O) was precast for 15 minutes before adding a layer of 7.5% stacking gel on top (monomer solution acrylamide, 4X stacking gel buffer at pH 6.8, 10% APS, 10% SDS, TEMED, and ddH_2O). Ten microliters of sample (at 1 μg/μL total protein concentration) was

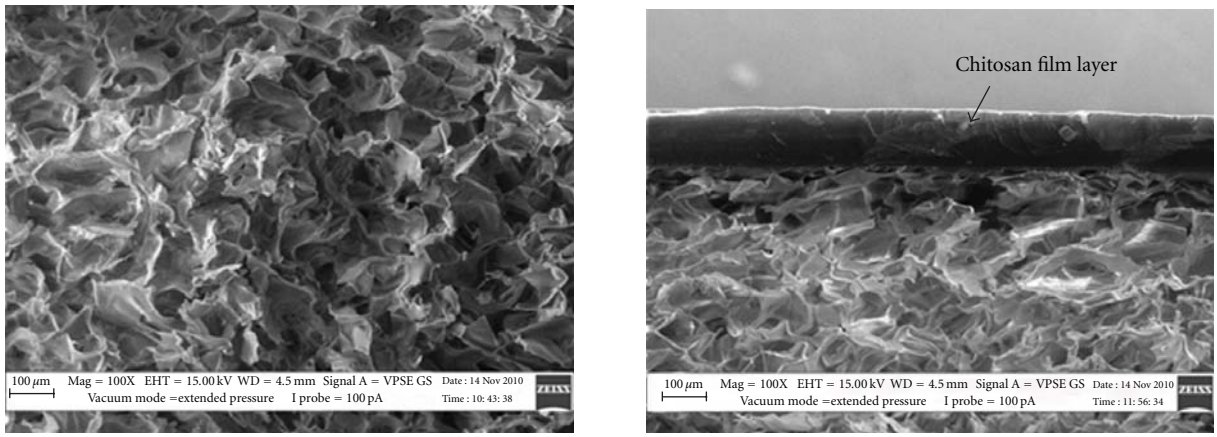

(a) (b)

Figure 1: SEM images of CPSRT. (a) Surface of sponge layer. (b) Cross-sectional view of CPSRT that indicates a chitosan film combining a chitosan porous layer.

mixed with 10 μL of 2X protein sample loading buffer. Protein samples were heated for 5 minutes at 96°C and loaded into wells, followed by the addition of 5 μL of prestained protein ladder in a different well. SDS polyacrylamide gel electrophoresis was performed at 150 V for 45 minutes. Transblotting was conducted at a constant 13 V for 90 minutes.

The transblotted polyvinylidene fluoride membrane was blocked with blocking buffer (5% w/v nonfat milk, 1X Tris buffered saline (TBS) and 0.05% Tween-20) for 1 hour, followed by washing buffer (1X TBS and 0.05% Tween-20) for 10 minutes. The membranes were then incubated with the following primary antibodies: mouse monoclonal anti-human IL-8 (dilution 1 : 1000) (Abcam), TNF-α (dilution 1 : 1000) (Abcam), and loading control alpha-tubulin (dilution 1 : 5000) (Abcam) for 120 minutes each. Goat antimouse HRP-conjugated secondary antibody (dilution at 1 : 2000) (Sigma-Aldrich) was added and incubated for 1 hour at room temperature. The membrane was then incubated with chemiluminescent horseradish peroxidase substrate for 3 minutes at room temperature before visualization and quantification of band intensity using a ChemiImager 4040 image analyzer. Protein band intensity was scored in arbitrary intensity units (AIUs) and was normalized to the alpha-tubulin loading control. Each experiment was repeated in three skin samples. Cultured pHEK in direct contact with low-density polyethylene (LDPE) served as negative control whereas the organotin-polyvinylchloride (PVC) as positive control.

2.5. Growth of pHDF within CPSRT Observed via CLSM Microscopy. pHDF cultures at passage 3 were dislodged from culture flasks and seeded at 2×10^6 viable cells/mL onto CPSRTs in 96-well plates. After 24 hours, the CPSRTs were transferred to 12-well plates. Growth medium was changed every day to mitigate nutrient depletion. Cultures were evaluated at days 5 and 14.

Briefly, CPSRTs were transferred back to 96-well plates and washed twice with Dulbecco's phosphate buffered saline (DPBS) before live/dead cell staining. One hundred microliters of live/dead cell reagents (Molecular Probe, Invitrogen) containing calcein (2 μM) and ethidium homodimer-1 (4 μM) was added to each CPSRT and incubated for 45 minutes at room temperature. CPSRTs were imaged both in cross-section and on the construct surface under a CLSM with excitation/emission wavelengths at 495 nm/515 nm for calcein and 495 nm/635 nm for ethidium-homodimer-1. CPSRTs incubated in growth medium without cultured cells served as the negative control.

2.6. Statistical Analyses. The results are expressed as mean ± standard deviation (SD). The Wilcoxon signed-rank test was used to assess significance among the different experimental conditions. Differences were regarded as significant at $P \leq 0.05$.

3. Results

3.1. Structure of CPSRT. The microstructure of the sponge layer and the cross-sectional view bilayer CPSRT was observed under an SEM (Figure 1). The pore sizes of CPSRT are ranging from 50 to 150 μm (Figure 1(a)). The chitosan film layer was intact to the chitosan porous layer, making up a bilayer structure (Figure 1(b)).

3.2. Cytotoxicity of CPSRT In Vitro. Cytotoxicity *in vitro* was assessed by measuring the amount of LDH released into the supernatant from damaged pHEKs after 72 hours of incubation with CPSRTs, as a percentage of the LDH values in positive controls. The LDH assay indicated that the CPSRTs displayed no measurable cytotoxic behavior when compared with positive controls at all time points (Figure 2). However, cytotoxicity was noticeably elevated after 48 hours of treatment with CPSRTs compared to the 6-hour CPSRT treatment. The CPSRT cytotoxicity was significantly reduced at 72 hours ($P < 0.05$).

3.3. Proinflammatory Cytokine Expression of CPSRT. IL-8 and TNF-α proteins were expressed by pHEKs at all time

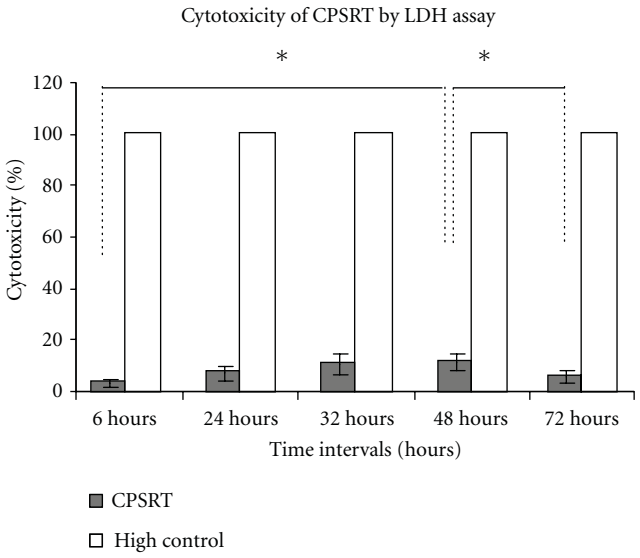

Figure 2: Cytotoxicity of CPSRT as determined by the release of LDH from the damaged cells. $n = 5$, *for $P \leq 0.05$.

points (Figures 3 and 4). pHEKs treated with organotin-PVC produced the most IL-8 and TNF-α at 24 hours, and both proteins were noticeably increased at 72 hours ($P < 0.05$). No significant difference in IL-8 expression was observed between pHEKs treated with CPSRT and LDPE at both time points. However, TNF-α expression remained unchanged in the treatment with CPSRTs at both time points and had the lowest value out of all three groups (CPSRT, organotin-PVC, LDPE). Although pHEKs treated with LDPE expressed higher TNF-α compared with CPSRT at 24 hours, LDPE-induced TNF-α levels declined at 72 hours.

3.4. Ingrowths of pHDF on CPSRT. The ingrowth of pHDF cells was observable at day 5 by CLSM (Figure 5). The viable cultured cells propagated in small groups within the CPSRT pores, as shown by the green fluorescence (Figure 5(a)). No significant quantity of dead or apoptosis cells was seen, indicated by the lack of red fluorescence emission. At fourteen days postseeding, the groups of pHDF cells had proliferated enough to fuse into a larger cell mass that covered the top surface of CPSRT (Figure 5(b)). Furthermore, pHDF cells had also infiltrated and proliferated into the porous structure of CPSRT, as visualized in the cross-sectional view (Figure 5(c)).

4. Discussion

In this study, a skin-like bilayer porous chitosan scaffold mimicking the thickness of natural skin was created for skin tissue engineering. For skin tissue engineering, pore size for a scaffold is recommended to be within the range between 100 to 200 μm [12]. Nevertheless, significant cell proliferation and differentiation were reported for the scaffolds with small pore sizes. Chitosan-gelatin-hydroxyapatite scaffold with pore sizes at the top (65–80 μm) and bottom (10–20 μm), resulted in proliferation of fibroblasts and keratinocytes [13].

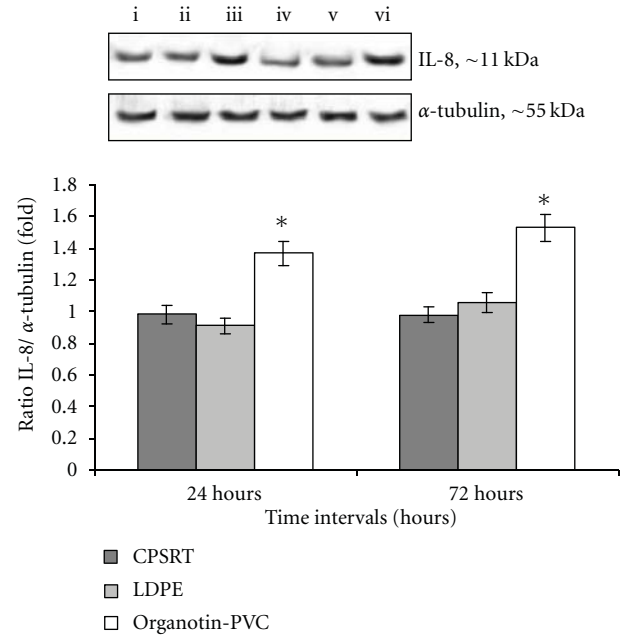

Figure 3: Western blot analysis of IL-8 in pHEK cultures. pHEK cultures were treated for 24 hours ((i) CPSRT, (ii) LDPE, and (iii) organotin-PVC) and 72 hours ((iv) CPSRT, (v) LDPE, and (vi) organotin-PVC) ($n = 3$). *For $P \leq 0.05$ compared with both CPSRT and LDPE.

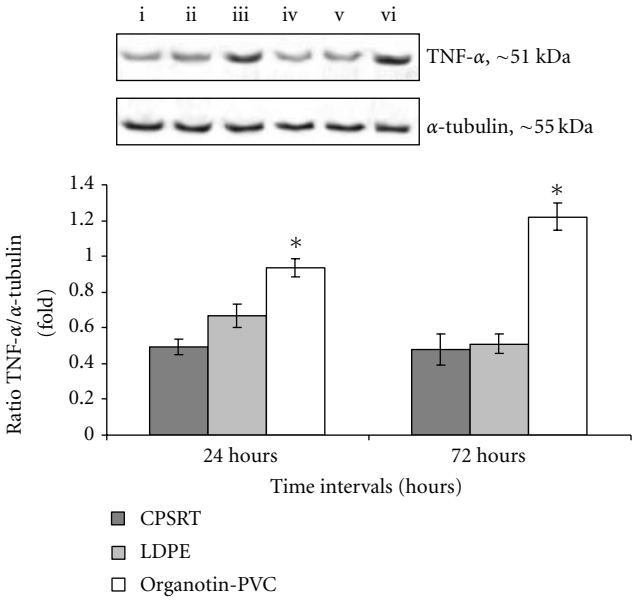

Figure 4: TNF-α protein expression in western blot analysis. pHEK cultures were treated for 24 hours [(i) CPSRT, (ii) LDPE and (iii) organotin-PVC] and 72 hours [(iv) CPSRT, (v) LDPE and (vi) organotin-PVC] ($n = 3$). *For $P \leq 0.05$ compared with CPSRT.

Similarly, lyophilized chitosan scaffold coated with collagen (40–100 μm pore sizes) was shown to have interconnected structure, which enhanced cell proliferation and wound-healing without inflammation [14].

However, although chitosan is biocompatible, to ensure the CPSRT fabrication process did not alter its natural

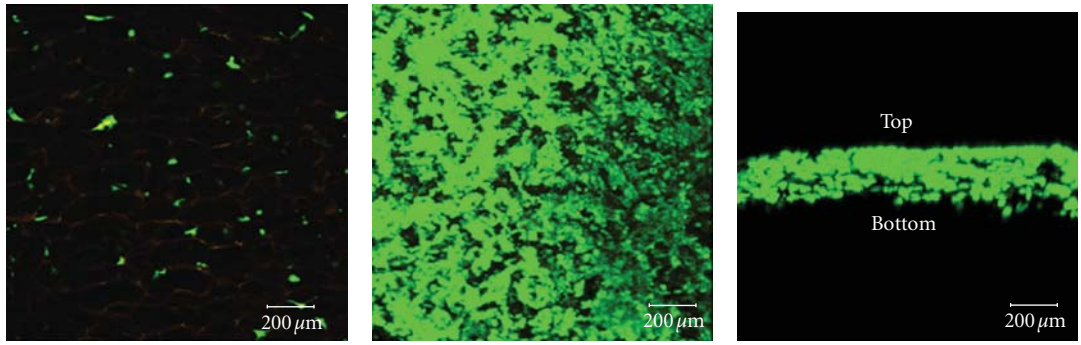

Figure 5: Live/dead cell staining of pHDF cultures seeded on CPSRTs. (a) Three-dimensional (3D) surfaces were scanned using a CLSM at day 5. (b) Viable pHDFs (green) were confluent at day 14. (c) Cross-sectional view of a CPSRT seeded with pHDFs at day 14.

biocompatibility, *in vitro* models of cytotoxicity were used to evaluate the construct. *In vitro* cytotoxicity models are often used to screen for potential harmful effects of chemical compounds because they have good reproducibility and sensitivity, while also minimizing the use of animals. Moreover, cellular cytotoxicity systems are better predictive tools for human toxicity than are whole organism models [5, 6, 15, 16].

By using primary human cell cultures, in this case pHEKs, these results should also better reflect the cytotoxicity outcomes expected in humans, compared with results from transformed cell lines, fibroblasts, or animal cell lines [6, 7, 17, 18]. LDH is a stable cytoplasmic enzyme present in most cells that is released when the plasma membrane is damaged or ruptured. Therefore, measuring LDH levels is a highly sensitive and accurate measure of cytotoxicity [19]. The CPSRTs in this study did not cause significant cytotoxicity compared with the positive control. However, the reduction in LDH observed at 72 hours may be attributed to chitosan-induced proliferation and cell growth, which is corroborated by the findings of Cho et al. [20]. Chitosan's oligomers *N*-acetylglucosamine and glucosamine have been implicated in enhancing cell growth. Glucosamine has been reported to be important for detoxification in the liver and kidneys, as well as in anti-inflammatory, hepatoprotective, antireactive, and antihypoxic activities [21, 22]. *N*-acetylglucosamine is a major component of dermal tissue that is essential for repairing scar tissue and is present in large quantity in the early phase of wound-healing. It has been effective in modulating keratinocyte cellular adhesion, proliferation, and differentiation, leading to the normalization of stratum corneum exfoliation [23]. Therefore, it is possible that CPSRTs could promote the proliferation of keratinocytes by functioning as a controlled delivery source for *N*-acetylglucosamine and glucosamine to the *in vitro* wound-like model in this study.

Because the CPSRT is intended to be a scaffold for skin transplantation, it should avoid irritating epidermal transplantation sites to avoid failure of the bioengineered skin graft. Keratinocytes are the primary cell type in the epidermis and serve as a major contributor of epidermal cytokines, particularly pro-inflammatory cytokines, that act as the first line of defense to protect the body from invaders [24]. Many of the currently identified cytokines, such as IL-6, IL-7, IL-8, and TNF-α, are produced by keratinocytes, either constitutively or upon induction by various stimuli [7, 25]. The findings of this study corroborate the cytokine expression profiles of keratinocytes. The pro-inflammatory cytokines IL-8 and TNF-α were expressed in the negative control cultures, suggesting that these cytokines are constitutively expressed. However, the expression of both cytokines was significantly higher in the positive control, indicating that higher levels of both IL-8 and TNF-α could indicate skin irritation *in vitro*. High expression of TNF-α has been found in patients with keratinocyte lesions, rendering it important role in inflammatory process [26]. Elevated levels of TNF-α expression could indicate activation of cytokine pathways associated with inflammation and disease progression [6]. CPSRTs did not induce increased production of either IL-8 or TNF-α, but maintained levels similar to those in the negative control, suggesting that these scaffolds did not provoke an irritation response *in vitro*.

Combining cells with natural or synthetic scaffolds is a fundamental approach in tissue engineering. The scaffolds help maintain a three-dimensional (3D) space for cells in order to facilitate cellular proliferation and differentiation and to eventually guide cellular organization into a defined architecture for tissue regeneration. Natural biopolymers have been the focus as they are biocompatible, biodegradable and come from renewable resources. Chitosan has structural characteristics similar to glycosaminoglycans, which can be useful for developing a skin replacement. Therefore, the CPSRT was produced in a skin-like format with a 3D porous structure to provide space for cellular ingrowth. Porous chitosan structures can be formed by freezing and lyophilizing chitosan salt solutions in suitable molds. During the freezing process, ice crystals nucleate along thermal gradients and generate a porous structure when removed by lyophilization.

Cultured pHDF cells adapted to the 3D environment by adhering to the 3D structure of the CPSRT at day 5, as verified by live/dead staining and imaging by CLSM.

This CPSRT supports cell attachment, as in agreement with Zhu et al. [27] and Fakhry et al. [28]. Cultured pHDFs grew rapidly and achieved confluence within the CPSRT at fourteen days post-seeding. This growth is likely due to the initial adaptation of cells to the 3D environment by adhering to the chitosan motifs in the construct. In addition, degraded chitosan oligomers have been effective at inducing cell migration and proliferation [29].

5. Conclusion

A naturally derived, bilayer porous biopolymer scaffold, termed a CPSRT, has been developed for skin tissue engineering with pore sizes ranging from 50 to 150 μm. It has been shown to be biocompatible, as it neither induced significant cytotoxic response in the LDH assay nor an irritation response *in vitro*. This biocompatibility is further supported by the observed ingrowth of pHDFs into the CPSRT.

Acknowledgments

This work was supported by a Grant (no. 03-03-01-0000-PR0071/05) from the Intensification of Research in Priority Area Program (IRPA), Ministry of Science, Technology and Innovation (MOSTI) Malaysia, a Grant by International Atomic Energy Agency (IAEA) (no. 304/PPSP/6150097/A127), and a Grant by Research University (RU) from Universiti Sains Malaysia (no. 1001/PPSP/812037).

References

[1] M. G. Peter, "Applications and environmental aspects of chitin and chitosan," *Journal of Macromolecular Science: Pure and Applied Chemistry*, vol. A32, pp. 629–640, 1995.

[2] M. N. V. Ravi Kumar, "A review of chitin and chitosan applications," *Reactive and Functional Polymers*, vol. 46, no. 1, pp. 1–27, 2000.

[3] M. Prabaharan, "Chitosan derivatives as promising materials for controlled drug delivery," *Journal of Biomaterials Applications*, vol. 23, no. 1, pp. 5–36, 2008.

[4] M. Morimoto, H. Saimoto, and Y. Shigemasa, "Control of functions of chitin and chitosan by chemical modification," *Trends in Glycoscience and Glycotechnology*, vol. 14, no. 78, pp. 205–222, 2002.

[5] C. K. Lim, A. S. Halim, H. Y. Lau, Z. Ujang, and A. Hazri, "In vitro cytocology model of oligo-chitosan and N, O-carboxymethyl chitosan using primary normal human epidermal keratinocyte cultures," *Journal of Applied Biomaterials & Biomechanics*, vol. 5, pp. 82–87, 2007.

[6] L. C. Keong and A. S. Halim, "In Vitro models in biocompatibility assessment for biomedical-grade chitosan derivatives in wound management," *International Journal of Molecular Sciences*, vol. 10, no. 3, pp. 1300–1313, 2009.

[7] C. K. Lim, N. S. Yaacob, Z. Ismail, and A. S. Halim, "In vitro biocompatibility of chitosan porous skin regenerating templates (PSRTs) using primary human skin keratinocytes," *Toxicology in Vitro*, vol. 24, no. 3, pp. 721–727, 2010.

[8] M. S. B. Abdull Rasad, A. S. Halim, K. Hashim, A. H. A. Rashid, N. Yusof, and S. Shamsuddin, "In vitro evaluation of novel chitosan derivatives sheet and paste cytocompatibility on human dermal fibroblasts," *Carbohydrate Polymers*, vol. 79, no. 4, pp. 1094–1100, 2010.

[9] D. K. Singh and A. R. Ray, "Biomedical applications of chitin, chitosan, and their derivatives," *Reviews in Macromolecular Chemistry and Physics*, vol. 40, pp. 69–83, 2000.

[10] I. Zainol, S. M. Ghani, A. Mastor, M. A. Derman, and M. F. Yahya, "Enzymatic degradation study of porous chitosan membrane," *Materials Research Innovations*, vol. 13, no. 3, pp. 316–319, 2009.

[11] M. Coufal, M. M. Maxwell, D. E. Russel et al., "Discovery of a novel small-molecule targeting selective clearance of mutant huntingtin fragments," *Journal of Biomolecular Screening*, vol. 12, no. 3, pp. 351–360, 2007.

[12] H. Liu, H. Fan, Y. Cui, Y. Chen, K. Yao, and J. C. H. Goh, "Effects of the controlled-released basic fibroblast growth factor from chitosan-gelatin microspheres on human fibroblasts cultured on a chitosan-gelatin scaffold," *Biomacromolecules*, vol. 8, no. 5, pp. 1446–1455, 2007.

[13] H. Liu, Y. Yin, and K. Yao, "Construction of chitosan-gelatin-hyaluronic acid artificial skin in vitro," *Journal of Biomaterials Applications*, vol. 21, no. 4, pp. 413–430, 2007.

[14] H. R. Lin, K. S. Chen, S. C. Chen et al., "Attachment of stem cells on porous chitosan scaffold crosslinked by Na5P3O10," *Materials Science and Engineering C*, vol. 27, no. 2, pp. 280–284, 2007.

[15] X. Ponsoda, C. Núñez, J. V. Castell, and M. J. Gómez-Lechón, "Evaluation of the cytotoxic effects of MEIC chemicals 31-50 on primary culture of rat hepatocytes and hepatic and non-hepatic cell lines," *ATLA Alternatives to Laboratory Animals*, vol. 25, no. 4, pp. 423–436, 1997.

[16] A. Yang, D. L. Cardona, and F. A. Barile, "Subacute cytotoxicity testing with cultured human lung cells," *Toxicology in Vitro*, vol. 16, no. 1, pp. 33–39, 2002.

[17] C. Clemedson, F. A. Barile, C. Chesné et al., "MEIC evaluation of acute systemic toxicity. Part VII. Prediction of human toxicity by results from testing of the first 30 reference chemicals with 27 further in vitro assays," *ATLA Alternatives to Laboratory Animals*, vol. 28, supplement 1, pp. 161–200, 2000.

[18] G. R. Sharpe and C. Fisher, "Time-dependent inhibition of growth of human keratinocytes and fibroblasts by cyclosporin A: effect on keratinocytes at therapeutic blood levels," *British Journal of Dermatology*, vol. 123, no. 2, pp. 207–213, 1990.

[19] C. Baba, K. Yanagida, T. Kanzaki, and M. Baba, "Colorimetric lactate dehydrogenase (LDH) assay for evaluation of antiviral activity against bovine viral diarrhoea virus (BVDV) in vitro," *Antiviral Chemistry and Chemotherapy*, vol. 16, no. 1, pp. 33–39, 2005.

[20] Y. W. Cho, Y. N. Cho, S. H. Chung, G. Yoo, and S. W. Ko, "Water-soluble chitin as a wound healing accelerator," *Biomaterials*, vol. 20, no. 22, pp. 2139–2145, 1999.

[21] D. W. Lee, S. A. Shirley, R. F. Lockey, and S. S. Mohapatra, "Thiolated chitosan nanoparticles enhance anti-inflammatory effects of intranasally delivered theophylline," *Respiratory Research*, vol. 7, article no. 112, 2006.

[22] I. Setnikar, R. Cereda, M. A. Pacini, and L. Revel, "Antireactive properties of glucosamine sulfate," *Arzneimittel-Forschung*, vol. 41, no. 2, pp. 157–161, 1991.

[23] T. Mammone, D. Gan, C. Fthenakis, and K. Marenus, "The effect of N-acetyl-glucosamine on stratum corneum desquamation and water content in human skin," *Journal of Cosmetic Science*, vol. 60, no. 4, pp. 423–428, 2009.

[24] D. N. Sauder, "The role of epidermal cytokines in inflammatory skin diseases," *Journal of Investigative Dermatology*, vol. 95, no. 5, pp. 27–28, 1990.

[25] A. Oxholm, M. Diamant, P. Oxholm, and K. Bendtzen, "Interleukin-6 and tumour necrosis factor alpha are expressed

by keratinocytes but not by Langerhans cells," *APMIS*, vol. 99, no. 1, pp. 58–64, 1991.

[26] D. Daliani, R. A. Ulmer, C. Jackow et al., "Tumor necrosis factor-α and interferon-γ, but not HTLV-I tax, are likely factors in the epidermotropism of cutaneous T-cell lymphoma via induction of interferon-inducible protein-10," *Leukemia and Lymphoma*, vol. 29, no. 3-4, pp. 315–328, 1998.

[27] A. P. Zhu, S. Q. Wang, D. M. Cheng et al., "Attachment and growth of cultured fibroblast cells on chitosan/PHEA-blended hydrogels," *Chinese Journal of Biotechnology*, vol. 18, no. 1, pp. 109–111, 2002.

[28] A. Fakhry, G. B. Schneider, R. Zaharias, and S. Şenel, "Chitosan supports the initial attachment and spreading of osteoblasts preferentially over fibroblasts," *Biomaterials*, vol. 25, no. 11, pp. 2075–2079, 2004.

[29] Y. Okamoto, A. Inoue, K. Miyatake, K. Ogihara, Y. Shigemasa, and S. Minami, "Effects of chitin/chitosan and their oligomers/ monomers on migrations of macrophages," *Macromolecular Bioscience*, vol. 3, no. 10, pp. 587–590, 2003.

Hindawi Publishing Corporation
International Journal of Polymer Science
Volume 2011, Article ID 290602, 19 pages
doi:10.1155/2011/290602

Review Article

Polymeric Scaffolds in Tissue Engineering Application: A Review

Brahatheeswaran Dhandayuthapani, Yasuhiko Yoshida, Toru Maekawa, and D. Sakthi Kumar

Bio-Nano Electronics Research Centre, Graduate School of Interdisciplinary New Science, Toyo University, Kawagoe, Saitama 350-8585, Japan

Correspondence should be addressed to D. Sakthi Kumar, sakthi@toyo.jp

Received 16 May 2011; Revised 29 June 2011; Accepted 9 July 2011

Academic Editor: Shanfeng Wang

Current strategies of regenerative medicine are focused on the restoration of pathologically altered tissue architectures by transplantation of cells in combination with supportive scaffolds and biomolecules. In recent years, considerable interest has been given to biologically active scaffolds which are based on similar analogs of the extracellular matrix that have induced synthesis of tissues and organs. To restore function or regenerate tissue, a scaffold is necessary that will act as a temporary matrix for cell proliferation and extracellular matrix deposition, with subsequent ingrowth until the tissues are totally restored or regenerated. Scaffolds have been used for tissue engineering such as bone, cartilage, ligament, skin, vascular tissues, neural tissues, and skeletal muscle and as vehicle for the controlled delivery of drugs, proteins, and DNA. Various technologies come together to construct porous scaffolds to regenerate the tissues/organs and also for controlled and targeted release of bioactive agents in tissue engineering applications. In this paper, an overview of the different types of scaffolds with their material properties is discussed. The fabrication technologies for tissue engineering scaffolds, including the basic and conventional techniques to the more recent ones, are tabulated.

1. Introduction

The field of tissue engineering has advanced dramatically in the last 10 years, offering the potential for regenerating almost every tissue and organ of the human body. Tissue engineering and the related discipline of regenerative medicine remain a flourishing area of research with potential new treatments for many more disease states. The advances involve researchers in a multitude of disciplines, including cell biology, biomaterials science, imaging, and characterization of surfaces and cell material interactions. Tissue engineering aims to restore, maintain, or improve tissue functions that are defective or have been lost by different pathological conditions, either by developing biological substitutes or by reconstructing tissues. The general strategies adopted by tissue engineering can be classified into three groups [1]: (i) Implantation of isolated cells or cell substitutes into the organism, (ii) delivering of tissue-inducing substances (such as growth factors), and (iii) placing cells on or within different matrices. The last of these strategies is more frequently associated with the concept of tissue engineering, that is, the use of living cells seeded on a natural or synthetic extracellular substrate to create implantable pieces of the organism [2].

Scaffold design and fabrication are major areas of biomaterial research, and they are also important subjects for tissue engineering and regenerative medicine research [1]. Scaffold plays a unique role in tissue regeneration and repair. During the past two decades, many works have been done to develop potentially applicable scaffold materials for tissue engineering. Scaffolds are defined as three-dimension porous solid biomaterials designed to perform some or all of the following functions: (i) promote cell-biomaterial interactions, cell adhesion, and ECM deposition, (ii) permit sufficient transport of gases, nutrients, and regulatory factors to allow cell survival, proliferation, and differentiation, (iii) biodegrade at a controllable rate that approximates the rate of tissue regeneration under the culture conditions of interest, and (iv) provoke a minimal degree of inflammation or toxicity *in vivo* [3]. The developing scaffolds with the optimal

characteristics, such as their strength, rate of degradation, porosity, and microstructure, as well as their shapes and sizes, are more readily and reproducibly controlled in polymeric scaffolds [4]. The few scaffolds that have displayed biological activity have induced regeneration of tissues and organs that do not regenerate spontaneously and have been referred as regeneration templates. Biological scaffolds are derived from human, animal tissues and synthetic scaffolds from polymers. The first biologically active scaffold was synthesized in 1974; its degradation behavior and exceptionally low antigenicity *in vivo*, as well as its thromboresistant behavior *in vitro,* were described [5]. The initial patent describing these scaffolds was granted in 1977 [6]. Principles for synthesizing a biologically active scaffold, including the critical importance of the degradation rate, was described in detail in 1980 [7]. The first reports of induced regeneration of tissue in an adult (dermis) by a scaffold in animals [8, 9] and humans [10], peripheral nerve regeneration across a gap of unprecedented length [11], and regeneration of the conjunctiva [12].

Biomaterials play a critical role in this technology by acting as synthetic frameworks referred as scaffolds, matrices, or constructs. The state of the art in biomaterials design has continuously evolved over the past few decades. In recent years, there has been increasing importance on materials that could be used in biomedical areas. Biomaterials intended for biomedical applications target to develop artificial materials that can be used to renovate or restore function of diseased or traumatized tissues in the human body and thus improve the quality of life. After an early empirical phase of biomaterials selection based on availability, design attempts were primarily focused on either achieving structural/mechanical performance or on rendering biomaterials inert and thus unrecognizable as foreign bodies by the immune system. Biomaterials used as implants in the form of sutures, bone plates, joint replacements, ligaments, vascular grafts, heart valves, intraocular lenses, dental implants, and medical devices like pacemakers, biosensors, and so forth [13, 14].

In the last four decades, significant advances have been made in the progress of scaffolds for biomedical applications. This paper is intended to illustrate the various scaffolds in the field of tissue engineering. It covers the most commonly used scaffold's fabrication technologies.

2. Natural Polymers and Synthetic Polymers for Scaffolds

Polymers have been widely used as biomaterials for the fabrication of medical device and tissue-engineering scaffolds [15, 16]. In biomedical applications, the criteria for selecting the materials as biomaterials are based on their material chemistry, molecular weight, solubility, shape and structure, hydrophilicity/hydrophobicity, lubricity, surface energy, water absorption degradation, and erosion mechanism. Polymeric scaffolds are drawing a great attention due to their unique properties such as high surface-to-volume ratio, high porosity with very small pore size, biodegradation, and mechanical property. They offer distinct advantages of biocompatibility, versatility of chemistry, and the biological properties which are significant in the application of tissue engineering and organ substitution. Researchers have attempted to grow skin and cartilage [17], bone and cartilage [18], liver [19], heart valves and arteries [20], bladder [21], pancreas [22], nerves [23], corneas [24], and various other soft tissues [25].

Scaffold materials can be synthetic or biologic, degradable or nondegradable, depending on the intended use [13]. The properties of polymers depend on the composition, structure, and arrangement of their constituent macromolecules. It can be categorized into different types in terms of their structural, chemical, and biological characteristics, for example, ceramics, glasses, polymers, and so forth. Naturally occurring polymers, synthetic biodegradable, and synthetic nonbiodegradable polymers are the main types of polymers used as biomaterials.

Natural polymers can be considered as the first biodegradable biomaterials used clinically [26]. Natural materials owing to the bioactive properties have better interactions with the cells which allow them to enhance the cells' performance in biological system. Natural polymers can be classified as proteins (silk, collagen, gelatin, fibrinogen, elastin, keratin, actin, and myosin), polysaccharides (cellulose, amylose, dextran, chitin, and glycosaminoglycans), or polynucleotides (DNA, RNA) [27].

Synthetic biomaterial guidance provided by biomaterials may facilitate restoration of structure and function of damaged or diseased tissues. Synthetic polymers are highly useful in biomedical field since their properties (e.g., porosity, degradation time, and mechanical characteristics) can be tailored for specific applications. Synthetic polymers are often cheaper than biologic scaffolds; it can be produced in large uniform quantities and have a long shelf time. Many commercially available synthetic polymers show physicochemical and mechanical properties comparable to those of biological tissues. Synthetic polymers represent the largest group of biodegradable polymers, and they can be produced under controlled conditions. They exhibit, in general, predictable and reproducible mechanical and physical properties such as tensile strength, elastic modulus, and degradation rate [28]. PLA, PGA, and PLGA copolymers are among the most commonly used synthetic polymers in tissue engineering [29]. PHA belongs to a class of microbial polyesters and is being increasingly considered for applications in tissue engineering [30].

Bioactive ceramics, such as HAP, TCP, and certain compositions of silicate and phosphate glasses (bioactive glasses) and glass-ceramics (such as apatite-wollastonite) react with physiological fluids and through cellular activity form tenacious bonds to hard and in some cases soft tissue engineering [31]. However, their biocompatibility and biodegradability are often insufficient, limiting their potential use in the clinical side. We can overcome these issues by blending synthetic and natural polymers or by using composite materials that improve the scaffold properties and thereby allowing controlled degradation [32] and improving the biocompatibility in tissue engineering applications [33]. The combination of degradable polymers and inorganic bioactive particles represents the approach in terms of achievable mechanical and biological performance in hard tissue [34].

3. Three-Dimensional Polymeric Scaffold Fabrication and Different Types of Scaffolds

In an era of decreasing availability of organs for transplantation and a growing need for suitable replacements, the emerging field of tissue engineering gives hope to patients who desperately require tissue and organ substitutes. Since 1980, researchers have developed many novel techniques to shape polymers into complex architectures that exhibit the desired properties for specific tissue-engineering applications. These fabrication techniques result in reproducible scaffolds for the regeneration of specific tissues. Polymer scaffolds can provide mechanical strength, interconnected porosity and surface area, varying surface chemistry, and unique geometries to direct tissue regeneration [138]. Scaffolding is essential in this endeavor to act as a three-dimensional template for tissue ingrowths by mimicking ECM [139]. These key scaffold characteristics can be tailored to the application by careful selection of the polymers, additional scaffold components, and the fabrication technique. Typical scaffold designs have included meshes, fibers, sponges and foams, and so forth. These designs are chosen because they promote uniform cell distribution, diffusion of nutrients, and the growth of organized cell communities [140]. The fabrication technique for tissue engineering scaffolds depends almost entirely on the bulk and surface properties of the material and the proposed function of the scaffold. Most techniques involve the application of heat and/or pressure to the polymer or dissolving it in an organic solvent to mold the material into its desired shape. While each method presents distinct advantages and disadvantages, the appropriate technique must be selected to meet the requirements for the specific type of tissue. Scaffolds structure development is directly related to many methods, which are listed in Table 1.

Large numbers of scaffolds from different biomaterials are available for clinical use which is listed in Table 2. In order to repair and regenerate lost or damaged tissue and organs, 3D scaffolds must be designed, fabricated, and utilized to regenerate the tissue similar in both anatomical structure and function to the original tissue or organ to be replaced or repaired. Different types of scaffolds, including porous scaffold, microsphere scaffold, hydrogel scaffold, fibrous scaffold, polymer-bioceramic composite scaffold, and acellular scaffolds are described in this paper.

4. Porous Scaffold

The three-dimensional polymeric porous scaffolds with higher porosities having homogeneous interconnected pore network are highly useful for tissue engineering. Sponge or foam porous scaffold have been used in tissue engineering applications [50], especially for growth of host tissue, bone regrowth, or organ vascularization. Their porous network simulates the ECM architecture allowing cells to interact effectively with their environment. Though foams and sponges are more mechanically stable compared to mesh structures, their use is still limited due to the open spaces present throughout the scaffold. A foam polymeric scaffold approach has several potential advantages for proliferating or adherent cell lines such as (a) provide a physical surface onto which the cells can lay their own ECM, (b) may inhibit cell growth of adherent contact-inhibited cells, (c) provides improved nutrient transport to the center of the device through the porous interconnecting channel network, and (d) may limit cluster size to the pore size of the foam and thereby eliminating very large clusters that can potentially develop a necrotic center. Depending on the choice of solvent and phase separating conditions, the foams can be controlled to form either random or oriented pore architectures [141].

Improvement in the structure and increased pore interconnectivity of the porous scaffold is required for the development of artificial blood vessels or peripheral nerve growth. Precise three-dimensional shapes are required which lead to the development of sophisticated extrusion technologies [142] and methods of adhering porous membranes to the desirable shapes [143]. Ideal pore sizes vary for different cells and tissues [144]. Porous scaffolds can be manufactured with specific pore size, porosity, surface-area-to-volume ratio and crystallinity. Porous controlled-release systems contain pores that are large enough to enable diffusion of the drug [145]. Synthetic biodegradable polymers such as PLLA, PGA, PLGA [50], PCL [146], PDLLA, PEE based on PEO, and PBT [147] are used as porous scaffolding materials. For enhanced control over porosity and pore diameter as compared to most fabrication methods, a solvent casting and particulate leaching technique was developed. A modern method for creating porous scaffolds composed of nano- and microscale biodegradable fibers by electrospinning is a latest development in this field.

5. Hydrogel Scaffold

In the last decade, hydrogels have played an ever increasing role in the revolutionary field of tissue engineering where they are used as scaffolds to guide the growth of new tissues. The design and application of biodegradable hydrogels has dramatically increased the potential impact of hydrogel materials in the biomedical field and enabled the development of exciting advances in controlled drug delivery and tissue engineering applications [148]. Hydrogels comprised of naturally derived macromolecules have potential advantages of biocompatibility, cell-controlled degradability, and intrinsic cellular interaction. They may exhibit batch variations and generally exhibit a narrow and limited range of mechanical properties. In contrast, synthetic polymers can be prepared with precisely controlled structures and functions. Hydrogels have structural similarity to the macromolecular-based components in the body and are considered biocompatible [149]. Gels are formed when the network is covalently crosslinked [150]. Hydrogels are made either from synthetic or natural polymers, which are crosslinked through either covalent or noncovalent bonds. Hydrogels in tissue engineering must meet a number of design criteria to function appropriately and promote new tissue formation. These criteria include both classical physical parameters (e.g., degradation and mechanics) as well as

Table 1: Scaffolds' fabrication techniques in tissue engineering applications.

Method	Polymers	Unique factors	Application
Biodegradable porous scaffold fabrication			
Solvent casting/salt leaching method [35–37]	Absorbable polymer (PLLA, PLGA, collagen, etc.)	Biodegradable controlled porous scaffolds	Bone and cartilage tissue engineering
Ice particle leaching method [38–40]	PLLA & PLGA	Control of pore structure and production of thicker scaffolds	Porous 3D scaffolds for bone tissue engineering
Gas foaming/salt leaching method [41–43]	PLLA, PLGA & PDLLA	Controlled porosity and pore structure sponge	Drug delivery and tissue engineering
Microsphere fabrication			
Solvent evaporation technique [44–46]	PLGA, PLAGA	High-density cell culture, due to the extended surface area	Bone repair
Particle aggregated scaffold [47–49]	Chitosan, HAP	High mechanical stability	Bone, cartilage, or osteochondral tissue engineering
Freeze drying method [50–52]	PLGA, PLLA, PGA, PLGA/PPF, Collagen, and Chitosan	3D porous sponge structure, durable and flexible	Tissue engineering scaffolds
Thermally induced phase separation [53, 54]	PEG, PLLA	Highly porous scaffold for cellular transplantation	Complicated shapes for tissue engineering applications
Injectable gel scaffold fabrication			
Ceramic-based injectable scaffolds [55–57]	CP ceramics, HAp, TCP, BCP, and BG	Porosity and bioresorbability	Cartilage tissue engineering
Hydrogel-basedinjectable scaffolds [58–60]	Hydrophilic/hydrophobic diblock and triblock copolymer combinations of PLA, PGA, PLGA, and PEG. Copolymers of PEO and PPO and polyoxamer. alginates, collagen, chitosan, HA, and fibroin	Biomimetically, exhibit biocompatibility and cause minimal inflammatory responses, thrombosis, and tissue damage	Cartilage, bone tissue engineering, and drug delivery
Hydrogel scaffold fabrication			
Micromolding [61–63]	Alginate, PMMA, HA, PEG	Microgels, biologically degradable, mechanical and physical Complexity	Insulin delivery, gene therapy, bioreactor, and immunoisolation
Photolithography [64–66]	Chitosan, fibronectin, HA, PEG, PNIAAm, PAA, PMMA, PAam, and PDMAEM	Microwells, microarrays, controlled size and shape	Microdevices, biosensors, growth factors, matrix components, forces, and cell-cell interactions
Microfluidics [67–69]	PGS, PEG, calcium alginate, silicon and PDMS	Microbeads, microrods, valves, and pumps	Sensing, cell separation, cell-based microreactors, and controlled microreactors,
Emulsification [70–72]	Gelatin, HA, and collagen	Microgels, microsensors, cell-based diagnostics	Sustainable and controllable drug delivery therapies
Acellular scaffold fabrication			
Decellularisation process [73–75]	Biological tissues	Retain anatomical structure, native ECM, and similar biomechanical properties	Tissue engineering
Keratin scaffold fabrication			
Self-assembled process [76–78]	Keratin	Biocompatibility	Drug delivery, wound healing, soft tissue augmentation, synthetic skin, coatings for implants, and scaffolds for tissue engineering

Table 1: Continued.

Method	Polymers	Unique factors	Application
Fibrous scaffold fabrication			
Nanofiber electrospinning process [79–81]	PGA, PLA, PLGA, PCL copolymers, collagen, elastin, and so forth	High surface area, biomechanical, and biocompatibility	Drug delivery, wound healing, soft tissue synthetic skin, and scaffolds for tissue engineering
Microfiber wet-spinning process [82–84]	PLGA, PLA, chitosan, and PCL	Biocompatible fibres with good mechanical properties	Solar sails, reinforcement, vascular grafts, nonwetting textile surfaces, and scaffolds for tissue
Nonwoven fibre by melt-blown process [85–87]	Polyesters, PGA, and PDO	Submicron fiber size, highly porous scaffold	Filtration, membrane separation, protective military clothing, biosensors, wound dressings, and scaffolds for tissue engineering
Functional scaffold fabrication			
Growth factor's release process [88–90]	Collagen, gelatin, alginate, chitosan, fibrin, PLGA, PLA, and PEG	Membranes, hydrogels, foams, microsphere, and particles	Angiogenesis, bone regeneration, and wound healing
Ceramic scaffold fabrication			
Sponge replication method [91–93]	PU sponge, PVA, TCP, BCP or calcium sulfate	Interconnected porous ceramic scaffolds	Bone tissue engineering
Simple calcium phosphate coating method [94–96]	Coating on: metals, glasses, inorganic ceramics and organic polymers (PLGA, PS, PP, silicone, and PTFE), collagens, fibres of silk, and hairs	Improve biocompatibility or enhance the bioreactivity	Orthopedic application
Automation and direct organ fabrication			
Inkjet printing process [97–100]	Sodium alginate	To build complex tissues composed of multiple cell types (Hydrogel scaffold)	Biosensor development, microdeposition of active proteins on cellulose, biochips and acellular polymeric scaffolds
Melt-based rapid prototyping process [101, 102]	Biodegradeable polymers or blends	Complex 3D solid object, good mechanical strength	Honey comb structure scaffold, hard-tissue scaffolds
Computer-aided design (CAD) data manipulation techniques [103–105]		Design and fabrication of patient-specific scaffolds and automated scaffold assembly algorithm	Develop a program algorithm that can be used to design scaffold internal architectures
Organ printing [106, 107]	Tubular collagen gel	Layer by layer deposition of cells or matrix	To print complex 3D organs with computer-controlled,
Scaffold sterilization			
Ethylene oxide gas (EOG) [108–110]		For degradable polymers and porous scaffolds, high penetration ability, and compatibility	Absolute freedom from biological contamination in scaffolds
Gamma-radiation sterilization [111–113]		Proven process is safe, reliable, and highly effective at treating single-use medical devices	Surgical disposables: surgical sutures, bandages, dressings, gauge pads, implants
Electron beam radiation [114–116]		Compatibility, low penetration, in line sterilization of thin products	Commercially successful technology for sterilizing a variety of disposable medical devices with a wide range of densities
Dry-heat sterilization [117, 118]		Efficacy, speed, process simplicity, and lack of toxic residues	Heat is absorbed by the exterior surface of scaffold and then passed inward to the next layer
Steam sterilization [119, 120]		Removal of all contamination, and scaffold can be reused	Porous scaffold for living cell immobilization

Table 2: List of commercial polymeric scaffolds' products.

Polymer	Property	Biomedical application	Trade name
PGA	Regenerate biological tissue [121]	First biodegradable synthetic suture in 1969	DEXON
	Good mechanical properties [122]	Bone internal fixation devices	Biofix
PLLA	Good tensile strength	Orthopaedic fixation devices	Bio-Anchor, Meniscal Stinger, The Clearfix Meniscal Dart
	Improved suture [123]	High-strength fibers (FDA approved at 1971)	DEXON
	Nondegradable fibers [124]	Ligament replacement or augmentation devices	Dacron
	Fiber-based devices [125]	Blood vessel conduits	
	Injectable form	People with human immunodeficiency virus or correction of facial fat loss	
PLDLA	Better property modulation [126]	Bioresorbable implant material	Resomer
PLGA	High degradation	Multifilament suture	Vicryl, Vicryl Rapid & CRYL
	Form of meshes	Skin graft	Vicryl Mesh
PLGA-collagen	Matrix	Tissue regeneration membrane	CYTOPLAST Resorb
PLGA	Prostate cancer	Drug delivery vehicle	LUPRON DEPOT
		First commercially developed monofilament suture (1980)	PDS
PDS	Fixation screws for small bone and osteochondral fragments	Orthopaedic applications	Pins
PCL	Long-term zero-order release [26]	Long-term contraceptive device	Capronor
PDLLA-CL	Fibers less stiff	Monofilament suture	MONACRYL
PGCL, PLCL, and PEG	Bioresorbable multiblock	Drug delivery vehicle for small, and medium-sized biologically active molecules	SynBiosys
PCLTMC	multiblock	Flexible suture materials	Maxon
and PGCL		Orthopaedic tacks and screws	Acufex
PHBHV	Piezoelectricity property [127]	Bone pins and plates and drug delivery	
PEU	High porous & no adverse effect [128]	Tissue engineering application	Degrapol
LDI-based PU	Injectable & good mechanical property [129]	Orthopaedic applications & bone cement	Polynova
PEAs	Potential bioresorbable suture materials	Site-specific delivery of small hydrophobic drugs and peptides	CAMEO
POE	Hydrophobic, surface eroding [130]	Drug delivery applications and ocular applications	Alzamer
Polyanhydrides	Surface erosion & biocompatibility Evaluations [131]	Chemotherapeutic, brain cancer (FDA approved)	Gliadel
PCA	Absorb or encapsulate a wide range of drug or protein molecules [132]	First biodegradable polymers used for developing nanoparticles for drug delivery application	
	Synthetic surgical glue, skin adhesive, and an embolic material	Tissue adhesives for topical skin application (FDA approved)	Dermabond
	Major component of skin and other musculoskeletal tissues [133]	Bilayer skin substitute (FDA approved)	Integra Dermal Regeneration Template
		Wound dressings	Biobrane &Alloderm
Collagen	Scaffolds for cardiovascular, musculoskeletal & nervous tissue engineering [133]	Bioengineered skin equivalents	TransCyte

Table 2: Continued.

Polymer	Property	Biomedical application	Trade name
HA	Promote angiogenesis [134]	Wound dressing application	HYAFF
	Sponge as a carrier vehicle for osteoinductive protein [135]	Synthetic bone graft	OSSIGEL
HMW viscous HA	Injectable soft tissue fillers [136]	Corneal transplantation and glaucoma surgery	AMVISC & AMVISC Plus
Viscous HA	Synovial fluid substitute [137]	To relieve pain and improve join mobility in osteoarthritis patients	SYNVISC,ORTHOVISC

biological performance parameters (e.g., cell adhesion). It is commonly believed that the degradation rates of tissue scaffolds must be matched to the rate of various cellular processes in order to optimize tissue regeneration [151, 152]. Therefore, the degradation behavior of all biodegradable hydrogels should be well defined, reproducible, and tunable via hydrogel chemistry or structure. Biocompatible hydrogels are currently used in cartilage wound healing, bone regeneration, wound dress, and as carriers for drug delivery [153]. Hydrogel with growth factor can act directly to support the development and differentiation of cells in the newly formed tissues [154]. Hydrogels are often favorable for promoting cell migration, angiogenesis, high water content, and rapid nutrient diffusion [155]. The hydrogel scaffolds have received intensive study for their use in the engineering of replacement connective tissues, primarily due to their biochemical similarity with the highly hydrated GAG components of connective tissues. Examples of hydrogel-forming polymers of natural origin are collagen [156], gelatin [157], fibrin [158], HA [159], alginate [160], and chitosan [161]. The synthetic polymers are PLA [162], PPF-derived Copolymers [163], PEG-derivatives, and PVA [164].

6. Fibrous Scaffold

The development of nanofibers has enhanced the scope for fabricating scaffolds that can potentially mimic the architecture of natural human tissue at the nanometer scale. Currently, there are three techniques available for the synthesis of nanofibers: electrospinning, self-assembly, and phase separation. Of these, electrospinning is the most widely studied technique and also seems to exhibit the most promising results for tissue engineering applications. Nanofibers synthesized by self-assembly [165] and phase separation [50] have had relatively limited studies that explored their application as scaffolds for tissue engineering. The high surface-area-to-volume ratio of the nanofibers combined with their microporous structure favors cell adhesion, proliferation, migration, and differentiation, all of which are highly desired properties for tissue engineering applications [166, 167]. Nanofibers used as scaffolds for musculoskeletal tissue engineering including bone, cartilage, ligament, and skeletal muscle, skin, vascular, neural tissue engineering, and as vehicle for the controlled delivery of drugs, proteins, and DNA [168]. Natural polymers and synthetic polymers explored for the fabrication of nanofibers such as collagen [169], gelatin [170], chitosan [171], HA [172], silk fibroin [173], PLA [174], PU [175], PCL [176], PLGA [177], PEVA [178], and PLLA-CL [179] are fibrous scaffold in biomedical application. The blending (or mixing) technique is a common choice for the nanofiber functionalization. However, most of the polymer nanofibers do not possess any specific functional groups, and they must be specifically functionalized for successful applications. The most popular and simplest nanofiber modification methods are physical blending and coating. Surface grafting polymerization has also been used for attaching ligand molecules and adhesive proteins on nanofiber surface for application of affinity membrane and tissue engineering scaffold, respectively. Drugs, growth factors, and genes can be directly mixed into the polymer solution and electrospun to prepare drug carriers with controlled release properties [180].

7. Microsphere Scaffold

Microsphere-based tissue engineering scaffold designs have attracted significant attention in recent years [181]. Laurencin et al. [44] initially used a microsphere-based approach for tissue engineering scaffold. Microsphere scaffolds are having spatial extension and temporal duration control which provides the stiffness gradients for interfacial tissue engineering [182]. Microsphere scaffolds are increasingly used as drug delivery systems and in advanced tissue engineering applications such as gene therapy, antibiotic treatment of infected bone, and so forth [183]. The influence of nanotechnology on scaffold design and the possibility of sustained release formulations of growth factors via microspheres are showing promising developments. Microsphere scaffolds are generally a polymer matrix used for drug encapsulation for the release of drugs at a relatively slow rate over a prolonged period of time [184]. Polymers with low molecular weight used in developing porous microspheres for the rapid release of the drug, while polymers with high molecular weight for developing microspheres for a slower drug release profile which can be achieved due to its dense nature [185]. Injectable microspheres have also been developed for the controlled delivery of drugs [186]. Microspheres as building blocks offer several benefits, including ease of fabrication, control over morphology, physicochemical characteristics, and its versatility of controlling the release kinetics of encapsulated factors [187]. The methods used to produce microsphere-based scaffolds have utilized heat

sintering [188, 189], solvent vapor treatment [190, 191], solvent/nonsolvent sintering method [192, 193] or nonsolvent sintering technique [181]. Particle aggregation methodology is proposed to fabricate bilayered scaffolds for osteochondral tissue engineering in order to achieve an improved integrative bone and cartilage interface which has been needed for this application. PLAGA microsphere scaffolds are in the range of trabecular bone, demonstrating the potential of the porous microsphere matrix to be used as a scaffold for load-bearing bone tissue engineering [47]. The sintered microsphere matrix shows promise as a bone regeneration scaffold. An advantage of the sintered microsphere structure is its pore interconnectivity and desirable three-dimension pore size. The gel microsphere matrix and the sintered microsphere matrix were designed using the random packing of PLAGA microspheres to create a three-dimensional porous structure for bone regeneration [194]. Composite microspheres are also used for the fabrication of polymer-ceramic matrices for bone applications [195]. Chitosan microsphere scaffolds have been produced for cartilage and osteochondral tissue engineering [48].

8. Polymer-Bioceramic Composite Scaffold

Development of composite materials for tissue engineering is attractive since their properties can be engineered to suit the mechanical and physiological demands of the host tissue by controlling the volume fraction, morphology, and arrangement of the reinforcing phase [196]. Ceramics used in fabricating implants can be classified as nonabsorbable (relatively inert), bioactive or surface reactive (semi-inert) [197], and biodegradable or resorbable (noninert) [198]. Alumina, zirconia, silicone nitrides, and carbons are inert bioceramics. Certain glass ceramics and dense HAP are semi-inert (bioreactive), and examples of resorbable ceramics are aluminum calcium phosphate, coralline, plaster of Paris, HAP, and TCP [199]. Ceramics are known for their good compatibility, corrosion resistance, and high compression resistance. Drawbacks of ceramics include brittleness, low fracture strength, difficulty to fabricate, low mechanical reliability, lack of resilience, and high density. In recent years, humans have realized that ceramics and their composites can also be used to augment or replace various parts of body, particularly bone. Thus, the ceramics used for the latter purposes are classified as bioceramics. Polymers by themselves are generally flexible and exhibit a lack of mechanical strength and stiffness, whereas inorganic materials such as ceramics and glasses are known to be too stiff and brittle. The combination of polymers and inorganic phases leads to composite materials with improved mechanical properties due to the inherent higher stiffness and strength of the inorganic material. Secondly, addition of bioactive phases to bioresorbable polymers can alter the polymer degradation behavior of the scaffolds [200, 201]. Complications in the development of polymer bioceramics composite scaffold are (i) maintenance of strength and the stability of the interface during the degradation period and replacement by the natural host tissue and (ii) matching resorption rates to the repair rates of body tissues developed for hard tissue implants and tissue engineering scaffolds, due to their excellent biocompatibility, bioactivity, and bioresorption in calcified tissue. Highly porous polymer/ceramic composite scaffolding appears to be a promising substrate for bone tissue engineering due to its excellent mechanical properties and osteoconductivity [40]. PLGA/HAP composite scaffold has excellent biocompatibility with hard tissues and high osteoconductivity and bioactivity [50]. The composite scaffolds supported uniform cell seeding, cell ingrowth, and tissue formation. The major inorganic component of natural bone; bioceramics, including CP, HAP, and TCP are composite with PLLA [46], collagen [202], gelatin [203], chitosan [204] are widely used as scaffolding materials for bone repair.

9. Acellular Scaffold

Acellular tissue matrices can be prepared by manufacturing artificial scaffolds or by removing cellular components from tissues by mechanical and chemical manipulation to produce collagen-rich matrices [205–207]. These matrices slowly degrade on implantation and are generally replaced by the ECM proteins secreted by the ingrowing cells. The ultimate goal of any decellularization protocol is to remove all cellular material without adversely affecting the composition, mechanical integrity, and eventual biological activity of the remaining ECM. The decellularized biological scaffold was introduced to obtain a physiological matrix scaffold that resembles that of native blood vessels [208]. Acellular tissue matrices have proven to support cell ingrowth and regeneration of genitourinary tissues, including urethra and bladder, with no evidence of immunogenic rejection [207]. Ureteral acellular matrices were utilized as a scaffold for the ingrowth of ureteral tissue in rats [209]. Acellular bladder matrix has served as a scaffold for the ingrowth of host bladder wall components in rats. Since the structures of the proteins (e.g., collagen and elastin) in acellular matrices are well conserved and normally arranged, the mechanical properties of the acellular matrices are not significantly different from those of native bladder submucosa [209]. The matrix was prepared by mechanically and chemically removing all cellular components from bladder tissue [210]. To engineer tissues successfully, the selection of scaffolds is critical. Although various synthetic biodegradable polymer scaffolds have been developed and improved by mimicking biological structures, comparing to other scaffolds, acellular scaffolds have the following advantages.

(i) Acellular scaffolds retain their correct anatomical structure even after the decellularisation process.

(ii) Acellular scaffolds retain native ECM architecture and possess the cell adhesion ligands.

(iii) The decellularisation process considerably reduces immunological responses by completely removing cellular components.

(iv) The decellularisation process facilitates similar biomechanical properties as those of native tissues that are critical for the long-term functionality of the grafts.

Various extracellular matrices have been utilized successfully for tissue engineering in animal models and products incorporating decellularized heart valves, small intestinal submucosa (SIS), and urinary bladder have received regulatory approval for use in human patients [211]. The obvious advantage of this scaffold is that it is composed of ECM proteins typically found in the body. When derived from a vessel, the three-dimension architecture is very similar to that of the original, thus conferring appropriate mechanical and physical properties, which is essential in identifying and predicting optimal cell environments in order to develop scaffolds for preliminary analysis and implantation. Naturally derived materials and acellular tissue matrices have the potential advantage of biological recognition. Polymer coating of a tissue-derived acellular scaffold can improve the mechanical stability and enhance the hemocompatibility of the protein matrix. Tissue engineering that has been introduced is the use of biological/polymeric composite materials as starter matrices. Such hybrids can be complex structures such as heart valves, for example, fabricated from decellularized porcine aortic valves and dip coated with a biodegradable polymer [212].

10. Physicochemical Characterization of Scaffolds

Polymeric scaffolds have evolved to serve not merely as carriers of cells and inductive factors, but to actively instruct cells and provide step by step guidance of tissue formation. To accomplish this goal, a thorough understanding of the chemistry and physicochemical properties of the tissue to be engineered and the materials used in this process are required. Several characterizations are required for the fabrication of successful 3D scaffolds. They are

(i) external geometry (e.g., macro-, microstructure, interconnectivity),

(ii) surface properties (e.g., surface energy, chemistry, charge, surface area),

(iii) porosity and pore size,

(iv) interface adherence & biocompatibility,

(v) degradation characterization (e.g., biodegradation),

(vi) mechanical competence (e.g., compressive and tensile strength).

Developing scaffolds that mimic the architecture of tissue at the nanoscale is one of the most important challenges in the field of tissue engineering [168]. Polymeric scaffolds show excellent potential with mechanical properties and with wide range of degradation, the qualities which are essential for a range of tissue engineering applications [213].

11. External Geometry

Physical characteristics are certainly the important factors to consider when scaffolds are applied for tissue reconstruction [214]. Scaffold with proper physical characters are smart materials that can mimic natural ECM. ECM plays a key role in tissue architecture by providing structural support and tensile strength. Attachment sites for cell surface receptors are related to a wide variety of processes related to cell differentiation, tissue formation, homeostasis, and regeneration [215, 216]. The fabrication and design of macro- to nanoscale structural architectures have received much attention in medical applications. Nano- to macroscale structure geometrically or topologically mimics the native state of ECM in living tissues. Three-dimensional scaffolds are capable of regenerating tissue and organs in their normal physiological shape. Mimicking the ECM using biomaterials would be a logical approach for engineering scaffold for a variety of tissue types. As polymer materials permit a most versatile variety of surface characteristics, efficient control over processes of ECM reconstitution can be achieved by the interaction with polymeric materials. The importance of scaffold geometry in maintaining highly interconnected porous fabrics of high surface density provides an extremely high surface-to-volume ratio, favoring cell attachment and proliferation.

12. Surface Properties

Surface properties include both chemical and topographical characteristics, which can control and affect cellular adhesion and proliferation [214]. The scaffold surface is the initial and primary site of interaction with surrounding cells and tissue. As most cells utilized in tissue engineering are anchorage dependent, it has been reasoned that the scaffold should facilitate their attachment. Thus, scaffolds with a large and accessible surface area are favorable. For example, high internal surface-area-to-volume ratios is essential in order to accommodate the number of cells required to replace or restore tissue or organ functions. The surface properties can be selectively modified to enhance the performance of the biomaterials. For instance, by altering the surface functionality using thin film deposition, the optimal surface, chemical, and physical properties can be attained [217, 218]. Hence, surface modification of biomaterials is becoming an increasingly popular method to improve device multifunctionality, tribological, and mechanical properties. Most of the surface modifications and immobilizations of biomolecules are performed to improve the biocompatibility of the polymeric scaffold; thereby, cells can specifically recognize the scaffold. These biomolecules include adhesive proteins like collagen, fibronectin, RGD peptides, and growth factors like bFGF, EGF, insulin, and so forth. The biomolecules can either be covalently attached, electrostatically adsorbed, or self-assembled on the biomaterial surfaces to develop brand new materials [219].

13. Porosity and Pore Size

Scaffolds must possess a highly porous structure with an open fully interconnected geometry for providing a large surface area that will allow cell ingrowth, uniform cell distribution, and facilitate the neovascularization of the

construct [220]. Average pore size, pore size distribution, pore volume, pore interconnectivity, pore shape, pore throat size, and pore wall roughness are important parameters to consider while designing a scaffold. It provides a porous biocompatible network into which the surrounding tissue is induced and acts as a temporary template for the new tissue's growth and reorganization [221]. Pore size is also a very important issue because if the pores employed are too small, pore occlusion by the cells will happen, which will prevent cellular penetration, extracellular matrix production, and neovascularization of the inner areas of the scaffold. The effects of pore size on tissue regeneration has been emphasized by experiments demonstrating optimum pore size of 5 μm for neovascularization [222], 5–15 μm for fibroblast ingrowth [223], 20 μm for the ingrowth of hepatocytes [224], 200–350 μm for osteoconduction [225], and 20–125 μm for regeneration of adult mammalian skin [226]. Pore interconnectivity is also critical to ensure that all cells are within 200 μm from blood supply in order to provide for mass transfer of oxygen and nutrients [224, 227].

14. Interface Adherence and Biocompatibility

The term biocompatibility has been defined in many and different ways. Historically, materials that caused minimal biological responses were considered biocompatible. Biocompatibility refers to the ability of a biomaterial to perform its desired function with respect to a medical therapy, without eliciting any undesirable local or systemic effects in the recipient or beneficiary of that therapy. It should generate the most appropriate beneficial cellular or tissue response in that specific situation and optimize the clinically relevant performance of that therapy [15]. Biocompatibility of a scaffold or matrix for a tissue engineering product refers to the ability to perform as a substrate that will support the appropriate cellular activity, including the facilitation of molecular and mechanical signalling systems [228]. Some important factors that determine scaffold's biocompatibility are their chemistry, structure, and their morphology, which in turn are affected by the polymer synthesis, scaffold processing, and sterilization conditions. Recently, several biodegradable polymers such as PLA, PGA, PLGA, PDO, PTMC, and so on are extensively used or tested on a wide range of medical applications due to their good biocompatibility [229]. The behavior of the adsorption and desorption of adhesion and proliferation of different types of mammalian cells on polymeric materials depends on the surface characteristics such as wettability, hydrophilicity/hydrophobicity ratio, bulk chemistry, surface charge and charge distribution, surface roughness, and rigidity. A number of surface treatments are available to optimize the biocompatibility of surfaces in contact with living tissue, to seal in undesirable residues or additives using a coating and to regulate excretion and/or absorption using a selectively permeable surface [230]. Recently, physical and chemical surface modification methods for polymeric biomaterials to influence cell adhesion and growth have been achieved by oxidized polystyrene surface [231], ammonia plasma-treated surface [232], and plasma-deposited acetone [233].

15. Degradation Rates

Biodegradable polymers have revolutionized the applications of biomaterial in the field of drug delivery and implants for tissue engineering applications. Scaffold degradation can occur through mechanisms that involve physical or chemical processes and/or biological processes that are mediated by biological agents, such as enzymes in tissue remodeling. The biodegradable scaffold gradually degrades by predetermined period to be replaced by newly grown tissue from the adhered cells [1]. Degradation results in scaffold dismantling and material dissolution/resorption through the scaffolds bulk and/or surface types of degradation [234]. Polymeric scaffolds that undergo bulk degradation tend to break down the internal structure of the scaffold thus reducing the molecular mass [235]. A polymeric scaffold that primarily undergoes surface degradation can be described similarly to the dissolution of soap. The rate at which the surface degrades is usually constant. Therefore, even though the size of the scaffold becomes smaller, the bulk structure is maintained. These types of degrading scaffolds provide longer mechanical stability for the tissue to regenerate. Biodegradation of polymeric biomaterials involves cleavage of hydrolytically or enzymatically sensitive bonds in the polymer leading to polymer erosion [131]. The biodegradation rate of a polymer depends mainly on the intrinsic properties of the polymer, including the chemical structure, thev presence of hydrolytically unstable bonds, the level ofv hydrophilicity/hydrophobicity, crystalline/amorphous morphology, glass transition temperatures (Tg), the copolymer ratio, and the molecular weight [236]. The Controllable degradation and restoration rates should match the rate of tissue growth *in vitro* and *in vivo* for biodegradable or restorable materials. The nonbiodegradable polymeric scaffolds are biologically stable, and it can provide a permanent support over time and should ideally perform during the life time of the patient. For example, PMMA is mainly used as bone cements in hip and knee replacements, and high-density PE forms the articulating surfaces of hip and knee joints [13].

16. Mechanical Properties

The proper mechanical properties for a biomaterial to be used in a tissue engineering application are critical to the success of the implant. The biostability of many scaffolds depends on the factors such as strength, elasticity, and absorption at the material interface and its chemical degradation. The scaffold should have proper mechanical properties and degradation rate with the bioactive surface to encourage the rapid regeneration of the tissue [26]. It is highly essential to retain the mechanical strength of the scaffolds structure after implantation for the reconstruction of hard, load bearing tissues such as bone and cartilages. To be used successfully in tissue engineering, it is critical that a biomaterial scaffold temporarily withstands and conducts the loads and stresses that the new tissue will ultimately bear. It is important, therefore, to evaluate one or more of the

following rheological parameters:

(i) *elastic modulus*—measured strain in response to a given tensile or compressive stress along the force;

(ii) *flexural modulus*—measured the relationship between a bending stress and the resulting strain in response to a given tensile or compressive stress perpendicular under load;

(iii) *tensile strength*—maximum stress that the material can withstand before it breaks;

(iv) *maximum strain*—ductility of a material or total strain exhibited prior to fracture.

The low strength and rigidity of the polysaccharides limit their use to soft tissue applications. Fortunately, the options for tissue engineering are expanded by the use of fibrous proteins, whose normal function is to provide mechanical integrity and stability to biological structures. Fibrous proteins are responsible for the transduction of external mechanical forces to associated cells in a manner that influences the outcome of tissue growth [169]. The mechanical properties of bulk biomaterials are altered by their processing into scaffolds of various pore sizes and pore orientations and further that these properties will rapidly diminish as a function of implantation time [237]. The mechanical rigidity of the surrounding matrix, as well as material roughness and physical confinement, determined by three-dimensional microstructure on a subcellular and supercellular scale, respectively, may significantly modulate the outcome of the balance between cell matrix forces, leading to the remodeling of cytoarchitecture, cell polarization, alteration of downstream intracellular signaling events as well as modification of the balance of cell-cell forces [238–240]. The major factor affecting the mechanical properties and structural integrity of scaffolds, however, is their porosity, for example, pore volume, size, shape, orientation, and connectivity.

Conclusions

In summary, tissue engineering is one of the most exciting interdisciplinary and multidisciplinary research areas and is growing exponentially over time. Scaffold materials and fabrication technologies play a crucial role in tissue engineering. A wide range of polymeric scaffold was used to date in the tissue engineering area. Scaffolds should meet certain design parameters to be useful in this area, regardless of whether they originate from natural resources or are synthetically created. All these techniques for scaffold fabrication are sensitive to the various processing parameters. Innovations in the material design and fabrication processes are raising the possibility of production of implants with good performance. The scaffold should be surface compatible as well as architecturally suitable with the host environment. The interest in the principles and theories of the fabrication process with polymers would be useful to develop a new design for implants and also to understand the behavior of the scaffold in the biomedical applications. Nanotechnology can provide strategies that can help to create features on a scaffold in a dimensional range that may be adequate for cells and biomolecules. There are clear indications that as the goals of biomedical engineering increase in complexity, there is need to develop novel scaffold structures.

Future Directions

Medical research continues to explore new scientific frontiers for diagnosing, treating, curing, and preventing diseases at the molecular/genetic level. Important advances have been made in the clinical use of medical implants and other devices. Presently, emphasis is placed on the design of polymeric scaffold, that is, materials that obtain specific, desired, and timely responses from surrounding cells and tissues. The need for alternative solutions to meet the demand for replacement organs and tissue parts will continue to drive advances in tissue engineering. Polymer scaffolds have all the prospective to provide a new means to control the physical and chemical environment of the biological system. There are several advantages to use biological polymers over widely utilized synthetic polymer in tissue engineering scaffold. Despite these recent improvements to the mechanical properties, porosity, and bioactivity of scaffolds, future researches are needed to overcome many remaining limitations in the fabricating process. We believe no one material will satisfy all design parameters in all applications, but a wide range of materials will find uses in various tissue engineering applications. The overall challenges in scaffold design and fabrication gives opportunity for new exciting application oriented research in scaffold design which includes polymer assembly, surface topography or chemical cues, nano-/macrostructure, biocompatibility, biodegradability, mechanical properties, directing cell function and induced formation of natural tissue.

Abbreviations

PU: Polyurethane
PS: Polysulfone
CP: Calcium phosphate
HA: Hyaluronic acid
PP: Polypropylene
BG: Bioactive glass
ECM: Extracellular matrix
PVA: Polyvinyl alcohol
PGA: Polyglycolide
PLA: Polylactide
PPF: Poly(propylene fumarate)
PCA: Polycyanoacrylate
PCL: Poly(ε-caprolactone)
PDO: Polydioxanone
PHA: Polyhydroxyalkanoates
POE: Poly(ortho ester)
PEE: Poly(ether ester)
PEO: Poly(ethylene oxide)
PBT: Polybutylene terephthalate
HAP: Hydroxyapatite

TCP: Tricalcium phosphate
PEG: Poly(ethylene glycol)
PEU: Poly(ester urethane)
PAA: Poly(acrylic acid)
LDI: Lysine diisocyanate
BCP: Biphasic calcium phosphate
HMW: High molecular weight
PAam: Polyacrylamide
PMMA: Polymethylmethacrylate
PLLA: Poly(L-lactic acid)
PLGA: Poly(l-lactide-co-glycolide)
PTMC: Poly(trimethylene carbonate)
PDMS: Polydimethylsiloxane
PTFE: Polytetrafluoroethylene
PEVA: Poly(ethylene-co-vinylacetate)
PGCL: Poly(glycolide-co-ε-caprolactone)
PLCL: Poly(l-lactide-co-caprolactone)
PDLLA: Poly(DL-lactide)
PLDLA: Poly-L/D-lactide
PLAGA: Poly(lactic acid-glycolic acid)
PHBHV: Poly(3-hydroxybutyrate)3-hydroxyvalerate
PCLTMC: Poly(caprolactone-co-trimethylene carbonate)
PNIPAAm: Poly(N-isopropylacrylamide)
PDMAEM: Poly(dimethylaminoethylmethacrylate) hydrochloride
PDLLA-CL: Poly(D,L-lactide-co- caprolactone)
PLLA-CL: Poly(l-lactide-co-ε-caprolactone)
TCP: Tricalcium phosphate.

Acknowledgment

D. Brahatheeswaran, would like to acknowledge the Japanese Government, Ministry of Education, Culture, Sports, Science and Technology (MEXT) for the scholarships provided for the doctoral studies.

References

[1] R. Langer and J. P. Vacanti, "Tissue engineering," *Science*, vol. 260, no. 5110, pp. 920–926, 1993.
[2] R. M. Nerem, "Tissue engineering in the USA," *Medical and Biological Engineering and Computing*, vol. 30, no. 4, pp. CE8–CE12, 1992.
[3] R. Langer and D. A. Tirrell, "Designing materials for biology and medicine," *Nature*, vol. 428, no. 6982, pp. 487–492, 2004.
[4] J. R. Fuchs, B. A. Nasseri, and J. P. Vacanti, "Tissue engineering: a 21st century solution to surgical reconstruction," *Annals of Thoracic Surgery*, vol. 72, no. 2, pp. 577–591, 2001.
[5] I. V. Yannas, J. F. Burke, C. Huang, and P. L. Gordon, "Suppression of in vivo degradability and of immunogenicity of collagen by reaction with glycosaminoglycans," *Polymer Preprints*, vol. 16, pp. 209–214, 1975.
[6] I. V. Yannas, J. F. Burke, P. L. Gordon, and C. Huang, "Multilayer membrane useful as synthetic skin," US patent 4060081, 1977.
[7] I. V. Yannas and J. F. Burke, "Design of an artificial skin. I. Basic design principles," *Journal of Biomedical Materials Research*, vol. 14, no. 1, pp. 65–81, 1980.
[8] I. V. Yannas, J. F. Burke, M. Warpehoski et al., "Prompt, long-term functional replacement of skin," *Transactions—American Society for Artificial Internal Organs*, vol. 27, pp. 19–23, 1981.
[9] I. V. Yannas, J. F. Burke, D. P. Orgill, and E. M. Skrabut, "Regeneration of skin following closure of deep wounds with a biodegradable template," *Transactions of the Society For Biomaterials*, vol. 5, pp. 24–29, 1982.
[10] J. F. Burke, O. V. Yannas, and W. C. Quinby Jr., "Successful use of a physiologically acceptable artificial skin in the treatment of extensive burn injury," *Annals of Surgery*, vol. 194, no. 4, pp. 413–427, 1981.
[11] I. V. Yannas, D. P. Orgill, J. Silver, T. V. Norregaard, N. T. Zervas, and W. C. Schoene, "Polymeric template facilitates regeneration of sciatic nerves across 15-mm gap," *Transactions of the Society For Biomaterials*, vol. 8, p. 146, 1985.
[12] W. C. Hsu, M. H. Spilker, I. V. Yannas, and P. A. D. Rubin, "Inhibition of conjunctival scarring and contraction by a porous collagen-glycosaminoglycan implant," *Investigative Ophthalmology and Visual Science*, vol. 41, no. 9, pp. 2404–2411, 2000.
[13] S. Ramakrishna, J. Mayer, E. Wintermantel, and K. W. Leong, "Biomedical applications of polymer-composite materials: a review," *Composites Science and Technology*, vol. 61, no. 9, pp. 1189–1224, 2001.
[14] M. Vert, "Aliphatic polyesters: great degradable polymers that cannot do everything," *Biomacromolecules*, vol. 6, no. 2, pp. 538–546, 2005.
[15] E. Piskin, "Biodegradable polymers as biomaterials," *Journal of Biomaterials Science Polymer Edition*, vol. 6, pp. 775–795, 1994.
[16] Y. Ji, K. Ghosh, X. Z. Shu et al., "Electrospun three-dimensional hyaluronic acid nanofibrous scaffolds," *Biomaterials*, vol. 27, no. 20, pp. 3782–3792, 2006.
[17] W. H. Eaglstein and V. Falanga, "Tissue engineering and the development of Apligraf a human skin equivalent," *Advances in Wound Care*, vol. 11, supplement 4, pp. 1–8, 1998.
[18] B. D. Boyan, C. H. Lohmann, J. Romero, and Z. Schwartz, "Bone and cartilage tissue engineering," *Clinics in Plastic Surgery*, vol. 26, no. 4, pp. 629–645, 1999.
[19] J. Mayer, E. Karamuk, T. Akaike, and E. Wintermantel, "Matrices for tissue engineering-scaffold structure for a bioartificial liver support system," *Journal of Controlled Release*, vol. 64, no. 1–3, pp. 81–90, 2000.
[20] J. E. Mayer, T. Shin'oka, and D. Shum-Tim, "Tissue engineering of cardiovascular structures," *Current Opinion in Cardiology*, vol. 12, no. 6, pp. 528–532, 1997.
[21] F. Oberpenning, J. Meng, J. J. Yoo, and A. Atala, "De novo reconstitution of a functional mammalian urinary bladder by tissue engineering," *Nature Biotechnology*, vol. 17, no. 2, pp. 149–155, 1999.
[22] E. Tziampazis and A. Sambanis, "Tissue engineering of a bioartificial pancreas: modeling the cell environment and device function," *Biotechnology Progress*, vol. 11, no. 2, pp. 115–126, 1995.
[23] J. Mohammad, J. Shenaq, E. Rabinovsky, and S. Shenaq, "Modulation of peripheral nerve regeneration: a tissue-engineering approach. The role of amnion tube nerve conduit across a 1-centimeter nerve gap," *Plastic and Reconstructive Surgery*, vol. 105, no. 2, pp. 660–666, 2000.
[24] L. Germain, F. A. Auger, E. Grandbois et al., "Reconstructed human cornea produced in vitro by tissue engineering," *Pathobiology*, vol. 67, no. 3, pp. 140–147, 1999.

[25] C. A. Diedwardo, P. Petrosko, T. O. Acarturk, P. A. Dimilia, W. A. Laframboise, and P. C. Johnson, "Muscle tissue engineering," *Clinics in Plastic Surgery*, vol. 26, no. 4, pp. 647–656, 1999.

[26] L. S. Nair and C. T. Laurencin, "Biodegradable polymers as biomaterials," *Progress in Polymer Science*, vol. 32, no. 8-9, pp. 762–798, 2007.

[27] I. V. Yannas, "Classes of materials used in medicine: natural materials," in *Biomaterials Science—An Introduction to Materials in Medicine*, B. D. Ratner, A. S. Hoffman, F. J. Schoen, and J. Lemons, Eds., pp. 127–136, Elsevier Academic Press, San Diego, Calif, USA, 2004.

[28] P. Gunatillake, R. Mayadunne, and R. Adhikari, "Recent developments in biodegradable synthetic polymers," *Biotechnology Annual Review*, vol. 12, pp. 301–347, 2006.

[29] P. X. Ma, "Scaffolds for tissue fabrication," *Materials Today*, vol. 7, no. 5, pp. 30–40, 2004.

[30] L. J. Chen and M. Wang, "Production and evaluation of biodegradable composites based on PHB-PHV copolymer," *Biomaterials*, vol. 23, no. 13, pp. 2631–2639, 2002.

[31] L. L. Hench, "Bioceramics," *Journal of the American Ceramic Society*, vol. 81, no. 7, pp. 1705–1727, 1998.

[32] M. G. Cascone, N. Barbani, C. Cristallini, P. Giusti, G. Ciardelli, and L. Lazzeri, "Bioartificial polymeric materials based on polysaccharides," *Journal of Biomaterials Science*, vol. 12, no. 3, pp. 267–281, 2001.

[33] G. Ciardelli, V. Chiono, G. Vozzi et al., "Blends of poly-(ε-caprolactone) and polysaccharides in tissue engineering applications," *Biomacromolecules*, vol. 6, no. 4, pp. 1961–1976, 2005.

[34] J. A. Roether, A. R. Boccaccini, L. L. Hench, V. Maquet, S. Gautier, and R. Jérôme, "Development and in vitro characterisation of novel bioresorbable and bioactive composite materials based on polylactide foams and Bioglass® for tissue engineering applications," *Biomaterials*, vol. 23, no. 18, pp. 3871–3878, 2002.

[35] A. G. Mikos, G. Sarakinos, S. M. Leite, J. P. Vacanti, and R. Langer, "Laminated three-dimensional biodegradable foams for use in tissue engineering," *Biomaterials*, vol. 14, no. 5, pp. 323–330, 1993.

[36] A. G. Mikos, A. J. Thorsen, L. A. Czerwonka et al., "Preparation and characterization of poly(l-lactic acid) foams," *Polymer*, vol. 35, no. 5, pp. 1068–1077, 1994.

[37] K. Ochi, G. Chen, T. Ushida et al., "Use of isolated mature osteoblasts in abundance acts as desired-shaped bone regeneration in combination with a modified poly-DL-lactic-co-glycolic acid (PLGA)-collagen sponge," *Journal of Cellular Physiology*, vol. 194, no. 1, pp. 45–53, 2003.

[38] C. E. Holy, M. S. Shoichet, and J. E. Davies, "Engineering three-dimensional bone tissue in vitro using biodegradable scaffolds: investigating initial cell-seeding density and culture period," *Journal of Biomedical Materials Research*, vol. 51, no. 3, pp. 376–382, 2000.

[39] J. M. Karp, M. S. Shoichet, and J. E. Davies, "Bone formation on two-dimensional poly(DL-lactide-co-glycolide) (PLGA) films and three-dimensional PLGA tissue engineering scaffolds in vitro," *Journal of Biomedical Materials Research A*, vol. 64, no. 2, pp. 388–396, 2003.

[40] H. G. Kang, S. Y. Kim, and Y. M. Lee, "Novel porous gelatin scaffolds by overrun/particle leaching process for tissue engineering applications," *Journal of Biomedical Materials Research B*, vol. 79, no. 2, pp. 388–397, 2006.

[41] D. J. Mooney, D. F. Baldwin, N. P. Suh, J. P. Vacanti, and R. Langer, "Novel approach to fabricate porous sponges of poly(D,L-lactic-co-glycolic acid) without the use of organic solvents," *Biomaterials*, vol. 17, no. 14, pp. 1417–1422, 1996.

[42] J. J. Yoon and T. G. Park, "Degradation behaviors of biodegradable macroporous scaffolds prepared by gas foaming of effervescent salts," *Journal of Biomedical Materials Research*, vol. 55, no. 3, pp. 401–408, 2001.

[43] W. L. Murphy, R. G. Dennis, J. L. Kileny, and D. J. Mooney, "Salt fusion: an approach to improve pore interconnectivity within tissue engineering scaffolds," *Tissue Engineering*, vol. 8, no. 1, pp. 43–52, 2002.

[44] C. T. Laurencin, M. A. Attawia, H. E. Elgendy, and K. M. Herbert, "Tissue engineered bone-regeneration using degradable polymers: the formation of mineralized matrices," *Bone*, vol. 19, no. 1, 1996.

[45] J. E. Devin, M. A. Attawia, and C. T. Laurencin, "Three-dimensional degradable porous polymer-ceramic matrices for use in bone repair," *Journal of Biomaterials Science*, vol. 7, no. 8, pp. 661–669, 1996.

[46] B. H. Woo, J. W. Kostanski, S. Gebrekidan, B. A. Dani, B. C. Thanoo, and P. P. DeLuca, "Preparation, characterization and in vivo evaluation of 120-day poly(D,L-lactide) leuprolide microspheres," *Journal of Controlled Release*, vol. 75, no. 3, pp. 307–315, 2001.

[47] M. Borden, S. F. El-Amin, M. Attawia, and C. T. Laurencin, "Structural and human cellular assessment of a novel microsphere-based tissue engineered scaffold for bone repair," *Biomaterials*, vol. 24, no. 4, pp. 597–609, 2003.

[48] P. B. Malafaya, A. J. Pedro, A. Peterbauer, C. Gabriel, H. Redl, and R. L. Reis, "Chitosan particles agglomerated scaffolds for cartilage and osteochondral tissue engineering approaches with adipose tissue derived stem cells," *Journal of Materials Science: Materials in Medicine*, vol. 16, no. 12, pp. 1077–1085, 2005.

[49] P. B. Malafaya, T. C. Santos, M. van Griensven, and R. L. Reis, "Morphology, mechanical characterization and in vivo neo-vascularization of chitosan particle aggregated scaffolds architectures," *Biomaterials*, vol. 29, no. 29, pp. 3914–3926, 2008.

[50] R. Zhang and P. X. Ma, "Porous poly(L-lactic acid)/apatite composites created by biomimetic process," *Journal of Biomedical Materials Research*, vol. 45, no. 4, pp. 285–293, 1999.

[51] Y. Ohya, H. Matsunami, E. Yamabe, and T. Ouchi, "Cell attachment and growth on films prepared from poly(depsipeptide-co-lactide) having various functional groups," *Journal of Biomedical Materials Research A*, vol. 65, no. 1, pp. 79–88, 2003.

[52] Y. Ohya, H. Matsunami, and T. Ouchi, "Cell growth on the porous sponges prepared from poly(depsipeptide-co-lactide) having various functional groups," *Journal of Biomaterials Science*, vol. 15, no. 1, pp. 111–123, 2004.

[53] M. Borden, M. Attawia, Y. Khan, and C. T. Laurencin, "Tissue engineered microsphere-based matrices for bone repair: design and evaluation," *Biomaterials*, vol. 23, no. 2, pp. 551–559, 2002.

[54] J. Guan, K. L. Fujimoto, M. S. Sacks, and W. R. Wagner, "Preparation and characterization of highly porous, biodegradable polyurethane scaffolds for soft tissue applications," *Biomaterials*, vol. 26, no. 18, pp. 3961–3971, 2005.

[55] T. J. Blokhuis, M. F. Termaat, F. C. Den Boer, P. Patka, F. C. Bakker, and H. J. T. M. Haarman, "Properties of calcium phosphate ceramics in relation to their in vivo behavior," *Journal of Trauma—Injury, Infection and Critical Care*, vol. 48, no. 1, pp. 179–186, 2000.

[56] T. A. Holland, J. K. V. Tessmar, Y. Tabata, and A. G. Mikos, "Transforming growth factor-β1 release from oligo(poly(ethylene glycol) fumarate) hydrogels in conditions that model the cartilage wound healing environment," *Journal of Controlled Release*, vol. 94, no. 1, pp. 101–114, 2004.

[57] O. Gauthier, R. Müller, D. Von Stechow et al., "In vivo bone regeneration with injectable calcium phosphate biomaterial: a three-dimensional micro-computed tomographic, biomechanical and SEM study," *Biomaterials*, vol. 26, no. 27, pp. 5444–5453, 2005.

[58] B. Jeong, Y. H. Bae, and S. W. Kim, "Thermoreversible gelation of PEG-PLGA-PEG triblock copolymer aqueous solutions," *Macromolecules*, vol. 32, no. 21, pp. 7064–7069, 1999.

[59] S. Ibusuki, Y. Fujii, Y. Iwamoto, and T. Matsuda, "Tissue-engineered cartilage using an injectable and in situ gelable thermoresponsive gelatin: fabrication and in vitro performance," *Tissue Engineering*, vol. 9, no. 2, pp. 371–384, 2003.

[60] J. Y. Seong, Y. J. Jun, B. Jeong, and Y. S. Sohn, "New thermogelling poly(organophosphazenes) with methoxy-poly(ethylene glycol) and oligopeptide as side groups," *Polymer*, vol. 46, no. 14, pp. 5075–5081, 2005.

[61] J. Yeh, Y. Ling, J. M. Karp et al., "Micromolding of shape-controlled, harvestable cell-laden hydrogels," *Biomaterials*, vol. 27, no. 31, pp. 5391–5398, 2006.

[62] J. Fukuda, A. Khademhosseini, Y. Yeo et al., "Micromolding of photocrosslinkable chitosan hydrogel for spheroid microarray and co-cultures," *Biomaterials*, vol. 27, no. 30, pp. 5259–5267, 2006.

[63] A. Khademhosseini, G. Eng, J. Yeh et al., "Micromolding of photocrosslinkable hyaluronic acid for cell encapsulation and entrapment," *Journal of Biomedical Materials Research A*, vol. 79, no. 3, pp. 522–532, 2006.

[64] D. J. Beebe, J. S. Moore, J. M. Bauer et al., "Functional hydrogel structures for autonomous flow control inside microfluidic channels," *Nature*, vol. 404, no. 6778, pp. 588–590, 2000.

[65] V. A. Liu and S. N. Bhatia, "Three-dimensional photopatterning of hydrogels containing living cells," *Biomedical Microdevices*, vol. 4, no. 4, pp. 257–266, 2002.

[66] D. Dendukuri, D. C. Pregibon, J. Collins, T. A. Hatton, and P. S. Doyle, "Continuous-flow lithography for high-throughput microparticle synthesis," *Nature Materials*, vol. 5, no. 5, pp. 365–369, 2006.

[67] T. Nisisako, T. Torii, and T. Higuchi, "Droplet formation in a microchannel network," *Lab on a Chip—Miniaturisation for Chemistry and Biology*, vol. 2, no. 1, pp. 24–26, 2002.

[68] J. A. Burdick, A. Khademhosseini, and R. Langer, "Fabrication of gradient hydrogels using a microfluidics/photopolymerization process," *Langmuir*, vol. 20, no. 13, pp. 5153–5156, 2004.

[69] S. Xu, Z. Nie, M. Seo et al., "Generation of monodisperse particles by using microfluidics: control over size, shape, and composition," *Angewandte Chemie International Edition*, vol. 44, no. 5, pp. 724–728, 2005.

[70] N. A. Peppas and A. R. Khare, "Preparation, structure and diffusional behavior of hydrogels in controlled release," *Advanced Drug Delivery Reviews*, vol. 11, no. 1-2, pp. 1–35, 1993.

[71] T. Alexakis, K. Boadid, D. Guong et al., "Microencapsulation of DNA within alginate microspheres and crosslinked chitosan membranes for in vivo application," *Applied Biochemistry and Biotechnology*, vol. 50, no. 1, pp. 93–106, 1995.

[72] C. P. Reis, A. J. Ribeiro, R. J. Neufeld, and F. Veiga, "Alginate microparticles as novel carrier for oral insulin delivery," *Biotechnology and Bioengineering*, vol. 96, no. 5, pp. 977–989, 2007.

[73] G. Steinhoff, U. Stock, N. Karim et al., "Tissue engineering of pulmonary heart valves on allogenic acellular matrix conduits: In vivo restoration of valve tissue," *Circulation*, vol. 102, no. 19, pp. III50–III55, 2000.

[74] D. E. Zhao, R. B. Li, W. Y. Liu et al., "Tissue-engineered heart valve on acellular aortic valve scaffold: in-vivo study," *Asian Cardiovascular and Thoracic Annals*, vol. 11, no. 2, pp. 153–156, 2003.

[75] H. C. Liang, Y. Chang, C. K. Hsu, M. H. Lee, and H. W. Sung, "Effects of crosslinking degree of an acellular biological tissue on its tissue regeneration pattern," *Biomaterials*, vol. 25, no. 17, pp. 3541–3552, 2004.

[76] A. Tachibana, Y. Furuta, H. Takeshima, T. Tanabe, and K. Yamauchi, "Fabrication of wool keratin sponge scaffolds for long-term cell cultivation," *Journal of Biotechnology*, vol. 93, no. 2, pp. 165–170, 2002.

[77] A. Tachibana, S. Kaneko, T. Tanabe, and K. Yamauchi, "Rapid fabrication of keratin-hydroxyapatite hybrid sponges toward osteoblast cultivation and differentiation," *Biomaterials*, vol. 26, no. 3, pp. 297–302, 2005.

[78] K. Katoh, T. Tanabe, and K. Yamauchi, "Novel approach to fabricate keratin sponge scaffolds with controlled pore size and porosity," *Biomaterials*, vol. 25, no. 18, pp. 4255–4262, 2004.

[79] J. Doshi and D. H. Reneker, "Electrospinning process and applications of electrospun fibers," *Journal of Electrostatics*, vol. 35, no. 2-3, pp. 151–160, 1995.

[80] W. J. Li, K. G. Danielson, P. G. Alexander, and R. S. Tuan, "Biological response of chondrocytes cultured in three-dimensional nanofibrous poly(ε-caprolactone) scaffolds," *Journal of Biomedical Materials Research A*, vol. 67, no. 4, pp. 1105–1114, 2003.

[81] J. Zeng, A. Aigner, F. Czubayko, T. Kissel, J. H. Wendorff, and A. Greiner, "Poly(vinyl alcohol) nanofibers by electrospinning as a protein delivery system and the retardation of enzyme release by additional polymer coatings," *Biomacromolecules*, vol. 6, no. 3, pp. 1484–1488, 2005.

[82] S. Hirano, M. Zhang, M. Nakagawa, and T. Miyata, "Wet spun chitosan-collagen fibers, their chemical N-modifications, and blood compatibility," *Biomaterials*, vol. 21, no. 10, pp. 997–1003, 2000.

[83] S. J. Pomfret, P. N. Adams, N. P. Comfort, and A. P. Monkman, "Electrical and mechanical properties of polyaniline fibres produced by a one-step wet spinning process," *Polymer*, vol. 41, no. 6, pp. 2265–2269, 2000.

[84] H. Okuzaki, Y. Harashina, and H. Yan, "Highly conductive PEDOT/PSS microfibers fabricated by wet-spinning and dip-treatment in ethylene glycol," *European Polymer Journal*, vol. 45, no. 1, pp. 256–261, 2009.

[85] J. Lyons, C. Li, and F. Ko, "Melt-electrospinning—part I: processing parameters and geometric properties," *Polymer*, vol. 45, no. 22, pp. 7597–7603, 2004.

[86] C. J. Ellison, A. Phatak, D. W. Giles, C. W. Macosko, and F. S. Bates, "Melt blown nanofibers: fiber diameter distributions and onset of fiber breakup," *Polymer*, vol. 48, no. 11, pp. 3306–3316, 2007.

[87] K. Kim, C. Lee, I. W. Kim, and J. Kim, "Performance modification of a melt-blown filter medium via an additional nano-web layer prepared by electrospinning," *Fibers and Polymers*, vol. 10, no. 1, pp. 60–64, 2009.

[88] M. J. B. Wissink, R. Beernink, J. S. Pieper et al., "Binding and release of basic fibroblast growth factor from heparinized

collagen matrices," *Biomaterials*, vol. 22, no. 16, pp. 2291–2299, 2001.

[89] F. Causa, P. A. Netti, and L. Ambrosio, "A multi-functional scaffold for tissue regeneration: the need to engineer a tissue analogue," *Biomaterials*, vol. 28, no. 34, pp. 5093–5099, 2007.

[90] Y. C. Ho, F. L. Mi, H. W. Sung, and P. L. Kuo, "Heparin-functionalized chitosan-alginate scaffolds for controlled release of growth factor," *International Journal of Pharmaceutics*, vol. 376, no. 1-2, pp. 69–75, 2009.

[91] P. Sepulveda and J. G. P. Binner, "Processing of cellular ceramics by foaming and in situ polymerisation of organic monomers," *Journal of the European Ceramic Society*, vol. 19, no. 12, pp. 2059–2066, 1999.

[92] Q. Z. Chen, I. D. Thompson, and A. R. Boccaccini, "45S5 Bioglass®-derived glass-ceramic scaffolds for bone tissue engineering," *Biomaterials*, vol. 27, no. 11, pp. 2414–2425, 2006.

[93] I. H. Jo, K. H. Shin, Y. M. Soon, Y. H. Koh, J. H. Lee, and H. E. Kim, "Highly porous hydroxyapatite scaffolds with elongated pores using stretched polymeric sponges as novel template," *Materials Letters*, vol. 63, no. 20, pp. 1702–1704, 2009.

[94] F. Li, Q. L. Feng, F. Z. Cui, H. D. Li, and H. Schubert, "A simple biomimetic method for calcium phosphate coating," *Surface and Coatings Technology*, vol. 154, no. 1, pp. 88–93, 2002.

[95] J. Chen, B. Chu, and B. S. Hsiao, "Mineralization of hydroxyapatite in electrospun nanofibrous poly(L-lactic acid) scaffolds," *Journal of Biomedical Materials Research A*, vol. 79, no. 2, pp. 307–317, 2006.

[96] F. Yang, J. G. C. Wolke, and J. A. Jansen, "Biomimetic calcium phosphate coating on electrospun poly(ε-caprolactone) scaffolds for bone tissue engineering," *Chemical Engineering Journal*, vol. 137, no. 1, pp. 154–161, 2008.

[97] A. V. Lemmo, D. J. Rose, and T. C. Tisone, "Inkjet dispensing technology: applications in drug discovery," *Current Opinion in Biotechnology*, vol. 9, no. 6, pp. 615–617, 1998.

[98] P. Calvert, "Inkjet printing for materials and devices," *Chemistry of Materials*, vol. 13, no. 10, pp. 3299–3305, 2001.

[99] L. Pardo, W. Cris Wilson, and T. Boland, "Characterization of patterned self-assembled monolayers and protein arrays generated by the ink-jet method," *Langmuir*, vol. 19, no. 5, pp. 1462–1466, 2003.

[100] W. Y. Yeong, C. K. Chua, K. F. Leong, M. Chandrasekaran, and M. W. Lee, "Indirect fabrication of collagen scaffold based on inkjet printing technique," *Rapid Prototyping Journal*, vol. 12, no. 4, pp. 229–237, 2006.

[101] V. Mironov, T. Boland, T. Trusk, G. Forgacs, and R. R. Markwald, "Organ printing: computer-aided jet-based 3D tissue engineering," *Trends in Biotechnology*, vol. 21, no. 4, pp. 157–161, 2003.

[102] W. Sun, A. Darling, B. Starly, and J. Nam, "Computer-aided tissue engineering: overview, scope and challenges," *Biotechnology and Applied Biochemistry*, vol. 39, part 1, pp. 29–47, 2004.

[103] W. Sun and P. Lal, "Recent development on computer aided tissue engineering—a review," *Computer Methods and Programs in Biomedicine*, vol. 67, no. 2, pp. 85–103, 2002.

[104] W. Sun, B. Starly, A. Darling, and C. Gomez, "Computer-aided tissue engineering: application to biomimetic modelling and design of tissue scaffolds," *Biotechnology and Applied Biochemistry*, vol. 39, no. 1, pp. 49–58, 2004.

[105] Z. Fang, B. Starly, and W. Sun, "Computer-aided characterization for effective mechanical properties of porous tissue scaffolds," *CAD Computer Aided Design*, vol. 37, no. 1, pp. 65–72, 2005.

[106] S. Lalan, I. Pomerantseva, and J. P. Vacanti, "Tissue engineering and its potential impact on surgery," *World Journal of Surgery*, vol. 25, no. 11, pp. 1458–1466, 2001.

[107] T. Boland, V. Mironov, A. Gutowska, E. A. Roth, and R. R. Markwald, "Cell and organ printing 2: fusion of cell aggregates in three-dimensional gels," *Anatomical Record A*, vol. 272, no. 2, pp. 497–502, 2003.

[108] N. Hirata, K. I. Matsumoto, T. Inishita, Y. Takenaka, Y. Suma, and H. Shintani, "Gamma-ray irradiation, autoclave and ethylene oxide sterilization to thermosetting polyurethane: sterilization to polyurethane," *Radiation Physics and Chemistry*, vol. 46, no. 3, pp. 377–381, 1995.

[109] K. A. Hooper, J. D. Cox, and J. Kohn, "Comparison of the effect of ethylene oxide and γ-irradiation on selected tyrosine-derived polycarbonates and poly(L-lactic acid)," *Journal of Applied Polymer Science*, vol. 63, no. 11, pp. 1499–1510, 1997.

[110] C. E. Holy, C. Cheng, J. E. Davies, and M. S. Shoichet, "Optimizing the sterilization of PLGA scaffolds for use in tissue engineering," *Biomaterials*, vol. 22, no. 1, pp. 25–31, 2001.

[111] C. Volland, M. Wolff, and T. Kissel, "The influence of terminal gamma-sterilization on captopril containing poly(D,L-lactide-co-glycolide) microspheres," *Journal of Controlled Release*, vol. 31, no. 3, pp. 293–304, 1994.

[112] M. B. Sintzel, K. S. Abdellaoui, K. Mader et al., "Influence of irradiation sterilization on a semi-solid poly(ortho ester)," *International Journal of Pharmaceutics*, vol. 175, pp. 165–176, 1998.

[113] L. Montanari, M. Costantini, E. C. Signoretti et al., "Gamma irradiation effects on poly(DL-lactictide-co-glycolide) microspheres," *Journal of Controlled Release*, vol. 56, no. 1–3, pp. 219–229, 1998.

[114] M. Ohrlander, R. Erickson, R. Palmgren, A. Wirsen, and A. C. Albertsson, "The effect of electron beam irradiation on PCL and PDXO-X monitored by luminescence and electron spin resonance measurements," *Polymer*, vol. 41, pp. 1277–1286, 1999.

[115] J. S. C. Loo, C. P. Ooi, and F. Y. C. Boey, "Degradation of poly(lactide-co-glycolide) (PLGA) and poly(L-lactide) (PLLA) by electron beam radiation," *Biomaterials*, vol. 26, no. 12, pp. 1359–1367, 2005.

[116] K. Odelius, P. Plikk, and A. C. Albertsson, "The influence of composition of porous copolyester scaffolds on reactions induced by irradiation sterilization," *Biomaterials*, vol. 29, no. 2, pp. 129–140, 2008.

[117] E. M. Darmady, K. E. Hughes, J. D. Jones, D. Prince, and W. Tuke, "Sterilization by dry heat," *Journal of Clinical Pathology*, vol. 14, pp. 38–44, 1961.

[118] Q. Fu, M. N. Rahaman, B. S. Bal, and R. F. Brown, "In vitro cellular response to hydroxyapatite scaffolds with oriented pore architectures," *Materials Science and Engineering C*, vol. 29, no. 7, pp. 2147–2153, 2009.

[119] F. A. Müller, L. Müller, I. Hofmann, P. Greil, M. M. Wenzel, and R. Staudenmaier, "Cellulose-based scaffold materials for cartilage tissue engineering," *Biomaterials*, vol. 27, no. 21, pp. 3955–3963, 2006.

[120] K. Gellynck, P. C. M. Verdonk, E. Van Nimmen et al., "Silkworm and spider silk scaffolds for chondrocyte support," *Journal of Materials Science: Materials in Medicine*, vol. 19, no. 11, pp. 3399–3409, 2008.

[121] S. Terasaka, Y. Iwasaki, N. Shinya, and T. Uchida, "Fibrin glue and polyglycolic acid nonwoven fabric as a biocompatible dural substitute," *Neurosurgery*, vol. 58, no. 1, pp. S-134–S-138, 2006.

[122] P. B. Maurus and C. C. Kaeding, "Bioabsorbable implant material review," *Operative Techniques in Sports Medicine*, vol. 12, no. 3, pp. 158–160, 2004.

[123] H. H. Lu, J. A. Cooper, S. Manuel et al., "Anterior cruciate ligament regeneration using braided biodegradable scaffolds: in vitro optimization studies," *Biomaterials*, vol. 26, no. 23, pp. 4805–4816, 2005.

[124] J. A. Cooper, H. H. Lu, F. K. Ko, J. W. Freeman, and C. T. Laurencin, "Fiber-based tissue-engineered scaffold for ligament replacement: design considerations and in vitro evaluation," *Biomaterials*, vol. 26, no. 13, pp. 1523–1532, 2005.

[125] M. Zilberman, K. D. Nelson, and R. C. Eberhart, "Mechanical properties and in vitro degradation of bioresorbable fibers and expandable fiber-based stents," *Journal of Biomedical Materials Research B*, vol. 74, no. 2, pp. 792–799, 2005.

[126] S. Leinonen, E. Suokas, M. Veiranto, P. Tormala, T. Waris, and N. Ashammakhi, "Healing power of bioadsorbable ciprofloxacin- containing self reinforced poly(L/DL-lactide 70/30 bioactive glass 13 miniscrews in human cadaver bone," *Journal of Craniofacial Surgery*, vol. 13, pp. 212–218, 2002.

[127] C. W. Pouton and S. Akhtar, "Biosynthetic polyhydroxyalkanoates and their potential in drug delivery," *Advanced Drug Delivery Reviews*, vol. 18, no. 2, pp. 133–162, 1996.

[128] B. Saad, T. D. Hirt, M. Welti, G. K. Uhlschmid, P. Neuenschwander, and U. W. Suter, "Development of degradable polyesterurethanes for medical applications: in vitro and in vivo evaluations," *Journal of Biomedical Materials Research*, vol. 36, no. 1, pp. 65–74, 1997.

[129] I. C. Bonzani, R. Adhikari, S. Houshyar, R. Mayadunne, P. Gunatillake, and M. M. Stevens, "Synthesis of two-component injectable polyurethanes for bone tissue engineering," *Biomaterials*, vol. 28, no. 3, pp. 423–433, 2007.

[130] J. Heller, "Ocular delivery using poly(ortho esters)," *Advanced Drug Delivery Reviews*, vol. 57, no. 14, pp. 2053–2062, 2005.

[131] D. S. Katti, S. Lakshmi, R. Langer, and C. T. Laurencin, "Toxicity, biodegradation and elimination of polyanhydrides," *Advanced Drug Delivery Reviews*, vol. 54, no. 7, pp. 933–961, 2002.

[132] C. Vauthier, C. Dubernet, C. Chauvierre, I. Brigger, and P. Couvreur, "Drug delivery to resistant tumors: the potential of poly(alkyl cyanoacrylate) nanoparticles," *Journal of Controlled Release*, vol. 93, no. 2, pp. 151–160, 2003.

[133] P. Sai and M. Babu, "Collagen based dressings—a review," *Burns*, vol. 26, no. 1, pp. 54–62, 2000.

[134] X. Duan, C. McLaughlin, M. Griffith, and H. Sheardown, "Biofunctionalization of collagen for improved biological response: scaffolds for corneal tissue engineering," *Biomaterials*, vol. 28, no. 1, pp. 78–88, 2007.

[135] D. R. Hunt, S. A. Joanovic, U. M. E. Wikesjo, J. M. Wozney, and D. W. Bernard, "Hyaluronan supports recombinant human bone morphogenetic protein-2 induced bone reconstruction of advanced alveolar ridge defects in dogs. A pilot study," *Journal of Periodontology*, vol. 72, pp. 651–657, 2001.

[136] B. L. Eppley and B. Dadvand, "Injectable soft-tissue fillers: clinical overview," *Plastic and Reconstructive Surgery*, vol. 118, no. 4, pp. 98e–106e, 2006.

[137] Y. Kato, S. Nakamura, and M. Nishimura, "Beneficial actions of hyaluronan (HA) on arthritic joints: effects of molecular weight of HA on elasticity of cartilage matrix," *Biorheology*, vol. 43, no. 3-4, pp. 347–354, 2006.

[138] D. W. Hutmacher, "Scaffold design and fabrication technologies for engineering tissues—State of the art and future perspectives," *Journal of Biomaterials Science*, vol. 12, no. 1, pp. 107–124, 2001.

[139] L. E. Freed, G. Vunjak-Novakovic, R. J. Biron et al., "Biodegradable polymer scaffolds for tissue engineering," *Biotechnology*, vol. 12, no. 7, pp. 689–693, 1994.

[140] L. E. Freed and G. Vunjak-Novakovic, "Culture of organized cell communities," *Advanced Drug Delivery Reviews*, vol. 33, no. 1-2, pp. 15–30, 1998.

[141] P. X. Ma and R. Zhang, "Microtubular architecture of biodegradable polymer scaffolds," *Journal of Biomedical Materials Research*, vol. 56, no. 4, pp. 469–477, 2001.

[142] S. Freiberg and X. X. Zhu, "Polymer microspheres for controlled drug release," *International Journal of Pharmaceutics*, vol. 282, no. 1-2, pp. 1–18, 2004.

[143] D. J. Mooney, G. Organ, J. P. Vacanti, and R. Langer, "Design and fabrication of biodegradable polymer devices to engineer tubular tissues," *Cell Transplantation*, vol. 3, no. 2, pp. 203–210, 1994.

[144] G. Wei and P. X. Ma, "Structure and properties of nano-hydroxyapatite/polymer composite scaffolds for bone tissue engineering," *Biomaterials*, vol. 25, no. 19, pp. 4749–4757, 2004.

[145] E. M. Ouriemchi and J. M. Vergnaud, "Processes of drug transfer with three different polymeric systems with transdermal drug delivery," *Computational and Theoretical Polymer Science*, vol. 10, no. 5, pp. 391–401, 2000.

[146] Q. Hou, D. W. Grijpma, and J. Feijen, "Preparation of porous poly(ε-caprolactone) structures," *Macromolecular Rapid Communications*, vol. 23, no. 4, pp. 247–252, 2002.

[147] Q. Hou, D. W. Grijpma, and J. Feijen, "Porous polymeric structures for tissue engineering prepared by a coagulation, compression moulding and salt leaching technique," *Biomaterials*, vol. 24, no. 11, pp. 1937–1947, 2003.

[148] M. Cabodi, N. W. Choi, J. P. Gleghorn, C. S. D. Lee, L. J. Bonassar, and A. D. Stroock, "A microfluidic biomaterial," *Journal of the American Chemical Society*, vol. 127, no. 40, pp. 13788–13789, 2005.

[149] M. S. Jhon and J. D. Andrade, "Water and hydrogels," *Journal of Biomedical Materials Research*, vol. 7, no. 6, pp. 509–522, 1973.

[150] A. S. Hoffman, "Hydrogels for biomedical applications," *Annals of the New York Academy of Sciences*, vol. 944, pp. 62–73, 2001.

[151] J. A. Hubbell, "Bioactive biomaterials," *Current Opinion in Biotechnology*, vol. 10, no. 2, pp. 123–129, 1999.

[152] K. Y. Lee and D. J. Mooney, "Hydrogels for tissue engineering," *Chemical Reviews*, vol. 101, no. 7, pp. 1869–1879, 2001.

[153] N. A. Peppas and A. R. Khare, "Preparation, structure and diffusional behavior of hydrogels in controlled release," *Advanced Drug Delivery Reviews*, vol. 11, no. 1-2, pp. 1–35, 1993.

[154] Y. Tabata, "Tissue regeneration based on growth factor release," *Tissue Engineering*, vol. 9, no. 4, pp. 5–15, 2003.

[155] S. J. Bryant and K. S. Anseth, "The effects of scaffold thickness on tissue engineered cartilage in photocrosslinked poly(ethylene oxide) hydrogels," *Biomaterials*, vol. 22, no. 6, pp. 619–626, 2001.

[156] D. G. Wallace and J. Rosenblatt, "Collagen gel systems for sustained delivery and tissue engineering," *Advanced Drug Delivery Reviews*, vol. 55, no. 12, pp. 1631–1649, 2003.

[157] U. J. Kim, J. Park, C. Li, H. J. Jin, R. Valluzzi, and D. L. Kaplan, "Structure and properties of silk hydrogels," *Biomacromolecules*, vol. 5, no. 3, pp. 786–792, 2004.

[158] D. Eyrich, F. Brandl, B. Appel et al., "Long-term stable fibrin gels for cartilage engineering," *Biomaterials*, vol. 28, no. 1, pp. 55–65, 2007.

[159] L. A. Solchaga, J. Gao, J. E. Dennis et al., "Treatment of osteochondral defects with autologous bone marrow in a hyaluronan-based delivery vehicle," *Tissue Engineering*, vol. 8, no. 2, pp. 333–347, 2002.

[160] H. J. Kong, M. K. Smith, and D. J. Mooney, "Designing alginate hydrogels to maintain viability of immobilized cells," *Biomaterials*, vol. 24, no. 22, pp. 4023–4029, 2003.

[161] J. K. Francis Suh and H. W. T. Matthew, "Application of chitosan-based polysaccharide biomaterials in cartilage tissue engineering: a review," *Biomaterials*, vol. 21, no. 24, pp. 2589–2598, 2000.

[162] R. H. Schmedlen, K. S. Masters, and J. L. West, "Photocrosslinkable polyvinyl alcohol hydrogels that can be modified with cell adhesion peptides for use in tissue engineering," *Biomaterials*, vol. 23, no. 22, pp. 4325–4332, 2002.

[163] E. Behravesh and A. G. Mikos, "Three-dimensional culture of differentiating marrow stromal osteoblasts in biomimetic poly(propylene fumarate-co-ethylene glycol)-based macroporous hydrogels," *Journal of Biomedical Materials Research A*, vol. 66, no. 3, pp. 698–706, 2003.

[164] S. J. Bryant, K. A. Davis-Arehart, N. Luo, R. K. Shoemaker, J. A. Arthur, and K. S. Anseth, "Synthesis and characterization of photopolymerized multifunctional hydrogels: water-soluble poly(vinyl alcohol) and chondroitin sulfate macromers for chondrocyte encapsulation," *Macromolecules*, vol. 37, no. 18, pp. 6726–6733, 2004.

[165] P. Berndt, G. B. Fields, and M. Tirrell, "Synthetic lipidation of peptides and amino acids: monolayer structure and properties," *Journal of the American Chemical Society*, vol. 117, no. 37, pp. 9515–9522, 1995.

[166] S. R. Bhattarai, N. Bhattarai, H. K. Yi, P. H. Hwang, D. I. Cha, and H. Y. Kim, "Novel biodegradable electrospun membrane: scaffold for tissue engineering," *Biomaterials*, vol. 25, no. 13, pp. 2595–2602, 2004.

[167] Z. Ma, M. Kotaki, R. Inai, and S. Ramakrishna, "Potential of nanofiber matrix as tissue-engineering scaffolds," *Tissue Engineering*, vol. 11, no. 1-2, pp. 101–109, 2005.

[168] R. Vasita and D. S. Katti, "Nanofibers and their applications in tissue engineering," *International Journal of Nanomedicine*, vol. 1, no. 1, pp. 15–30, 2006.

[169] J. A. Matthews, G. E. Wnek, D. G. Simpson, and G. L. Bowlin, "Electrospinning of collagen nanofibers," *Biomacromolecules*, vol. 3, no. 2, pp. 232–238, 2002.

[170] Y. Zhang, H. Ouyang, T. L. Chwee, S. Ramakrishna, and Z. M. Huang, "Electrospinning of gelatin fibers and gelatin/PCL composite fibrous scaffolds," *Journal of Biomedical Materials Research B*, vol. 72, no. 1, pp. 156–165, 2005.

[171] X. Geng, O. H. Kwon, and J. Jang, "Electrospinning of chitosan dissolved in concentrated acetic acid solution," *Biomaterials*, vol. 26, no. 27, pp. 5427–5432, 2005.

[172] I. C. Um, D. Fang, B. S. Hsiao, A. Okamoto, and B. Chu, "Electro-spinning and electro-blowing of hyaluronic acid," *Biomacromolecules*, vol. 5, no. 4, pp. 1428–1436, 2004.

[173] H. J. Jin, J. Chen, V. Karageorgiou, G. H. Altman, and D. L. Kaplan, "Human bone marrow stromal cell responses on electrospun silk fibroin mats," *Biomaterials*, vol. 25, no. 6, pp. 1039–1047, 2004.

[174] F. Yang, R. Murugan, S. Wang, and S. Ramakrishna, "Electrospinning of nano/micro scale poly(l-lactic acid) aligned fibers and their potential in neural tissue engineering," *Biomaterials*, vol. 26, no. 15, pp. 2603–2610, 2005.

[175] S. A. Riboldi, M. Sampaolesi, P. Neuenschwander, G. Cossu, and S. Mantero, "Electrospun degradable polyesterurethane membranes: potential scaffolds for skeletal muscle tissue engineering," *Biomaterials*, vol. 26, no. 22, pp. 4606–4615, 2005.

[176] W. J. Li, K. G. Danielson, P. G. Alexander, and R. S. Tuan, "Biological response of chondrocytes cultured in three-dimensional nanofibrous poly(ε-caprolactone) scaffolds," *Journal of Biomedical Materials Research A*, vol. 67, no. 4, pp. 1105–1114, 2003.

[177] K. Uematsu, K. Hattori, Y. Ishimoto et al., "Cartilage regeneration using mesenchymal stem cells and a three-dimensional poly-lactic-glycolic acid (PLGA) scaffold," *Biomaterials*, vol. 26, no. 20, pp. 4273–4279, 2005.

[178] E. R. Kenawy, G. L. Bowlin, K. Mansfield et al., "Release of tetracycline hydrochloride from electrospun poly(ethylene-co-vinylacetate), poly(lactic acid), and a blend," *Journal of Controlled Release*, vol. 81, no. 1-2, pp. 57–64, 2002.

[179] X. M. Mo, C. Y. Xu, M. Kotaki, and S. Ramakrishna, "Electrospun P(LLA-CL) nanofiber: a biomimetic extracellular matrix for smooth muscle cell and endothelial cell proliferation," *Biomaterials*, vol. 25, no. 10, pp. 1883–1890, 2004.

[180] G. Verreck, I. Chun, J. Rosenblatt et al., "Incorporation of drugs in an amorphous state into electrospun nanofibers composed of a water-insoluble, nonbiodegradable polymer," *Journal of Controlled Release*, vol. 92, no. 3, pp. 349–360, 2003.

[181] M. Singh, C. P. Morris, R. J. Ellis, M. S. Detamore, and C. Berkland, "Microsphere-based seamless scaffolds containing macroscopic gradients of encapsulated factors for tissue engineering," *Tissue Engineering C*, vol. 14, no. 4, pp. 299–309, 2008.

[182] M. Singh, B. Sandhu, A. Scurto, C. Berkland, and M. S. Detamore, "Microsphere-based scaffolds for cartilage tissue engineering: using subcritical CO_2 as a sintering agent," *Acta Biomaterialia*, vol. 6, no. 1, pp. 137–143, 2010.

[183] D. Stephens, L. Li, D. Robinson et al., "Investigation of the in vitro release of gentamicin from a polyanhydride matrix," *Journal of Controlled Release*, vol. 63, no. 3, pp. 305–317, 2000.

[184] C. Berkland, M. King, A. Cox, K. Kim, and D. W. Pack, "Precise control of PLG microsphere size provides enhanced control of drug release rate," *Journal of Controlled Release*, vol. 82, no. 1, pp. 137–147, 2002.

[185] H. B. Ravivarapu, K. Burton, and P. P. DeLuca, "Polymer and microsphere blending to alter the release of a peptide from PLGA microspheres," *European Journal of Pharmaceutics and Biopharmaceutics*, vol. 50, no. 2, pp. 263–270, 2000.

[186] R. A. Jain, C. T. Rhodes, A. M. Railkar, A. W. Malick, and N. H. Shah, "Controlled delivery of drugs from a novel injectable in situ formed biodegradable PLGA microsphere system," *Journal of Microencapsulation*, vol. 17, no. 3, pp. 343–362, 2000.

[187] C. Berkland, K. Kim, and D. W. Pack, "PLG microsphere size controls drug release rate through several competing factors," *Pharmaceutical Research*, vol. 20, no. 7, pp. 1055–1062, 2003.

[188] M. Borden, M. Attawia, Y. Khan, S. F. El-Amin, and C. T. Laurencin, "Tissue-engineered bone formation in vivo using a novel sintered polymeric microsphere matrix," *Journal of Bone and Joint Surgery B*, vol. 86, no. 8, pp. 1200–1208, 2004.

[189] J. Yao, S. Radin, P. S. Leboy P., and P. Ducheyne, "The effect of bioactive glass content on synthesis and bioactivity of composite poly (lactic-co-glycolic acid)/bioactive glass substrate for tissue engineering," *Biomaterials*, vol. 26, no. 14, pp. 1935–1943, 2005.

[190] A. Jaklenec, E. Wan, M. E. Murray, and E. Mathiowitz, "Novel scaffolds fabricated from protein-loaded microspheres for tissue engineering," *Biomaterials*, vol. 29, no. 2, pp. 185–192, 2008.

[191] A. Jaklenec, A. Hinckfuss, B. Bilgen, D. M. Ciombor, R. Aaron, and E. Mathiowitz, "Sequential release of bioactive IGF-I and TGF-β1 from PLGA microsphere-based scaffolds," *Biomaterials*, vol. 29, no. 10, pp. 1518–1525, 2008.

[192] J. L. Brown, L. S. Nair, and C. T. Laurencin, "Solvent/non-solvent sintering: a novel route to create porous microsphere scaffolds for tissue regeneration," *Journal of Biomedical Materials Research B*, vol. 86, no. 2, pp. 396–406, 2008.

[193] S. P. Nukavarapu, S. G. Kumbar, J. L. Brown et al., "Polyphosphazene/nano-hydroxyapatite composite microsphere scaffolds for bone tissue engineering," *Biomacromolecules*, vol. 9, no. 7, pp. 1818–1825, 2008.

[194] M. Borden, M. Attawia, and C. T. Laurencin, "The sintered microsphere matrix for bone tissue engineering: in vitro osteoconductivity studies," *Journal of Biomedical Materials Research*, vol. 61, no. 3, pp. 421–429, 2002.

[195] Y. M. Khan, D. S. Katti, and C. T. Laurencin, "Novel polymer-synthesized ceramic composite-based system for bone repair: an in vitro evaluation," *Journal of Biomedical Materials Research A*, vol. 69, no. 4, pp. 728–737, 2004.

[196] K. Rezwan, Q. Z. Chen, J. J. Blaker, and A. R. Boccaccini, "Biodegradable and bioactive porous polymer/inorganic composite scaffolds for bone tissue engineering," *Biomaterials*, vol. 27, no. 18, pp. 3413–3431, 2006.

[197] L. L. Hench, "Bioceramics: from concept to clinic," *American Ceramic Society Bulletin*, vol. 72, pp. 93–98, 1993.

[198] R. L. Hentrich Jr., G. A. Graves Jr., H. G. Stein, and P. K. Bajpai, "Evaluation of inert and resorbable ceramics for future clinical orthopedic applications," *Journal of Biomedical Materials Research*, vol. 5, no. 1, pp. 25–51, 1971.

[199] J. B. Park and R. S. Lakes, *Biomaterials—An Introduction*, Plenum Press, New York, NY, USA, 2nd edition, 1992.

[200] J. J. Blaker, J. E. Gough, V. Maquet, I. Notingher, and A. R. Boccaccini, "In vitro evaluation of novel bioactive composites based on Bioglass®-filled polylactide foams for bone tissue engineering scaffolds," *Journal of Biomedical Materials Research A*, vol. 67, no. 4, pp. 1401–1411, 2003.

[201] H. W. Kim, E. J. Lee, I. K. Jun, H. E. Kim, and J. C. Knowles, "Degradation and drug release of phosphate glass/polycaprolactone biological composites for hard-tissue regeneration," *Journal of Biomedical Materials Research B*, vol. 75, no. 1, pp. 34–41, 2005.

[202] C. Du, F. Z. Cui, X. D. Zhu, and K. De Groot, "Three-dimensional nano-HAp/collagen matrix loading with osteogenic cells in organ culture," *Journal of Biomedical Materials Research*, vol. 44, no. 4, pp. 407–415, 1999.

[203] A. Bigi, E. Boanini, S. Panzavolta, N. Roveri, and K. Rubini, "Bonelike apatite growth on hydroxyapatite-gelatin sponges from simulated body fluid," *Journal of Biomedical Materials Research*, vol. 59, no. 4, pp. 709–715, 2002.

[204] Y. Zhang and M. Zhang, "Synthesis and characterization of macroporous chitosan/calcium phosphate composite scaffolds for tissue engineering," *Journal of Biomedical Materials Research*, vol. 55, no. 3, pp. 304–312, 2001.

[205] S. E. Dahms, H. J. Piechota, R. Dahiya, T. F. Lue, and E. A. Tanagho, "Composition and biomechanical properties of the bladder acellular matrix graft: comparative analysis in rat, pig and human," *British Journal of Urology*, vol. 82, no. 3, pp. 411–419, 1998.

[206] J. J. Yoo, J. Meng, F. Oberpenning, and A. Atala, "Bladder augmentation using allogenic bladder submucosa seeded with cells," *Urology*, vol. 51, no. 2, pp. 221–225, 1998.

[207] F. Chen, J. J. Yoo, and A. Atala, "Acellular collagen matrix as a possible 'off the shelf' biomaterial for urethral repair," *Urology*, vol. 54, no. 3, pp. 407–410, 1999.

[208] G. J. Wilson, D. W. Courtman, P. Klement, J. M. Lee, and H. Yeger, "Acellular matrix: a biomaterials approach for coronary artery bypass and heart valve replacement," *Annals of Thoracic Surgery*, vol. 60, supplement 2, pp. S353–S358, 1995.

[209] S. E. Dahms, H. J. Piechota, L. Nunes, R. Dahiya, T. F. Lue, and E. A. Tanagho, "Free ureteral replacement in rats: regeneration of ureteral wall components in the acellular matrix graft," *Urology*, vol. 50, no. 5, pp. 818–825, 1997.

[210] M. Probst, R. Dahiya, S. Carrier, and E. A. Tanagho, "Reproduction of functional smooth muscle tissue and partial bladder replacement," *British Journal of Urology*, vol. 79, no. 4, pp. 505–515, 1997.

[211] T. W. Gilbert, T. L. Sellaro, and S. F. Badylak, "Decellularization of tissues and organs," *Biomaterials*, vol. 27, no. 19, pp. 3675–3683, 2006.

[212] C. Stamm, A. Khosravi, N. Grabow et al., "Biomatrix/polymer composite material for heart valve tissue engineering," *Annals of Thoracic Surgery*, vol. 78, no. 6, pp. 2084–2093, 2004.

[213] M. Sokolsky-Papkov, K. Agashi, A. Olaye, K. Shakesheff, and A. J. Domb, "Polymer carriers for drug delivery in tissue engineering," *Advanced Drug Delivery Reviews*, vol. 59, no. 4-5, pp. 187–206, 2007.

[214] B. D. Boyan, T. W. Hummert, D. D. Dean, and Z. Schwartz, "Role of material surfaces in regulating bone and cartilage cell response," *Biomaterials*, vol. 17, no. 2, pp. 137–146, 1996.

[215] K. T. Tran, L. Griffith, and A. Wells, "Extracellular matrix signaling through growth factor receptors during wound healing," *Wound Repair and Regeneration*, vol. 12, no. 3, pp. 262–268, 2004.

[216] K. S. Midwood, L. V. Williams, and J. E. Schwarzbauer, "Tissue repair and the dynamics of the extracellular matrix," *International Journal of Biochemistry and Cell Biology*, vol. 36, no. 6, pp. 1031–1037, 2004.

[217] R. N. S. Sodhi, "Application of surface analytical and modification techniques to biomaterial research," *Journal of Electron Spectroscopy and Related Phenomena*, vol. 81, no. 3, pp. 269–284, 1996.

[218] D. M. Brewis and D. Briggs, "Adhesion to polyethylene and polypropylene," *Polymer*, vol. 22, no. 1, pp. 7–16, 1981.

[219] D. L. Elbert and J. A. Hubbell, "Surface treatments of polymers for biocompatibility," *Annual Review of Materials Science*, vol. 26, no. 1, pp. 365–394, 1996.

[220] C. A. Léon y León, "New perspectives in mercury porosimetry," *Advances in Colloid and Interface Science*, vol. 76-77, pp. 341–372, 1998.

[221] A. G. A. Coombes, S. C. Rizzi, M. Williamson, J. E. Barralet, S. Downes, and W. A. Wallace, "Precipitation casting of polycaprolactone for applications in tissue engineering and drug delivery," *Biomaterials*, vol. 25, no. 2, pp. 315–325, 2004.

[222] J. H. Brauker, V. E. Carr-Brendel, L. A. Martinson, J. Crudele, W. D. Johnston, and R. C. Johnson, "Neovascularization of synthetic membranes directed by membrane micro architecture," *Journal of Biomedical Materials Research*, vol. 29, pp. 1517–1524, 1995.

[223] J. J. Klawitter and S. F. Hulbert, "Application of porous ceramics for the attachment of load-bearing internal orthopedic applications," *Journal of Biomedical Materials Research A Symposium*, vol. 2, pp. 161–168, 1971.

[224] S. Yang, K. F. Leong, Z. Du, and C. K. Chua, "The design of scaffolds for use in tissue engineering—part I: traditional factors," *Tissue Engineering*, vol. 7, no. 6, pp. 679–689, 2001.

[225] K. Whang, K. E. Healy, D. R. Elenz et al., "Engineering bone regeneration with bioabsorbable scaffolds with novel microarchitecture," *Tissue Engineering*, vol. 5, no. 1, pp. 35–51, 1999.

[226] I. V. Yannas, E. Lee, D. P. Orgill, E. M. Skrabut, and G. F. Murphy, "Synthesis and characterization of a model extracellular matrix that induces partial regeneration of adult mammalian skin," *Proceedings of the National Academy of Sciences of the United States of America*, vol. 86, no. 3, pp. 933–937, 1989.

[227] A. J. Salgado, O. P. Coutinho, and R. L. Reis, "Bone tissue engineering: state of the art and future trends," *Macromolecular Bioscience*, vol. 4, no. 8, pp. 743–765, 2004.

[228] D. F. Williams, "On the mechanisms of biocompatibility," *Biomaterials*, vol. 29, no. 20, pp. 2941–2953, 2008.

[229] G. Khang, J. H. Jeon, J. W. Lee, S. C. Cho, and H. B. Lee, "Cell and platelet adhesions on plasma glow discharge-treated poly(lactide-co-glycolide)," *Bio-Medical Materials and Engineering*, vol. 7, no. 6, pp. 357–368, 1997.

[230] K. D. Colter, M. Shen, and A. T. Bell, "Reduction of progesterone release rate through silicone membranes by plasma polymerization," *Biomaterials Medical Devices and Artificial Organs*, vol. 5, no. 1, pp. 13–24, 1977.

[231] M. Sato, M. Ishihara, M. Ishihara et al., "Effects of growth factors on heparin-carrying polystyrene-coated atelocollagen scaffold for articular cartilage tissue engineering," *Journal of Biomedical Materials Research B*, vol. 83, no. 1, pp. 181–188, 2007.

[232] H. Park, K. Y. Lee, S. J. Lee, K. E. Park, and W. H. Park, "Plasma-treated poly(lactic-co-glycolic acid) nanofibers for tissue engineering," *Macromolecular Research*, vol. 15, no. 3, pp. 238–243, 2007.

[233] S. A. Mitchell, M. R. Davidson, and R. H. Bradley, "Improved cellular adhesion to acetone plasma modified polystyrene surfaces," *Journal of Colloid and Interface Science*, vol. 281, no. 1, pp. 122–129, 2005.

[234] J. C. Middleton and A. J. Tipton, "Synthetic biodegradable polymers as orthopedic devices," *Biomaterials*, vol. 21, no. 23, pp. 2335–2346, 2000.

[235] M. A. Woodruff and D. W. Hutmacher, "The return of a forgotten polymer—polycaprolactone in the 21st century," *Progress in Polymer Science*, vol. 35, no. 10, pp. 1217–1256, 2010.

[236] W. P. Ye, F. S. Du, W. H. Jin, J. Y. Yang, and Y. Xu, "In vitro degradation of poly(caprolactone), poly(lactide) and their block copolymers: influence of composition, temperature and morphology," *Reactive and Functional Polymers*, vol. 32, no. 2, pp. 161–168, 1997.

[237] K. S. Anseth, C. N. Bowman, and L. Brannon-Peppas, "Mechanical properties of hydrogels and their experimental determination," *Biomaterials*, vol. 17, no. 17, pp. 1647–1657, 1996.

[238] P. V. Moghe, F. Berthiaume, R. M. Ezzell, M. Toner, R. G. Tompkins, and M. L. Yarmush, "Culture matrix configuration and composition in the maintenance of hepatocyte polarity and function," *Biomaterials*, vol. 17, no. 3, pp. 373–385, 1996.

[239] P. L. Ryan, R. A. Foty, J. Kohn, and M. S. Steinberg, "Tissue spreading on implantable substrates is a competitive outcome of cell-cell vs. cell-substratum adhesivity," *Proceedings of the National Academy of Sciences of the United States of America*, vol. 98, no. 8, pp. 4323–4327, 2001.

[240] D. E. Ingber, "Mechanical signaling and the cellular response to extracellular matrix in angiogenesis and cardiovascular physiology," *Circulation Research*, vol. 91, no. 10, pp. 877–887, 2002.

Hindawi Publishing Corporation
International Journal of Polymer Science
Volume 2011, Article ID 814163, 9 pages
doi:10.1155/2011/814163

Review Article

Hydrogel Contact Lens for Extended Delivery of Ophthalmic Drugs

Xiaohong Hu, Lingyun Hao, Huaiqing Wang, Xiaoli Yang, Guojun Zhang, Guoyu Wang, and Xiao Zhang

School of Material Engineering, Jinling Institute of Technology, Nanjing 211169, China

Correspondence should be addressed to Xiaohong Hu, huxiaohong07@163.com

Received 24 February 2011; Revised 5 April 2011; Accepted 12 April 2011

Academic Editor: Shanfeng Wang

Soft contact lenses can improve the bioavailability and prolong the residence time of drugs and, therefore, are ideal drug carriers for ophthalmic drug delivery. Hydrogels are the leading materials of soft contact lenses because of their biocompatibility and transparent characteristic. In order to increase the amount of load drug and to control their release at the expected intervals, many strategies are developed to modify the conventional contact lens as well as the novel hydrogel contact lenses that include (i) polymeric hydrogels with controlled hydrophilic/hydrophobic copolymer ratio; (ii) hydrogels for inclusion of drugs in a colloidal structure dispersed in the contact lenses; (iii) ligand-containing hydrogels; (iv) molecularly imprinted polymeric hydrogels; (v) hydrogel with the surface containing multilayer structure for drugs loading and releasing. The advantages and disadvantages of these strategies in modifying or designing hydrogel contact lenses for extended ophthalmic drug delivery are analyzed in this paper.

1. Introduction

Ocular disorders frequently occur in human body, which are mainly treated by drugs. In therapy uses, the drugs could present some side effects to the human body and even harm the normal tissues when their concentration is too high. On the other side, the drugs will not treat the diseases effectively when their concentration is too low [1]. Moreover, the treatments of ocular disorders are frequently slow processes extending from several days to several weeks. Therefore, the effective therapy must depend on the rational drug concentration and residence time. 90% or more of drugs used in ocular disorder therapy are in the form of eye drops or eye ointments [1]. Only 1–5% of the drugs contained in the eye drops can be effectively used, while a large part of the drugs enters the systemic circulation by either conjunctival uptake or drainage into the nasal cavity. Moreover, the residence time of eye drops is only 2 min or so [2]. These characteristics of eye drops cause inconvenient use, low efficiency, ineffective therapy, severe side effects, and so forth. Although eye ointments may be resident on the eye much longer than eye drops, they may affect the sight and irritate eye tissue [1, 3–5]. In order to overcome the disadvantages of eye drops and eye ointments, numerous strategies have been developed for the treatment of ocular disorders including increasing the viscosity of the eye drops and increasing the corneal permeability. Though these strategies may increase the drugs residence time and the bioactivities, they cannot completely satisfy the need for treatments of ocular disorders, especially for ocular disorders which need long-time therapy [6].

With the development of drug delivery, drug carriers such as particles, hydrogels, insert films, and contact lens have been developed to control the release of ophthalmic drugs [4, 6, 7]. Among these carriers contact lenses are particularly attractive because of their ability to prolong the residence time of drugs and improve their bioavailability, ease of control, and convenient use. Some research reported that in theory the use of efficient ocular drugs delivered by contact lens was 35 times better than that delivered by eye drops [8–11]. Hydrogels are the leading materials of soft contact lenses because of their biocompatibility and transparent characteristic [12, 13]. Therefore, hydrogel contact lenses are widely used in ophthalmic drug delivery.

Most conventional hydrogel contact lenses were used to deliver the ophthalmic drugs by soaking the contact lenses in drug solution to load the drugs, applying eye drops on contact lenses after being inserted into eyes, or incorporating the drugs into the monomer of hydrogel contact lenses. Recently, supercritical fluid- (SCF-) assisted method was used to enhance the drug loading amount in hydrogel contact lenses and to control their release [14, 15]. However, the sustained release time of drugs using the above-mentioned methods is no longer than 24 h, which is not suitable for extended drug delivery [9, 16, 17]. In recent years, many strategies are operated to modify the conventional contact lenses for extended drug delivery with the emergence and development of novel hydrogel contact lens. In this paper, the modifications of conventional contact lenses as well as novel contact lenses based hydrogels for extended ophthalmic drug delivery are introduced.

2. Hydrophilic/Hydrophobic Copolymer Hydrogel

Hydrogels are water-swollen polymeric materials that can absorb a large amount of water but not be dissolved in water [18]. After poly-hydroxyethyl methacrylate (pHEMA) hydrogels were first prepared as soft contact lenses in the 1960s, the hydrogel contact lenses have been used to deliver ophthalmic drugs. However, the conventional contact lenses have some limitations in the application of long-time therapy due to fast release rate of drugs and low loaded drug amount [11, 16, 17]. In order to enhance the potential capacity of hydrogel to load drugs and prolong the sustained release time of drugs, hydrophobic monomer such as 4-vinylpyridine (VP) or ionic monomer such as N-(3-aminopropyl)methacrylamide (APMA) was incorporated to pHEMA hydrogels [19]. The incorporation of ionic/hydrophobic monomer would increase the interaction between hydrogel and drugs so that the drugs had more difficulties diffusing from the hydrogel. Andrade-Vivero et al. also reported that the incorporated monomers remarkably increased the amount of loaded drugs (ibuprofen up to 10-fold or diclofenac up to 20-fold) without changing the viscoelastic properties and the state of water of hydrogel. The drug release profile of pHEMA-APMA could be controlled by ions in the media, the sustaining release process of pHEMA-VP lasted for at least 24 h for the ibuprofen and almost 1 week for the diclofenac [19].

In order to increase the oxygen permeability, silicone polymers replace the conventional contact lenses monomers [20–22]. Kim et al. used silicone macromer (bis-alpha, omega-(methacryloxypropyl) polydimethylsiloxane), hydrophobic monomer containing silicon (3-methacryloxypropyltris (trimethylsiloxy) silane, TRIS) and hydrophilic monomer (N,N-dimethylacrylamide, DMA) to synthesize extended wear of silicone hydrogel contact lenses and transport ophthalmic drugs (timolol, dexamethasone, and dexamethasone 21-acetate). It was found that the sustained drug release process of silicone hydrogels varied from 20 days up to more than three months depending on the compositions of hydrophobic and hydrophilic components of silicone hydrogels. The result also showed that the properties of silicone hydrogels such as mechanical properties, ion permeability, equilibrium water content, transparency, and surface contact angles were suitable for contact lens application [22]. However, if hydrophilic/hydrophobic ratio was improper, hydrophilic/hydrophobic copolymer hydrogel would became opaque because of phase separation. Although silicone hydrogel contact lenses possess high oxygen permeability, their stiffness also increases with the decrease of water content, which will be uncomfortable to patients because the cornea is soft.

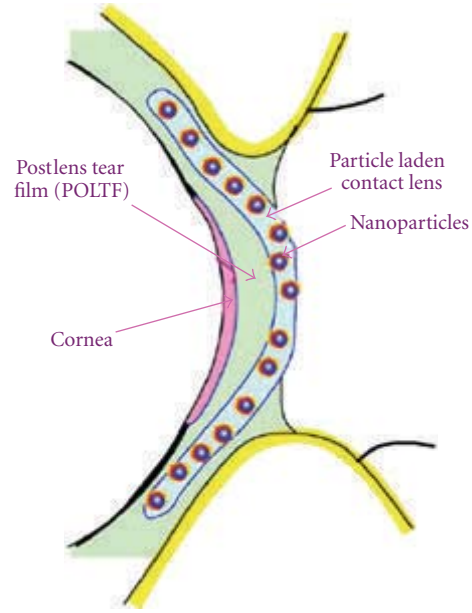

Figure 1: Schematic illustration of the particle-laden lens inserted in the eye [27, 28].

3. Colloid-Laden Hydrogel

Colloidal carriers have been exploited to achieve ophthalmic drug delivery [7]. These colloidal systems consist of micro-/nanoparticles, micro-/nanoemulsions, nanosuspensions, and liposomes [7]. It is reported that drug carriers via nanotechnology are favourable in enhancing drug permeation, controlling the release of drug and targeting drug [24]. Encapsulation of drugs in these colloidal carriers can also significantly prevent degradation from the ocular enzymes [25, 26]. Moreover, the size of these nanocarriers is small enough so as not to affect the vision of patient. Therefore, colloid carriers can be incorporated into hydrogels contact lens in order to prolong sustained release time of drugs and increase their bioavailability further [23, 27–29].

Gulsen and Chauhan encapsulated the ophthalmic drug formulations in microemulsion drops, and the drug-laden microemulsion drops were dispersed in the p-HEMA hydrogels, which was further inserted into the eyes as shown in Figure 1. The results of their study showed that the p-HEMA

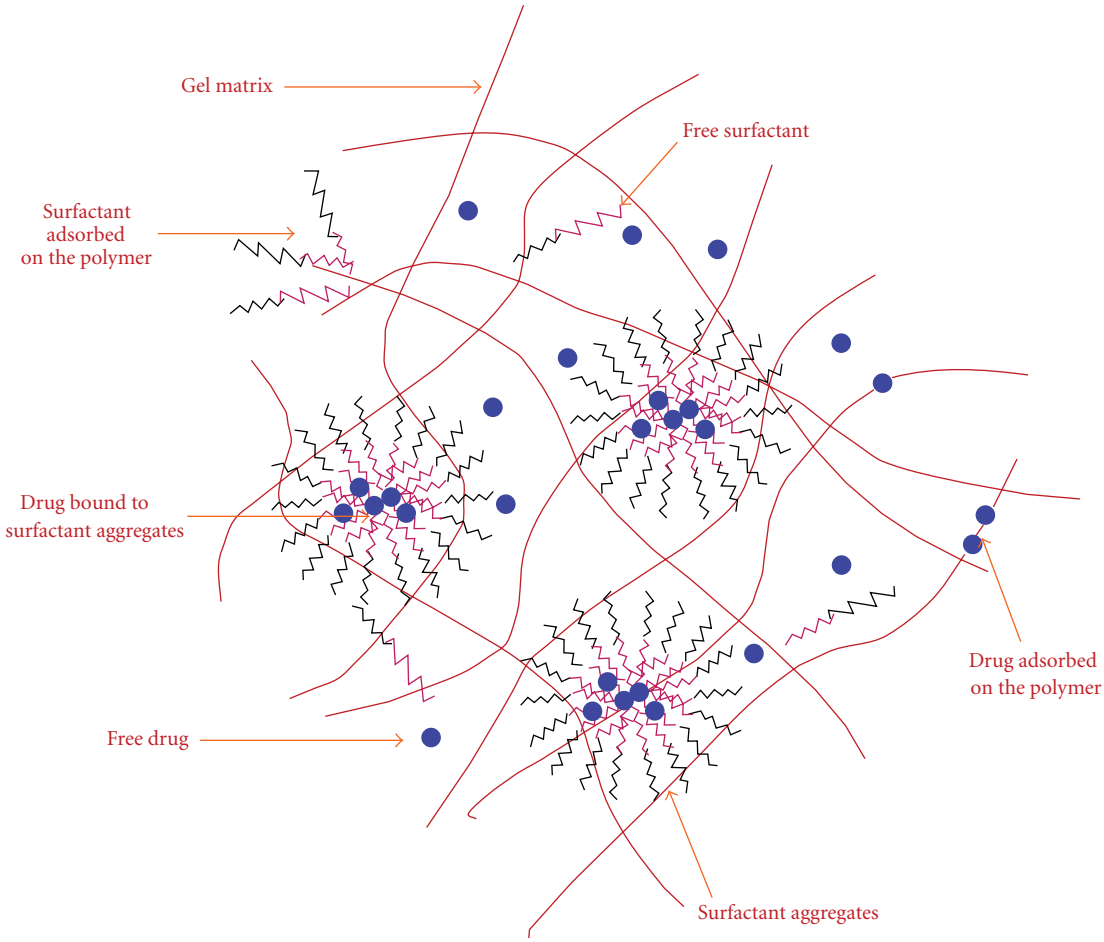

Figure 2: A schematic of the microstructure of the surfactant-laden gels [23].

gels loaded with microemulsions were transparent; these gels released drugs for a period of over 8 days, and the delivery rates could be tailored by controlling the particle and the drug loading. They also found that this system might provide lubricants to alleviate eye problems prevalent in extended lens wear as well as cure the ailments of eyes. However, the fabrication processes of microemulsion-loaded hydrogels require two-step processes: preparation of microemulsion drops, followed by entrapment in the hydrogels [27, 28].

It has also been proposed to create colloid-laden hydrogel *in situ* in one step. Surfactant-laden hydrogels can be prepared by addition of surfactants to the polymerizing mixture. A schematic of the microstructure of the surfactant-laden gels is shown in Figure 2. During the process of fabrication, the surfactants interact with polymer chains and form micelles creating hydrophobic cores, where the hydrophobic drugs will preferentially enter into. The drug transport is inhibited due to the presence of surfactant micelles. Kapoor et al. prepared Brij surfactant-laden p-HEMA hydrogels that can release Cyclosporine A (CyA) at a controlled rate for extended periods of time (20 days). Their results show that Brij surfactant-laden p-HEMA gels provide extended release of CyA and possess suitable mechanical and optical properties for contact lens applications. However, the hydrogels are not as effective for extended release of two other hydrophobic ophthalmic drugs, that is, dexamethasone (DMS) and dexamethasone 21 acetate (DMSA), because of insufficient partitioning inside the surfactant aggregates [23, 29].

However, there are some drawbacks of using colloid-laden hydrogel contact lenses. One is the instability of the colloid-laden hydrogel during preservation and transportation because the loaded drugs diffused into the hydrogel matrix. Another is the decaying release rate of colloid-laden hydrogel in ophthalmic drug delivery [11, 28].

4. Ligand-Containing Hydrogels

Weak interactions between drugs and ligands in polymer matrix including hydrogen bond, electrostatic interactions, and host-guest interactions can induce the drug loading and control its release by ions in solution [15, 30, 34–39].

Sato et al. synthesized hydrogels containing cationic functional groups for delivery of anionic drugs and hydrogels containing anionic functional groups for delivery of cationic drugs. The resulting hydrogels are capable of storing the anionic drugs or cationic drugs depending on the charge of functional groups based on ion-exchange reaction. The

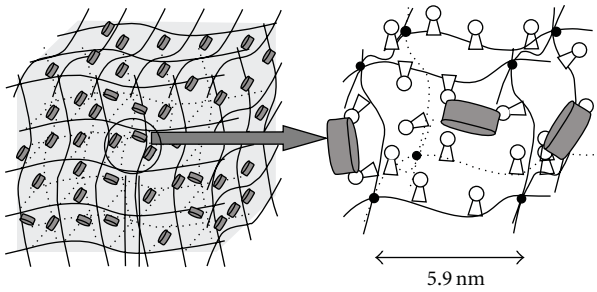

Figure 3: Scheme of a pHEMA-co-GMA hydrogel with pendant β-CDs [30].

incorporated drugs would be released into tear fluid by ion exchange. Their results also show that these hydrogels are suitable for soft contact lenses as ophthalmic drug delivery. However, the sustained release time of these ions ligand-containing hydrogels is only several hours, which made these hydrogels unsuitable for extended delivery of ophthalmic drugs [36, 37].

Cyclodextrins (CDs) are known as "host" molecules having hydrophobic internal cavities that can include "guest" drug molecules. These inclusion complexes are actually dynamic processes that result from noncovalent bonds between the CDs and their guests just as other weak interactions, and this means that CDs have found widespread applications in the fields of drug delivery [15, 34, 35]. Some efforts have been made to incorporate CDs into various polymer matrices in order to increase aqueous solubility and the stability in ophthalmic formulations, increase loaded drugs, and sustain the drug release for several days. dos Santos et al. developed acrylic hydrogels containing β-cyclodextrin (β-CD) by grafting reaction under mild conditions. The structure of hydrogel is shown in Figure 3 [30]. The hydrogels containing β-CD present similar light transmittance, glass transition temperature, swelling degree, viscoelasticity, oxygen permeability, surface contact angle, mechanical properties, and biocompatibility with acrylic hydrogels without β-CD but notably improving their ability to load drugs and sustaining drug delivery in lacrimal fluid for two weeks [30]. Jinku et al. synthesized pHEMA/β-CD hydrogel platform by photopolymerization of HEMA, monomethacrylated β-CD (mono-MA-β-CD), and trimethylolpropane trimethacrylate for sustained release of ophthalmic drugs. Their results showed that the incorporation of β-CD in the hydrogels increased the equilibrium swelling ratio and tensile strength. The drug (puerarin) loading and *in vitro* release rate were dependent on β-CD content in the pHEMA/β-CD hydrogels. The puerarin-loaded pHEMA/β-CD hydrogel contact lenses provided sustained drug release in the precorneal area of rabbits with longer retention time and higher bioavailability [39].

5. Molecularly Imprinted Polymeric Hydrogels

Molecularly imprinted polymers (MIPs) are investigated for the field of drug delivery due to their active sites of specific recognition [31, 40–42]. The general imprinting process includes five steps, as shown in Figure 4. First, template, functional monomer, crosslinking monomer, and initiator (Figure 4(a)) in solution are self-assembled into the prepolymerization complex (Figure 4(b)) via covalent or noncovalent chemistry. Second, the complex is initiated via UV light or heat to form crosslinked network (Figure 4(c)). Third, original template is removed via wash step, the crosslinked polymer network with cavities (Figure 4(d)) is formed. Fourth, new template (potential drug) is rebinding into the crosslinked polymer (Figure 4(e)). Fifth, the new template diffuses into solution via stimulation such as swelling (Figure 4(f)). During this imprinting process, the bioactivity of drugs can also be preserved [31].

In recent years, researchers incorporate MIPs into hydrogel contact lenses for increasing drugs loading and prolonging their sustained release time, considering advantages of MIPs and soft contact lenses in delivering ophthalmic drugs. Imprinted hydrogels with single functional monomer as well as multiple functional monomers are synthesized as soft contact lenses to deliver ophthalmic drugs [43–54]. More recently, some reviews presented comprehensive introduction of molecularly imprinted therapeutic contact lenses [51, 54]. Some representative drug-imprinted soft contact lenses as well as potential technology in drug-imprinted hydrogel are introduced as follows.

Hiratani and Alvarez-Lorenzo prepared imprinted contact lenses made of HEMA or N,N-diethylacrylamide (DEAA), low cross-linker proportions, and a small proportion of functional monomer (methacrylic acid, MAA), which was able to interact with drug (timolol maleate) via ionic and hydrogen bonds. It was found that imprinted HEMA-based and DEAA-based contact lenses uptook more timolol than the corresponding nonimprinted systems, the loaded lenses could sustain drug release in lacrimal fluid for more than 12 h, and the empty lenses could reload drug overnight for the next day use [45, 50]. The effects of four kinds of backbone monomers and the template/functional monomer proportion on the drug loading capacity, released behaviours, and properties such as the hydrophilic character, swelling degree, and mechanical properties were further researched [46, 48]. *In vivo* experiments, it was found that the imprinted contact lenses could be capable of prolonging the retention time of timolol in the precorneal area, compared to conventional contact lenses and eye drops [47]. Later, they designed imprinted HEMA-based hydrogel contact lens using acrylic acid (AA) as functional monomer to load and to release norfloxacin for several hours or even days in a sustained way [44]. However, the duration of drug release in these imprinted hydrogel contact lenses using one functional monomer was limited to less than 1 day *in vitro* and *in vivo* experiments.

Venkatesh et al. synthesized imprinted HEMA-co-polyethylene glycol (200) dimethacrylate- (PEG200DMA-) based contact lenses containing multiple functional monomers of AA, acrylamide (AM), and N-vinyl 2-pyrrolidinone (NVP) for the delivery of ocular medication such as H1-antihistamines. Their results showed that these contact lenses had the potential to load significant amounts of drug, as

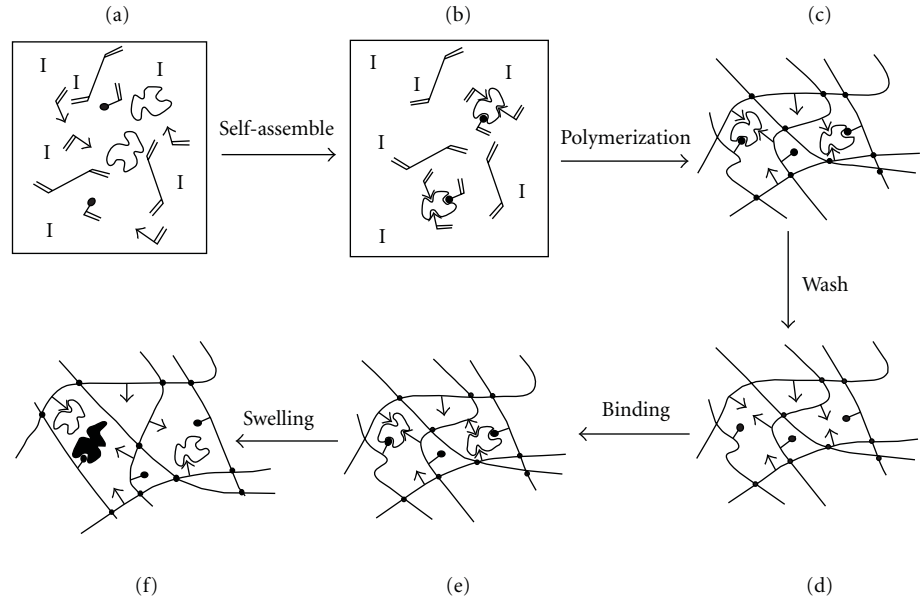

Figure 4: Imprinting process. (a) Solution mixture of template, functional monomer(s) (triangles and circles), crosslinking monomer, solvent, and initiator (I). (b) The prepolymerization complex is formed via covalent or noncovalent chemistry. (c) The formation of the network. (d) Wash step where original template is removed. (e) Rebinding of template. (f) In less crosslinked systems, movement of the macromolecular chains will produce areas of differing affinity and specificity (filled molecule is isomer of template) [31].

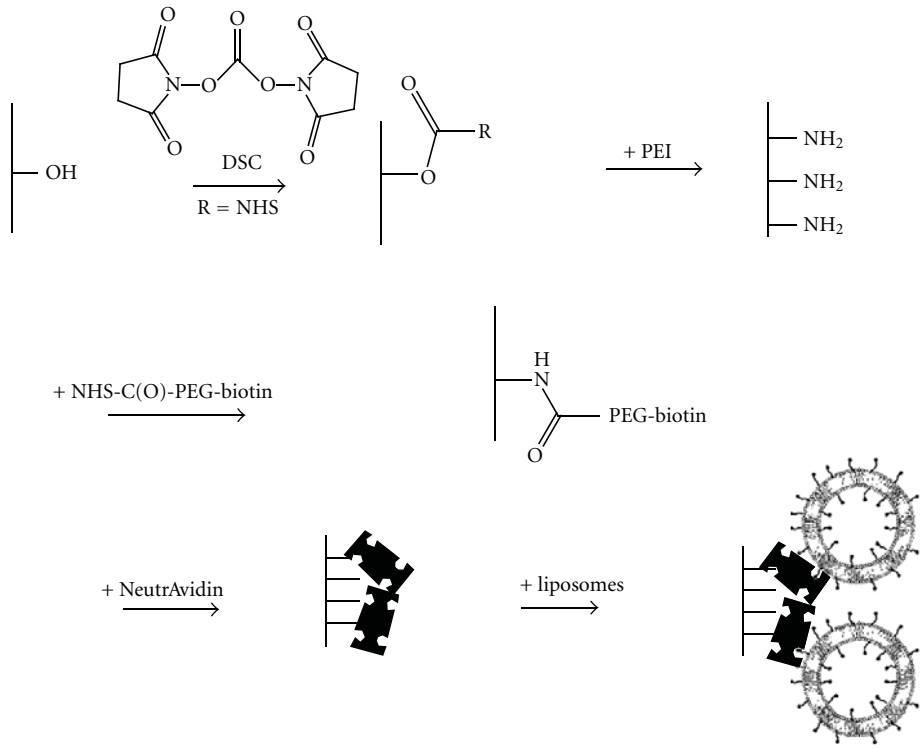

Figure 5: Chemical reactions leading to the attachment of liposomes onto the surfaces of soft contact lenses [32].

well as to release a therapeutic dosage of drug *in vitro* in a controlled fashion for 5 days with an even further extension in the presence of protein. It was also found that hydrogels of multiple complexation points with varying functionalities outperformed hydrogels formed with less diverse functional monomers, mechanical and optical properties of these hydrogels agreed with conventional lenses, and increased loading was reflected in a reduced propagation of polymer chains [49]. Ali and Byrne designed imprinted poly(vinyl alcohol)- (PVA-) based contact lenses containing multiple

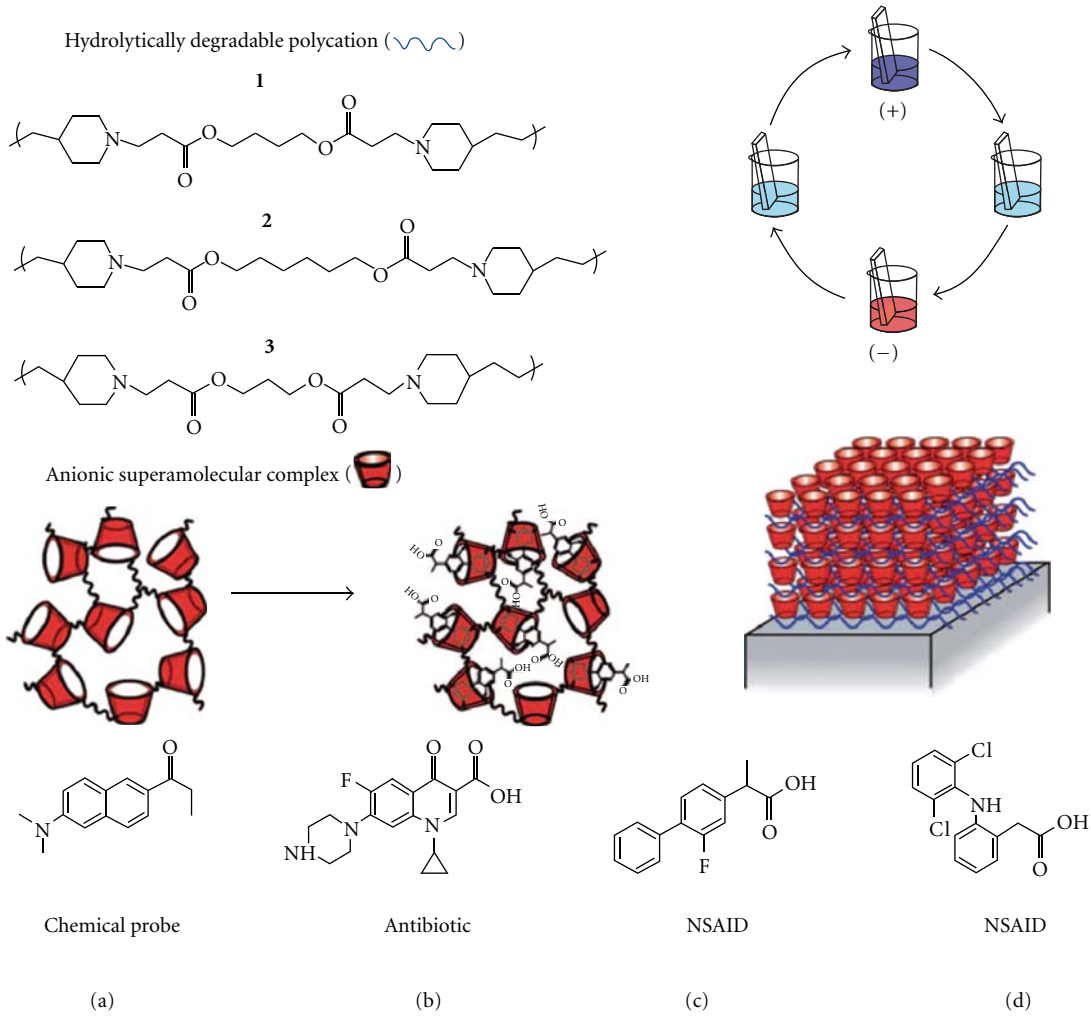

Figure 6: Methodology for LbL films. Left: film components. Three poly(β-amino esters) were investigated as degradable polycations. Poly(carboxymethyl-β-cyclodextrin) was used as the anionic supramolecular complex. Right: electrostatic assembly. Light blue: water. (+) indicates addition of polycation. (−) indicates addition of anionic supramolecular complex. Bottom shows molecules used in experimentation. NSAID: nonsteroidal anti-inflammatory drug [33].

functional monomers of AM, NVP, and 2-(diethylamino) ethyl methacrylate (DEAEM) for the therapeutic delivery of hyaluronic acid (HA) to the eye surface in desired release kinetics, to improve the wettability of lenses and to treat symptoms of dry eye [43].

More recently, Ribeiro et al. designed bioinspired imprinted hydrogels using HEMA as the backbone component. Zinc methacrylate, 1- or 4-vinylimidazole (1VI or 4VI), and N-hydroxyethyl acrylamide (HEAA) were combined to reproduce in the hydrogels the cone-shaped cavity of the CA, which contains a Zn^{2+} ion coordinated to three histidine residues. Consequently, biomimetic networks can load more drug and control better drug release than conventionally synthesized pHEMA hydrogels, being useful for the development of advanced controlled release systems. Nevertheless, aspects such as optical transparency, the effect of thickness on drug release length, and long-term durability of the biomimetic receptors require further studies to elucidate fully the practical potential of enzyme-mimicking networks [52].

6. Surface-Modified Hydrogels

Besides the efforts of modification during the hydrogel contact lenses fabrication to load drugs for ocular disorders' therapy, some efforts have been made to modify the surface of commercial contact lenses for the ophthalmic drug delivery. Danion et al. encapsulated drugs into liposomes and then subsequently bound these intact lipid vesicles onto both the anterior and posterior surfaces of commercial contact lenses. The process of immobilizing liposomes included three steps, as shown in Figure 5. In first step, polyethylenimine was grafted onto the surface of a commercial contact lens (Hioxifilcon B) via amidation under the catalyzation of disuccinimidyl carbonate (DSC). NHS-PEG-biotin molecules were following covalently bounded onto the surface by

carbodiimide chemistry. In the second step, NeutrAvidin was immobilized to the PEG-biotin layer via biotin-avidin affinity. Liposomes containing PEG-biotinylated lipids were then docked onto the surface-immobilized NeutrAvidin. In the third step, multilayers of liposomes were fabricated by consecutive addition of further NeutrAvidin and liposome layers or by exposing contact lenses coated with Neutr-Avidin to liposome aggregates produced by the addition of free biotin in solution. The results showed that the surface-immobilized, drug-filled liposome multilayers provide a promising avenue for site-specific delivery. However, no actual drug was investigated in this research [32].

Recently, layer-by-layer (LbL) platforms have been applied for drug delivery due to its simple, mild aqueous manufacturing conditions at room temperature [33, 55, 56]. Yet, LbL platforms cannot deliver small molecule drug with highly controlled release kinetics, and the release time scales delivered by LbL platforms is short. Some efforts have been made to modify the conventional LbL technique for small molecule drug delivery such as incorporating the cyclodextrin into LbL platform. Smith et al. designed layer-by-layer platforms to deliver small-molecule therapeutics from virtually any surface, regardless of geometry or surface chemistry, with programmable zero-order release kinetics through hydrolytic top-down degradation. Methodology for LbL films was shown in Figure 6 [33]. Poly(carboxymethyl-β-cyclodextrin) (polyCD) was complexed with a small molecule (Figures 6(a)–6(d)) as the anionic supramolecular complex. Poly(β-amino esters) (PBAEs) as the degradable polycations and the anionic supramolecular complex were alternately immobilized on the surface of the films via LbL technique. The drug of diclofenac or flurbiprofen in the LbL film could sustain release for 15 days in zero-order release kinetics [33].

7. Conclusions and Perspectives

It is estimated that nearly 100 million people wear contact lenses and the number is still increasing. Although contact lenses are designed to correct ametropia, they also show great perspective as therapeutic devices for delivery of ophthalmic drugs. An ideal contact lens-based ophthalmic drug delivery system would have the capacity of loading large amount of drugs and controlling the release in zero-order release profiles without influencing its own properties such as shape retaining, transparency stability, and oxygen permeability. The modification either during or after the manufacture of hydrogel contact lenses including the controlled hydrophilic/hydrophobic ratio, colloid-laden incorporation, ligand modification, MIPs, and multilayer technique broadens their applications in the field of ophthalmic drug delivery. According to the different properties of ophthalmic drugs, different measures must be made. For hydrophobic ophthalmic drugs, CD-containing hydrogels show potential application in therapeutic contact lenses, because hydrophobic internal cavities of CD can regulate hydrophobic drug release profiles though host-guest interaction. Imprinted hydrogels show great advantages to control hydrophilic drugs release and reload drugs. According to different usage of contact lenses such as daily disposable, monthly disposable, and yearly disposable, different hydrogel design must be made. For extended delivery of ophthalmic drugs, contact lens is often required prolonged use time. However, some ocular disorders are caused by contact lens wearing because of protein absorption or lacking biocompatibility surface. Therefore, some special hydrogel designs must be made to decrease the protein absorbing and increase biocompatibility of hydrogel. Moreover, *in vivo* studies are also needed for ocular therapeutic contact lenses application.

Acknowledgments

This paper is financially supported by the Research Fund of Jinling Institute of Technology in China (no. JIT40610008), the Doctoral Fund of Jinling Institute of Technology in China (no. JIT-b-201014), and the Natural Science Fund for Colleges and Universities in Jiangsu Province of China (no. 09kjd150011).

References

[1] J. C. Lang, "Ocular drug delivery conventional ocular formulations," *Advanced Drug Delivery Reviews*, vol. 16, no. 1, pp. 39–43, 1995.

[2] S. G. Deshpande and S. Shirolkar, "Sustained release ophthalmic formulations of pilocarpine," *Journal of Pharmacy and Pharmacology*, vol. 41, no. 3, pp. 197–200, 1989.

[3] M. T. Dorigo, R. De Natale, and P. A. Miglioli, "Collagen shields delivery of netilmicin: a study of ocular pharmacokinetics," *Chemotherapy*, vol. 41, no. 1, pp. 1–4, 1995.

[4] E. Barbu, L. Verestiuc, T. G. Nevell, and J. Tsibouklis, "Polymeric materials for ophthalmic drug delivery: trends and perspectives," *Journal of Materials Chemistry*, vol. 16, no. 34, pp. 3439–3443, 2006.

[5] H. R. Lin and K. C. Sung, "Carbopol/pluronic phase change solutions for ophthalmic drug delivery," *Journal of Controlled Release*, vol. 69, no. 3, pp. 379–388, 2000.

[6] A. Ludwig, "The use of mucoadhesive polymers in ocular drug delivery," *Advanced Drug Delivery Reviews*, vol. 57, no. 11, pp. 1595–1639, 2005.

[7] R. Gaudana, J. Jwala, S. H. Boddu, and A. K. Mitra, "Recent perspectives in ocular drug delivery," *Pharmaceutical Research*, vol. 26, no. 5, pp. 1197–1216, 2009.

[8] D. Shulin, "Recent developments in ophthalmic drug delivery," *Pharmaceutical Science and Technology Today*, vol. 1, no. 8, pp. 328–335, 1998.

[9] E. M. Hehl, R. Beck, K. Luthard, R. Guthoff, and B. Drewelow, "Improved penetration of aminoglycosides and fluoroquinolones into the aqueous humour of patients by means of Acuvue contact lenses," *European Journal of Clinical Pharmacology*, vol. 55, no. 4, pp. 317–323, 1999.

[10] M. L. McDermott and J. W. Chandler, "Therapeutic uses of contact lenses," *Survey of Ophthalmology*, vol. 33, no. 5, pp. 381–394, 1989.

[11] L. Xinming, C. Yingde, A. W. Lloyd et al., "Polymeric hydrogels for novel contact lens-based ophthalmic drug delivery systems: a review," *Contact Lens and Anterior Eye*, vol. 31, no. 2, pp. 57–64, 2008.

[12] J. Kopeček, "Hydrogels: from soft contact lenses and implants to self-assembled nanomaterials," *Journal of Polymer Science, Part A*, vol. 47, no. 22, pp. 5929–5946, 2009.

[13] P. C. Nicolson and J. Vogt, "Soft contact lens polymers: an evolution," *Biomaterials*, vol. 22, no. 24, pp. 3273–3283, 2001.

[14] V. P. Costa, M. E. M. Braga, C. M. M. Duarte et al., "Anti-glaucoma drug-loaded contact lenses prepared using supercritical solvent impregnation," *Journal of Supercritical Fluids*, vol. 53, pp. 165–173, 2010.

[15] Z. Jianxiang, S. Hongli, and X. M. Peter, "Host-guest interaction mediated polymeric assemblies: multifunctional nanoparticles for drug and gene delivery," *ACS Nano*, vol. 4, no. 2, pp. 1049–1059, 2010.

[16] R. C. Peterson, J. S. Wolffsohn, J. Nick, L. Winterton, and J. Lally, "Clinical performance of daily disposable soft contact lenses using sustained release technology," *Contact Lens and Anterior Eye*, vol. 29, no. 3, pp. 127–134, 2006.

[17] L. ChiChung and A. Chauhan, "Modeling ophthalmic drug delivery by soaked contact lenses," *Industrial and Engineering Chemistry Research*, vol. 45, no. 10, pp. 3718–3734, 2006.

[18] C. C. Lin and A. T. Metters, "Hydrogels in controlled release formulations: network design and mathematical modeling," *Advanced Drug Delivery Reviews*, vol. 58, no. 12-13, pp. 1379–1408, 2006.

[19] P. Andrade-Vivero, E. Fernandez-Gabriel, C. Alvarez-Lorenzo, and A. Concheiro, "Improving the loading and release of NSAIDs from pHEMA hydrogels by copolymerization with functionalized monomers," *Journal of Pharmaceutical Sciences*, vol. 96, no. 4, pp. 802–813, 2007.

[20] J. L. Court, R. P. Redman, J. H. Wang et al., "A novel phosphorylcholine-coated contact lens for extended wear use," *Biomaterials*, vol. 22, no. 24, pp. 3261–3272, 2001.

[21] C. C. Karlgard, N. S. Wong, L. W. Jones, and C. Moresoli, "In vitro uptake and release studies of ocular pharmaceutical agents by silicon-containing and p-HEMA hydrogel contact lens materials," *International Journal of Pharmaceutics*, vol. 257, no. 1-2, pp. 141–151, 2003.

[22] J. Kim, A. Conway, and A. Chauhan, "Extended delivery of ophthalmic drugs by silicone hydrogel contact lenses," *Biomaterials*, vol. 29, no. 14, pp. 2259–2269, 2008.

[23] Y. Kapoor, J. C. Thomas, G. Tan, V. T. John, and A. Chauhan, "Surfactant-laden soft contact lenses for extended delivery of ophthalmic drugs," *Biomaterials*, vol. 30, no. 5, pp. 867–878, 2009.

[24] S. K. Sahoo, F. Dilnawaz, and S. Krishnakumar, "Nanotechnology in ocular drug delivery," *Drug Discovery Today*, vol. 13, no. 3-4, pp. 144–151, 2008.

[25] O. Kayser, A. Lemke, and N. Hernández-Trejo, "The impact of nanobiotechnology on the development of new drug delivery systems," *Current Pharmaceutical Biotechnology*, vol. 6, no. 1, pp. 3–5, 2005.

[26] J. Vandervoort and A. Ludwig, "Ocular drug delivery: nanomedicine applications," *Nanomedicine*, vol. 2, no. 1, pp. 11–21, 2007.

[27] D. Gulsen and A. Chauhan, "Ophthalmic drug delivery through contact lenses," *Investigative Ophthalmology and Visual Science*, vol. 45, no. 7, pp. 2342–2347, 2004.

[28] D. Gulsen and A. Chauhan, "Dispersion of microemulsion drops in HEMA hydrogel: a potential ophthalmic drug delivery vehicle," *International Journal of Pharmaceutics*, vol. 292, no. 1-2, pp. 95–117, 2005.

[29] Y. Kapoor and A. Chauhan, "Drug and surfactant transport in Cyclosporine A and Brij 98 laden p-HEMA hydrogels," *Journal of Colloid and Interface Science*, vol. 322, no. 2, pp. 624–633, 2008.

[30] J. F. dos Santos, C. Alvarez-Lorenzo, M. Silva et al., "Soft contact lenses functionalized with pendant cyclodextrins for controlled drug delivery," *Biomaterials*, vol. 30, no. 7, pp. 1348–1355, 2009.

[31] M. E. Byrne, K. Park, and N. A. Peppas, "Molecular imprinting within hydrogels," *Advanced Drug Delivery Reviews*, vol. 54, no. 1, pp. 149–161, 2002.

[32] A. Danion, H. Brochu, Y. Martin, and P. Vermette, "Fabrication and characterization of contact lenses bearing surface-immobilized layers of intact liposomes," *Journal of Biomedical Materials Research—Part A*, vol. 82, no. 1, pp. 41–51, 2007.

[33] R. C. Smith, M. Riollano, A. Leung, and P. T. Hammond, "Layer-by-layer platform technology for small-molecule delivery," *Angewandte Chemie—International Edition*, vol. 48, no. 47, pp. 8974–8977, 2009.

[34] T. R. Thatiparti, A. J. Shoffstall, and H. A. von Recum, "Cyclodextrin-based device coatings for affinity-based release of antibiotics," *Biomaterials*, vol. 31, no. 8, pp. 2335–2347, 2010.

[35] T. R. Thatiparti and H. A. von Recum, "Cyclodextrin complexation for affinity-based antibiotic delivery," *Macromolecular Bioscience*, vol. 10, no. 1, pp. 82–90, 2010.

[36] T. Sato, R. Uchida, H. Tanigawa, K. Uno, and A. Murakami, "Application of polymer gels containing side-chain phosphate groups to drug-delivery contact lenses," *Journal of Applied Polymer Science*, vol. 98, no. 2, pp. 731–735, 2005.

[37] R. Uchida, T. Sato, H. Tanigawa, and K. Uno, "Azulene incorporation and release by hydrogel containing methacrylamide propyltrimenthylammonium chloride, and its application to soft contact lens," *Journal of Controlled Release*, vol. 92, no. 3, pp. 259–264, 2003.

[38] V. Dulong, D. Le Cerf, L. Picton, and G. Muller, "Carboxymethylpullulan hydrogels with a ionic and/or amphiphilic behavior: swelling properties and entrapment of cationic and/or hydrophobic molecules," *Colloids and Surfaces A: Physicochemical and Engineering Aspects*, vol. 274, pp. 163–169, 2006.

[39] X. Jinku, L. Xinsong, and S. Fuqian, "Cyclodextrin-containing hydrogels for contact lenses as a platform for drug incorporation and release," *Acta Biomaterialia*, vol. 6, no. 2, pp. 486–493, 2010.

[40] M. E. Byrne and V. Salian, "Molecular imprinting within hydrogels II: progress and analysis of the field," *International Journal of Pharmaceutics*, vol. 364, no. 2, pp. 188–212, 2008.

[41] D. Cunliffe, A. Kirby, and C. Alexander, "Molecularly imprinted drug delivery systems," *Advanced Drug Delivery Reviews*, vol. 57, no. 12, pp. 1836–1853, 2005.

[42] N. M. Bergmann and N. A. Peppas, "Molecularly imprinted polymers with specific recognition for macromolecules and proteins," *Progress in Polymer Science*, vol. 33, no. 3, pp. 271–288, 2008.

[43] M. Ali and M. E. Byrne, "Controlled release of high molecular weight hyaluronic acid from molecularly imprinted hydrogel contact lenses," *Pharmaceutical Research*, vol. 26, no. 3, pp. 714–726, 2009.

[44] C. Alvarez-Lorenzo, F. Yañez, R. Barreiro-Iglesias, and A. Concheiro, "Imprinted soft contact lenses as norfloxacin delivery systems," *Journal of Controlled Release*, vol. 113, no. 3, pp. 236–244, 2006.

[45] H. Hiratani and C. Alvarez-Lorenzo, "Timolol uptake and release by imprinted soft contact lenses made of N,N-diethylacrylamide and methacrylic acid," *Journal of Controlled Release*, vol. 83, no. 2, pp. 223–230, 2002.

[46] H. Hiratani and C. Alvarez-Lorenzo, "The nature of backbone monomers determines the performance of imprinted soft contact lenses as timolol drug delivery systems," *Biomaterials*, vol. 25, no. 6, pp. 1105–1113, 2004.

[47] H. Hiratani, A. Fujiwara, Y. Tamiya, Y. Mizutani, and C. Alvarez-Lorenzo, "Ocular release of timolol from molecularly imprinted soft contact lenses," *Biomaterials*, vol. 26, no. 11, pp. 1293–1298, 2005.

[48] H. Hiratani, Y. Mizutani, and C. Alvarez-Lorenzo, "Controlling drug release from imprinted hydrogels by modifying the characteristics of the imprinted cavities," *Macromolecular Bioscience*, vol. 5, no. 8, pp. 728–733, 2005.

[49] S. Venkatesh, S. P. Sizemore, and M. E. Byrne, "Biomimetic hydrogels for enhanced loading and extended release of ocular therapeutics," *Biomaterials*, vol. 28, no. 4, pp. 717–724, 2007.

[50] C. Alvarez-Lorenzo, H. Hiratani, J. L. Gómez-Amoza, R. Martínez-Pacheco, C. Souto, and A. Concheiro, "Soft contact lenses capable of sustained delivery of timolol," *Journal of Pharmaceutical Sciences*, vol. 91, no. 10, pp. 2182–2192, 2002.

[51] C. Alvarez-Lorenzo, F. Yañez, and A. Concheiro, "Ocular drug delivery from molecularly-imprinted contact lenses," *Journal of Drug Delivery Science and Technology*, vol. 20, pp. 237–248, 2010.

[52] A. Ribeiro, F. Veiga, D. Santos, J. J. Torres-Labandeira, A. Concheiro, and C. Alvarez-Lorenzo, "Bioinspired imprinted PHEMA-hydrogels for ocular delivery of carbonic anhydrase inhibitor drugs," *Biomacromolecules*, vol. 12, pp. 701–709, 2011.

[53] F. Yanez, L. Martikainen, M. E. Braga et al., "Supercritical fluid-assisted preparation of imprinted contact lenses for drug delivery," *Acta Biomaterialia*, vol. 7, pp. 1019–1030, 2011.

[54] C. J. White and M. E. Byrne, "Molecularly imprinted therapeutic contact lenses," *Expert Opinion on Drug Delivery*, vol. 7, no. 6, pp. 765–780, 2010.

[55] C. J. Ochs, G. K. Such, Y. Yan, M. P. van Koeverden, and F. Caruso, "Biodegradable click capsules with engineered drug-loaded multilayers," *ACS Nano*, vol. 4, no. 3, pp. 1653–1663, 2010.

[56] S. Xingfang, K. Byeong-Su, R. K. Sara, T. H. Paula, and J. I. Darrell, "Layer-by-layer-assembled multilayer films for transcutaneous drug and vaccine delivery," *ACS Nano*, vol. 3, no. 11, pp. 3719–3729, 2009.

Hindawi Publishing Corporation
International Journal of Polymer Science
Volume 2011, Article ID 161749, 20 pages
doi:10.1155/2011/161749

Review Article

Poly(amidoamine) Hydrogels as Scaffolds for Cell Culturing and Conduits for Peripheral Nerve Regeneration

Fabio Fenili, Amedea Manfredi, Elisabetta Ranucci, and Paolo Ferruti

Department of Industrial and Organic Chemistry, The University of Milan, Via Venezian 21, 20133 Milan, Italy

Correspondence should be addressed to Paolo Ferruti, paolo.ferruti@unimi.it

Received 6 June 2011; Revised 27 July 2011; Accepted 27 July 2011

Academic Editor: Shanfeng Wang

Biodegradable and biocompatible poly(amidoamine)-(PAA-) based hydrogels have been considered for different tissue engineering applications. First-generation AGMA1 hydrogels, amphoteric but prevailing cationic hydrogels containing carboxylic and guanidine groups as side substituents, show satisfactory results in terms of adhesion and proliferation properties towards different cell lines. Unfortunately, these hydrogels are very swellable materials, breakable on handling, and have been found inadequate for other applications. To overcome this problem, second-generation AGMA1 hydrogels have been prepared adopting a new synthetic method. These new hydrogels exhibit good biological properties *in vitro* with satisfactory mechanical characteristics. They are obtained in different forms and shapes and successfully tested *in vivo* for the regeneration of peripheral nerves. This paper reports on our recent efforts in the use of first-and second-generation PAA hydrogels as substrates for cell culturing and tubular scaffold for peripheral nerve regeneration.

1. Introduction

Tissue loss or end-stage organ failure caused by injury or other types of damage is one of the most devastating and costly problems in human health care. Surgical strategies that have been developed to address these problems include organ transplantation from one individual to another, tissue transfer from a healthy site to the diseased site in the same individual, and replacement by using mechanical devices such as joint prosthesis or dialysis machine. Moreover, medical treatment encompassed supplementation of metabolic products of the nonfunctional tissue. Though significant advances have been achieved in terms of health care by these therapeutic options, many limitations and unsolved issues remain [1]. The number of organs available for transplantation is far exceeded by the number of patients needing such procedures. In Europe in 2010 alone, approximately 9,300 people were on the waiting list for an organ transplant due to end-stage organ failure, but only 3,100 transplants were performed [2]. Tissue transfer cannot replace all the functions of the original tissue and bears the risk of donor-site complications.

Tissue engineering "is an interdisciplinary field that applies the principles of engineering and of life science towards the development of biological substitutes that restore, maintain or improve tissue or organ function." This definition is based on several articles, by Langer and Vacanti, that were published in the 1990s [3–6]. In those articles tissue engineering is proposed as an alternative to organ transplantation when all the other treatments fail using three main strategies. The first, the utilization of isolated cells, which has the great advantage to replace just the cells that are really needed and to eventually genetically manipulate them before infusion. This strategy allows for minimal invasive surgery, but there is always the possibility of immunological rejection or failure in maintaining new functions. The second approach is that of using tissue-inducing substances such as growth factors or cytokines. However, drawbacks of this solution are purification and large-scale production issues, and it is always necessary to have a system to deliver the bioactive molecule to its target. Finally, the third strategy utilizes cells placed on a scaffold that serve as a synthetic extracellular matrix to organize cells into a three-dimensional architecture and to present stimuli

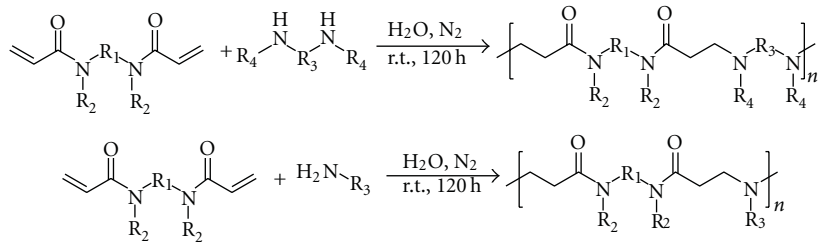

Scheme 1: Synthesis of linear PAAs. R_1, R_2, R_3, and R_4 can be any alkyl residues eventually containing carboxyl, amide, ester, and ether groups.

Table 1: Acid-base properties of the same PAA polymers.

PAA name and structure	pK_a	I.P.	Percentage of charged units		IC_{50} B16F10 cell
			pH = 5.5	pH = 7.4	(mg/mL)
ISA23 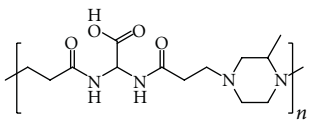	pK_{a1} = 2.1 pK_{a2} = 3.25 pK_{a3} = 7.5	5.5	2% (+)	40% (−)	>5
ISA1 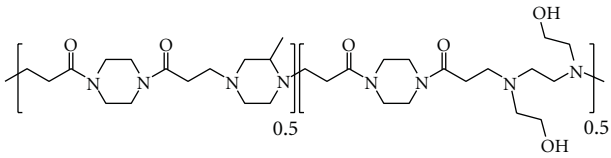	pK_{a1} = 8.1 pK_{a2} = 6.9 pK_{a3} = 3.8 pK_{a4} = 2.8	>10	95% (+)	55% (+)	3

which direct the growth and formation of a desired tissue [7]. This strategy is currently used in tissue engineering.

Scaffolds can be produced from natural materials or synthetic polymers. In general, the ideal scaffold should be three dimensional, highly porous with an interconnected pore network, and biocompatible with a controlled degradation rate, should have an appropriate surface for cell adhesion, proliferation, and differentiation, and should maintain proper mechanical properties. Among all the synthetic polymeric materials that have been found to be suitable for tissue engineering applications, special attention has been recently given to biodegradable polymers and hydrogels. Several reviews in literature the describe the use of natural [8–15] and synthetic [16–20] biodegradable polymers as well as some nonbiodegradable [21, 22] ones, which are currently used for cartilage, nerve repair, bone, cardiac, vascular graft, and many other tissue engineering applications. Among synthetic materials, increasing attention has been paid to hydrogels due to their tissue-like properties for interaction with living cells, such as similar water content and permeability to oxygen and metabolites [23]. Synthetic hydrogels, as opposed to naturally derived materials, are more advantageous, giving the possibility of a complete control over hydrogel composition, surface properties, and other key parameters such as water absorption and (bio)degradation time. Moreover, hydrogel structures could be used to encapsulate cells, proteins, and signaling factors, as well as bioactive moieties to be slowly released during cell growth [24]. This paper reports on our recent efforts in the use of first-and second-generation poly(amidoamine) hydrogels as substrates for cell culturing and tubular scaffold for peripheral nerve regeneration.

2. Poly(amidoamine) Hydrogels: Synthesis and Properties

PAAs are a family of synthetic polymers containing tertiary amino and amido groups regularly arranged along their polymer chain [25, 26]. They are obtained by Michael-type polyaddition of primary or secondary amines to bis-acrylamides (Scheme 1).

PAAs are extremely versatile materials. PAAs containing as side substituents other chemical functions, such as additional tertiary amino groups, carboxyl groups, hydroxyl groups, and allyl groups, can be easily obtained by using suitably functionalized monomers, as for instance amino-carbohydrate derivatives [27]. Peptides and proteins can also participate in the polyaddition reaction through their terminal amino groups as well as ε-lysine amino groups, if present [26–28]. Many PAAs exhibit a combination of properties imparting them a considerable potential in the biomedical field (see Table 1). They are highly hydrophilic and usually degrade in aqueous media at a rate

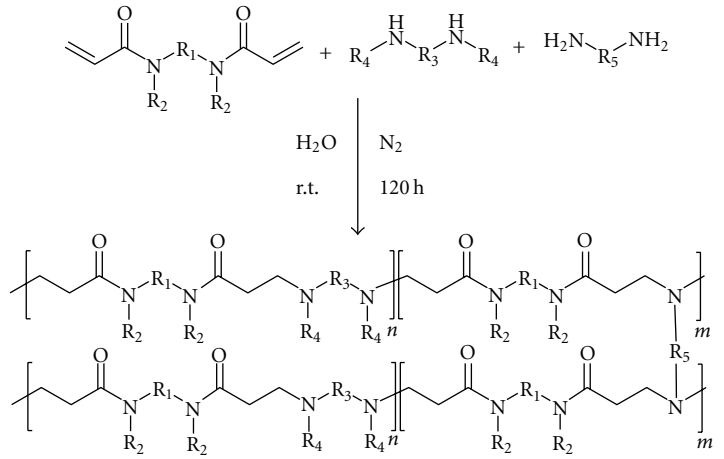

Scheme 2: General synthesis of PAA-based hydrogels.

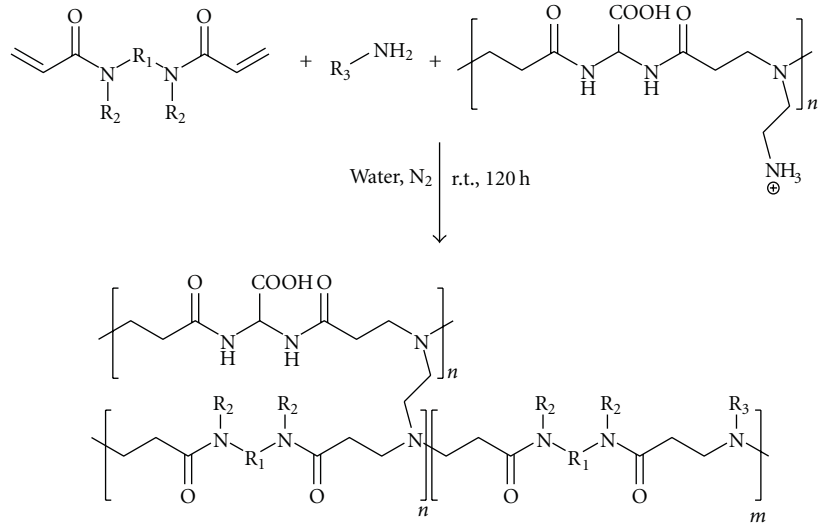

Scheme 3: Synthesis of PAA hydrogels using NH_2–BAC.

depending on their structure [29]. Moreover, many of them are almost nontoxic, in spite of their polycationic nature, with IC_{50} values ranging from 0.5 to 3.0 mg/mL [30, 31]. Amphoteric PAAs, that is, PAAs carrying carboxyl groups as side substituents, are even less toxic and may be approximately as biocompatible as dextran [32].

Crosslinked PAAs can be easily obtained by different methods. So far, the most often employed method is to introduce primary diamines as crosslinking agents into the polymerization mixture [33]. Primary diamines carry four different mobile hydrogens and hence behave as tetrafunctional monomers in PAA synthesis (Scheme 2). Crosslinked PAAs are typical hydrogels, absorbing large amounts of water if their crosslinking degree is not too high.

Another synthetic procedure leading to PAA-hydrogels involves the preparation of a linear PAA carrying primary amino pendants, such as the amphoteric one (NH_2–BAC) prepared by polyaddition of monoprotonated EDA to BAC (Scheme 3) [34]. This PAA can be used as multifunctional crosslinking agent in the place of diamines [35].

Amphoteric PAAs, whose polymer chain contains amide, amine, and carboxylate groups in regular sequence, can be considered in a sense protein-like synthetic materials. In fact, they exhibit good compatibility with proteins, as for instance albumin. It has also been demonstrated that different molecules and biomolecules, as oligopeptides and proteins [36], are capable of reproducing the receptorial sites of proteins playing a fundamental role in cell adhesion, such as fibronectin, laminin, and vitronectin [37]. Among these, the tripeptide RGD is presently the most popular [38].

Recently a peptidomimetic PAA, labeled AGMA1, has been obtained by polyaddition reaction of 2,2-bis(acrylamido)acetic acid and agmatine (4-aminobutyl guanidine) [39–41]. As reported in Figure 1, AGMA1 carries guanidine and carboxyl groups and shows a strong structural resemblance to the RGD sequence.

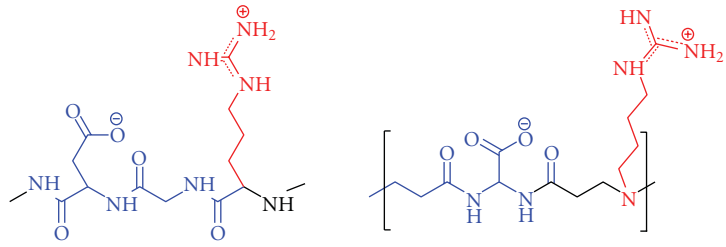

Figure 1: Structure of agmatine containing amphoteric poly(amidoamine) (right part) compared to the RGD tripeptide sequence.

Table 2: Acid-base properties of AGMA1.

PAA name and structure	pK_a	I.P.	Percentage of charged units		IC_{50} B16F10 cell
			pH = 5.5	pH = 7.4	(mg/mL)
AGMA1 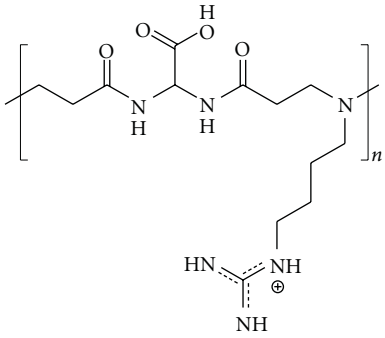	pK_{a1} = 2.25 pK_{a2} = 7.45 pK_{a3} = 12.1	10.0	55% (+)	90% (+)	>5

Agmatine-containing PAAs hydrogels, easily obtained using 4-aminobutyl guanidine as amine monomer, are fully cytocompatible and also show remarkable adhesion and proliferation properties towards several cell lines [42].

Agmatine contains a primary amino group and a guanidine group carrying five potentially mobile hydrogens that might participate in the polyaddition reaction. It is, therefore, a potential cross-linking agent in PAA synthesis like primary diamines as EDA. Nevertheless, a large difference in basic properties exists between the amine and the guanidine groups of agmatine. The latter has $pK_a > 12$, much higher than that of any aliphatic amine, and remains protonated under the conditions employed in PAA synthesis (Table 2).

Degradation tests carried out on selected PAA hydrogels under conditions mimicking the body fluids (pH 7.4 and 37°C) reveal that their degradation products are completely nontoxic [42]. The mechanism of PAAs degradation seems to be purely hydrolytic as no vinyl groups, such as those that would be derived from a β-elimination reaction, can be determined. Furthermore, degradation seems not to be affected by the presence of isolated lysosomal enzymes at pH 5.5 [43, 44].

3. Poly(amidoamine) Hydrogels as Substrates for Cell Culturing

In the last few years the progress of biological sciences has led to outstanding developments in the field of cell culturing in vitro. Several new techniques, such as cell microarray or cells on chips, require reliable support materials with good biocompatibility and cell adhesion, preferentially disposable and simple to use [45, 46]. Traditionally, cells culturing has been performed on two-dimensional substrates or on the surface of tissue analogs. Currently, various polymer-based materials, that is, polystyrene (PS), polycarbonate (PC), and polypropylene (PP), are applied as common bulk materials in two-dimensional cell culture systems, such as cell culture dishes and cell culture membranes. Tissue culture polystyrene (TCPS) is the most common cell culture substrate due to its easy processability and optical transparency, but it still needs to be modified with poly(D-lysine) to ensure cell adhesion [47]. Among all the synthetic polymeric materials that have been found to be suitable substrates for cell culturing, special attention has been recently given to hydrogels. Hydrogels present unique tissue-like properties for interactions with living cells [23, 48], such as water

content and permeability to oxygen and metabolites. In principle, fully synthetic hydrogels, as opposed to naturally derived media (e.g., gelatin, chitosan, etc.), should be more advantageous, coupling the aforementioned properties with the possibility of complete control over hydrogel composition, crosslinking, and swelling. Hydrogels can be produced with tailored shape and thickness, even in 3D structures, and their surface can be patterned with lithographic techniques [49, 50]. Moreover, hydrogels can be fittingly functionalized with biomolecules for obtaining customized properties. Cell adhesion on fully synthetic hydrogels, however, is still an issue for many of these materials, such as PHEMA or crosslinked PEG derivatives [51]. A number of chemical and physical modifications have been proposed to overcome this problem, often relying on modification of the synthetic surface with biological or biomimetic moieties, as peptides or proteins [52] typically, arginine-glycine-aspartate (RGD). The process of cell adhesion to a substrate, both on the natural ECM and synthetic materials, is mediated by interactions between surface ligands and cell receptors, such as transmembrane integrins and proteoglycans [53]. The tripeptide RGD, present in several ECM proteins, has been the object of intensive research in the last years [54]. In fact, several studies have shown that this tripeptide, and some of its analogues, can interact with adhesion-regulating proteins of the integrin family and play a role in promoting cell adhesion and spreading, mimicking the effect of some ECM proteins, such as fibronectin or vitronectin [55–57]. The overall action mechanism is still not completely clear, but some studies have associated it to the conformation of the guanidine side group of arginine, and its distance and angle from the acidic pendant of aspartic acid [58, 59]. Modification of chemical structures in order to include an RGD or RGD-like group has been proposed for a number of applications where cells interaction is desired to enhance adhesion or recognition by cellular receptors [60, 61].

Different PAA hydrogels have been tested as substrates for cell culture. They have been prepared using different crosslinkers, such as EDA, 1,10-diaminododecane, or the linear NH_2–BAC carrying primary amino pendants (Table 3).

Cytotoxicity tests have been carried out by the direct contact method with fibroblast cell lines on the hydrogels both in their native state (i.e., as free bases), and as salts with acids of different strength, namely, hydrochloric, sulfuric, acetic, and lactic acid. This has been done in order to ascertain if there is any counterion-specific influence on cytotoxicity. It has been found that all the amphoteric PAA hydrogels considered are cytobiocompatible both as free bases and salts (Figure 2), and their biological performance is independent of the counterion's nature [33] (Figure 3).

Degradation tests have been performed on selected hydrogels samples under controlled conditions simulating biological environments, that is, Dulbecco medium at pH 7.4 and 37°C. All samples degrade completely and dissolve within 10 days. The degradation products of all samples have demonstrated to be noncytotoxic [33].

PAA-AG1 and PAA-AG2 are bioactive in terms of allowing cell adhesion and further proliferation. The morphology of cells grown onto the surfaces of both hydrogels is comparable with that of cells grown on TCPS used as control. In all cases, cell confluence has been reached after 10 days from the beginning of the experiments [42] (Figure 4).

Swelling tests have demonstrated that all PAA hydrogels have a high swelling capability. This property, not unexpected considering the hydrophilic and ionic nature of all investigated PAA hydrogels, ensures an efficient diffusion of low molecular weight substances, thus facilitating purification processes consisting in extensive extraction with water. However, the mechanical strength of the hydrogels in the swollen form is modest and the materials appear relatively fragile. The swelling of PAA hydrogels protonated with different acids is still very high, and not significantly different from that of the corresponding free bases, with the exception of the sulfates, which are slightly less swollen.

A systematic comparative study of the response of an epithelial cell line has been performed on AGMA1-EDA hydrogels, on nonfunctionalized amphoteric ISA23-EDA hydrogels, and tissue culture plastic substrates [62, 65]. As previously pointed out, the AGMA1 repeating units (Figure 1) are very similar to the well-known adhesion-modulating RGD peptide sequence. Since ISA23 does not carry any guanidine pendant group, it is expected to show no significant cell adhesion properties [33] and is used as a nonfunctionalized control. In order to make the hydrogels more handy, a new bilayered system has been designed, prepared and tested. It is composed by a functionalized glass support covered with a thin hydrogel layer. MDCK cells have been plated on the two types of hydrogels and on TCPS. Within 1 hour after plating, no evident differences are observed between AGMA1-EDA and ISA23-EDA, and the amount of adhered cells on these substrates is significantly lower than on TCPS (Figure 5). After 3 hours, the trend is substantially different, and the adhesion on AGMA1-EDA is comparable to that on TCPS (within one standard deviation) whereas on ISA23-EDA remains definitely lower (Figure 5).

After 1-2 days, effective MDCK cells proliferation on TCPS is observed, whereas this process on AGMA1-EDA appears to be slowed down (Figure 6).

After 3 days, meanwhile the cells on TCPS achieve confluence, the cells on AGMA1-EDA form clusters and no confluence is observed as reported in Figure 7.

This effect may be explained considering that, despite the fact that PAA hydrogel layer are supported by a rigid material, cells probably experience a more compliant substrate than TCPS. Optical images indicate that the cells adhered on AGMA1-EDA are less spread with respect to TCPS. This behavior could be ascribed to the occurrence of opposite stimuli to the cells: the compliance of the hydrogel surface, which can prevent a strong cell-substratum interaction and stress fiber formation, and the presence of integrin ligands, which favors a more effective cell-substratum adhesion. The behavior of the actin stress fibers on the different substrates is shown in Figure 8. Slower actin stress fiber formation on AGMA1-EDA and ISA23-EDA matches the slower spreading on these hydrogels. Chemical properties can participate with physical characteristics of substrates to affect cell adhesion. It has been shown that the presentation of integrin ligands in a clusterized form enables the formation of focal contacts

Table 3: Partial structures of PAA hydrogels.

Code	Structure	Reference
ISA23-EDA	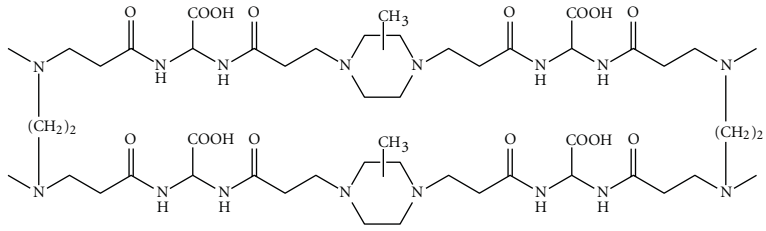	[33, 62]
AGMA1-EDA	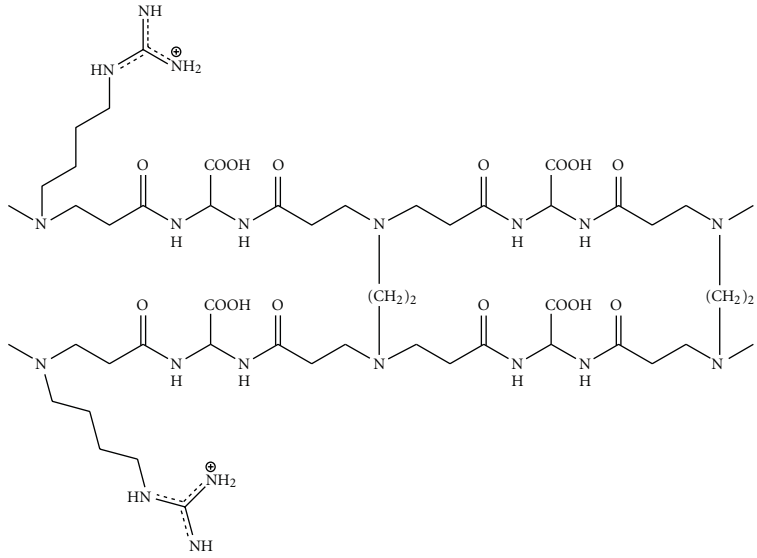	[62, 65]
PAA-DD	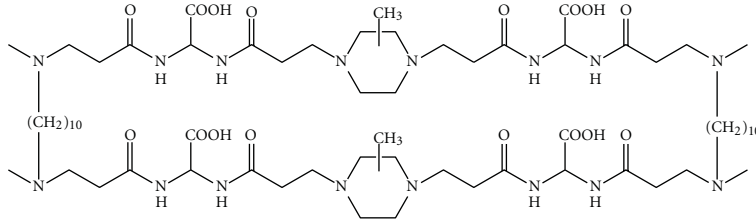	[33]
PAA-ED2	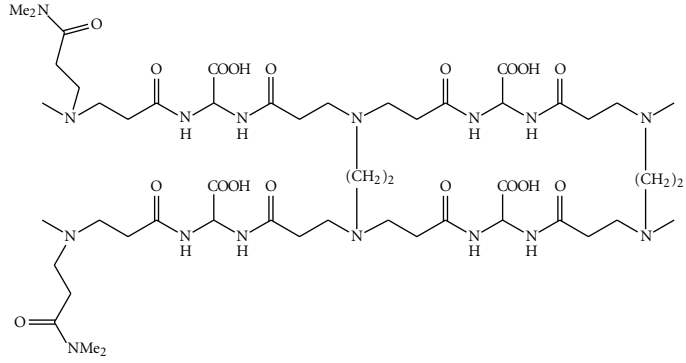	[33]

Table 3: Continued.

Code	Structure	Reference
PAA-ED3	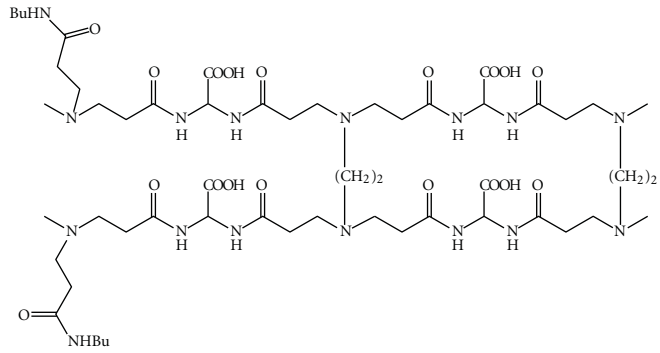	[33]
PAA-ED4	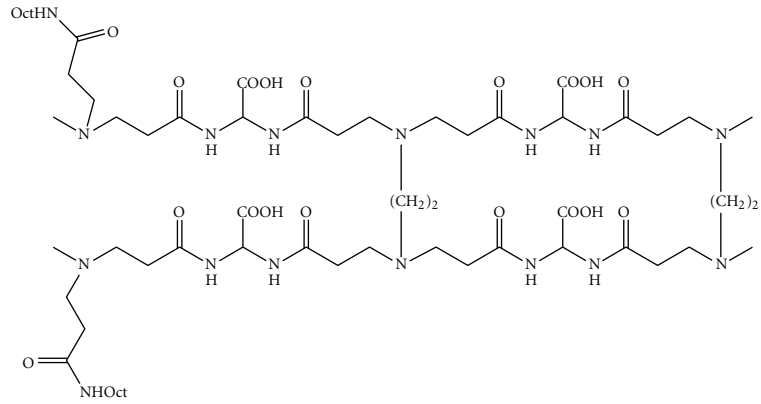	[33]
PAA-AG1	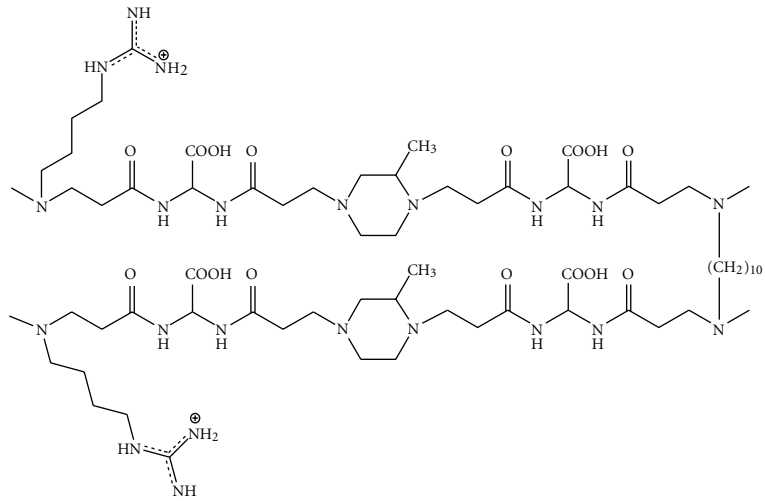	[42]

Table 3: Continued.

Code	Structure	Reference
PAA-AG2	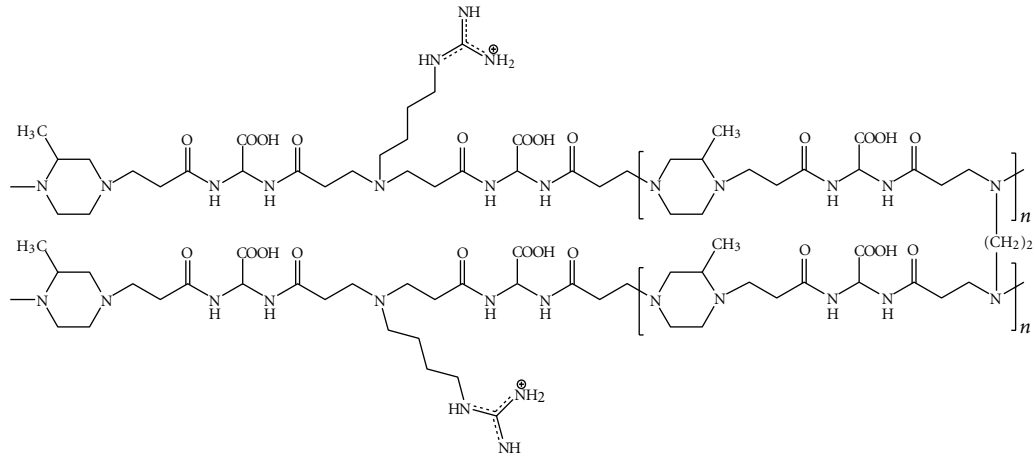	[42]

and stress fibers [66] and determines cell spreading [67]. A uniform low density of integrin ligands, instead, is unable to support stress fiber formation [66]. Therefore, slower spreading and stress fiber formation on AGMA1-EDA hydrogels could be also due to a more uniform (i.e. not clusterized) presentation of integrin ligands compared to the TCPS. It is also interesting to note that on ISA23-EDA cell islands often show membrane structures as filopodia and lamellipodia indicating not stable focal contacts and a tendency to cell migration [68].

4. PAA Hydrogels for Microfluidics and Lab-on-Chip Applications

Microfluidics deals with the precise control and manipulation of fluids that are geometrically constrained to a small, typically submillimeter, scale. It is a multidisciplinary field intersecting engineering, physics, chemistry, microtechnology, and biotechnology, with practical applications to the design of systems in which such small volumes of fluids will be used.

Microfluidics has emerged at the beginning of the 1980s and is used in the development of DNA chips, lab-on-chip technology, micropropulsion, and microthermal technologies [69–71].

In addition to functionalizing biomaterials with ECM-derived cell adhesive molecules, there is emerging evidence indicating that the surface topography, stiffness, and electrical properties play an important role in cells adhesion and growth [72]. Based on these premises, ISA23-EDA hydrogels have been used for the preparation of patterned substrate using a scanning electron microscope. The method consists of exposing dry hydrogel films to electron beam (computer assisted) in high vacuum chamber [63]. Fluorescent labelled, FITC or TRITC, proteins such as BSA, the hormone EGF FITC, and the biomolecule Phalloidin-TRITC, attach selectively to an electron-beam-modified surface in a dose dependent manner. Higher exposure doses lead to a higher protein or biomolecules attachment. Cells lines, such as MDCK and PC12, have been plated on the patterned surface. MDCK cells growth is observed along all surfaces, independently of pattern or other physic, and chemical modifications. The PC12 cell line, able to differentiate into neural cells when induced by NGF, presents a strong preference for the electron-beam-modified substrate. A 24-hours-PC12 cell culture, NGF non-treated, has been grown on the top of a hydrogel patterned with a chess-like area according to Figure 9 (total area $600 \times 600\,\mu$m). Containing alternate exposed and nonexposed squares ($100 \times 100\,\mu$m), 84% of the total cells (400 cells) are in the electron-beam-exposed squares (Figure 9) [63].

By exploiting the selective attachment growth and differentiation of PC12 cells on microwells connected by thin channels, we have fabricated a neural network of single cells connected by neurites extending along the microchannels [63]. The fine control of this neural network is further strengthened by the fact that the number of outcoming neurites is determined by the number of microchannels originating from each microwell (Figure 10).

E-beam lithography on PAA hydrogels opens up the opportunity of producing multifunctional microfluidics devices supported on a small glass chip and incorporating complex topographies, allowing precise control of the growth and organization of individual cells and providing the capability to study physiologic and pharmacologic responses at a single cell level.

5. PAA Hydrogels as Scaffolds for Peripheral Nerve Regeneration

Peripheral nerve injuries present a significant clinical challenge across the world [73]. Injuries to the peripheral

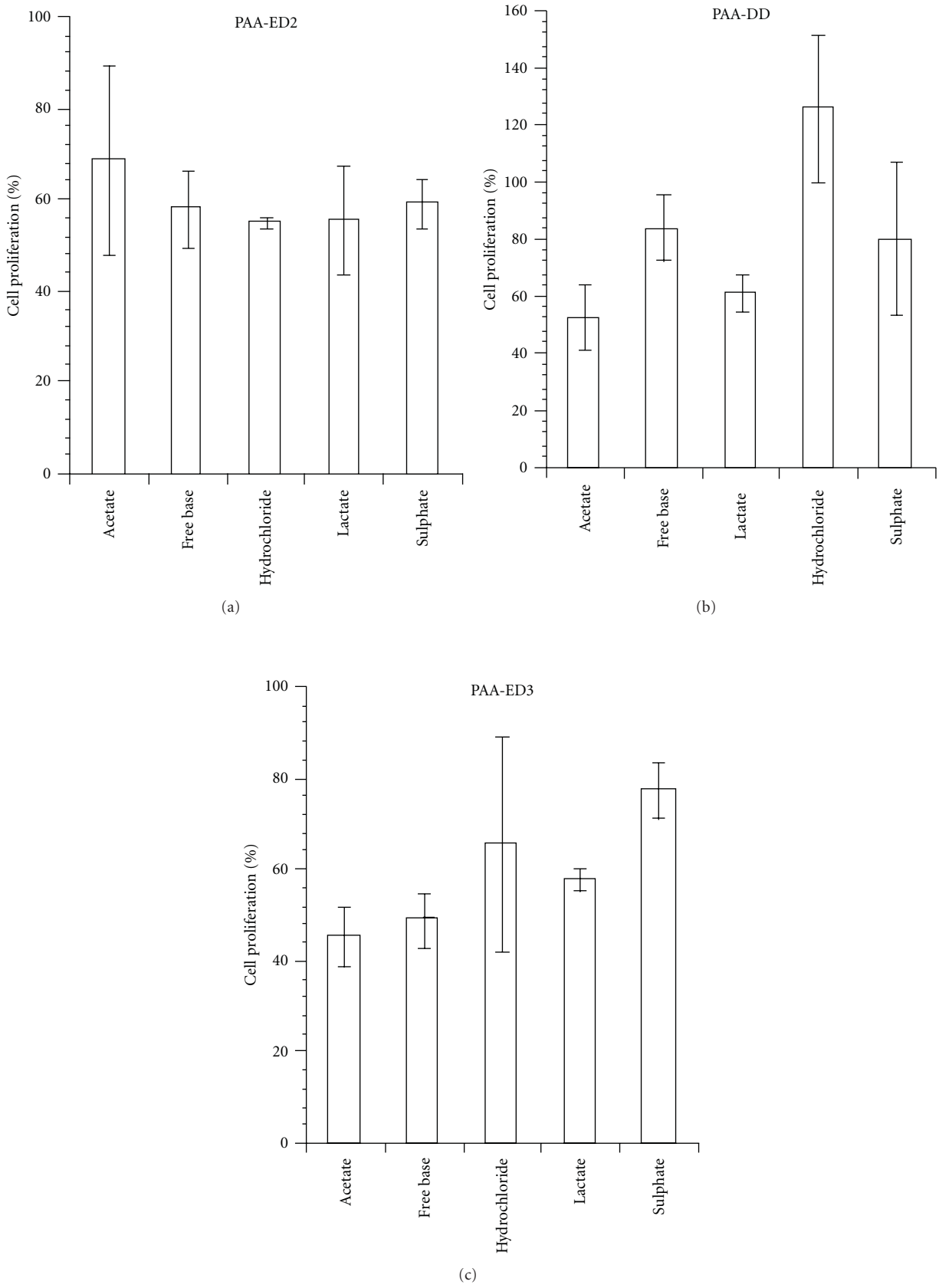

Figure 2: Results of the cytotoxicity tests of PAA-ED2, PAA-DD and PAA-ED3 hydrogels, as free base and ammonium salts, carried out on fibroblast cells by means of the direct contact method [33].

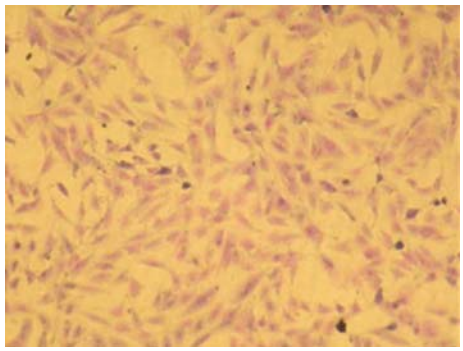

Figure 3: Morphology of mouse embryo fibroblasts in the cell proliferation experiment carried out by the direct contact method in the presence of PAA-DD as lactate ammonium salt [33].

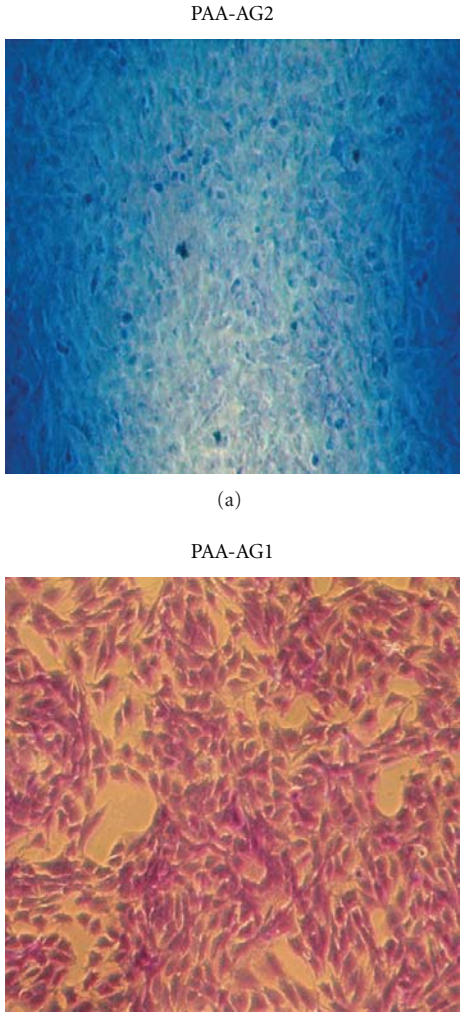

Figure 4: Morphology of mouse embryo fibroblasts grown on PAA-AG2 and PAA-AG1 after 10 days of culture [42].

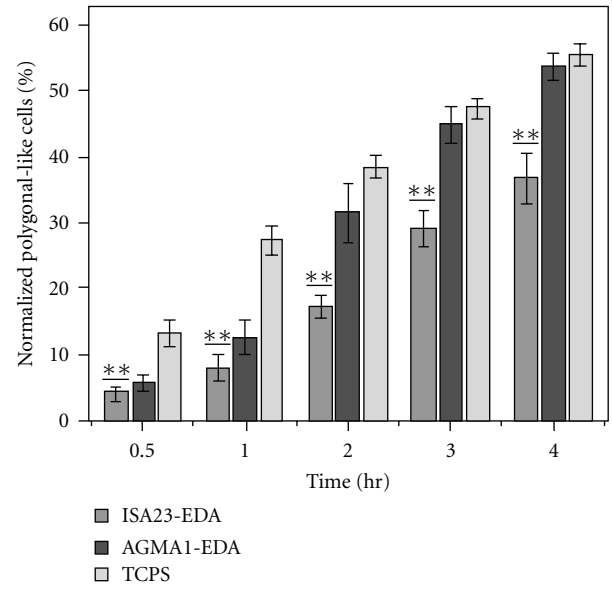

Figure 5: MDCK cells adhesion versus time on ISA23-EDA, AGMA1-EDA, and TCPS [62].

nervous system are common and are a major source of disability, impairing the ability to move muscles and/or feel normal sensations or resulting in painful neuropathies. Due to the difficulties in treating such injuries, many patients are left without any benefit of medical intervention. Even among the patients who receive treatment for traumatic peripheral nerve injuries, more than 50% show no measurable signs of recovery or else suffer from drastically reduced muscle strength [74].

After nerve trauma, the standard clinical operating procedure consists of opposing the two nerve ends and suture them together without generating tension where possible. When the defect is so large that the severed nerve ends cannot be directly sutured, nerve injury is bridged by autologous nerve grafting. While autografts are the best clinical bridges available today because they are biocompatible, nontoxic and provide a support structure to promote axonal adhesion, there are many drawbacks to this procedure. These include the need for a secondary surgery, loss of donor site function, limited availability, modality mismatch (arising from a sensory nerve being used to repair a motor or mixed nerve), and neuroma formation at the donor or graft site.

Various tissue engineering strategies have been used to influence different aspects of the regenerative process with hope for functional recovery using natural and synthetic tubular scaffolds. The design criteria for fabrication of scaffolds should address various factors including composition [75] and dimensions of the tubular scaffold [76], the addition of exogenous factors such as fibrin precursors [77] and growth factors, the incorporation of glial cells, most often Schwann cells and fibroblasts [78, 79], the elastic modulus, permeability, topography, swelling ratio, degradation rate, size, and clearance of the degradation products [80]. In particular the elastic modulus of the scaffold should be at least 1,200 kPa in order to resist compressive and tensile forces that are generated both during the surgery as well as from surrounding tissue after implantation [81]. Different

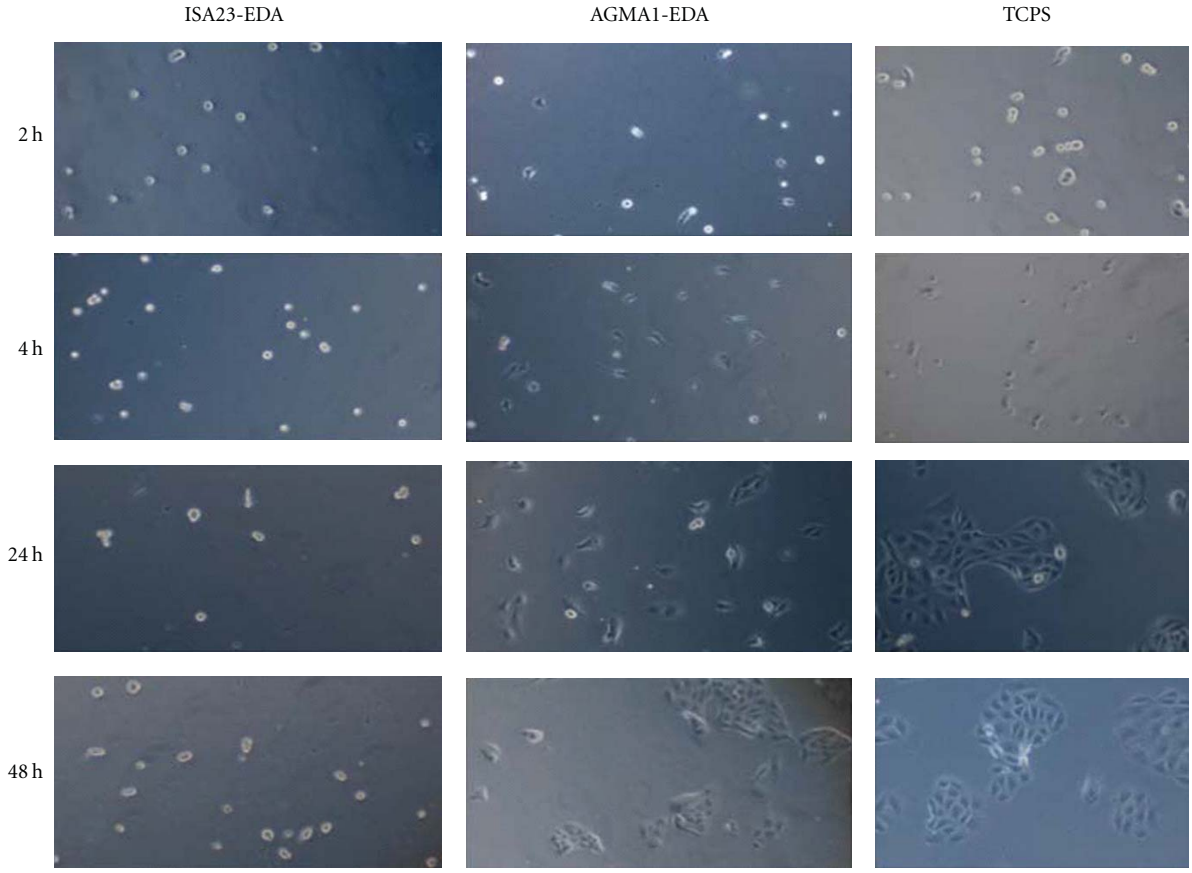

Figure 6: Optical microscopy images showing time evolution of MDCK cells on ISA23-EDA, AGMA1-EDA and TCPS [62].

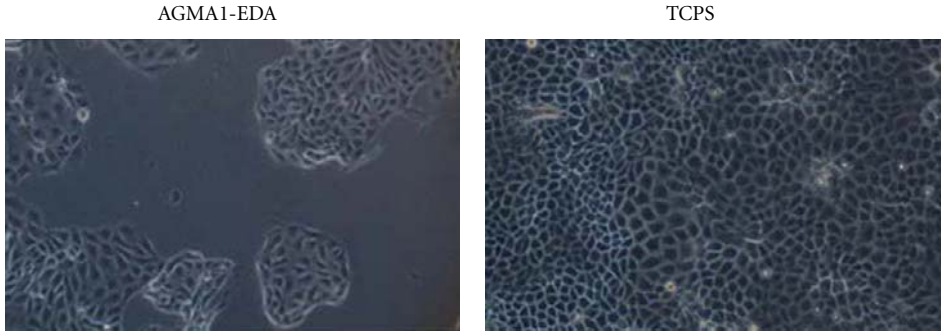

Figure 7: Optical microscopy images showing MDCK on TCPS and AGMA1-EDA at 72 hour after seeding [62].

natural and synthetic materials have been used to facilitate nerve regeneration. Among natural tubular scaffolds, autogenous venous and arterial nerve grafts have been the most successful in achieving functional recovery across 10-mm nerve gaps [82–84]. Venous grafts remain intact throughout the process of nerve regeneration and are easier to extract compared to arterial grafts [82]. While natural materials have good biocompatibility, they often collapse when used in longer nerve gaps. Additionally, issues related to the limited availability of these explants, as well as autograft-triggered immune response, are a few among many reasons that prompted exploration of alternative materials to direct nerve growth [85]. Synthetic tubular scaffolds have similar advantages to natural scaffolds but additionally provide mechanical and structural control [86]. In the recent past, several guidance techniques using artificial nerve conduits have been developed to guide nerve regeneration towards the distal stump [87]. The isolated environment provided by guidance channels helps confinement and concentrate neurotrophic factors that are released by supporting cells

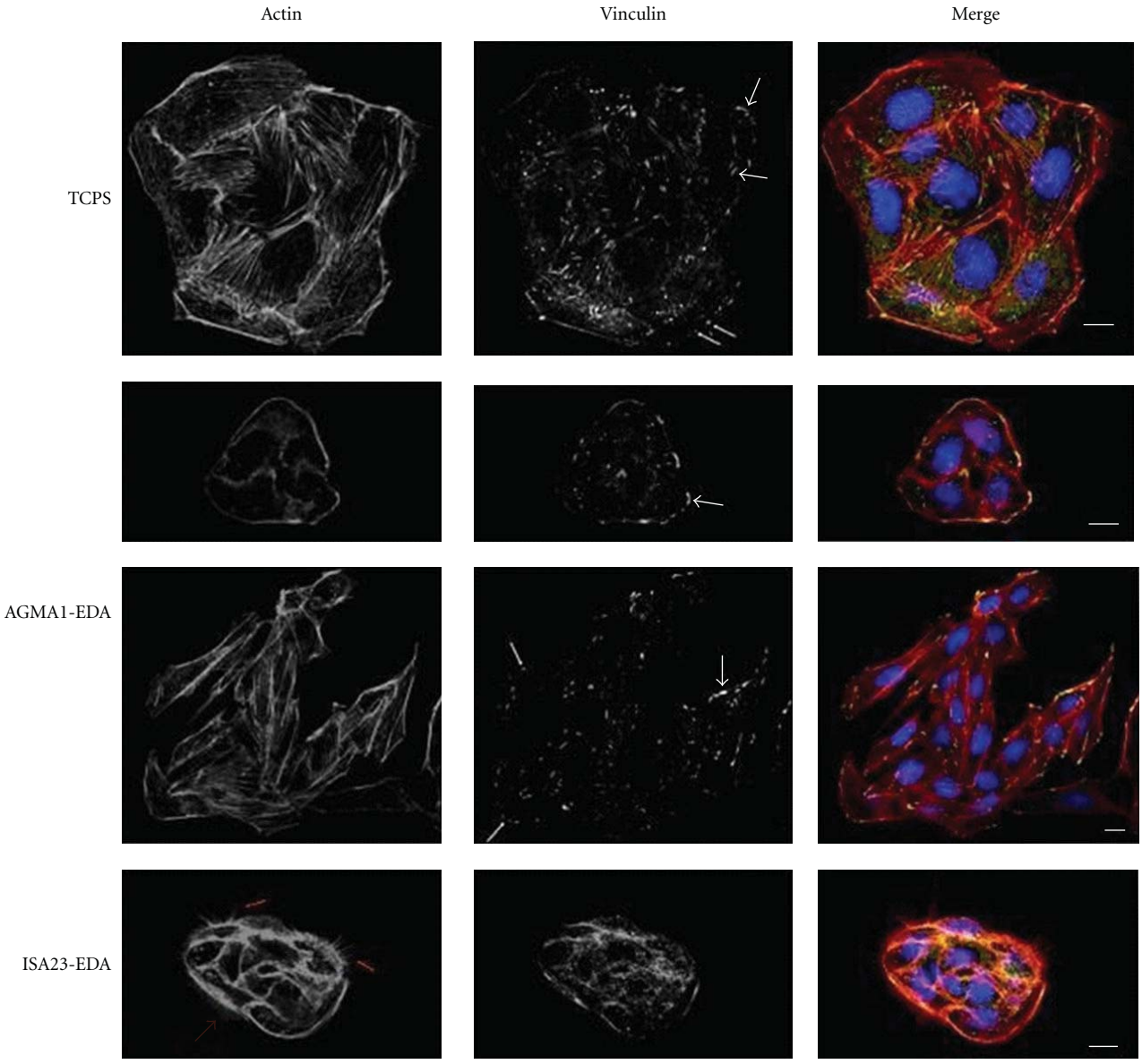

Figure 8: Immunofluorescence analysis of actin cytoskeleton and focal contacts of TCPS or hydrogel MDCK growing cells [62].

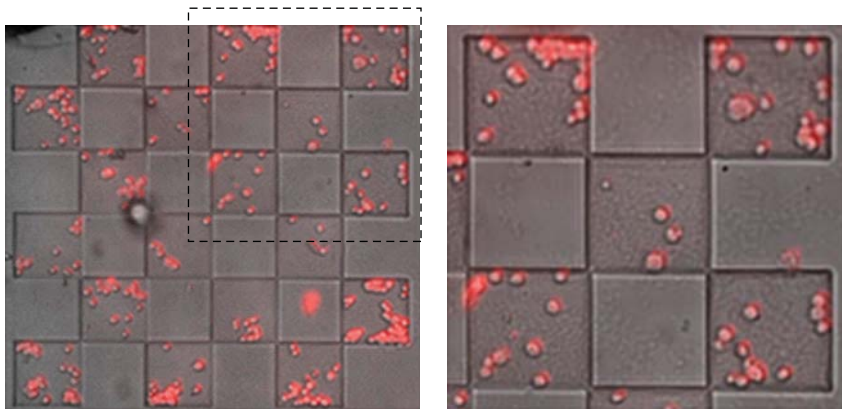

(a) (b)

Figure 9: PC12 adhesion on electron-beam-exposed areas [63].

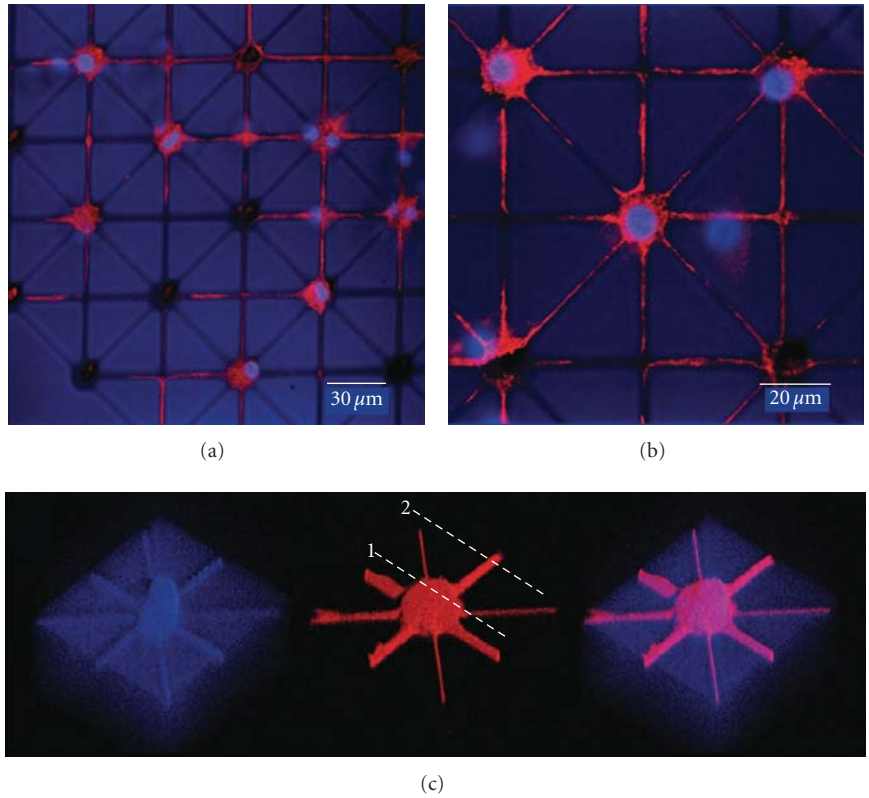

Figure 10: Confocal microscopy images of PC12 cells grown on electron-beam-lithography-patterned network of microwells (10 mm diameter) connected by microchannels (1 mm width). The cells were treated with NGF (for 48 hours) and immunostained with DAPI (cell nuclei, blue), FITC antivinculin antibody (focal contacts, red), and TRITC phalloidin (actin filaments, red) [63].

while protecting the axons against collapse and invasion from immune cells [82]. The use of guidance channels eliminates functional loss at the donor site, a condition that is commonly associated to autografts. Initial studies employing the use of short impermeable silicone tubes have shown promising nerve regeneration across 3 mm gaps [88], although significant fibrosis and nerve compression have been subsequently associated with the use of these tubes [89–91]. Biodegradable polymers such as poly(L-lactic acid), polyglycolic acid, and poly(lactic-co-glycolic) acid have been originally the materials of choice for synthesizing conduits, due to their relative abundance and applicability [92–101]. In addition to poly(esters), biodegradable poly(urethane) [102–104], poly(organo-phosphazene) [16], and poly(3-hydroxybutyrate) [105–107] have shown a capacity for guiding regeneration. Nevertheless, these materials do not fulfill all the requirements that a scaffold for *in vivo* application should have. For instance, a common inconvenience of biodegradable polyesters is to cause inflammation in the surrounding tissues giving rise to a local concentration of acids upon degradation.

In recent years, special attention has been given to hydrogels. Hydrogels exhibit overall properties similar to those of soft tissues, having tunable elasticity, nutrient permeability, biocompatibility, and low interfacial tension. Among natural hydrogels, gelatin-based tubular scaffolds [108], alginate-based capillary hydrogels [109], and multichannel collagen nerve conduits [110] have been used to guide axonal growth in animal experiments. Synthetic hydrogels include PEG [111] and poly(2-hydroxyethyl methacrylate-co-methyl methacrylate) [112]. Although these materials have shown promising results in terms of nerve regeneration, their properties such as permeability, degradability, and mechanical strength are not yet satisfactory [113].

AGMA1-EDA hydrogels have a definite potential as biomimetic materials and deserve to be further considered for different biotechnological applications such as substrates for cell culture [62]. Unfortunately, their mechanical properties are not satisfactory in view of a use as scaffolds for tissue engineering, in that their strength is still very low and they are very soft and breakable on handling. To overcome this problem, a new synthetic method has been developed leading to second-generation AGMA1 hydrogels with similar composition and exhibiting the same biological properties but with improved mechanical strength [64]. In particular, a different two-step synthetic pathway has been followed as reported in Scheme 4. In the first step an acryloyl end-capped linear AGMA1 oligomer is synthesized using a controlled excess of the bisacrylamide; in the second step the oligomer is photopolymerized by UV irradiation producing AGMA1-UV hydrogels with the required mechanical characteristics.

Hydrogel tubes of different dimensions (length 10–30 mm, 3 mm external diameter, and 0.5–1.2 mm internal

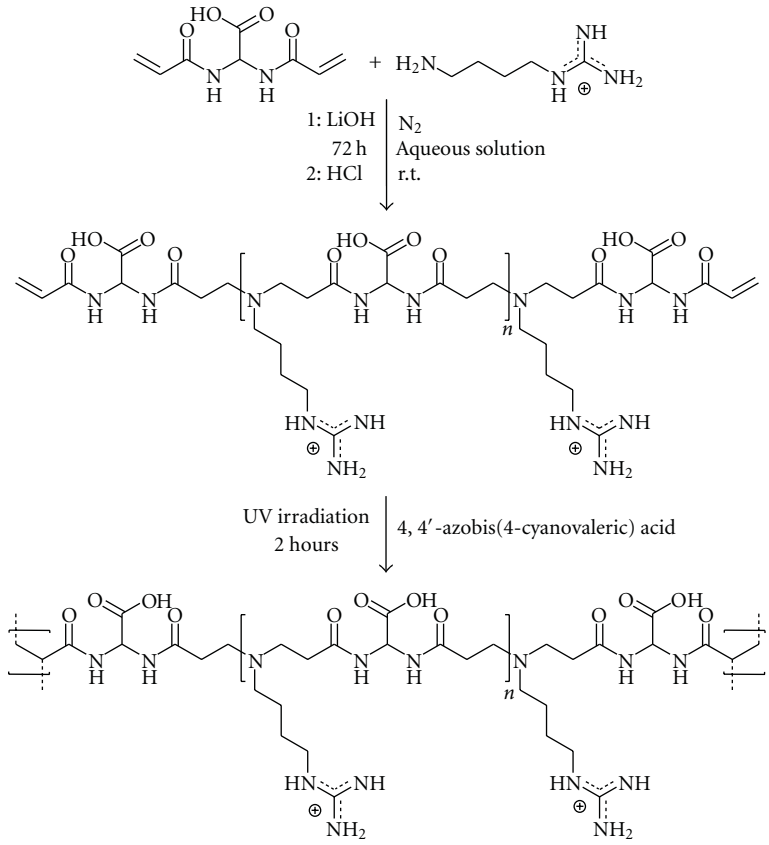

Scheme 4: Synthetic pathway leading to AGMA1 hydrogels.

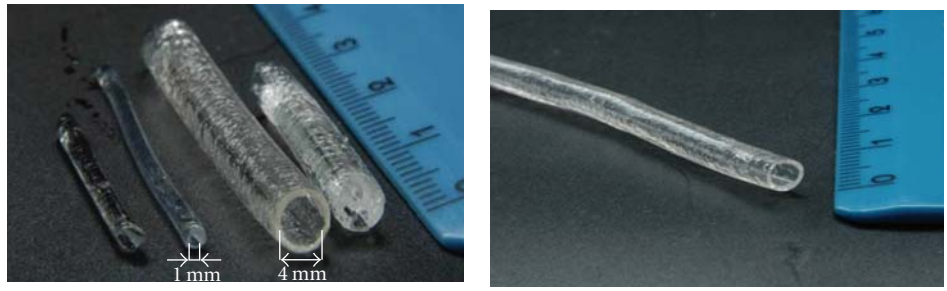

(a) (b)

Figure 11: AGMA1 tubular hydrogels obtained by UV photopolymerization [64].

diameter) are obtained (Figure 11); however, the preferred dimensions for rat implantation are 10 mm length and 1 mm inner diameter [64].

Cross-linked PAAs, obtained by ethylenediamine as cross-linking agent, swell in water giving very soft hydrogels [33, 42, 62, 65]. Swelling tests carried out on the AGMA1-UV hydrogels in doubly distilled water and 0.1 M PBS solution pH 7.4 show a 200% absorption in both cases, 3 times lower than the AGMA1-EDA hydrogels.

AGMA1-UV tubular scaffolds have been tested *in vivo* as conduit for nerve regeneration in living rats. The right sciatic nerve of the rats has been cut in the middle, and hydrogel conduit having 10 mm length and 1 mm inner diameters implanted leaving the nerve gap of 5 mm (Figure 12). All rats have survived, and no complications related to operation occurred, since all wounds have healed spontaneously [64].

The progression of the nerve regeneration has been extensively analyzed at different time points, namely, 30, 90, and 180 days after surgery [64]. 30 days after implantation the conduit appears well integrated and no dislocations are observed. The regenerated nerve is resistant to mechanical traction showing no evidence of interruption. No apparent signs of inflammatory reaction or serum infiltrate are found, even if a thin fibrotic sheet surrounding the conduit is observed. Regeneration between the upper and lower nerve stump occurs inside the scaffold guide as demonstrated by

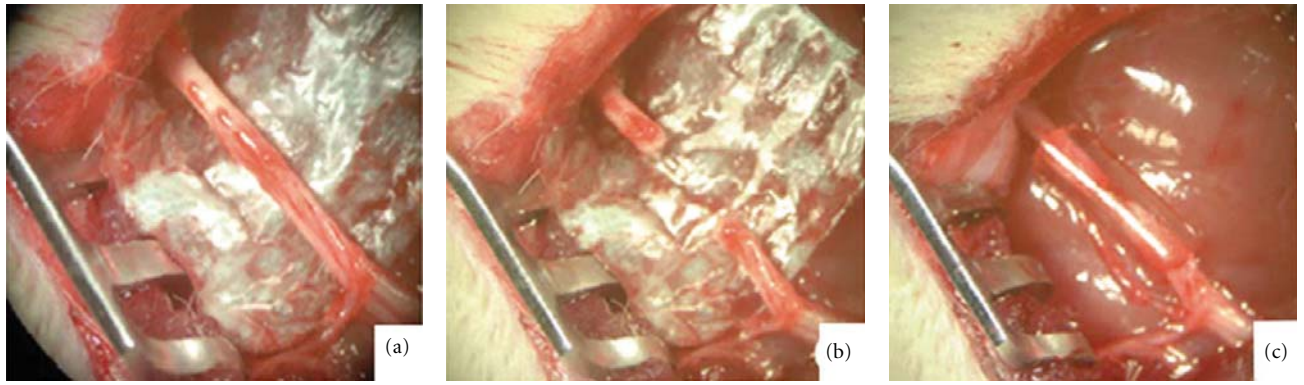

Figure 12: Normal intact right sciatic nerve was cut in the middle (a), removing 4-5 mm nervous tissue. AGMA1 hydrogel tube has been used to regenerate the gap (c) [64].

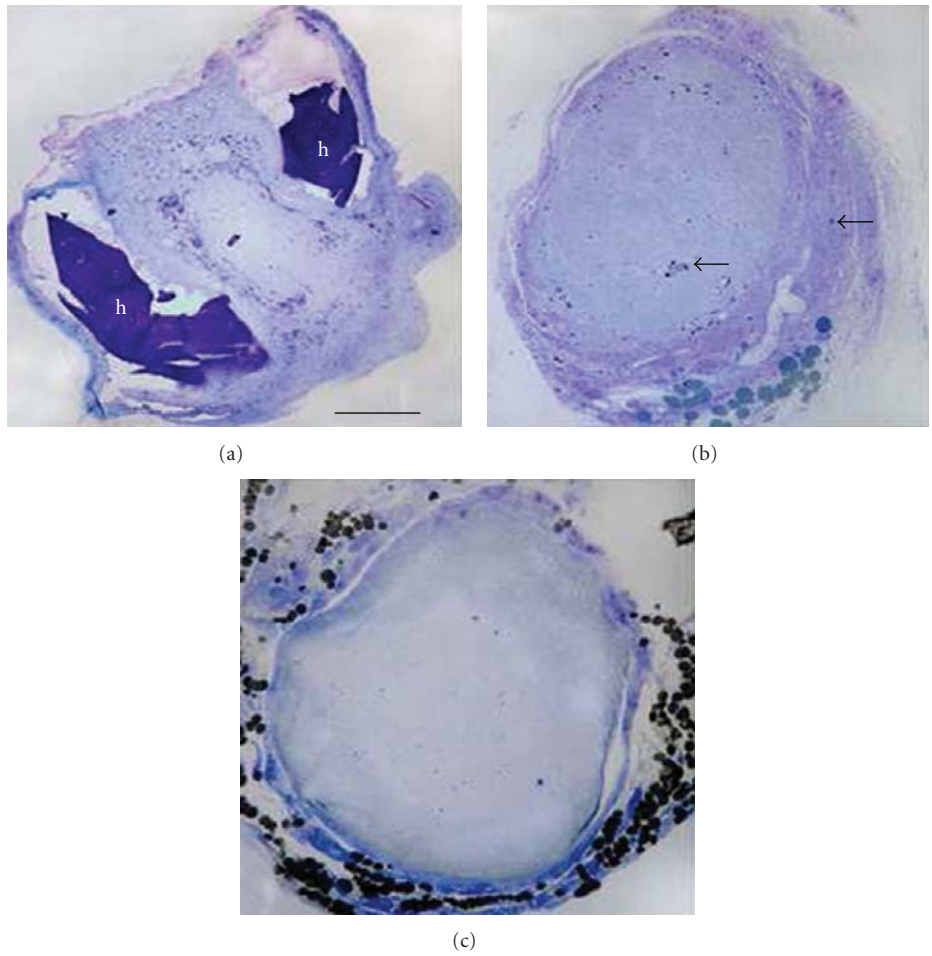

Figure 13: Toluidine-blue semithin transverse section of regenerating nerves in the medial part of the nerve guide at 30 (a), 90 (b), and 180 (c) days after surgery [64].

the presence of nerve fibers filling the original gap. The conduit is largely degraded but not completely reabsorbed, since two large scaffold fragments (h) are embedded in the epineurium surrounding the nerve (Figure 13(a)). At 90 days after surgery, a complete nerve structure is evident with some detritus still included in the fibrotic tissue around the nerve (Figure 13(b)), whereas at 180 days the scaffold is grossly reabsorbed, with only a few detritus in the surrounding epineurium (Figure 13(c)).

Morphological evaluations have been focused on 30 days after surgery, since the nerve regeneration is apparently satisfactory and not significantly different from that observed

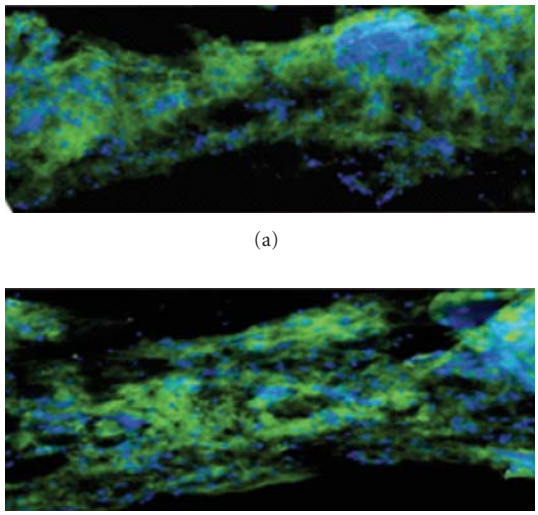

(a)

(b)

Figure 14: Immunofluorescence image of the regenerated nerve inside the hydrogel tube at 30 (a) and 90 (b) days after surgery [64].

at 90 and 180 days after implantation [64]. The axonal regeneration at 30 days is confirmed by immunofluorescent analysis of longitudinal sections of the sciatic nerve stump through the conduit.

Nerve fibers have been labeled in green with anti neurofilament M/H antibody and Schwann cells nuclei stained in blue with nuclear marker DAPI. Figure 14(a) shows the continuity of green labeling for the heavy chain of axon neurofilaments. A stronger neurofilament immunopositivity at 90 days after surgery is consistent with a higher, complete axonal regeneration (Figure 14(b)).

6. Conclusions and Perspectives

PAAs constitute a family of highly hydrophilic ionic polymers that are easily synthesized and can be designed to be biocompatible and degradable in the body fluids. Linear PAAs are usually water soluble. Cross-linked PAAs can be obtained by several means, forming highly swollen hydrogels some of which definitely warrant potential as scaffolds for tissue engineering applications both *in vitro* and *in vivo*, being highly biocompatible and biodegradable to nontoxic, self-buffered products that do not elicit inflammatory response from the surrounding tissues.

In more general terms, PAAs are highly versatile functional polymers whose biotechnological applications are still waiting to be fully exploited.

Abbreviations

PAAs: Poly(amidoamine)s
I.P.: Isoelectric point
EPR: Enhanced permeation and retention effect
BAC: 2,2-bis(acrylamido) acetic acid
EDA: Ethylenediamine
RGD: Tripeptide arginine-glycine-aspartic acid
PHEMA: Poly(2-hydroxyethyl methacrylate)
PEG: Poly(ethylene glycol)
ECM: Extracellular matrix
TCPS: Tissue culture polystyrene plates
MDCK: Madin-Darby canine kidney cell line
FITC: Fluorescein Isothiocyanate
TRITC: Tetramethylrhodamine isothiocyanate
BSA: Bovine serum albumin
EGF: Epidermal growth factor
PC12: Rat pheochromocytoma cell line
NGF: Nerve growth factor
DAPI: 4′,6-diamidino-2-phenylindole.

Acknowledgment

This work has been supported by Fondazione CARIPLO under the Project "Functional Polymeric Hydrogels for Tissue Regeneration" (no. 2010-0501), call for the Scientific Research on Advanced Materials, 2010.

References

[1] S. J. Shieh and J. P. Vacanti, "State-of-the-art tissue engineering: from tissue engineering to organ building," *Surgery*, vol. 137, no. 1, pp. 1–7, 2005.

[2] Italian Ministry of Health, National Center for Transplant, 2009-2010.

[3] R. Langer and J. P. Vacanti, "Tissue engineering," *Science*, vol. 260, no. 5110, pp. 920–926, 1993.

[4] J. P. Vacanti and R. Langer, "Tissue engineering: the design and fabrication of living replacement devices for surgical reconstruction and transplantation," *The Lancet*, vol. 354, no. 1, pp. 32–34, 1999.

[5] R. S. Langer and J. P. Vacanti, "Tissue engineering: the challenges ahead," *Scientific American*, vol. 280, no. 4, pp. 86–89, 1999.

[6] R. Langer and J. P. Vacanti, "Artificial organs," *Scientific American*, vol. 273, no. 3, pp. 130–133, 1995.

[7] S. Yang, K. F. Leong, Z. Du, and C. K. Chua, "The design of scaffolds for use in tissue engineering. Part I. Traditional factors," *Tissue Engineering*, vol. 7, no. 6, pp. 679–689, 2001.

[8] M. H. Spilker, K. Asano, I. V. Yannas, and M. Spector, "Contraction of collagen-glycosaminoglycan matrices by peripheral nerve cells in vitro," *Biomaterials*, vol. 22, no. 10, pp. 1085–1093, 2001.

[9] J. D. Guest, A. Rao, L. Olson, M. B. Bunge, and R. P. Bunge, "The ability of human schwann cell grafts to promote regeneration in the transected nude rat spinal cord," *Experimental Neurology*, vol. 148, no. 2, pp. 502–522, 1997.

[10] W. J. C. M. Marijnissen, G. J. V. M. Van Osch, J. Aigner et al., "Alginate as a chondrocyte-delivery substance in combination with a non-woven scaffold for cartilage tissue engineering," *Biomaterials*, vol. 23, no. 6, pp. 1511–1517, 2002.

[11] B. Pomahač, T. Svensjö, F. Yao, H. Brown, and E. Eriksson, "Tissue engineering of skin," *Critical Reviews in Oral Biology and Medicine*, vol. 9, no. 3, pp. 333–334, 1998.

[12] S. Liu, P. Peulve, O. Jin et al., "Axonal regrowth through collagen tubes bridging the spinal cord to nerve roots," *Journal of Neuroscience Research*, vol. 49, no. 4, pp. 425–432, 1997.

[13] X. M. Xu, S. X. Zhang, H. Li, P. Aebischer, and M. Bunge, "Regrowth of axons into the distal spinal cord through a Schwann-cell-seeded mini-channel implanted into hemisected adult rat spinal cord," *European Journal of Neuroscience*, vol. 11, no. 5, pp. 1723–1740, 1999.

[14] A. L. Sieminski, R. F. Padera, T. Blunk, and K. J. Gooch, "Systemic delivery of human growth hormone using genetically modified tissue-engineered microvascular networks: prolonged delivery and endothelial survival with inclusion of nonendothelial cells," *Tissue Engineering*, vol. 8, no. 6, pp. 1057–1069, 2002.

[15] A. Dar, M. Shachar, J. Leor, and S. Cohen, "Optimization of cardiac cell seeding and distribution in 3D porous alginate scaffolds," *Biotechnology and Bioengineering*, vol. 80, no. 3, pp. 305–312, 2002.

[16] N. Nicoli Aldini, M. Fini, M. Rocca, G. Giavaresi, and R. Giardino, "Guided regeneration with resorbable conduits in experimental peripheral nerve injuries," *International Orthopaedics*, vol. 24, no. 3, pp. 121–125, 2000.

[17] Y. L. Jae, J. W. Lee, and C. E. Schmidt, "Neuroactive conducting scaffolds: nerve growth factor conjugation on active ester-functionalized polypyrrole," *Journal of the Royal Society Interface*, vol. 6, no. 38, pp. 801–810, 2009.

[18] R. A. Dubin, G. C. Callegari, J. Kohn, and A. V. Neimark, "Carbon nanotube fibers are compatible with mammalian cells and neurons," *IEEE Transactions on Nanobioscience*, vol. 7, no. 1, pp. 11–14, 2008.

[19] E. B. Malarkey and V. Parpura, "Applications of carbon nanotubes in neurobiology," *Neurodegenerative Diseases*, vol. 4, no. 4, pp. 292–299, 2007.

[20] G. Cellot, E. Cilia, S. Cipollone et al., "Carbon nanotubes might improve neuronal performance by favouring electrical shortcuts," *Nature Nanotechnology*, vol. 4, no. 2, pp. 126–133, 2009.

[21] W. J. Li and R. S. Tuan, "Polymeric scaffolds for cartilage tissue engineering," *Macromolecular Symposia*, vol. 227, pp. 65–75, 2005.

[22] W. T. Godbey, "Polymeric scaffolds for stem cell growth," *Australian Journal of Chemistry*, vol. 58, no. 10, pp. 689–690, 2005.

[23] C. Alexander and K. M. Shakesheff, "Responsive polymers at the biology/materials science interface," *Advanced Materials*, vol. 18, no. 24, pp. 3321–3328, 2006.

[24] K. Y. Lee and D. J. Mooney, "Hydrogels for tissue engineering," *Chemical Reviews*, vol. 101, no. 7, pp. 1869–1879, 2001.

[25] P. Ferruti, "Ion-chelating polymers (Medical Applications)," in *Polymeric Materials Encyclopedia*, J. C. Salamone, Ed., pp. 3334–3359, CRC Press, Boca Raton, Fla, USA, 1996.

[26] P. Ferruti, M. A. Marchisio, and R. Duncan, "Poly(amidoamine)s: biomedical applications," *Macromolecular Rapid Communications*, vol. 23, no. 5-6, pp. 332–355, 2002.

[27] M. Casali, S. Riva, and P. Ferruti, "Use of new aminosugar derivatives as comonomers for the synthesis of glycosylated poly(amido-amines)," *Journal of Bioactive and Compatible Polymers*, vol. 16, no. 6, pp. 479–491, 2001.

[28] E. Ranucci, F. Bignotti, P. L. Paderno, and P. Ferruti, "Modification of albumins by grafting poly(amido amine) chains," *Polymer*, vol. 36, no. 15, pp. 2989–2994, 1995.

[29] P. Ferruti, M. E. Ranucci, L. Sartore et al., "Recent results on functional polymers and macromonomers of interest as biomaterials or for biomaterial modification," *Biomaterials*, vol. 15, no. 15, pp. 1235–1241, 1994.

[30] N. Lavignac, M. Lazenby, P. Foka et al., "Synthesis and endosomolytic properties of poly(amidoamine) block copolymers," *Macromolecular Bioscience*, vol. 4, no. 10, pp. 922–929, 2004.

[31] E. Ranucci, P. Ferruti, E. Lattanzio et al., "Acid-base properties of Poly(amidoamine)s," *Journal of Polymer Science, Part A*, vol. 47, no. 24, pp. 6977–6991, 2009.

[32] S. Richardson, P. Ferruti, and R. Duncan, "Poly(amidoamine)s as potential endosomolytic polymers: evaluation in vitro and body distribution in normal and tumour-bearing animals," *Journal of Drug Targeting*, vol. 6, no. 6, pp. 391–404, 1999.

[33] P. Ferruti, S. Bianchi, E. Ranucci, F. Chiellini, and V. Caruso, "Novel poly(amido-amine)-based hydrogels as scaffolds for tissue engineering," *Macromolecular Bioscience*, vol. 5, no. 7, pp. 613–622, 2005.

[34] B. Malgesini, I. Verpilio, R. Duncan, and P. Ferruti, "Poly(amido-amine)s carrying primary amino groups as side substituents," *Macromolecular Bioscience*, vol. 3, no. 1, pp. 59–66, 2003.

[35] P. Ferruti, E. Ranucci, S. Bianchi, L. Falciola, P. R. Mussini, and M. Rossi, "Novel polyamidoamine-based hydrogel with an innovative molecular architecture as a Co^{2+}-, Ni^{2+}, and Cu^{2+} sorbing material: cyclovoltammetry and extended X-ray absorption fine structure studies," *Journal of Polymer Science, Part A*, vol. 44, no. 7, pp. 2316–2327, 2006.

[36] S. P. Massia and J. A. Hubbell, "An RGD spacing of 440 nm is sufficient for integrin $\alpha(v)\beta 3$-mediated fibroblast spreading and 140 nm for focal contact and stress fiber formation," *The Journal of Cell Biology*, vol. 114, no. 5, pp. 1089–1100, 1991.

[37] K. Tanahashi, S. Jo, and A. G. Mikos, "Synthesis and characterization of biodegradable cationic poly(propylene fumarate-co-ethylene glycol) copolymer hydrogels modified with agmatine for enhanced cell adhesion," *Biomacromolecules*, vol. 3, no. 5, pp. 1030–1037, 2002.

[38] W. Raasch, U. Schäfer, J. Chun, and P. Dominiak, "Biological significance of agmatine, an endogenous ligand at imidazoline binding sites," *British Journal of Pharmacology*, vol. 133, no. 6, pp. 755–780, 2001.

[39] J. Franchini, E. Ranucci, P. Ferruti, M. Rossi, and R. Cavalli, "Synthesis, physicochemical properties, and preliminary biological characterizations of a novel amphoteric agmatine-based poly(amidoamine) with RGD-like repeating units," *Biomacromolecules*, vol. 7, no. 4, pp. 1215–1222, 2006.

[40] P. Ferruti, J. Franchini, M. Bencini et al., "Prevailingly cationic agmatine-based amphoteric polyamidoamine as a nontoxic, nonhemolytic, and "stealthlike" DNA complexing agent and transfection promoter," *Biomacromolecules*, vol. 8, no. 5, pp. 1498–1504, 2007.

[41] R. Annunziata, J. Franchini, E. Ranucci, and P. Ferruti, "Structural characterisation of poly(amidoamine) networks via high-resolution magic angle spinning NMR," *Magnetic Resonance in Chemistry*, vol. 45, no. 1, pp. 51–58, 2007.

[42] P. Ferruti, S. Bianchi, E. Ranucci, F. Chiellini, and A. M. Piras, "Novel agmatine-containing poly(amidoamine) hydrogels as scaffolds for tissue engineering," *Biomacromolecules*, vol. 6, no. 4, pp. 2229–2235, 2005.

[43] F. Bignotti, P. Sozzani, E. Ranucci, and P. Ferruti, "NMR studies, molecular characterization, and degradation behavior of poly(amido amine)s. 1. Poly(amido amine) deriving

from the polyaddition of 2-methylpiperazine to 1,4-bis(acryloyl)piperazine," *Macromolecules*, vol. 27, no. 24, pp. 7171–7178, 1994.

[44] E. Ranucci, G. Spagnoli, P. Ferruti, D. Sgouras, and R. Duncan, "Poly(amidoamine)s with potential as drug carriers: degradation and cellular toxicity," *Journal of Biomaterials Science*, vol. 2, no. 4, pp. 303–315, 1991.

[45] J. C. Adams, "Cell-matrix contact structures," *Cellular and Molecular Life Sciences*, vol. 58, no. 3, pp. 371–392, 2001.

[46] J. El-Ali, P. K. Sorger, and K. F. Jensen, "Cells on chips," *Nature*, vol. 442, no. 7101, pp. 403–411, 2006.

[47] N. Scharnagl, S. Lee, B. Hiebl, A. Sisson, and A. Lendlein, "Design principles for polymers as substratum for adherent cells," *Journal of Materials Chemistry*, vol. 20, no. 40, pp. 8789–8802, 2010.

[48] M. P. Lutolf and J. A. Hubbell, "Synthetic biomaterials as instructive extracellular microenvironments for morphogenesis in tissue engineering," *Nature Biotechnology*, vol. 23, no. 1, pp. 47–55, 2005.

[49] P. Krsko and M. Libera, "Biointeractive hydrogels," *Materials Today*, vol. 8, no. 12, pp. 36–44, 2005.

[50] V. L. Tsang, A. A. Chen, L. M. Cho et al., "Fabrication of 3D hepatic tissues by additive photopatterning of cellular hydrogels," *The FASEB Journal*, vol. 21, no. 3, pp. 790–801, 2007.

[51] S. Nayak and L. Andrew Lyon, "Soft nanotechnology with soft nanoparticles," *Angewandte Chemie—International Edition*, vol. 44, no. 47, pp. 7686–7708, 2005.

[52] M. R. Hynd, J. P. Frampton, N. Dowell-Mesfin, J. N. Turner, and W. Shain, "Directed cell growth on protein-functionalized hydrogel surfaces," *Journal of Neuroscience Methods*, vol. 162, no. 1-2, pp. 255–263, 2007.

[53] F. Toyoshima and E. Nishida, "Integrin-mediated adhesion orients the spindle parallel to the substratum in an EB1- and myosin X-dependent manner," *The EMBO Journal*, vol. 26, no. 6, pp. 1487–1498, 2007.

[54] E. Ruoslahti, "RGD and other recognition sequences for integrins," *Annual Review of Cell and Developmental Biology*, vol. 12, pp. 697–715, 1996.

[55] U. Hersel, C. Dahmen, and H. Kessler, "RGD modified polymers: biomaterials for stimulated cell adhesion and beyond," *Biomaterials*, vol. 24, no. 24, pp. 4385–4415, 2003.

[56] T. G. Kim and T. G. Park, "Biomimicking extracellular matrix: cell adhesive RGD peptide modified electrospun poly(D,L-lactic-co-glycolic acid) nanofiber mesh," *Tissue Engineering*, vol. 12, no. 2, pp. 221–233, 2006.

[57] P. M. D. Watson, M. J. Humphries, J. Relton, N. J. Rothwell, A. Verkhratsky, and R. M. Gibson, "Integrin-binding RGD peptides induce rapid intracellular calcium increases and MAPK signaling in cortical neurons," *Molecular and Cellular Neuroscience*, vol. 34, no. 2, pp. 147–154, 2007.

[58] S. Kostidis, A. Stavrakoudis, N. Biris, D. Tsoukatos, C. Sakarellos, and V. Tsikaris, "The relative orientation of the Arg and Asp side chains defined by a pseudodihedral angle as a key criterion for evaluating the structure-activity relationship of RGD peptides," *Journal of Peptide Science*, vol. 10, no. 8, pp. 494–509, 2004.

[59] E. Puklin-Faucher, M. Gao, K. Schulten, and V. Vogel, "How the headpiece hinge angle is opened: new insights into the dynamics of integrin activation," *The Journal of Cell Biology*, vol. 175, no. 2, pp. 349–360, 2006.

[60] W. A. Comisar, S. X. Hsiong, H. J. Kong, D. J. Mooney, and J. J. Linderman, "Multi-scale modeling to predict ligand presentation within RGD nanopatterned hydrogels," *Biomaterials*, vol. 27, no. 10, pp. 2322–2329, 2006.

[61] A. Bodin, L. Ahrenstedt, H. Fink, H. Brumer, B. Risberg, and P. Gatenholm, "Modification of nanocellulose with a xyloglucan-RGD conjugate enhances adhesion and proliferation of endothelial cells: implications for tissue engineering," *Biomacromolecules*, vol. 8, no. 12, pp. 3697–3704, 2007.

[62] E. Jacchetti, E. Emilitri, S. Rodighiero et al., "Biomimetic poly(amidoamine) hydrogels as synthetic materials for cell culture," *Journal of Nanobiotechnology*, vol. 6, article 14, 2008.

[63] G. Dos Reis, F. Fenili, A. Gianfelice et al., "Direct microfabrication of topographical and chemical cues for the guided growth of neural cell networks on polyamidoamine hydrogels," *Macromolecular Bioscience*, vol. 10, no. 8, pp. 842–852, 2010.

[64] V. Magnaghi, V. Conte, P. Procacci et al., "Biological performance of a novel biodegradable polyamidoamine hydrogel as guide for peripheral nerve regeneration," *Journal of Biomedical Materials Research Part A*, vol. 98, no. 1, pp. 19–30, 2011.

[65] E. Emilitri, F. Guizzardi, C. Lenardi, M. Suardi, E. Ranucci, and P. Ferruti, "Novel poly(amidoamine)-based hydrogels as scaffolds for tissue engineering," *Macromolecular Symposia*, vol. 266, no. 1, pp. 41–47, 2008.

[66] G. Maheshwari, G. Brown, D. A. Lauffenburger, A. Wells, and L. G. Griffith, "Cell adhesion and motility depend on nanoscale RGD clustering," *Journal of Cell Science*, vol. 113, no. 10, pp. 1677–1686, 2000.

[67] E. A. Cavalcanti-Adam, T. Volberg, A. Micoulet, H. Kessler, B. Geiger, and J. P. Spatz, "Cell spreading and focal adhesion dynamics are regulated by spacing of integrin ligands," *Biophysical Journal*, vol. 92, no. 8, pp. 2964–2974, 2007.

[68] J. C. Adams, "Roles of fascin in cell adhesion and motility," *Current Opinion in Cell Biology*, vol. 16, no. 5, pp. 590–596, 2004.

[69] J. Melin and S. R. Quake, "Microfluidic large-scale integration: the evolution of design rules for biological automation," *Annual Review of Biophysics and Biomolecular Structure*, vol. 36, pp. 213–231, 2007.

[70] N. M. Elman, B. C. Masi, M. J. Cima, and R. Langer, "Electro-thermally induced structural failure actuator (ETISFA) for implantable controlled drug delivery devices based on Micro-Electro-Mechanical- Systems," *Lab on a Chip*, vol. 10, no. 20, pp. 2796–2804, 2010.

[71] Y. Mei, K. Saha, S. R. Bogatyrev et al., "Combinatorial development of biomaterials for clonal growth of human pluripotent stem cells," *Nature Materials*, vol. 9, no. 9, pp. 768–778, 2010.

[72] L. M. Y. Yu, N. D. Leipzig, and M. S. Shoichet, "Promoting neuron adhesion and growth," *Materials Today*, vol. 11, no. 5, pp. 36–43, 2008.

[73] L. R. Robinson, "Traumatic injury to peripheral nerves," *Muscle and Nerve*, vol. 23, no. 6, pp. 863–873, 2000.

[74] S. K. Lee and S. W. Wolfe, "Peripheral nerve injury and repair," *The Journal of the American Academy of Orthopaedic Surgeons*, vol. 8, no. 4, pp. 243–252, 2000.

[75] P. Aebischer, V. Guenard, S. R. Winn, R. F. Valentini, and P. M. Galletti, "Blind-ended semipermeable guidance channels support peripheral nerve regeneration in the absence of a distal nerve stump," *Brain Research*, vol. 454, no. 1-2, pp. 179–187, 1988.

[76] L. R. Williams and S. Varon, "Modification of fibrin matrix formation in situ enhances nerve regeneration in silicone chambers," *The Journal of Comparative Neurology*, vol. 231, no. 2, pp. 209–220, 1985.

[77] L. R. Williams, N. Danielsen, H. Muller, and S. Varon, "Exogenous matrix percursors promote functional nerve regneration across a 15-mm gap within a silicone chamber in the rat," *The Journal of Comparative Neurology*, vol. 264, no. 2, pp. 284–290, 1987.

[78] A. D. Ansselin, T. Fink, and D. F. Davey, "Collagen—chitosan nerve guides for peripheral nerve repair: a histomorphometric study," *Neuropathology and Applied Neurobiology*, vol. 23, pp. 387–398, 1997.

[79] M. Koshimune, K. Takamatsu, H. Nakatsuka, K. Inui, Y. Yamano, and Y. Ikada, "Creating bioabsorbable Schwann cell coated conduits through tissue engineering," *Bio-Medical Materials and Engineering*, vol. 13, no. 3, pp. 223–229, 2003.

[80] S. Atzet, S. Curtin, P. Trinh, S. Bryant, and B. Ratner, "Degradable poly(2-hydroxyethyl methacrylate)-co-polycaprolactone hydrogels for tissue engineering scaffolds," *Biomacromolecules*, vol. 9, no. 12, pp. 3370–3377, 2008.

[81] R. Midha, C. A. Munro, P. D. Dalton, C. H. Tator, and M. S. Shoichet, "Growth factor enhancement of peripheral nerve regeneration through a novel synthetic hydrogel tube," *Journal of Neurosurgery*, vol. 99, no. 3, pp. 555–565, 2003.

[82] P. Weiss, "Reunion of stumps of small nerves by tubulation instead of suture," *Science*, vol. 93, no. 2403, pp. 67–68, 1941.

[83] M. Foidart-Dessalle, A. Dubuisson, A. Lejeune et al., "Sciatic nerve regeneration through venous or nervous grafts in the rat," *Experimental Neurology*, vol. 148, no. 1, pp. 236–246, 1997.

[84] C. Y. Tseng, G. Hu, R. T. Ambron, and D. T. W. Chiu, "Histologic analysis of Schwann cell migration and peripheral nerve regeneration in the autogenous venous nerve conduit (AVNC)," *Journal of Reconstructive Microsurgery*, vol. 19, no. 5, pp. 331–339, 2003.

[85] Y. T. Kim, V. K. Haftel, S. Kumar, and R. V. Bellamkonda, "The role of aligned polymer fiber-based constructs in the bridging of long peripheral nerve gaps," *Biomaterials*, vol. 29, no. 21, pp. 3117–3127, 2008.

[86] J. S. Belkas, C. A. Munro, M. S. Shoichet, and R. Midha, "Peripheral nerve regeneration through a synthetic hydrogel nerve tube," *Restorative Neurology and Neuroscience*, vol. 23, no. 1, pp. 19–29, 2005.

[87] N. N. Aldini, G. Perego, G. D. Cella et al., "Effectiveness of a bioabsorbable conduit in the repair of peripheral nerves," *Biomaterials*, vol. 17, no. 10, pp. 959–962, 1996.

[88] G. Lundborg, L. B. Dahlin, and N. Danielsen, "Ulnar nerve repair by the silicone chamber technique. Case report," *Scandinavian Journal of Plastic and Reconstructive Surgery and Hand Surgery*, vol. 25, no. 1, pp. 79–82, 1991.

[89] M. Merle, A. L. Dellon, J. N. Campbell, and P. S. Chang, "Complications from silicon-polymer intubulation of nerves," *Microsurgery*, vol. 10, no. 2, pp. 130–133, 1989.

[90] G. Lundborg, B. Rosén, L. Dahlin, J. Holmberg, and I. Rosén, "Tubular repair of the median or ulnar nerve in the human forearm: a 5—year follow—up," *Journal of Hand Surgery*, vol. 29, no. 2, pp. 100–107, 2004.

[91] J. Braga-Silva, "The use of silicone tubing in the late repair of the median and ulnar nerves in the forearm," *Journal of Hand Surgery*, vol. 24, no. 6, pp. 703–706, 1999.

[92] J. S. Belkas, M. S. Shoichet, and R. Midha, "Peripheral nerve regeneration through guidance tubes," *Neurological Research*, vol. 26, no. 2, pp. 151–160, 2004.

[93] T. W. Hudson, G. R. D. Evans, and C. E. Schmidt, "Engineering strategies for peripheral nerve repair," *Clinics in Plastic Surgery*, vol. 26, no. 4, pp. 617–628, 1999.

[94] V. B. Doolabh, M. C. Hertl, and S. E. Mackinnon, "The role of conduits in nerve repair: a review," *Reviews in the Neurosciences*, vol. 7, no. 1, pp. 47–84, 1996.

[95] S. H. Oh, J. H. Kim, K. S. Song et al., "Peripheral nerve regeneration within an asymmetrically porous PLGA/Pluronic F127 nerve guide conduit," *Biomaterials*, vol. 29, no. 11, pp. 1601–1609, 2008.

[96] Z. H. Zhou, X. P. Liu, and L. H. Liu, "Preparation and biocompatibility of poly(L-lactide-co-glycolide) scaffold materials for nerve conduits," *Designed Monomers and Polymers*, vol. 11, no. 5, pp. 447–456, 2008.

[97] L. He, Y. Zhang, C. Zeng et al., "Manufacture of plga multiple-channel conduits with precise hierarchical pore architectures and in vitro/vivo evaluation for spinal cord injury," *Tissue Engineering Part C*, vol. 15, no. 2, pp. 243–255, 2009.

[98] S. Ichihara, Y. Inada, A. Nakada et al., "Development of new nerve guide tube for repair of long nerve defects," *Tissue Engineering Part C*, vol. 15, no. 3, pp. 387–402, 2009.

[99] M. Yoshitani, S. Fukuda, S. I. Itoi et al., "Experimental repair of phrenic nerve using a polyglycolic acid and collagen tube," *Journal of Thoracic and Cardiovascular Surgery*, vol. 133, no. 3, pp. 726–733, 2007.

[100] M. C. Lu, Y. T. Huang, J. H. Lin et al., "Evaluation of a multilayer microbraided polylactic acid fiber-reinforced conduit for peripheral nerve regeneration," *Journal of Materials Science*, vol. 20, no. 5, pp. 1175–1180, 2009.

[101] G. R. D. Evans, K. Brandt, S. Katz et al., "Bioactive poly(L-lactic acid) conduits seeded with Schwann cells for peripheral nerve regeneration," *Biomaterials*, vol. 23, no. 3, pp. 841–848, 2002.

[102] G. Soldani, G. Varelli, A. Minnocci, and P. Dario, "Manufacturing and microscopical characterisation of polyurethane nerve guidance channel featuring a highly smooth internal surface," *Biomaterials*, vol. 19, no. 21, pp. 1919–1924, 1998.

[103] D. Yin, X. Wang, Y. Yan, and R. Zhang, "Preliminary studies on peripheral nerve regeneration using a new polyurethane conduit," *Journal of Bioactive and Compatible Polymers*, vol. 22, no. 2, pp. 143–159, 2007.

[104] T. Cui, Y. Yan, R. Zhang, L. Liu, W. Xu, and X. Wang, "Rapid prototyping of a double-layer polyurethane-collagen conduit for peripheral nerve regeneration," *Tissue Engineering Part C*, vol. 15, no. 1, pp. 1–9, 2009.

[105] R. C. Young, G. Terenghi, and M. Wiberg, "Poly-3-hydroxybutyrate (PHB): a resorbable conduit for long-gap repair in peripheral nerves," *British Journal of Plastic Surgery*, vol. 55, no. 3, pp. 235–240, 2002.

[106] D. F. Kalbermatten, P. J. Kingham, D. Mahay et al., "Fibrin matrix for suspension of regenerative cells in an artificial nerve conduit," *Journal of Plastic, Reconstructive and Aesthetic Surgery*, vol. 61, no. 6, pp. 669–675, 2008.

[107] A. Mosahebi, M. Wiberg, and G. Terenghi, "Addition of fibronectin to alginate matrix improves peripheral nerve regeneration in tissue-engineered conduits," *Tissue Engineering*, vol. 9, no. 2, pp. 209–218, 2003.

[108] E. Gámez, Y. Goto, K. Nagata, T. Iwaki, T. Sasaki, and T. Matsuda, "Photofabricated gelatin-based nerve conduits: nerve tissue regeneration potentials," *Cell Transplantation*, vol. 13, no. 5, pp. 549–564, 2004.

[109] P. Prang, R. Müller, A. Eljaouhari et al., "The promotion of oriented axonal regrowth in the injured spinal cord by alginate-based anisotropic capillary hydrogels," *Biomaterials*, vol. 27, no. 19, pp. 3560–3569, 2006.

[110] L. Yao, G. C. W. de Ruiter, H. Wang et al., "Controlling dispersion of axonal regeneration using a multichannel collagen nerve conduit," *Biomaterials*, vol. 31, no. 22, pp. 5789–5797, 2010.

[111] M. B. Runge, M. Dadsetan, J. Baltrusaitis et al., "Development of electrically conductive oligo(polyethylene glycol) fumarate-polypyrrole hydrogels for nerve regeneration," *Biomacromolecules*, vol. 11, no. 11, pp. 2845–2853, 2010.

[112] J. S. Belkas, C. A. Munro, M. S. Shoichet, M. Johnston, and R. Midha, "Long-term in vivo biomechanical properties and biocompatibility of poly(2-hydroxyethyl methacrylate-co-methyl methacrylate) nerve conduits," *Biomaterials*, vol. 26, no. 14, pp. 1741–1749, 2005.

[113] J. W. Gunn, S. D. Turner, and B. K. Mann, "Polymer gel systems for nerve repair and regeneration," *Journal of Biomedical Materials Research Part A*, vol. 72, no. 1, pp. 91–97, 2005.

Hindawi Publishing Corporation
International Journal of Polymer Science
Volume 2011, Article ID 343062, 14 pages
doi:10.1155/2011/343062

Review Article

Hydrogel Synthesis Directed Toward Tissue Engineering: Impact of Reaction Condition on Structural Parameters and Macroscopic Properties of Xerogels

Borivoj Adnadjević and Jelena Jovanović

Faculty of Physical Chemistry, Belgrade University, Studentski Trg 12-16, 11001 Belgrade, Serbia

Correspondence should be addressed to Jelena Jovanović, jelenaj@ffh.bg.ac.rs

Received 1 June 2011; Revised 13 July 2011; Accepted 13 July 2011

Academic Editor: Shanfeng Wang

The existence of correlation and functional relationships between reaction conditions (concentrations of crosslinker, monomer and initiator, and neutralization degree of monomer), primary structural parameters (crosslinking density of network, average molar mass between crosslinks, and distance between macromolecular chains), and macroscopic properties (equilibrium swelling degree and xerogel density) of the synthesized xerogels which are important for application in tissue engineering is investigated. The structurally different xerogels samples of poly(acrylic acid), poly(methacrylic acid), and poly(acrylic acid-*g*-gelatin) were synthesized by applying different methods of polymerization: crosslinking polymerization, crosslinking polymerization in high concentrated aqueous solution, and crosslinking graft polymerization. The values of primary structural parameters and macroscopic properties were determined for the synthesized xerogels samples. For all of the investigated methods of polymerization, an existence of empirical power function of the dependence of primary structural parameters and macroscopic properties on the reaction conditions was established. The scaling laws between primary structural parameters and macroscopic properties on average molar mass between crosslinks were established. It is shown that scaling exponent is independent from the type of monomer and other reaction conditions within the same polymerization method. The physicochemical model that could be used for xerogel synthesis with predetermined macroscopic properties was suggested.

1. Application of Hydrogels in Tissue Engineering

Every year, millions of patients suffer the loss or failure of an organ or tissue as a result of accidents or disease. The field of tissue engineering has developed to meet the tremendous need for organs and tissues [1–3].

Hydrogels are commonly defined as three-dimensional networks of hydrophilic polymers, capable of absorbing significant amounts of water (from 20 g/g up to 2000 g/g of their dry mass) without dissolving or losing their structural integrity [4, 5].

They are also called smart, intelligent, stimuli-responsive, or environmental sensitive materials when a rather sharp change can be induced by changes in the environmental conditions, for example, small changes in temperature. Stimuli-responsive hydrogels are described as smart or intelligent when their sol-gel transition occurs at conditions that can be induced in a living body [6].

Due to their characteristic properties (high swellability in water, hydrophilicity, biocompatibility, and intoxicity) and to their abilities to respond to a variety of changes in the surrounding medium (pH, temperature, ionic strength, light intensity, electric and magnetic field, and presence and concentration of some chemicals), hydrogels have been utilized in a wide range of biological, medical, pharmaceutical, and environmental applications. Hydrogels have structural similarity to the macromolecular-based components in the body and are considered biocompatible, and so, they have found numerous applications as biomaterials, both in tissue engineering and in drug delivery [7, 8].

Grodzinski [1] provided comprehensive overview of using gels and hydrogels for biomedical and pharmaceutical applications pointing out on some useful reviewers on

stimuli-responsive polymeric systems, their applications, and modes of activity [9, 10]. Hydrogels have been shown to be very useful for controlling cell adhesion in tissue engineering [11, 12] components of extracellular matrix [13] for reconstruction or repair of soft tissues [14, 15], as biosensors [16] and actuators, [17] and for many other biomedical applications [18, 19]. They have been utilized as scaffold materials for drug and growth factor delivery, engineering tissue replacements, and a variety of other applications.

They can be applied as space filling scaffolds, scaffolds for bioactive molecule delivery or for cell delivery [20]. An extensive review of the applications of hydrogels for scaffolds and ECMs has been published by Varghese and Elisseeff [21]. They indicated that collagen gels provide a good milieu for chondrocytes that enables preservation of their morphology. Application of these gels for bone regeneration was investigated. Their applications are, however, limited by their mechanical weakness.

Tuzlakoglu et al. [22] described the wet spinning technique of the chitosan fibers as a 3D fiber mesh, as a potential method of production of scaffolds for tissue engineering. In this context, they investigated their mechanical properties, swelling, cytotoxicity, and bioactivity. Their mesh structures were suitable for cell growth. Tuzlakoglu et al. believe that the scaffolds developed by them might be used for bone tissue engineering.

Guo et al. [23] prepared gene-activated porous chitosan-gelatin matrices (GAMs) for in vitro expression of the transforming growth factor (TFG-b1) for chondrocytes proliferation.

Liu and Chen-Park presented a novel cell-encapsulating hydrogel family based on the interpenetrating polymer network (IPN) of gelatin and dextran bifunctionalized with methacrylate (MA) and aldehyde (AD) (Dex-MA-AD). It was demonstrated that the dextran-based IPN hydrogels not only supported endothelial cells (ECs) adhesion and spreading on the surface, but also allowed encapsulated smooth muscle cells (SMCs) to proliferate and spread in the bulk interior of the hydrogel. Further, these IPN hydrogels have higher dynamic storage moduli than polyethylene glycol-based hydrogels commonly used for smooth muscle cells (SMCs) encapsulation. These IPN hydrogels appear promising as 3D scaffolds for vascular tissue engineering [24]. It is shown that rather than using adhesive peptide, gelatin which has good biodegradability and low level of immunogenicity and cytotoxicity [25] can also be incorporated into dextran hydrogel [26–28].

Lu et al. [29] investigated the feasibility of tailoring poly(vinyl alcohol)/poly(acrylic acid) interpenetrating polymer networks (PVA/PAA-IPN) as coatings for implantable neural electrodes. They presented a new approach for improving the electrode-neural tissue interface by using hydrogel PVA/PAA-IPN tailored as coatings for poly-(dimethylsiloxane)-based neural electrodes. Although PVA is a kind of polyhydroxyl polymer which is not degradable in most physiological situations [30], the PVA-based hydrogels are broadly applied in tissue engineering because of its excellent mechanical strength and good film formation property [31–34]. The crosslinked poly(acrylic acid) (PAA) is a high water absorbing and protein resistive material widely used in medical field [35, 36].

Poly(*N*-isopropylacrylamide) (PNIPAAm) is potentially very attractive for tissue engineering applications, as it exhibits phase transition behavior above the lower critical solution temperature (LCST). The LCST of PNIPAAm in water is approximately 32°C and can be matched to body temperature by copolymerization [37]. This will result in the formation of a solid cell/polymer construct, as the gel warms to body temperature. The NIPAAm has been copolymerized with acrylic acid, methacrylic acid, or butylmethacrylic acid, depending on the desired final applications [38–40]. Acrylamide derivatives have also been cross-linked with native proteins [41] or oligodeoxyribonucleotides [42] to form temperature responsive gels. In this situation, conventional polymers could potentially be modified to exhibit thermal transition behavior by utilizing a variety of crosslinking molecules that can induce phase separation in response to temperature changes. This mechanism of phase transition may be ideal for delivery of cells, as crosslinking due the temperature change happened upon introduction to the body. The unique temperature-responsive nature of these polymers is leading to a variety of biological applications. These polymers are also being investigated as an injectable delivery vehicle for cartilage and pancreas engineering [38, 43]. However, limitations of these gels are the nondegradable crosslinks, and the vinyl monomers and crosslinking molecules are toxic, carcinogenic, or teratogenic [44]. In an effort to obviate these issues, dextran-grafted PNIPAAm copolymers have been synthesized, and these may modulate degradation in synchronization with temperature [45].

The possibility of applying PAA-based hydrogels crosslinked by macro-di-isocyanates for retarded drug release was investigated [46]. The work presented by Changez et al. lead to the conclusion that it is possible to deliver gentamicin sulphate using IPNs based on PAA and gelatin in a controlled manner. The authors recommended that these devices may have good therapeutic potential for the treatment of local infections like osteomyelitis [47]. A mucoadhesive polymer complex composed of chitosan and PAA loaded with triamcinolone acetonide (TAA) was prepared. It was found that the TAA was released from the chitosan/PAA complex by non-Fickian diffusion [48].

The isothermal kinetics of the release of the drug (*E*)-4-(4-metoxyphenyl)-4-oxo-2-butenoic acid (MEPBA) structurally similar to (*E*)-4-aryl-(4-oxo-2-butenoic acid) whose antiproliferative activity towards human cervix carcinoma HeLa has been reported [49] from poly(acrylic acid) hydrogel and poly(acrylic-co-methacrylic acid) (PAMA) hydrogels were studied by Adnadjevic et al. [50, 51]. The process of MEPBA release from PAA hydrogel, almost in entire range, can be described with the model of the drug desorption from the active centers with different specific energies.

The delivery system composed of a dual pH-sensitive and thermosensitive smart polymer gel composed of a random terpolymer of *N*-isopropylacrylamide, butylmethacrylate, and acrylic acid was designed as a new anti-HIV agent [52].

In recent years, hydrogels based on poly(acrylic acid) (PAA), poly(methacrylic acid) (PMA), and their copolymers, complexes, IPNs, or grafted networks have often been used as carriers in drug release systems in recent years because of their multifunctional nature, unique properties, and good biocompatibility [53, 54].

2. Biocompatibility of Hydrogels in Tissue Engineering

The application of polymers and hydrogels in tissue engineering requires them to be biocompatible, nontoxic and nonimflammatory [55].

An absolutely critical parameter for application in tissue engineering is the biocompatibility of hydrogels. Naturally derived polymers in general demonstrate adequate biocompatibility, while synthetic polymers sometimes may produce negative responses from the body. The processes that follow implantation (inflammation, wound healing, and the foreign-body reaction) depend on the chemical structure, physical structure (porosity), and surface microarchitecture of hydrogels. Kopeček and Yang in their comprehensive review [56] presented a summary of systematic study of the biocompatibility of hydrogels based on crosslinked polyHEMA, poly(*N*-substituted methacrylamide)s, poly(*N*monosubstituted acrylamide)s, and poly(*N*,*N*disubstituted acrylamide)s and their copolymers with ionogenic comonomers and revealed that all these structures were well tolerated after subcutaneous implantation in rats and pigs. No significant differences were observed with healing-in of hydrogels of different chemical compositions although significant differences were observed for hydrogels with different morphology. Hoffman revealed that hydrogels designed for use as tissue engineering scaffolds may contain pores large enough to accommodate living cells, or they may be designed to dissolve or degrade away, releasing growth factors and creating pores into which living cells may penetrate and proliferate [57]. The biocompatibility of hydrogels with identical chemical structure but differing in porosity using the models hydrogels of HEMA was compared. Hydrogels of HEMA were prepared by crosslinking copolymerization with ethylene dimethacrylate with different water-to-monomer ratio, which resulted in the formation of homogeneous hydrogels, microporous and macroporous spongy hydrogels with interconnecting channels. The implantation of porous hydrogels resulted in fibrous capsule formation. However, in contrast to homogeneous hydrogels, newly formed blood capillaries and an eosinophilically stained exudate penetrated into the implant. The intensity of the response was greater with higher hydrogel porosity [56].

The interactions of cells with hydrogels significantly affects their adhesion as well as migration and differentiation. The adhesion may be cell-type specific and is dependent on the interaction of specific cell receptors with ligands that are a component or adsorbed onto the materials [57].

3. Design Synthesis of Xerogels for Tissue Engineering

Hydrogels in tissue engineering must meet a number of design criteria to function appropriately and promote new tissue formation. These criteria include both classical physical parameters (e.g., degradation and mechanics) and mass transport parameters (diffusion requirements) as well as biological performance parameters and biological interaction requirements of each specific application (e.g., cell adhesion). For example, scaffolds designed to encapsulate cells must be capable of being gelled without damaging the cells, must be nontoxic to the cells and the surrounding tissue after gelling, must allow appropriate diffusion of nutrients and metabolites to and from the encapsulated cells and surrounding tissue, and require sufficient mechanical integrity and strength to withstand manipulations associated with implantation and in vivo existence [58].

For a rational design of biomaterials, all variables influencing cell function and tissue morphogenesis have to be considered. Brandl et al. give comprehensive review which promote a rational design of hydrogels for tissue engineering application with a special emphasizes on their physical properties. Adjusting these parameters to the requirements of each specific application would allow for the creation of "custom-made" biomaterials that direct the development of desired tissues. In the review of Brandl et al., the basic principles of cellular mechanosensitivity, highlighting the problems of characterizing the mechanical properties of biological tissues and hydrogels, are summarized and followed by a discussion on the rational design of hydrogels for tissue-engineering applications, while the impact of mechanical characteristics and degradability on cell function and tissue morphogenesis was pointed out [59].

The areas of active research in tissue engineering include biomaterials design-incorporation of the appropriate chemical, physical, and mechanical/structural properties to guide cell and tissue organization, cell and scaffold integration-inclusion into the biomaterial scaffold of either cells for transplantation or biomolecules to attract cells, including stem cells, from the host to promote integration with the tissue after implantation, and biomolecule delivery inclusion of growth factors and/or small molecules or peptides that promote cell survival and tissue regeneration. The review of Shoichet emphasizes polymers used in medicine and specifically those designed as scaffolds for use in tissue engineering and regenerative medicine and particularly polymer scaffolds used for delivery of cells and biomolecules. The challenges and solutions pursued in designing polymeric biomaterial scaffolds with the appropriate 3-dimensional structure have been explored [60].

The results of the rapid development of advanced materials science are processing of materials with predicted functional physical, technological, and exploitation characteristics. However, progress in the field of synthesis of needed materials is considerably slow due to the lack of effective methods that can define new technologies with minimal research.

The predictions of the materials properties, firstly have been based on the association principle in order to be further replaced by the principle of correlation when quantity of information about materials enhanced. The findings of various correlation relationships type property-property and property-composition lead to the development of its significance. Finally, the correlation method reaches its ultimate expression in the so called multivariation analyses which enable discovering limited number of parameters which can be used for defining physicochemical properties of material. Principal limitations specific for the multivariation analyses used for predicting the properties of materials reveal that the structure of material was the crucial point in the process of predicting properties of materials.

In accordance with that, creation of material with predictable properties can be assumed that is solved if the triad technology-structure- property (T-S-P) is known, that is, if functional relationship type: property-structure and structure-technology are established and in that relations, structure has a role of parameter which express relationship: technology-property.

On this manner, prediction of the materials properties, that is, production of materials of predictable properties riches qualitatively new, higher level.

Bearing that in mind, this paper summarizes the effects of reaction conditions (concentrations of crosslinker (Cc), monomer (Cm), and initiator (Ci) and neutralization degree of monomer (ND) on primary structural properties of xerogels (average molar mass between crosslinks (M_c), crosslinking density of network (ρ_c) distance between macromolecular chains (d) and xerogels macroscopic properties (xerogel density (ρ_x), and equilibrium swelling degree (SD_{eq}) for different processes of xerogels/hydrogels synthesis (crosslinking polymerization (CLP), high concentrated aqueous solution crosslinking polymerization (CCLP), and crosslinking graft polymerization (CLGP)) with the aim to elucidate triad T-S-P as presented in Figure 1.

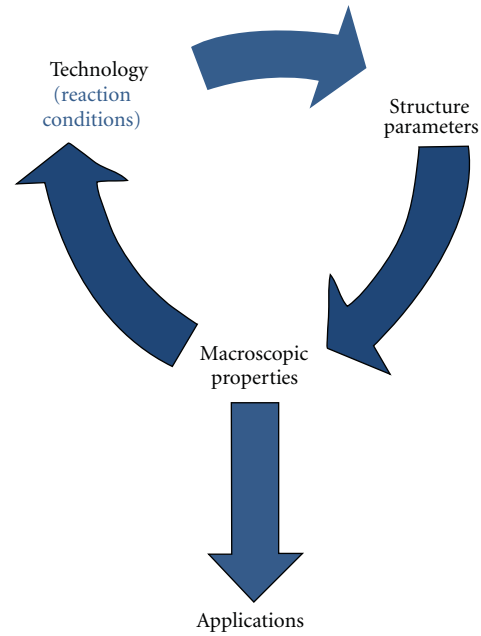

Figure 1: Triad technology-structure-property.

4. Design of Poly(Acrylic Acid) Xerogel Synthesis via High Concentrated Aqueous Solution Crosslinking Polymerization

4.1. Synthesis of Poly(Acrylic Acid) Hydrogels. Poly(acrylic acid) (PAA) hydrogels with different concentrations of crosslinker and initiator in reaction mixture were synthesized *via* high concentrated aqueous solution crosslinking polymerization (CCLP).

For the synthesis, the following materials were used. The monomer, acrylic acid (99.5%) (AA), was purchased from Merck KGaA, Darmstadt Germany, stored in a refrigerator, and melted at room temperature before use. The crosslinker N,N′-methylene bisacrylamide (MBA) (p.a) was supplied by Aldrich Chemical Co., Milwaukee, USA. The initiator, ammonium peroxodisulphate (p.a) (APS), was purchased from BDH Prolab, USA. Sodium hydroxide (p.a) was obtained from Aldrich Chemical Co., Milwaukee, USA.

The general procedure was as follows. Firstly, 10 mL of cooled acrylic acid in ice bath to 5°C was neutralized to required degree of neutralization by dropwise adding necessary amount of potassium hydroxide aqueous solution (50 wt%) under constant stirring. Then, crosslinker aqueous solution (0.1 wt%) was added and was stirred approximately 5 min at ambient temperature. Then, the initiator solution (10 wt% APS) was added to the reaction mixture. The reaction mixture was once again rapidly stirred, and immediately, the prepared reaction mixture was poured into teflon mold and placed in an thermostat oven at 70°C for 0.5 hours.

The resulting products were taken out the teflon mold and sliced into small pieces which were subsequently immersed in excess distilled water. The water was changed every 2-3 hours except overnights for 7 days in order to remove the sol fraction of polymer and unreacted monomer. Subsequently, the washed-out hydrogel was dried in air oven at 100°C approximately 8 h until constant mass was attained. The obtained products were stored in a vacuum exicator until use.

4.2. Structural Characterization of the Synthesized Poly(Acrylic Acid) Xerogels

4.2.1. Macroscopic Properties of Xerogels. Macroscopic properties (MP) of xerogels (equilibrium swelling degree (SD_{eq}) and xerogel density (ρ_{xg})) were determined using the following procedures.

Determination of the Equilibrium Swelling Degree. Dry hydrogel (xerogel) disks with an average weight of 0.10 g (±10%) were left to swell in distilled water in excess distilled water at ambient temperature. The swollen hydrogels samples were taken out from water, wiped to remove excess surface water, and weighted. This was done until the hydrogels attained constant mass, that is, until equilibrium was reached (m_{eq}). The equilibrium swelling degree (SD_{eq})

defined as the difference between the weight of the swollen hydrogel sample at equilibrium swollen state, that is, when the hydrogel sample attained constant mass (m_{eq}), and the weight of the xerogel (dry hydrogel) (m_0) divided by the weight of the xerogel sample (m_0) was determined as a function of time at constant temperature and calculated using:

$$\mathrm{SD} = \frac{m_{eq} - m_0}{m_0}. \quad (1)$$

For each sample, at least three swelling measurements were performed, and the mean values were used.

The xerogel densities of the synthesized samples were determined by the pycnometer method, using:

$$\rho_{xg} = \frac{m_{xg}\rho_T}{m_1 + m_{xg} - m_2}, \quad (2)$$

where m_{xg} is the weight of the xerogel sample, m_1 is the weight of pycnometer filled with toluene, used as the nonsolvent, m_2 is the weight of pycnometer filled with toluene with the xerogel sample in it, and ρ_T is the density of toluene ($\rho_T = 0.864\,\mathrm{g/cm^3}$).

4.2.2. Primary Structural Parameters of the Synthesized Poly(Acrylic Acid) Hydrogels. The primary structural parameters (PSP) of the synthesized poly(acrylic acid) xerogels: average molar mass between the network crosslinks (M_c), crosslinking degree (ρ_c), and the distance between the macromolecular chains (d) were calculated by application of Flory and Rehner Equation [61]

$$M_c = \frac{-\rho_{xg} V_{H_2O} v_{2,s}^{1/3}}{\ln(1 - v_{2,s}) + v_{2,s} + \chi v_{2,s}^2}, \quad (3)$$

where V_{H_2O} is the molar volume of H_2O, $v_{2,s}$ is the polymer volume fraction in the equilibrium swollen state, and χ is the Flory-Huggins interaction parameter between a solvent (H_2O) and a polymer (PMAA). The values of $v_{2,s}$ and χ were calculated using the following expressions:

$$v_{2,s} = \frac{1}{1 + \rho_{xg}\mathrm{SD}_{eq}},$$
$$\chi = \frac{\ln(1 - v_{2,s}) + v_{2,s}}{v_{2,s}^2}. \quad (4)$$

The degree of crosslinking was calculated as

$$\rho_c = \frac{\rho_x}{M_c}, \quad (5)$$

where M_0 is the molar mass of the repeating unit.

The distance between the macromolecular chains was calculated as

$$d = l v_{2,s}^{-1/3} \left(2C_n \frac{M_c}{M_0}\right)^{1/2}, \quad (6)$$

where C_n is the Flory characteristic ratio (C_n (AA) = 6.7 Å, (C_n (MAA) = 14.6 Å) and l is the carbon-carbon bond length (1.54 Å) [62].

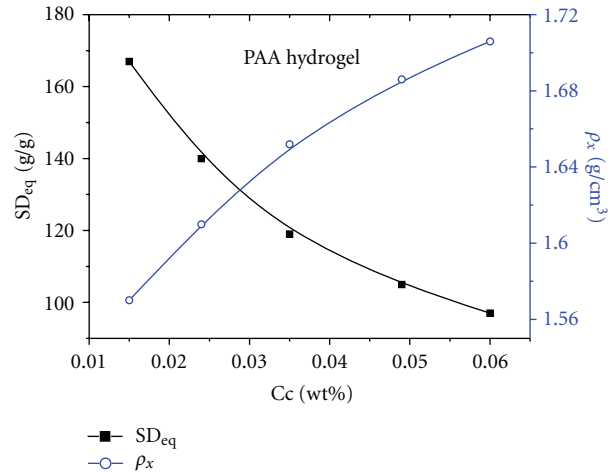

Figure 2: The effect of Cc on macroscopic properties of the synthesized PAA xerogels.

Table 1: Effect of changes in Cc on primary structural parameters of PAA xerogels.

Cc, wt%	$M_c \cdot 10^{-5}$, g/mol	ρ_c, mol/m^3	d, nm	χ
0.015	3.13	5.083	239	−0.499
0.024	2.51	6.506	203	−0.497
0.035	1.95	8.472	170	−0.503
0.049	1.66	10.149	152	−0.503
0.060	1.51	11.261	142	−0.502

4.3. Effects of Crosslinker Concentration on MP and PSP of PAA Xerogel. The samples of PAA hydrogels were synthesized by using reaction mixtures with variable crosslinker concentration within the range 0.015–0.06 wt% and keeping constant all the others reaction conditions (Cm = 72 wt%, Ci = 0.07 wt%, ND = 75%, T = 70°C, and t = 30 min) with the aim to evaluate the effects of changing Cc on the values of primary structural parameters and macroscopic properties of the synthesized xerogels.

Figure 2 presents the changes of MP of the synthesized PAA xerogels with the variation in the Cc in reaction mixture.

Table 1 presents the changes of PSP of the synthesized xerogels with the variation in the Cc in reaction mixture.

From the results presented in Figure 2 and Table 1, we can conclude that the increasing Cc leads to the increasing values of xerogel density and crosslinking density of xerogel and to the decreasing values of equilibrium swelling degrees, average molar mass between crosslinks, and the distance between the macromolecular chains, while the value of Flory-Huggins interaction parameter between solvent and polymer remains practically unaffected.

An analyses of the established changes of the primary structural parameters and macroscopic properties of synthesized xerogels caused with the variation in crosslinker concentration in reaction mixture revealed an existence of functional ($R \geq 0.99$) and correlation relationships ($R \leq 0.99$)

between them. The found relationship are presented by following empirical Equation (7):

$$\begin{aligned} \mathrm{SD_{eq}} &= 32.5 \cdot C_c^{-0.40} \quad R = 0.99, \\ \rho_x &= 2.02 \cdot C_c^{0.06} \quad R = 0.99, \\ M_c &= 3.3 \cdot 10^4 \cdot C_c^{-0.5} \quad R = 0.99, \\ \rho_c &= 60 \cdot C_c^{0.59} \quad R = 0.99, \\ d &= 47 \cdot C_c^{-0.39} \quad R = 0.99, \end{aligned} \tag{7}$$

where R is correlation coefficient. The data were analyzed using the commercial program Origin Microcal 8.0 and relations with the best correlation coefficient (R) are presented.

Based on above empirical Equation (7), it is easy to conclude that primary structural parameters and macroscopic properties of xerogels (Y) are power functions of concentration of crosslinker in reaction mixture (X) (8)

$$Y = a \cdot X^b, \tag{8}$$

where a is prefactor and b is exponent.

Assuming that equilibrium swelling degree is in functional relationship with the primary structural parameters of xerogel, an existence of dependence between $\mathrm{SD_{eq}}$ and primary structural parameters was investigated. The found relationship are presented by empirical Equation (9).

$$\begin{aligned} \mathrm{SD_{eq}} &= 0.015 \cdot M_c^{0.74} \quad R = 0.99, \\ \mathrm{SD_{eq}} &= 498 \cdot \rho_c^{-0.67} \quad R = 0.94, \\ \mathrm{SD_{eq}} &= 0.63 \cdot d^{1.02} \quad R = 0.99. \end{aligned} \tag{9}$$

The dependences of equilibrium swelling degree on primary structural parameters of xerogel are also power function with different values of prefactor and exponent for different structural parameters. The established power law dependences of equilibrium swelling degree on different primary structural parameters of xerogel confirm the validity of the previously given propose about existing functional relationship between them. The obtained different values of prefactor and exponent for different structural parameters of xerogels point out on dependence of equilibrium swelling degree on structural details of xerogel.

We proposed that the basic structural detail of xerogel is average molar mass of polymer chain between crosslinking points (M_c), and so, the dependences of primary structural parameters (ρ_c and d) and macroscopic property ρ_x of xerogel on M_c were investigated and obtained dependences are given by empirical Equation (10)

$$\begin{aligned} \rho_x &= 4.95 \cdot M_c^{-0.10} \quad R = 0.98, \\ \rho_c &= 5.44 \cdot M_c^{-1.1} \quad R = 0.99, \\ d &= 0.02 \cdot M_c^{0.73} \quad R = 0.99. \end{aligned} \tag{10}$$

As we can see, the MP and PSP may be scaled with M_c through scaling laws. This confirms the previous assumption that the basic structural detail of xerogel structure which further determine other primary structural parameters and macroscopic properties of xerogel is average molar mass of polymer chain between crosslinks and implies on law by which macromolecules scaling their PSP.

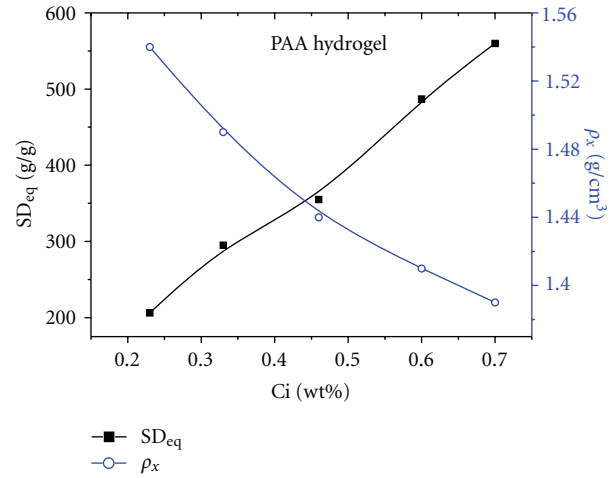

Figure 3: Effect of Ci on $\mathrm{SD_{eq}}$ and ρ_x of PAA xerogels.

Table 2: Effect of changes in Ci on primary structural parameters of PAA xerogel.

Ci, wt%	$M_c \cdot 10^{-5}$, g/mol	ρ_c, mol/m^3	d, nm	χ
0.23	3.96	3.85	284	−0.50
0.33	7.08	2.11	425	−0.48
0.46	8.64	1.70	496	−0.51
0.60	13.1	1.08	671	−0.52
0.70	16.7	0.82	794	−0.48

4.4. Effects of Initiator Concentration on MP and PSP of PAA Xerogel. PAA hydrogels with different concentrations of initiator (from 0.23 wt% to 0.70 wt%) were prepared, while other reaction parameters were kept constant (Cm = 72 wt%, ND = 75%, Cc = 0.015 wt%, T =70°C, t = 30 min).

The effects of concentration of initiator in reaction mixture on macroscopic properties of synthesized xerogels are presented in Figure 3.

The effects of concentration of initiator in reaction mixture on primary structural parameters of synthesized xerogels are presented in Table 2.

The increase in the initiator concentration leads to the increase in the equilibrium swelling degree, average molar mass of polymer chain between crosslinks, and distance between the macromolecular chains, while the values of xerogel density and crosslinking density of xerogel decrease. On the contrary to these effects, the value of Flory-Huggins interaction parameter between solvent and polymer is practically unaffected with the changes in the initiator concentration.

Like in the case of effects of crosslinker concentration, the changes of primary structural parameters and macroscopic

properties are in functional and correlation relationships with the concentration of initiator in the reaction mixture, as presented by

$$\begin{aligned} \mathrm{SD_{eq}} &= 750 \cdot C_i^{-0.87} \quad R = 0.98, \\ \rho_x &= 1.35 \cdot C_i^{-0.09} \quad R = 0.97, \\ M_c &= 2.5 \cdot 10^6 \cdot C_i^{1.23} \quad R = 0.99, \\ \rho_c &= 0.54 \cdot C_i^{-1.32} \quad R = 0.99, \\ d &= 1053 \cdot C_i^{0.89} \quad R = 0.99. \end{aligned} \tag{11}$$

The values of MP and PSP are power functions of the initiator concentration in reaction mixture, with different prefactors and exponents.

Starting from the point that the basic structural detail of xerogel is average molar mass of polymer chain between crosslinking points, as in the case when the effect of Cc evaluated, we again found relationship between the primary structural parameters and properties of xerogel and M_c in the form of scaling law, as can be seen from the following empirical equations:

$$\begin{aligned} \mathrm{SD_{eq}} &= 0.02 \cdot M_c^{0.71} \quad R = 0.99, \\ \rho_x &= 3.85 \cdot M_c^{-0.07} \quad R = 0.97, \\ \rho_\mathrm{c} &= 3.83 \cdot M_c^{-1.07} \quad R = 0.99, \\ d &= 0.03 \cdot M_c^{0.72} \quad R = 0.99. \end{aligned} \tag{12}$$

The established changes of average molar mass of polymer chain between crosslinks with the increasing concentration of initiator are in disagreement with the predictable values of the results which would be obtained by calculation based on the model of kinetics of radical polymerization [63]. In fact, according to that model, the increase in the initiator concentration should lead to the decrease in the average distance of kinetically chains, and therefore, also the average molar mass of polymer chain between crosslinks would decrease.

The found increase in the molar mass of polymer chain between crosslinks in the case of crosslinking polymerization of acrylic acid is in agreement with the theoretically presumption of kinetics model of CLP suggested by Tobita and Hamielec [64], Dusek [65], and Elliott and Bowman [66]. In accordance with them, the increasing initiator concentration in reaction mixture in the course of crosslinking polymerization favors an intramolecular cyclization process over the crosslinking process which leads to the increase in M_c of the formed polymer network. Further, the increase in M_c causes decrease in the network's crosslink density and increase in the distance between the macromolecular chains and so the equilibrium swelling degree increases.

Therefore, it is possible to completely define technology for preparation xerogels with predetermined macroscopic properties (synthesis design) if the equations listed below are known:

$$\begin{aligned} \mathrm{MP}_j &= \alpha \cdot M_c^{\beta}, \\ \mathrm{RC}_i &= \alpha \cdot M_c^{\beta 1}, \end{aligned} \tag{13}$$

where MP_j are the macroscopic properties of the xerogel (equilibrium swelling degree and xerogel density), RC are reaction condition, α and α_1 are the prefactors, and β and β_1 are the exponents.

In that case, the choose of reaction conditions aimed at preparing xerogel with desired macroscopic properties is based on the calculation of the values of molar mass between crosslinks (M_c) according to

$$M_c = \left(\frac{\mathrm{MP}_j}{\alpha}\right)^{1/\beta}, \tag{14}$$

and then, the reaction conditions under which will be synthesized xerogel with predefined value of M_c can be calculated by using

$$\mathrm{RC}_i = \left(\frac{M_c}{\alpha_1}\right)^{1/\beta_1}. \tag{15}$$

5. Design of Poly(Methacrylic Acid) Xerogel Synthesis via Crosslinking Polymerization

5.1. Synthesis of Poly(Methacrylic Acid) Hydrogels. Poly (methacrylic acid) hydrogels (PMA) with different concentrations of crosslinker and monomer in reaction mixture were prepared *via* crosslinking polymerization (CLP) in aqueous media using the modified procedure for poly(acrylic acid) hydrogel synthesis [67].

The general procedure was as follows. Firstly, methacrylic acid (99.5%) (MA) (purchased from Merck KGaA) (20 wt% aqueous solution) was neutralized to the required neutralization degree with 25 wt% sodium hydroxide solution (Sodium hydroxide (p.a) obtained from Aldrich Chemical Co., Milwaukee, USA) under the nitrogen atmosphere and with constant stirring. Then, crosslinker (MBA) aqueous solution (1 wt%) was added under stirring and nitrogen bubbling through the mixture for half an hour. Then, the initiator (2,2′-Azobis-[2-(2-imidazolin-2-yl)propane] Dihydrochloride (VA-044) (99.8%) supplied by Wako Pure Chemical Industries, Ltd. (VA-044)) was added (1 wt% solution of) and the reaction mixture was once again rapidly stirred and bubbled with nitrogen for a further 20 min. Immediately, the prepared reaction mixture was poured into glass moulds (plates separated by a rubber gasket 2 mm thick) and placed in an oven at 80°C, for 3 h.

After the completion the reaction, the resulting products were handled in the same way as the PAA hydrogel. The primary structural parameters and macroscopic properties were determined using the methods given for the PAA xerogels.

5.2. Effects of Crosslinker Concentration MP and PSP of PMA Xerogel. The samples of PMA hydrogels were synthesized by using reaction mixtures with different crosslinker concentration (Cc) within the range from 0.003 wt% to 0.006 wt%, while the other reaction conditions were kept constant (Cm = 20 wt%, Ci = 0.2 wt%, ND = 40%, T = 80°C, and t = 3 h). The effect of crosslinker concentration on the macroscopic properties of PMA xerogels are presented in Figure 4.

The effects of Cc on primary structural parameters of PMA xerogels are given in Table 3.

It is clear that the increase in crosslinker concentration in reaction mixture results in the increase in the values of xerogel density and crosslinking density of xerogel, while the values of equilibrium swelling degrees, average molar mass between crosslinks, and the distance between the macromolecular chains decrease.

The evaluated changes of primary structural parameters and macroscopic properties of PMMA xerogels are in correlation relationships with the crosslinker concentration in the reaction mixture, which are presented by the empirical Equation (16)

$$\begin{aligned} \mathrm{SD_{eq}} &= 0.152 \cdot C_c^{-1.26} \quad R = 0.98, \\ \rho_x &= 4.05 \cdot C_c^{0.20} \quad R = 0.99, \\ M_c &= 33.44 \cdot C_c^{-1.56} \quad R = 0.97, \\ \rho_c &= 2.83 \cdot C_c^{1.57} \quad R = 0.97, \\ d &= 0.42 \cdot C_c^{-1.14} \quad R = 0.97. \end{aligned} \tag{16}$$

As in the case of PAA xerogels, the relationships between average molar mass between crosslinks and each particular value of primary structural parameters and macroscopic properties of PMA xerogels are given in the form of scaling law (see (17))

$$\begin{aligned} \mathrm{SD_{eq}} &= 0.01 \cdot M_c^{0.79} \quad R = 0.99, \\ \rho_x &= 5.6 \cdot M_c^{-0.12} \quad R = 0.97, \\ \rho_c &= 100 \cdot M_c^{-1.0} \quad R = 0.99, \\ d &= 0.03 \cdot M_c^{0.73} \quad R = 0.99. \end{aligned} \tag{17}$$

The changes in the values of MP and PSP with the increasing Cc in the reaction mixture may be attributed to the increased degree of crosslinking of polymer chains which is caused with the increased concentration of crosslinker in reaction mixture. As the network's crosslinking density increases, the space between polymer chains decreases as well as the M_c, and therefore, network rigidity and density of xerogel increases, while the $\mathrm{SD_{eq}}$ decreases.

5.3. Effects of Monomer Concentration on MP and PSP of PMA Xerogel. In order to examine the effects of changing monomer concentration in reaction mixture on the values of primary structural parameters and macroscopic properties of the synthesized PMA xerogels, samples of PMA hydrogels were synthesized. For that reason, reaction mixtures with monomer concentration varying within the range of 20–40 wt% were prepared and reactions proceed with constant all the others parameters (Ci = 0.2 wt%, Cc = 0.04 wt%, ND = 40%, T = 80°C, and t = 3 h). Figure 5 presents the effects of monomer concentration on the MP of the synthesized PMA xerogels.

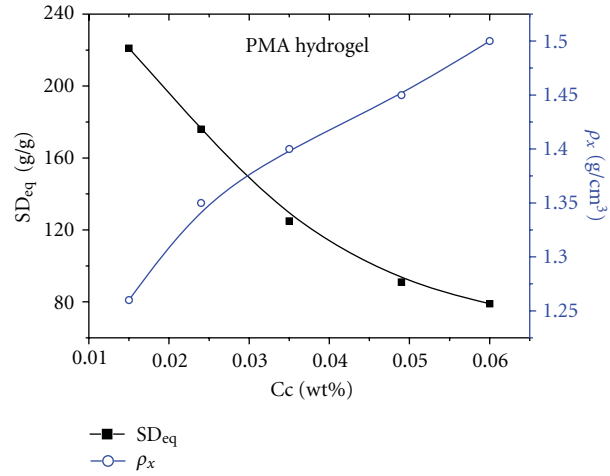

Figure 4: The effect of crosslinker concentration on the macroscopic properties of PMA xerogels.

Table 3: Effect of changes in Cc on primary structural parameters of PMA xerogels.

Cc, wt%	$M_c \cdot 10^{-5}$, g/mol	$\rho_c \cdot 10^4$, mol/cm^3	d, nm
0.015	2.7	3.5	290
0.024	2.2	4.2	250
0.035	1.4	6.7	180
0.049	0.91	10.4	132
0.060	0.75	11.7	118

Table 4 summarizes the effects of monomer concentration on the MP and PSP of the synthesized PMA xerogels.

Likewise in the case of crosslinker concentration, the increase in the methacrylic acid concentration in the reaction mixture leads to the increase in the values of xerogel density and crosslinking density of xerogel, while the values of equilibrium swelling degree, average molar mass between crosslinks, and the distance between the macromolecular chains decrease.

The primary structural parameters and macroscopic properties of PMA xerogels are power functions on the monomer concentration. Functional dependences of MP and PSP on monomer concentration are given by the empirical Equation (18)

$$\begin{aligned} \mathrm{SD_{eq}} &= 2.7 \cdot 10^6 C_m^{-3.18} \quad R = 0.98, \\ \rho_x &= 1.02 \cdot C_m^{0.09} \quad R = 0.99, \\ M_c &= 9.5 \cdot 10^{11} \cdot C_m^{-5.04} \quad R = 0.98, \end{aligned}$$

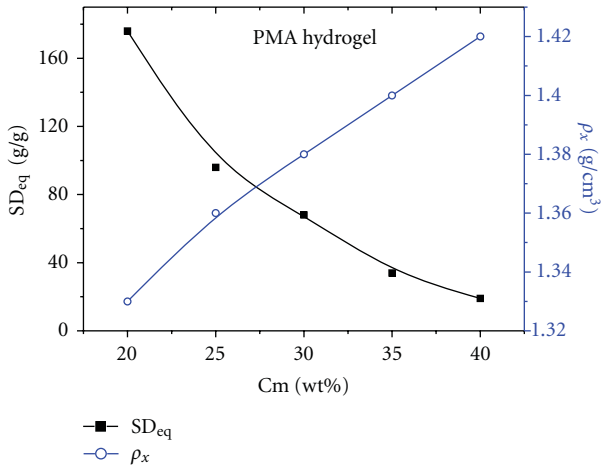

Figure 5: Effect of monomer concentration on macroscopic properties for PMA xerogels.

$$\rho_c = 8.8 \cdot 10^{-11} \cdot C_m^{5.10} \quad R = 0.98,$$
$$d = 1.05 \cdot 10^{7} \cdot C_m^{-3.5} \quad R = 0.97. \tag{18}$$

As was previously seen for crosslinker concentration, once again, the values of MP and PSP of synthesized PMA xerogels may be scaled with molar mass between crosslinks through scaling law (see (19))

$$\mathrm{SD_{eq}} = 0.08 \cdot M_c^{0.63} \quad R = 0.99,$$
$$\rho_x = 1.65 \cdot M_c^{0.02} \quad R = 0.96,$$
$$\rho_c = 99.5 \cdot M_c^{-1.0} \quad R = 1.0, \tag{19}$$
$$d = 0.05 \cdot M_c^{0.71} \quad R = 0.99.$$

The established changes of MP and PSP with the increasing monomer concentration in reaction mixture can be attributed to the fact that the increasing Cm leads to the increase in the rate of crosslinking polymerization, which causes the decreased values of average molar mass between crosslinks, and crosslinking density of xerogel increases which has as consequence the increase in the xerogel density while the value of $\mathrm{SD_{eq}}$ decreases.

6. Design of Poly(Acrylic Acid)-*G*-Gelatin Xerogel Synthesis via Crosslinking Graft Polymerization

6.1. Synthesis of Poly(Acrylic Acid)-G-Gelatin Hydrogels. A series of poly(acrylic acid)-*g*-gelatin (PAAG) xerogels with different neutralization degrees (ND) of acrylic acid and different crosslinker (MBA) concentration were synthesized *via* crosslinking graft polymerization of AA onto gelatin. The procedure of synthesis goes as follows. Firstly, 0.5 g of gelatin (Gelatin (70–100 Blooma), puriss, Kemika d.d. Zagreb, Croatia) was dissolved in 35 mL of distilled water at 45°C under stirring, until clear, homogenous solution was performed. Then, the initiator solution (VA-044, 1% wt) was added to gelatin solution and left for 15 min under stirring. In the meantime, AA was neutralized to required degree of neutralization, by dropwise adding potassium hydroxide aqueous solution (50 wt%) under cooling (5°C) with constant stirring. After that, crosslinker (0.1 wt%) was added and subsequently was added to the gelatine-initiator solution. The reaction mixture was once again rapidly stirred and immediately poured into teflons mold and placed in a thermostated oven at 80°C, for 3 hours.

After the completion the reaction, the resulting products were handled in the same way as the PAA hydrogel.

The primary structural parameters and macroscopic properties were determined using the methods given for the PAA xerogels.

Table 4: Effect of monomer concentration on primary structural parameters of PMA xerogels.

Cm, wt%	$M_c \cdot 10^{-4}$, g/mol	$\rho_c \cdot 10^4$, mol/cm^3	d, nm
20	22	4.2	250
25	8.8	4.8	134
30	5.1	19	88
35	1.6	66	40
40	0.64	149	21

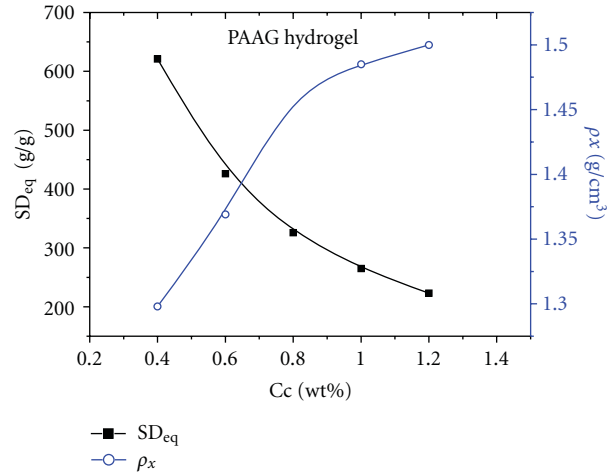

Figure 6: The effects of Cc on MP of PAAG xerogels.

6.2. The Effects of Crosslinker Concentration on MP and PSP of PAAG Xerogel. The effect of crosslinker concentration on the primary structural parameters and properties of poly(acrylic acid-g-gelatine (PAAG) xerogels was investigated within the range of crosslinker concentration varying from 0.4 wt%–1.2 wt% respective to monomer AA. The samples were synthesized keeping constant all other reaction parameters (Cm = 30 wt%, Ci = 1.0 wt%, ND = 50%, C_g = 5 wt%T = 80°C, and t = 3 h). The changes of values of MP of PAAG xerogels with change in the Cc are shown in Figure 6.

The changes of values of PSP of PAAG xerogels with change in the Cc are presented in Table 5.

The results above presented reveal that the increase in crosslinker concentration has the same effect on MP and PSP of PAAG xerogels as in the case of both PAA and PMA xerogels. In fact, once again, the increasing crosslinker concentration leads to the increasing values of xerogel density and network's crosslinking density on the contrary to the decreasing values of equilibrium swelling degrees, average molar mass between crosslinks and the distance between the macromolecular chains.

The relationships between crosslinker concentration in reaction mixture and the primary structural parameters and properties of the synthesized PAAG xerogels are found to be as follows:

$$\begin{aligned} \mathrm{SD_{eq}} &= 265 \cdot C_c^{-0.93} \quad R = 0.99, \\ \rho_x &= 1.49 \cdot C_c^{0.15} \quad R = 0.98, \\ M_c &= 6.5 \cdot 10^5 \cdot C_c^{-1.08} \quad R = 0.97, \\ \rho_c &= 2.31 \cdot 10^{-3} \cdot C_c^{1.25} \quad R = 0.98, \\ d &= 260 \cdot C_c^{-0.78} \quad R = 0.97. \end{aligned} \tag{20}$$

Scaling law of MP and PSP with M_c was found and given with empirical Equations (21)

$$\begin{aligned} \mathrm{SD_{eq}} &= 4.3 \cdot 10^{-3} \cdot M_c^{0.83} \quad R = 0.99, \\ \rho_x &= 8.6 \cdot M_c^{-0.13} \quad R = 0.94, \\ \rho_c &= 1.1 \cdot 10^4 \cdot M_c^{-1.15} \quad R = 0.99, \\ d &= 0.016 \cdot M_c^{0.72} \quad R = 0.99. \end{aligned} \tag{21}$$

The found changes in MP and PSP of xerogels synthesized by the crosslinking polymerization with the increased crosslinker concentration can be explained as follows. With the increase in crosslinker concentration, the network crosslinking density increases, which in turn causes the decrease in M_c and d, while the xerogel density and $\mathrm{SD_{eq}}$ decrease.

6.3. The Effects of Neutralization Degree on MP and PSP of PAAG Xerogel. The samples of PAAG xerogels with different degrees of neutralization from 0%–100% were synthesized by varying neutralization degree of AA while the other reaction parameters were kept constant (Cm = 30 wt%, Cc = 0.8 wt%, Ci = 0.27 wt%, C_g = 5 wt%, T = 80°C, and t = 3 h) aimed at investigating the effects of neutralization degree on MP and PSP of PAAG xerogels. The effect of neutralization degree on MP of PAAG xerogels are shown in Figure 7.

Table 6 presents the effect of neutralization degree on PSP of PAAG xerogels.

It is clear that the increasing degree of neutralization of acrylic acid results in xerogels with increased values of M_c, d, and $\mathrm{SD_{eq}}$ and decreased values of crosslinking density of xerogel and xerogel density. The found changes in the MP and PSP values of synthesized xerogels, like in the case of effects of crosslinker concentration, revealed power functional relationships with the degree of neutralization, as can be seen from the following empirical Equation (22)

$$\begin{aligned} \mathrm{SD_{eq}} &= 15.33 \cdot \mathrm{ND}^{0.79} \quad R = 0.99, \\ \rho_x &= 2.27 \cdot \mathrm{ND}^{-0.12} \quad R = 0.99, \\ M_c &= 1.56 \cdot 10^4 \cdot \mathrm{ND}^{0.99} \quad R = 0.99, \\ \rho_c &= 0.15 \cdot \mathrm{ND}^{-1.17} \quad R = 0.99, \\ d &= 17.6 \cdot \mathrm{ND}^{0.72} \quad R = 0.99. \end{aligned} \tag{22}$$

The existence of scaling law between the values of MP and PSP of PAAG xerogels with different degrees of neutralization of acrylic acid and M_c is given with empirical Equation (23)

$$\begin{aligned} \mathrm{SD_{eq}} &= 1.5 \cdot 10^{-4} \cdot M_c^{1.08} \quad R = 0.99, \\ \rho_x &= 3.16 \cdot M_c^{-0.06} \quad R = 0.93, \\ \rho_c &= 1.71 \cdot M_c^{-1.87} \quad R = 0.99, \\ d &= 2.7 \cdot 10^{-5} M_c^{1.19} \quad R = 0.99. \end{aligned} \tag{23}$$

Flory described the mechanism of the swelling of ionic networks [68]. According to Flory's theory, if the polymer chains making up the network containing ionizable group, the swelling forces may be greatly increased as a result of the localization of charges on the polymer chains and their repulsion effects. When acrylic acid is neutralized with KOH, the negatively charged carboxyl groups attached to the polymer chains set up an electrostatic repulsion which tends to expand the network. Therefore, if the increasing neutralization degree results in decrease of electrostatic repulsion between the polymer chains, then the $\mathrm{SD_{eq}}$ will decrease also.

On the contrary, however, during the CLGP of acrylic acid and gelatin, the increased degree of neutralization of AA increases the contraction of K-acrylate in reaction mixture. Bearing in mind that during the CLGP, the dominant effect on the structure of formed polymer network have the process of intermolecular cyclization, it is logical to propose that the increased degree of neutralization, that is, the K-acrylate concentration results in increased values of average molar mass between crosslinks and the distance between the macromolecular chains. Therefore, the values of crosslinking density and xerogel density of the synthesized xerogels are decreased, while the values of $\mathrm{SD_{eq}}$ are increased.

Table 5: The effect of Cc on primary structural parameters of PAAG xerogels.

Cc, wt%	$M_c \cdot 10^{-6}$, g/mol	ρ_c, mol·10^3/cm^3	d, nm
0.4	1.59	0.80	503
0.6	1.27	1.08	426
0.8	0.82	1.73	310
1.0	0.72	2.03	284
1.2	0.46	3.34	205

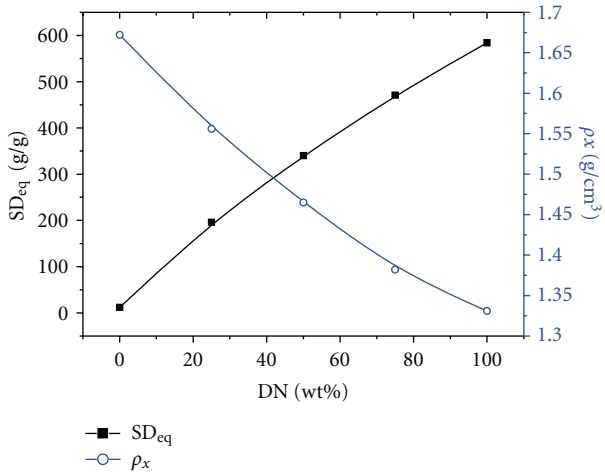

Figure 7: Effect of degree of neutralization on macroscopic properties of PAAG xerogels.

Table 6: The effect of neutralization degree on PSPP of PAAG xerogels.

DN, wt%	$M_c \cdot 10^{-5}$, g/mol	$\rho_c \cdot 10^3$, mol/cm^3	d, nm
0	0.41	411	7
25	3.85	4.04	180
50	8.23	1.78	310
75	12.14	1.14	412
100	15.10	0.87	485

The effects of reaction conditions on crosslinking density and equilibrium swelling for xerogels samples synthesized by radical polymerization (RP), crosslinking polymerization (CLP), and crosslinking graft polymerization (CLPG) were evaluated in numerous of theoretical considerations [68–70].

According to the model of ionic networks proposed by Flory [71], it is predictable that the dependence of equilibrium swelling degree on crosslinker concentration is in power law form, given by

$$\mathrm{SD}_{\mathrm{eq}} = k \cdot C_c^{-0.6}. \tag{24}$$

This dependence is experimentally confirmed by Chen and Zhao, for CLP of acrylic acid [72], and Pourjavadi et al., for CLPG of acrylic acid onto kappa-carageenan [73]. Pacios et al. found stoichiometry relationship between crosslink density of product and total concentration of comonomers and crosslinker concentration for the CLP of *n*-vynilimidizol [74]. For the same system, Obukhov et al. [75] found that equilibrium swelling degree is power function of monomer concentrations in reaction mixture

$$\mathrm{SD}_{\mathrm{eq}} \propto C_m^{-b}, \tag{25}$$

where b is parameters depending of solvent; in good solvent $b = 1$ and in theta solvent $b = 3/4$.

Table 7 summarizes values of prefactor (a) and exponent (b) calculated for established power function of the PSPP on different reaction conditions, for the investigated process of polymerization.

The results presented in Table 7 reveal that the values of prefactor (a) and exponent (b) for each particular MP and PSP are dependent on the method of polymerization and reaction conditions, and accordingly, they cannot be used as a base for making a general model that would be applied to predict the MP and PSP of xerogels that would be synthesized.

Furukawa [76] investigated effects of reaction conditions on $\mathrm{SD}_{\mathrm{eq}}$ for CLP of poly(acrylamide) and established the following relationship:

$$\mathrm{SD}_{\mathrm{eq}} \propto N^{3\upsilon-1}, \tag{26}$$

where N means polymerization index and υ is parameter of the deGenne's blob model [77]. The $\upsilon = 3/5$ in good solvent and $\upsilon = 1/2$ in theta solvent).

In all of the above evaluated crosslinking-polymerization systems, it is established that MP and PSP can be scaled with M_c. The values of prefactor and scaling exponent are given in Table 8.

The results presented in Table 8 show that the scaling exponent presents a constant value within the experimental error for CLP even in the case when deferent monomers are used and different reaction conditions are applied. That value considerably differs than the value for the exponent obtained for CLGP. Therefore, we may conclude that for the particular type of polymerization the model for prediction the PSP has to be based on the scaling law of PSP and M_c, because the M_c is the basic structural detail of synthesized xerogel.

The generality in that law presents the equality of the value of exponent b for the xerogels synthesized by the same method of polymerization and that value present a global physical property of the obtained xerogel and implies on the way of scaling structural property of xerogel.

In contrast to this, the prefactor a in scaling law is not universal. The prefactor a depends on the structural details of xerogel and accordingly is changeable depending on type of polymerization and reaction conditions and type of monomer.

The established functional dependences of PSP on reaction condition for different methods of polymerization and the possibility of their scaling with M_c enable us to model directed synthesis of xerogels/hydrogels. That modeling, as was previously said, is based on (13) and (30) which serves for calculation reaction conditions for synthesis of xerogel with predetermined macroscopic properties.

Based on the suggested "model of synthesis design", the selection of reaction conditions under which will be synthesized xerogel with predefined macroscopic properties is performed in two steps. Firstly, the values of molar mass between crosslinks which generate desired macroscopic property of xerogel, are calculated by (14) and in the following step, the reaction condition which will results in synthesis of xerogel with desired M_c is performed according to (15).

7. Conclusions

In all of the investigated methods of synthesis xerogels/hydrogels (CLP, CCLP, and CLPG), the existence of

Table 7: The values of prefactor and exponent for established power function of the MP PSP on different reaction conditions.

Xerogel	Reaction parmeter	SD_{eq}		ρ_x		M_c		ρ_c		d	
		a	b	a	b	A	b	a	b	a	b
PAA	Cc	32.5	−0.40	2.02	0.06	$3.3\cdot10^{4}$	−0.50	60	0.59	47	−0.39
PMA	Cc	0.152	−1.26	4.05	0.20	33.44	−1.56	2.83	1.57	0.42	−1.14
PAAG	Cc	265	−0.93	1.49	0.15	$6.5\cdot10^{5}$	−1.08	$2.31\cdot10^{-3}$	1.25	260	−0.78
PAA	Ci	750	−0.87	1.35	−0.09	$2.5\cdot10^{6}$	1.23	0.54	-1.32	1053	0.89
PMA	Cm	$2.7\cdot10^{6}$	−3.18	1.02	0.1	$9.5\cdot10^{11}$	−5.04	$8.8\cdot10^{-11}$	5.10	$1.05\cdot10^{7}$	−3.50
PAAG	ND	15.33	0.79	2.27	−0.12	$1.56\cdot10^{4}$	0.99	0.15	−1.17	17.6	0.72

Table 8: The values of prefactor and scaling exponent of the MP and PSP on M_c.

Xerogel	Reaction parmeter	SD_{eq}		ρ_x		ρ_c		d	
		a	B	a	b	a	b	a	b
PAA	Cc	0.015	0.74	4.95	−0.10	5.44	−1.1	0.02	0.73
PMA	Cc	0.01	0.79	5.6	−0.12	100	−1.0	0.03	0.73
PAAG	Cc	$4.3\cdot10^{-3}$	0.83	8.6	−0.13	$1.1\cdot10^{4}$	−1.15	0.016	0.72
PAA	Ci	0.02	0.71	3.85	−0.07	3.83	−1.07	0.03	0.72
PMA	Cm	0.08	0.63	1.65	002	99.5	−1.0	0.05	0.71
PAAG	ND	$1.5\cdot10^{-4}$	1.08	3.16	−0.06	1.7·	−1.87	$2.7\cdot10^{-5}$	1.19

empirical functional relationships between reaction conditions (concentration of crosslinker, monomer and initiator, and degree of neutralization of monomer), values of structural parameters of xerogel (M_c, d, and crosslinking density of network), and macroscopic properties (xerogel density and equilibrium swelling degree) are found.

In all of the investigated methods of polymerization, the presence of functional relationship between reaction conditions (RCi) and primary structural parameters and properties (PSP_j) of power form and power function was established

$$PSP_j = a \cdot RC_i^b. \quad (27)$$

The values of parameters (a and b) of the above power function are dependent on the method of polymerization, monomer type, and reaction conditions.

For all of the investigated process, the possibility of scaling of MP and PSP with M_c is reveled.

The values of scaling exponent of that function for the same method of polymerization are independent on the monomer type and other reaction condition and present a structural parameter of the xerogel. The M_c is structural parameter based on which may be predicted macroscopic physicochemical properties of xerogels and their application in tissue engineering.

Acknowledgment

This investigation was supported by the Ministry of Science and Technical Development of the Republic of Serbia through Project no. 172015 OI.

References

[1] J. J. Grodzinski, "Polymeric gels and hydrogels for biomedical and pharmaceutical applications," *Polymers for Advanced Technologies*, vol. 21, no. 1, pp. 27–47, 2010.

[2] R. Langer and D. A. Tirrell, "Designing materials for biology and medicine," *Nature*, vol. 428, no. 6982, pp. 487–492, 2004.

[3] E. S. Place, N. D. Evans, and M. M. Stevens, "Complexity in biomaterials for tissue engineering," *Nature Materials*, vol. 8, no. 6, pp. 457–470, 2009.

[4] N. A. Peppas and A. G. Mikos, "Preparation methods and structure of hydrogels," in *Hydrogels in Medicine and Pharmacy*, N. A. Peppas, Ed., pp. 2–23, CRC Press, Boca Raton, Fla, USA, 1986.

[5] K. Park, W. C. W. Shalaby, and H. Park, "Hydrogels, definition, hydrogel as a biomaterial, biodegradable hydrogels, biodegradation," in *Biodegradable Hydrogels for Drug Delivery*, K. Park, W. C. W. Shalaby, and H. Park, Eds., pp. 1–12, Technomic, Lancaster, UK, 1993.

[6] S. Chaterji, I. K. Kwon, and K. Park, "Smart polymeric gels: redefining the limits of biomedical devices," *Progress in Polymer Science*, vol. 32, no. 8-9, pp. 1083–1122, 2007.

[7] A. Kikuchi and T. Okano, "Pulsatile drug release control using hydrogels," *Advanced Drug Delivery Reviews*, vol. 54, no. 1, pp. 53–77, 2002.

[8] S. H. Hu, T. Y. Liu, D. M. Liu, and S. Y. Chen, "Controlled pulsatile drug release from a ferrogel by a high-frequency magnetic field," *Macromolecules*, vol. 40, no. 19, pp. 6786–6788, 2007.

[9] D. S. Kohane and R. Langer, "Polymeric biomaterials in tissue engineering," *Pediatric Research*, vol. 63, no. 5, pp. 487–491, 2008.

[10] J. F. Mano, "Stimuli-responsive polymeric systems for biomedical applications," *Advanced Engineering Materials*, vol. 10, no. 6, pp. 515–527, 2008.

[11] M. Yamato, C. Konno, M. Utsumi, A. Kikuchi, and T. Okano, "Thermally responsive polymer-grafted surfaces facilitate patterned cell seeding and co-culture," *Biomaterials*, vol. 23, no. 2, pp. 561–567, 2002.

[12] Y. Yeo and D. S. Kohane, "Polymers in the prevention of peritoneal adhesions," *European Journal of Pharmaceutics and Biopharmaceutics*, vol. 68, no. 1, pp. 57–66, 2008.

[13] N. E. Fedorovich, J. Alblas, J. R. de Wijn, W. E. Hennink, A. B.J. Verbout, and W. J.A. Dhert, "Hydrogels as extracellular matrices for skeletal tissue engineering: state-of-the-art and novel application in organ printing," *Tissue Engineering*, vol. 13, no. 8, pp. 1905–1925, 2007.

[14] S. Möller, J. Weisser, S. Bischoff, and M. Schnabelrauch, "Dextran and hyaluronan methacrylate based hydrogels as matrices for soft tissue reconstruction," *Biomolecular Engineering*, vol. 24, no. 5, pp. 496–504, 2007.

[15] E. Ho, A. Lowman, and M. Marcolongo, "Synthesis and characterization of an injectable hydrogel with tunable mechanical properties for soft tissue repair," *Biomacromolecules*, vol. 7, no. 11, pp. 3223–3228, 2006.

[16] W. Lee, D. Choi, Y. Lee, D. N. Kim, J. Park, and W. G. Koh, "Preparation of micropatterned hydrogel substrate via surface graft polymerization combined with photolithography for biosensor application," *Sensors and Actuators, B*, vol. 129, no. 2, pp. 841–849, 2008.

[17] J. Hoffmann, M. Plotner, D. Kucling, and W.-J. Fischer, "Photopatterning of thermally sensitive hydrogel useful for micro actuators," *Sens Actuators*, vol. 77, pp. 139–144, 1999.

[18] J. D. Kretlow, L. Klouda, and A. G. Mikos, "Injectable matrices and scaffolds for drug delivery in tissue engineering," *Advanced Drug Delivery Reviews*, vol. 59, no. 4-5, pp. 263–273, 2007.

[19] Z. M. O. Rzaev, S. Dinçer, and E. Pişkin, "Functional copolymers of N-isopropylacrylamide for bioengineering applications," *Progress in Polymer Science*, vol. 32, no. 5, pp. 534–595, 2007.

[20] J. L. Drury and D. J. Mooney, "Hydrogels for tissue engineering: scaffold design variables and applications," *Biomaterials*, vol. 24, no. 24, pp. 4337–4351, 2003.

[21] S. Varghese and J. H. Elisseeff, "Hydrogels for musculoskeletal tissue engineering," *Advances in Polymer Science*, vol. 203, no. 1, pp. 95–144, 2006.

[22] K. Tuzlakoglu, C. M. Alves, J. F. Mano, and R. L. Reis, "Production and characterization of chitosan fibers and 3-D fiber mesh scaffolds for tissue engineering applications," *Macromolecular Bioscience*, vol. 4, no. 8, pp. 811–819, 2004.

[23] T. Guo, J. Zhao, J. Chang et al., "Porous chitosan-gelatin scaffold containing plasmid DNA encoding transforming growth factor-β1 for chondrocytes proliferation," *Biomaterials*, vol. 27, no. 7, pp. 1095–1103, 2006.

[24] Y. Liu and M. B. Chan-Park, "Hydrogel based on interpenetrating polymer networks of dextran and gelatin for vascular tissue engineering," *Biomaterials*, vol. 30, no. 2, pp. 196–207, 2009.

[25] S. Young, M. Wong, Y. Tabata, and A. G. Mikos, "Gelatin as a delivery vehicle for the controlled release of bioactive molecules," *Journal of Controlled Release*, vol. 109, no. 1–3, pp. 256–274, 2005.

[26] F. M. Chen, Y. M. Zhao, H. H. Sun et al., "Novel glycidyl methacrylated dextran (Dex-GMA)/gelatin hydrogel scaffolds containing microspheres loaded with bone morphogenetic proteins: formulation and characteristics," *Journal of Controlled Release*, vol. 118, no. 1, pp. 65–77, 2007.

[27] F. M. Chen, Y. M. Zhao, R. Zhang et al., "Periodontal regeneration using novel glycidyl methacrylated dextran (Dex-GMA)/gelatin scaffolds containing microspheres loaded with bone morphogenetic proteins," *Journal of Controlled Release*, vol. 121, no. 1-2, pp. 81–90, 2007.

[28] J. D. Kosmala, D. B. Henthorn, and L. Brannon-Peppas, "Preparation of interpenetrating networks of gelatin and dextran as degradable biomaterials," *Biomaterials*, vol. 21, no. 20, pp. 2019–2023, 2000.

[29] Y. Lu, D. Wang, T. Li et al., "Poly(vinyl alcohol)/poly(acrylic acid) hydrogel coatings for improving electrode-neural tissue interface," *Biomaterials*, vol. 30, no. 25, pp. 4143–4151, 2009.

[30] K. Y. Lee and D. J. Mooney, "Hydrogels for tissue engineering," *Chemical Reviews*, vol. 101, no. 7, pp. 1869–1879, 2001.

[31] Y. Teramura, Y. Kaneda, and H. Iwata, "Islet-encapsulation in ultra-thin layer-by-layer membranes of poly(vinyl alcohol) anchored to poly(ethylene glycol)-lipids in the cell membrane," *Biomaterials*, vol. 28, no. 32, pp. 4818–4825, 2007.

[32] D. Mawad, P. J. Martens, R. A. Odell, and L. A. Poole-Warren, "The effect of redox polymerisation on degradation and cell responses to poly (vinyl alcohol) hydrogels," *Biomaterials*, vol. 28, no. 6, pp. 947–955, 2007.

[33] J. Choi, H. Bodugoz-Senturk, H. J. Kung, A. S. Malhi, and O. K. Muratoglu, "Effects of solvent dehydration on creep resistance of poly(vinyl alcohol) hydrogel," *Biomaterials*, vol. 28, no. 5, pp. 772–780, 2007.

[34] Y. M. Yue, K. Xu, X. G. Liu, Q. Chen, X. Sheng, and P. X. Wang, "Preparation and characterization of interpenetration polymer network films based on poly(vinyl alcohol) and poly(acrylic acid) for drug delivery," *Journal of Applied Polymer Science*, vol. 108, no. 6, pp. 3836–3842, 2008.

[35] E. De Giglio, S. Cometa, N. Cioffi, L. Torsi, and L. Sabbatini, "Analytical investigations of poly(acrylic acid) coatings electrodeposited on titanium-based implants: a versatile approach to biocompatibility enhancement," *Analytical and Bioanalytical Chemistry*, vol. 389, no. 7-8, pp. 2055–2063, 2007.

[36] J. Dai, Z. Bao, L. Sun, S. U. Hong, G. L. Baker, and M. L. Bruening, "High-capacity binding of proteins by poly(acrylic acid) brushes and their derivatives," *Langmuir*, vol. 22, no. 9, pp. 4274–4281, 2006.

[37] J. A. Hubbell, "Bioactive biomaterials," *Current Opinion in Biotechnology*, vol. 10, no. 2, pp. 123–129, 1999.

[38] J. A. Rowley, G. Madlambayan, and D. J. Mooney, "Alginate hydrogels as synthetic extracellular matrix materials," *Biomaterials*, vol. 20, no. 1, pp. 45–53, 1999.

[39] D. L. Hern and J. A. Hubbell, "Incorporation of adhesion peptides into nonadhesive hydrogels useful for tissue resurfacing," *Journal of Biomedical Materials Research*, vol. 39, no. 2, pp. 266–276, 1998.

[40] B. K. Mann, R. H. Schmedlen, and J. L. West, "Tethered-TGF-β increases extracellular matrix production of vascular smooth muscle cells," *Biomaterials*, vol. 22, no. 5, pp. 439–444, 2001.

[41] Y. Suzuki, M. Tanihara, K. Suzuki, A. Saitou, W. Sufan, and Y. Nishimura, "Alginate hydrogel linked with syntheticoligiopeptide derived from BMP-2 allows ectopic osteoinduction in vivo," *Journal of Biomedical Materials Research*, vol. 50, pp. 405–409, 2000.

[42] J. Elisseeff, W. McIntosh, K. Fu, T. Blunk, and R. Langer, "Controlled-release of IGF-I and TGF-β1 in a photopolymerizing hydrogel for cartilage tissue engineering," *Journal of Orthopaedic Research*, vol. 19, no. 6, pp. 1098–1104, 2001.

[43] A. E. Bent, J. Foote, S. Siegel, G. Faerber, R. Chao, and E. A. Gormley, "Collagen implant for treating stress urinary

incontinence in women with urethral hypermobility," *Journal of Urology*, vol. 166, no. 4, pp. 1354–1357, 2001.

[44] C. R. Nuttelman, D. J. Mortisen, S. M. Henry, and K. S. Anseth, "Attachment of fibronectin to poly(vinyl alcohol) hydrogels promotes NIH3T3 cell adhesion, proliferation, and migration," *Journal of Biomedical Materials Research*, vol. 57, no. 2, pp. 217–223, 2001.

[45] R. C. Thomson, M. C. Wake, M. J. Yaszemski, and A. G. Mikos, "Biodegradable polymer scaffolds to regenerate organs," *Advances in Polymer Science*, vol. 122, pp. 245–274, 1995.

[46] M. Dimitrov, N. Lambov, S. Shenkov, V. Dosseva, and V. Y. Baranovski, "Hydrogels based on the chemically crosslinked polyacrylic acid: biopharmaceutical characterization," *Acta Pharmaceutica*, vol. 53, no. 1, pp. 25–31, 2003.

[47] M. Changez, V. Koul, B. Krishna, A. K. Dinda, and V. Choudhary, "Studies on biodegradation and release of gentamicin sulphate from interpenetrating network hydrogels based on poly(acrylic acid) and gelatin: in vitro and in vivo," *Biomaterials*, vol. 25, no. 1, pp. 139–146, 2004.

[48] J. S. Ahn, H. K. Choi, M. K. Chun et al., "Release of triamcinolone acetonide from mucoadhesive polymer composed of chitosan and poly(acrylic acid) in vitro," *Biomaterials*, vol. 23, no. 6, pp. 1411–1416, 2002.

[49] Z. Juranic, L. Stevovic, B. Drakulic, T. Stanojkovic, S. Radulovic, and I. Juranic, "Substituted (E)-(benzoil) acrylic acid suppressed survival of neoplastic HeLacels," *Journal of the Serbian Chemical Society*, vol. 64, no. 9, pp. 505–512, 1999.

[50] B. Adnadjevic, J. Jovanovic, and B. Drakulic, "Isothermal kinetics of (E)-4-(4-metoxyphenyl)-4-oxo-2-butenoic acid release from poly(acrylic acid) hydrogel," *Thermochimica Acta*, vol. 466, no. 1-2, pp. 38–48, 2007.

[51] B. Adnadjevic and J. Jovanovic, "A comparative kinetics study of isothermal drug release from poly(acrylic acid) and poly(acrylic-co-methacrylic acid) hydrogels," *Colloids and Surfaces B*, vol. 69, no. 1, pp. 31–42, 2009.

[52] K. M. Gupta, S. R. Barnes, R. A. Tangaro et al., "Temperature and pH sensitive hydrogels: an approach towards smart semen-triggered vaginal microbicidal vehicles," *Journal of Pharmaceutical Sciences*, vol. 96, no. 3, pp. 670–681, 2007.

[53] M. Dittgen, M. Durrani, and K. Lehmann, "Acrylic polymers—a review of pharmaceutical applications," *S.T.P. Pharma Sciences*, vol. 7, no. 6, pp. 403–437, 1997.

[54] A. Besheer, K. M. Wood, N. A. Peppas, and K. Mäder, "Loading and mobility of spin-labeled insulin in physiologically responsive complexation hydrogels intended for oral administration," *Journal of Controlled Release*, vol. 111, no. 1-2, pp. 73–80, 2006.

[55] D. F. Williams, "On the mechanisms of biocompatibility," *Biomaterials*, vol. 29, no. 20, pp. 2941–2953, 2008.

[56] J. Kopeček and J. Yang, "Hydrogels as smart biomaterials," *Polymer International*, vol. 56, no. 9, pp. 1078–1098, 2007.

[57] A. S. Hoffman, "Hydrogels for biomedical applications," *Advanced Drug Delivery Reviews*, vol. 54, no. 1, pp. 3–12, 2002.

[58] F. Lim, "Microencapsulation of living cells and tissues—theory and practice," in *Biomedical Applications of Microencapsulation*, pp. 137–154, CRC Press, Boca Raton, Fla, USA, 1984.

[59] F. Brandl, F. Sommer, and A. Goepferich, "Rational design of hydrogels for tissue engineering: impact of physical factors on cell behavior," *Biomaterials*, vol. 28, no. 2, pp. 134–146, 2007.

[60] M. S. Shoichet, "Polymer scaffolds for biomaterials applications," *Macromolecules*, vol. 43, no. 2, pp. 581–591, 2010.

[61] P. J. Flory and J. Rehner, "Statistical mechanics of cross-linked polymer networks I. Rubberlike elasticity," *The Journal of Chemical Physics*, vol. 11, no. 11, pp. 512–520, 1943.

[62] J. Brandrup and E. H. Immergut, *Polymer Handbook*, John Wiley & Sons, New York, NY, USA, 2nd edition, 1975.

[63] H. R. Allcock and W. L. Frederick, *Contemporary Polymer Chemistry*, Prentice Hall, Englewood Cliffs, NJ, USA, 1981.

[64] H. Tobita and A. E. Hamielec, "Control of network structure in free-radical crosslinking copolymerization," *Polymer*, vol. 33, no. 17, pp. 3647–3657, 1992.

[65] K. Dusek, "Network formation involving polyfunctional polymer chains," in *Polymer Networks: Principles of Their Formation Structure and Properties*, R. F. T. Stepto, Ed., pp. 64–92, Blackie Academic and Professional, London, UK, 1998.

[66] J. E. Elliott and C. N. Bowman, "Kinetics of primary cyclization reactions in cross-linked polymers: an analytical and numerical approach to heterogeneity in network formation," *Macromolecules*, vol. 32, no. 25, pp. 8621–8628, 1999.

[67] B. Adnadjevic and J. Jovanovic, "Novel approach in investigation of the poly(acrylic acid) hydrogel swelling kinetics in water," *Journal of Applied Polymer Science*, vol. 107, no. 6, pp. 3579–3587, 2008.

[68] L. Bromberg, A. Y. Grosberg, E. S. Matsuo, Y. Suzuki, and T. Tanaka, "Dependency of swelling on the length of subchain in poly(N,N-dimethylacrylamide)-based gels," *Journal of Chemical Physics*, vol. 106, no. 7, pp. 2906–2910, 1997.

[69] A. Pastoriza, I. E. Pacios, and I. F. Piérola, "Kinetics of solvent responsiveness in poly(N,N-dimethylacrylamide) hydrogels of different morphology," *Polymer International*, vol. 54, no. 8, pp. 1205–1211, 2005.

[70] Z. Chen, C. Cohen, and F. A. Escobedo, "Monte Carlo simulation of the effect of entanglements on the swelling and deformation behavior of end-linked polymeric networks," *Macromolecules*, vol. 35, no. 8, pp. 3296–3305, 2002.

[71] P. J. Flory, *Principles of Polymeric Chemistry*, Cornell University Press, Ithaca, NY, USA, 1953.

[72] J. Chen and Y. Zhao, "Relationship between water absorbency and reaction conditions in aqueous solution polymerization of polyacrylate superabsorbents," *Journal of Applied Polymer Science*, vol. 75, no. 6, pp. 808–814, 2000.

[73] A. Pourjavadi, A. M. Harzandy, and H. Hosseinzadeh, "Synthesis of novel polysaccharide—based superabsorbent hydtogel via graft coplymerization of acrylic acid onto kappa-carragenan in air," *European Polymer Journal*, vol. 40, pp. 1363–1370, 2004.

[74] I. E. Pacios, M. J. Molina, M. Rosa Gonez-Anton, and I. F. Pierola, "Correlation of swelling and crosslinking density with the composition of the reactiong mixture employed in radical crosslinking copolymerization," *Journal of Applied Polymer Science*, vol. 103, pp. 263–269, 2007.

[75] S. P. Obukhov, M. Rubinstein, and R. H. Colby, "Network modulus and superelasticity," *Macromolecules*, vol. 27, no. 12, pp. 3191–3198, 1994.

[76] H. Furukawa, "Effect of varying preparing-concentration on the equilibrium swelling of polyacrylamide gels," *Journal of Molecular Structure*, vol. 554, no. 1, pp. 11–19, 2000.

[77] P. G. De Gennes, *Scaling Concepts in Polymer Ohysics*, Cornell University Press, Ithaca, NY, USA, 1979.